University of Glasgow

Identification and Characterisation of the Missing Components of the ER Reductive Pathway

Xiaofei Cao BSc (Hons) MRes

Supervisor: Prof Neil Bulleid

Submitted in fulfilment of the requirements for the Degree of Doctor of Philosophy

Institute of Molecular, Cell and Systems Biology

College of Medical, Veterinary & Life Sciences

University of Glasgow

June 2020

Abstract

Efficient folding of proteins frequently requires the introduction of disulfide bonds. The insertion of disulfide bonds could result in native disulfides, which can be found in the correctly folded and functional protein structure, and non-native disulfides which are not present in the native protein. The resolution of non-native disulfides is absolutely required for cells to fold secreted proteins correctly and to remove misfolded proteins to alleviate cell stress. The pathways for disulfide formation are well characterised. However, our understanding of the reduction of non-native disulfides is still limited. How the reducing equivalents are transferred across the ER membrane and whether there are additional components needed in the reduction pathway either in cytosol or ER lumen are the questions we need to address.

Microsomes including redox-sensitive green fluorescence protein (roGFP) were used to address which membrane protein was involved in the ER reductive pathway. We demonstrated that a membrane protein is required for the reduction of microsomal proteins by the membrane impermeable reducing agent Tris(2-carboxyethyl)phosphine (TCEP) or a reconstituted thioredoxin/thioredoxin reductase (Trx/TrxR) pathway.

Previous research in our group suggests that ERp57 has a specific role in the isomerisation of non-native disulfide bonds in specific glycoprotein. We optimised the determination of redox state of ERp57 in semi-permeabilised (SP) cells. It was found that the reduction of ERp57 in SP cells required reducing equivalents generated by the Trx/TrxR pathway and the reduction was dependent on catalytic cysteines in the Trx motif. It was also shown by proteinase experiments that different membrane proteins are required for the transduction of electrons from TCEP and the Trx/TrxR pathway.

In addition, we took advantage of an *in vitro* translational system supplemented with SP cells. A post-translationally folding assay was developed to evaluate the ability of the cytosolic components to resolve non-native disulfides in nascent polypeptides proteins in the ER. We showed that the minimal components in the cytosolic Trx/TrxR pathway are sufficient for disulfide rearrangement in the ER and that the reduction process is Trx - dependent.

Table of Contents

List of Tables

List of Figures

Acknowledgement

It has been my great honour to complete my four-year doctoral research in Prof Neil Bulleid's group.

Firstly, I would like to sincerely thank my supervisor Prof Neil Bulleid for his guidance and continuous support during my PhD study. Neil deeply impressed me by his enthusiasm for scientific research, extensive knowledge, and rigorous work attitude. Neil always provided valuable advice and positive encouragement whenever I needed. He has created a harmonious research environment of mutual promotion and assistance allowing everyone enjoy to working in his group. With his help, I became a more independent researcher.

I also received precious advice, help, feedback, and encouragement from everyone in Neil's group throughout my PhD project. I sincerely thank the post-docs (Marcel van Lith, Phil Robinson, Zhenbo Cao, Ojore Oka, Chloe Stoyle), research technicians (Marie Anne Pringle, Lorna Mitchell, and Bethany Fleming), and PhD students (Esraa Haji, Tomasz Szmaja, Wanida Tungkum, and Arvin Pierre). In addition, I would like to thank Sergio Lilla and Sara Zanivan in Cancer Research UK Beatson Institute for their contribution to the roGFP MS experiment.

I would like to thank all my family and friends for their support and encouragement. In particularly, I would like to thank Dr John McGinty for proofreading my thesis.

Finally, I would like to thank the China Scholarship Council for funding my PhD study at the University of Glasgow.

Author's Declaration

I declare that, except where explicit reference is made to the contribution of others, that this dissertation is the result of my own work and has not been submitted for any other degree at the University of Glasgow or any other institution.

Printed Name: XIAOFEI CAO

Signature: 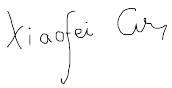

Definitions/Abbreviations

aa-tRNA: Aminoacyl-transfer RNA

ABCDE1: ATP-binding cassette (ABC) protein

Adam 10: Adam disintegrin and metalloprotease 10

Amp: Ampicillin

AMS: 4-acetamido-4'-maleimidylstilbene-2, 2'-disulfonic acid

AF: Auranofin

AP-1: Activator protein 1

ATP: Adenosine triphosphate

avGFP: *Aequorea victoria* green fluorescence protein

BSA: Bovine serum albumin

C: Reconstituted Trx/TrxR pathway using purified cytosol components (NADPH, G6P, G6PDH, Trx and TrxR)

CLD: Conserved loop C domain

CNX: Calnexin

CRT: Calreticulin

C-Trx (C-T): Reconstituted Trx/TrxR pathway using purified cytosol components in absence of Trx

CTP: 25 mM Cytidine triphosphate

Cys: Cysteine

Dia: Diamide

DHA: Dehydroascorbate

DMEM: Dulbecco's Modified Eagle Medium

DTT: Dithiothreitol

DR: Disulfide bond rearrangement

ECM: extracellular matrix

EDEM1: Degradation-enhancing a-mannosidase-like protein 1

EDTA: Ethylenediaminetetraacetic acid

eEFs: Eukaryotic elongation factors

EGTA: Ethylene glycol-bis(2-aminoethylether)-N, N, N′, N′-tetraacetic acid

eIFs: Eukaryotic initiation factors

EL: Endothelial lipase

ER: Endoplasmic reticulum

ERQC: ER quality control

ERAD: ER-associated protein degradation

eRFs: Eukaryotic release factors

Ero1: ER oxidoreductin 1

ERp: Endoplasmic reticulum-resident protein

ERQC: ER quality control

FAD: flavin adenine dinucleotide

$FADH_2$: Reduced form of FAD

G6P: Glucose 6-phosphate

G6PDH: Glucose 6-phosphate dehydrogenase

GFC buffer: Gel filtration chromatography

GFP: Green fluorescence protein

Gly-: Glycosylated

GRP58: Glucose-regulated protein 58

GSH: Reduced glutathione

GSSG: Oxidised glutathione

GPAA1: Glycosylphosphatidylinositol anchor attachment 1 protein

GPx1: Glutathione peroxidase 1

GPX 7/8: Glutathione peroxidase 7/8

GTP: Guanosine triphosphate

HA: Hemagglutinin

HL: Hepatic lipase

Hsp: Heat shock protein

IAA: Iodoacetamide

IMS: Mitochondrial intermembrane space

IP: Immunoprecipitation

IPTG: Isopropyl ß-D-1-thiogalactopyranoside

LB: Luria Broth

LC-MS-MS: Liquid Chromatography with tandem mass spectrometry

LMF1: Lipase maturation factor 1

LMAN1: Human lectin mannose-binding 1

LPL: Lipoprotein lipase

Met: Methionine

Met-tRNA^{iMet}: Methionine transfer RNA

MP: Unknown membrane protein

mPEG: Methoxy Polyethylene Glycol

mRNA: Massager RNA

MS: Mass Spectrometry

MsrB1: Methionine sulfoxide reductase

MTP: Microsomal triglyceride transfer protein

NADP+: Nicotinamide adenine dinucleotide phosphate

NADPH: Adenine dinucleotide phosphate (Reduced form of $NADP^+$)

NEM: N-ethylmaleimide

NF-kB: Nuclear factor-kB

ORF: Open reading frame

Ox: Oxidised

OxR: Oxidoreductase

OST: Oligosaccharyl transferase

P4H: prolyl 4-hydroxylases

PAS: Recombinant Protein A Sepharose FF Resin

PBS buffer: Dulbecco's Phosphate Buffered Saline

PCR: Polymerase chain reaction

PDI: Protein disulfide isomerise

PGL: 6-phosphogluconolacetone

PL: Pancreatic lipase

PM: Plasma membrane

PMSF: Phenylmethanesulfonyl fluoride

PRDX 4: Peroxiredoxin 4

PPIases: Peptidyl prolyl cis/trans isomerases

pp-tRNA: Peptidyl-tRNA

Pro K: Proteinase

PrxIV: Peroxiredoxin IV

PT: Peptidyl-transferase

QSOX: Quiescin sulfhydryl oxidase

Ratio (390nm/460nm): The emission fluorescence intensity at 525 nm that is excited at 390 nm wavelength is divided by that is excited at 460 nm wavelength

Re: Reduced

RRL: Rabbit reticulocyte lysate

RT: Room temperature

roGFP: Reduction-oxidation sensitive green fluorescent protein

SDS: Sodium dodecyl sulfate

SDS-PAGE: Sodium dodecyl sulfate polyacrylamide gel electrophoresis

Sec: Selenocysteine

SECIS: Selenocysteine insertion sequence

SEPN1: Selenoprotein N

SRP: Signal recognition particle

SP cell: Semi-permeabilised cell

SPC: Signal sequence peptidase complex

TCEP: Tris(2-carboxyethyl)phosphine

TMX2: Thioredoxin-related transmembrane protein 2

tRNA: Transfer RNA

Trx: Thioredoxin

TrxR1: Thioredoxin reductase 1

TXNDC11: thioredoxin domain containing 11

UGT1: Glycoprotein glucosyltransferase 1

Untrans: Untranslocated

UPR: Unfolded protein response

UT: Untreated

UTP: Uridine triphosphate

UTR: Untranslated region

VKOR: Vitamin K epoxide reductase

VKORC1L1: Vitamin K epoxide reductase complex subunit 1-like protein 1

Chapter 1 Introduction

1.1 Protein biogenesis

In mammalian cells, most proteins in the secretion pathway and membrane proteins need to translocate into the endoplasmic reticulum (ER) to undergo a series of modifications to obtain their native and functional structure (Figure 1-1). The correctly folded proteins will be transported to the Golgi apparatus or other intracellular organelles and then finally trafficked to their target location. Misfolded proteins will be retained and identified by the ER quality control system and then translocated back to the cytosol and degraded by the ER associated degradation system (ERAD) (Sitia and Braakman, 2003). The whole process is called protein biogenesis (Hegde and Lingappa, 1999).

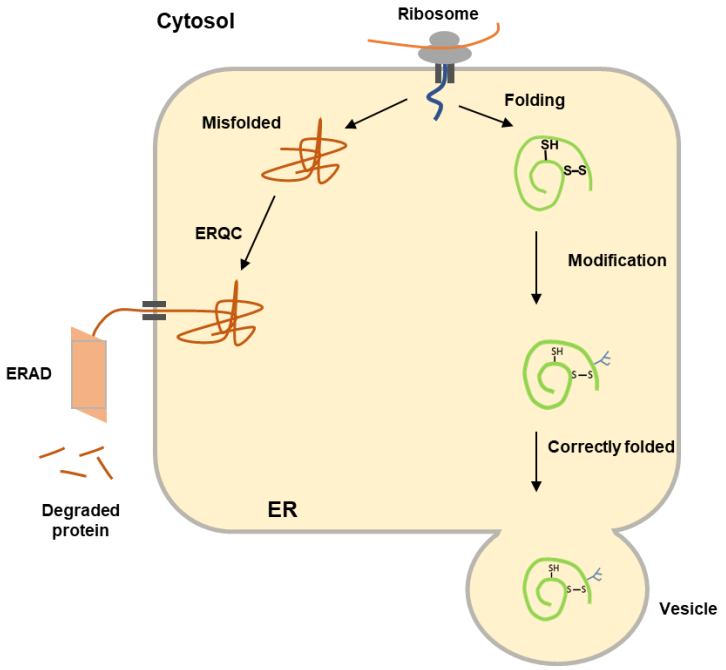

Figure 1-1 Protein biogenesis of membrane proteins and secretion proteins. The ribosome sits on the Sec61 translocon to support co translational translocation of the nascent chain into the ER lumen. After folding and modifications, the correctly folded proteins are delivered to the Golgi apparatus and other intracellular organelles by vesicular transport. Misfolded polypeptides are recognised by the ER quality control (ERQC) system and transported to the cytosol and finally degraded by the ER associated degradation (ERAD) ubiquitin-proteasome system (Sitia and Braakman, 2003).

1.2 Endoplasmic reticulum

The ER is a large membrane-enclosed cellular organelle which can be found in all eukaryotic cells (English and Voeltz, 2013, Kleizen and Braakman, 2004). The ER contacts with the plasma membrane, mitochondria, Golgi, endosomes, and peroxisomes at different sites. It is the entry site of the secretion pathway and plays crucial roles in protein synthesis and transport, protein folding, lipid and steroid synthesis, drug and carbohydrate metabolism and calcium storage (Lin et al., 2008, Schwarz and Blower, 2016). It has been demonstrated that a third of all proteins coded by human genome enter the ER where they undergo protein folding and modification to help them obtain their native structure and function (Braakman and Bulleid, 2011).

The ER can be divided into different domains, such as the nuclear envelope, peripheral tubular ER and peripheral cisternae which are required for different cellular processes (Figure 1-2) (English and Voeltz, 2013). The nuclear envelope is a double membrane bilayer surrounding the nucleus acting as a barrier that selectively controls the transporting of molecules in and out. The peripheral ER (peripheral tubular ER and peripheral cisternae) branches out from outer nuclear membranes as an interconnected network. The ER cisternae is generally localised closer to the nuclear envelope than ER tubules (Puhka et al., 2012). The peripheral tubular ER and peripheral cisternae is historically named smooth ER and rough ER due to the attachment of ribosomes (West et al., 2011). Compared with the ER tubulars, the cisternae has more ribosomes and a larger luminal volume to surface which is specialised for the protein folding process.

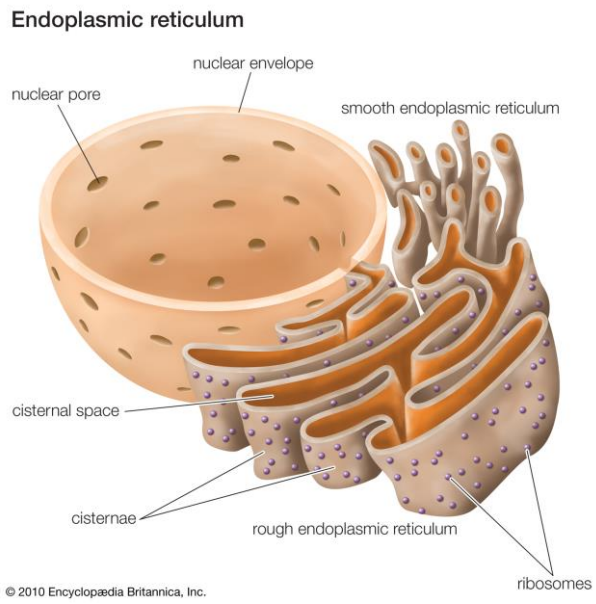

Figure 1-2 Structure of ER. ER is a continuous membrane system in all eukaryotic cells (Encyclopædia Britannica). It contains functionally and structurally distinct domains such as the nuclear envelope, peripheral tubular ER and peripheral cisternae which are required for different cellular processes, like the biosynthesis, processing, and transport of proteins and lipids. Due to the attachment of ribosomes, the peripheral tubular ER and peripheral cisternae are also named as smooth ER and rough ER. Figure obtained from (https: //www.britannica.com/science/endoplasmic-reticulum#/media/1/187020/114952).

a) Microsomes

ER derived microsomal membrane are universally used in *in vitro* protein biogenesis research. Microsomes are ER derived vesicles with a diameter of 100 – 200 nm which and are isolated from homogenates of liver and other tissues (Claude, 1943, Kriechbaumer, 2018) or cultured cells (Sukhodub and Burchell, 2005) by differential centrifugation (Figure 1-3). Microsomes are composed of rough ER, smooth ER and ribosomes. Numerous enzyme activities are associated with the microsomal fraction due to the chaperones and folding enzymes which are contained in the lumen of microsomes. The microsomes can still carry out protein synthesis, protein translocation, protein folding, and modifications as happens in intact cells (Palade and Siekevitz, 1956, Sabatini, 2014). Because the microsomes are RNA rich (Yamada et al., 1960), nuclease treatment of microsomes is performed to remove endogenous RNA before it is used in protein synthesis experiments (Robinson et al., 2017).

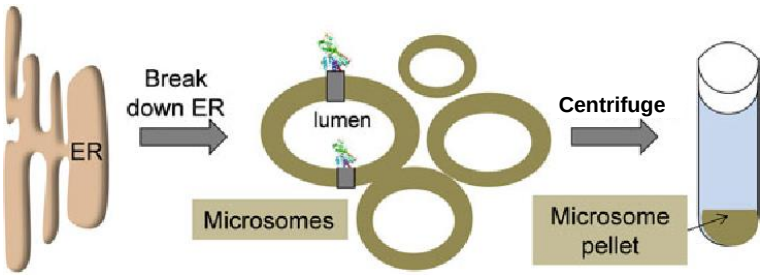

Figure 1-3 Schematic preparation of microsomes. Microsomes are prepared from ER by differential centrifugation. (Kriechbaumer, 2018)

b) Semi-permeabilised cells

The semi-permeabilised SP cells are prepared from cultured cells by treatment with the mild non-ionic detergent digitonin which was initially used in the nuclear protein import assay (Adam et al., 1990). The digitonin can permeabilise the membrane by creating pores in the plasma membrane by replacing cholesterol (Aits et al., 2015) (Figure 1-4). In eukaryotic cells, the cholesterol content differs in different membranes, such as 40-90% of total cellular cholesterol in plasma membrane (Liscum and Munn, 1999), but only 0.5% in ER membrane (Lange et al., 1999). The cholesterol content of the Golgi is lower than plasma membrane but higher than ER membrane in a cis-to-trans firection (Ikonen, 2018). The huge differences of cholesterol content between the plasma membrane and intracelluar membrane ensure the permeabilization of plasma membrane but leaves the membrane of the intracellular organelles, like ER and Golgi, intact if the incubation time and concentration of digitonin are accurately controlled (Figure 1-4) (Litvinov et al., 2018). It was proved that the digitonin treatment (concentration range 20-40 µg/ml) for 5 min on ice can permeabilise the plasma membrane but allow the ER and cis/medial-Golgi to retain their function and morphologically intactness (Plutner et al., 1992).

Subsequently, an efficient *in vitro* translational system using RRL with the addition of digitonin-permeabilised cells acting as an ER source was developed to study the *in vitro* protein biogenesis (Wilson et al., 1995). The SP cells are added into an *in vitro* translocation system like wheatgerm or RRL. The membrane and secreted proteins can be translated following the addition of an RNA template and the protein efficiently translocated, folded, and modified in the ER.

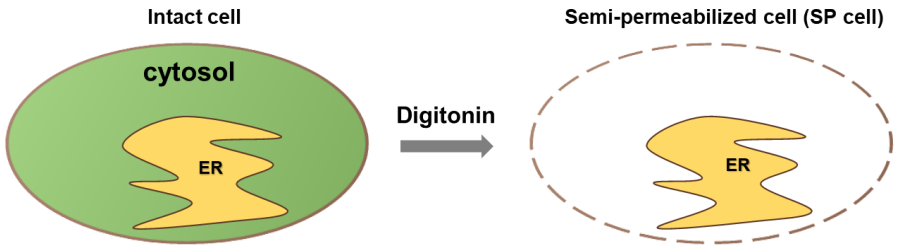

Figure 1-4 Schematic preparation of SP cells. The digitonin treatment can permeabilise the plasma membrane but leaving the membrane of intracellular organelle intact, like ER, Golgi apparatus.

1.3 Eukaryotic translation

a) *In vivo* translation

In eukaryotic cells, translation happens in the cytosol and the process of cytosolic translation contains four steps: initiation, elongation, termination and recycling (Figure 1-5) (Schuller and Green, 2018). The whole process of translation starts with initiation involving the formation process of an elongation-competent 80S ribosome complex. At least 9 eukaryotic initiation factors (eIFs) are involved to facilitate the formation of 80S ribosome complex (Jackson et al., 2010). During the initiation stage, the anticodon loop of initiator methionyl-tRNA (Met-tRNA ^{iMet}) base-pairs with the start codon (AUG) on the messenger RNA (mRNA) in the P site of 80S ribosome complexes, which is following by the elongation stage in a 5' to 3' direction.

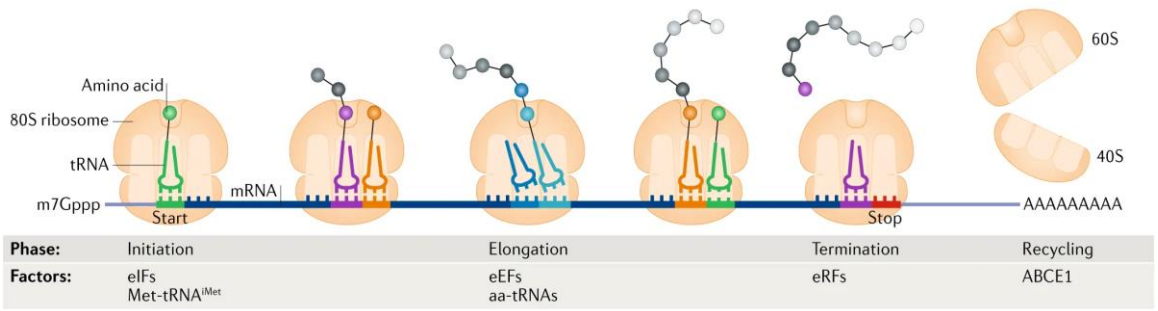

Figure 1-5 Translation in eukaryotic cells. In eukaryotic cells, translation happens in cytosol and the process of cytosolic translation contains four steps: initiation, elongation, termination and recycling (Schuller and Green, 2018).

Polypeptide is synthesised during elongation with the help of eukaryotic elongation factors (eEFs), aminoacyl-tRNAs (aa-tRNAs), and the peptidyl-transferase (PT) (Dever and Green, 2012). The anticodon of aa-tRNA recognises and pairs with the codon in the open reading frame (ORF) of mRNA in the ribosomal A site. A peptide bond forms between the α-amino group of aa-tRNA in A site and the carbonyl carbon of the peptidyl-tRNA (pp-tRNA) in the P site (Beringer and Rodnina, 2007). The reaction is catalysed by peptidyl-transferase (PT). The new peptide which is one amino acid longer is transferred into the A site. The deacylated tRNA and pp-tRNA are translocated to E and P site in the 80S ribosomal complex respectively. The deacylated tRNA is then released from the E site and a new cycle of elongation process will repeat with the exposure of a new codon in the ribosomal A site until the stop codon is exposed in A site (Schuller and Green, 2018).

In eukaryotes, the translation process stops when the stop codon (UAG, UAA and UGA) at the end of ORF is recognised in the ribosomal A site with the recruitment of eukaryotic release factors 1 (eRF1) and eukaryotic release factors 3 (eRF3) (Dever and Green, 2012). The eRF1 is also responsible for the hydrolysis of pp-RNA to release the nascent polypeptide (Alkalaeva et al., 2006). eRF3 promotes the activity of eRF1 by the interaction with eRF1 in the presence of GTP (Frolova et al., 1996).

After termination of translation, the ribosome complex is split into subunits (40S and 60S) that will be reused in the next cycle of translation, which is named the recycling process (Nurenberg and Tampe, 2013). This process links the successful termination process in the last translation and a new initiation process of next run of translation. In eukaryotic cells, the ribosome recycling needs an ATP energised factor, ATP-binding cassette (ABC) protein (ABCDE1) (Nurenberg-Goloub et al., 2018).

b) Cell-free protein synthesis

To study proteins structure and function, usually a large amount of homogeneous proteins is required. However, the overexpression of some toxic or membrane proteins *in vivo* can be harmful for cells and can disrupt protein homeostasis. As an alternative, cell-free protein synthesis (*cell-free translation*) has been

universally used in protein structure and function research in molecular biology due to its timesaving and easy-to-use features (Katzen et al., 2005, Chong, 2014).

The cell-free translation system was first established using lysate (extract) from *E. coli* by Marshall Warren Nirenberg (Nirenberg and Matthaei, 1961). Extracts from wheat germ (Roberts and Paterson, 1973) and rabbit reticulocyte lysate (RRL) (Pelham and Jackson, 1976) were then used to develop alternative cell free translation systems. These three kinds of lysates became the most popular lysates which are commonly used for cell-free translation. Recently, cell extracts from mammalian cells, like Hela cells (Mikami et al., 2006), have been used to develop a cell-free translation system with supplements of translation factors.

An efficient cell free lysate contents components for translation, such as ribosomes, tRNAs, amino acids (AA), enzymes and factors (Figure 1-6) (Katzen et al., 2005). Transcription products, mRNA, is added to the system to be the translation template. In addition, the template for cell-free translation can be DNA (plasmid DNA or PCR product) in a coupled cell-free transcription/translation synthesis system with the addition of RNA polymerase. Compared with in vivo translation, the conditions are easy to adjust and a variety of different reagents like protein disulfide isomerase (PDI) and chaperones can be supplemented to the cell free protein synthesis reactions to assist folding. The addition of ER derived microsomal membranes or SP cells allows the translocation from cytosol into ER lumen where glycosylation can occur, opening up more possibilities for protein research.

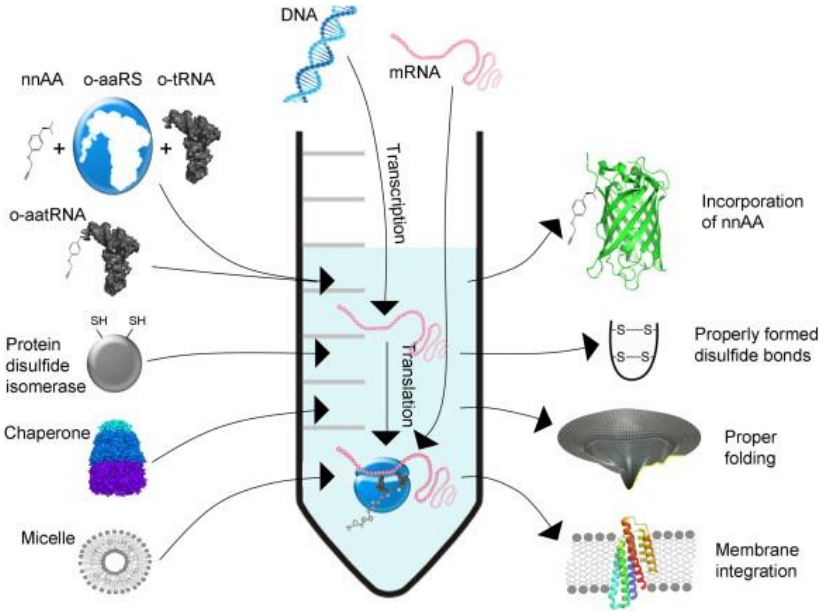

Figure 1-6 Cell-free translation system. Cell-free translation system has two forms: coupled (transcription and translation) cell-free protein synthesis which use plasmid DNA, or PCR product as template and uncoupled (only translation) that use the transcription product (mRNA) as template (Rosenblum and Cooperman, 2014).

1.4 Protein Translocation across ER membrane in eukaryotes

In eukaryotic cells, an indispensable step for secretory proteins and the majority of membrane proteins is their translocation from the cytosol to the ER lumen where protein folding and modifications can occur (Braakman, 2006). This process called protein translocation can be divided into two types: co-translationally and post-translationally that depends on whether the translocation happens at the same time with translation or after translation is completed (Figure 1-7) (Rapoport, 2007).

The newly synthesised polypeptides are translocated from the cytosol to the ER lumen by a protein-conducting channel named the Sec61 complex which is formed of three subunits, α , ß and γ (Rapoport et al., 2017). Two halves of α subunit form the pore of the Sec61 channel and the γ subunit is responsible for linking the two halves of α subunit while the dispensable ß subunit is attached to the periphery outside of the α subunit (Zimmermann et al., 2011). The Sec61 channel is a passive channel and the polypeptide can slide in or out of the channel in both directions which means that a driving force is necessary to ensure the right

direction of translocation of the nascent polypeptide chain. The driving force is provided by the translocation partners, ribosomes in co-translational translocation, the Sec62/63 membrane complex and the ER luminal chaperone BiP that is a member of Hsp70 ATPase family for post-translational protein translocation.

The co-translational translocation starts with the association of signal recognition particle (SRP) with signal sequence (7-15 residues) at the N-terminal of secretory proteins or the transmembrane sequence (TM) (≧20 residues) in the membrane proteins during translation at ribosomes (Figure 1-7A) (Rapoport et al., 2017, Halic and Beckmann, 2005). The SRP is then recognised by the signal recognition receptor (SRP receptor) and the ribosome interacts with the Sec61 channel (Luirink and Sinning, 2004). The growing polypeptide inserts as a loop into the Sec61 channel with translocation being driven by the elongation of translation and signal peptide cleavage. The nascent polypeptide chain is then released into the lumen after the translation is fully finished. For some membrane proteins, the certain segments do not insert to the channel rather they stay in the cytosol.

Post-translational translocation occurs when nascent polypeptide chains destined for the secretory pathway are not recognised by the SRP during their translation (Figure 1-7B) (Ng et al., 1996). These polypeptides need to remain in an unfolded, reduced state to ensure the successful translocation into the ER lumen. In this case, the signal sequence is targeted and bound to the Sec61 channel with the help of cytosolic chaperones. The polypeptide then inserts into the channel. The membrane complex Sec62/63 and ER luminal BiP (Hsp70 ATPase) interacts with the channel to facilitate the translocating process by a ratcheting mechanism to ensure the direction of polypeptide insertion (Deshaies et al., 1991, Panzner et al., 1995). Once the polypeptide is fully translocated into the ER lumen, the conversion from ADP to ATP allows the release of BiP (Matlack et al., 1999). The post-translational translocation process is then completed.

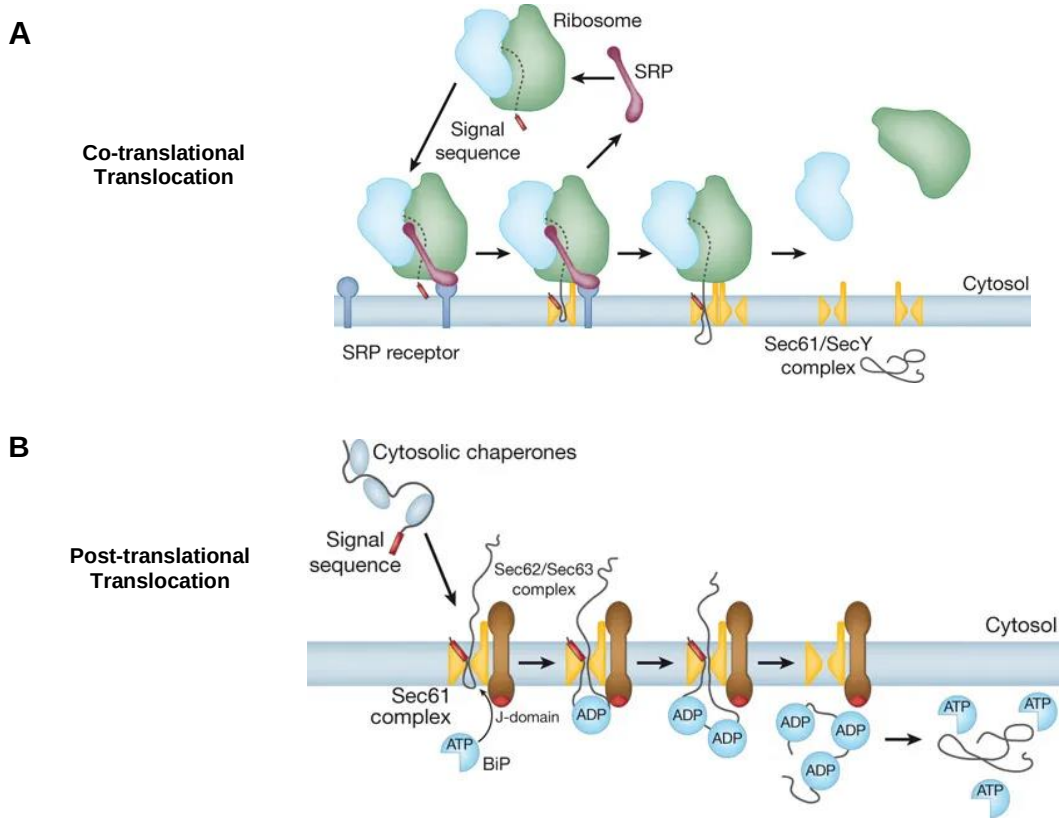

Figure 1-7 Models of eukaryotic protein co- and post- translational translocation. A. Co-translation translocation. The signal peptide of a nascent polypeptide chain is recognised by the signal recognition receptor (SRP receptor). The ribosome interacts with the Sec61 channel. The growing polypeptide inserts as a loop into the Sec61 channel with translocation being driven by the elongation of translation and signal peptide cleavage. The nascent polypeptide chain is then released into the lumen after the translation is fully finished. **B**. Post-translational translocation. The translation of the polypeptide is completed in the cytosol. The cytosolic chaperones maintain the nascent chain in the reduced state. With the facilitation of the cytosolic chaperones, the signal peptide is recognised by the Sec61 complex and inserted into the channel. The tetrameric Sec62/Sec63 complex and the ATP dependent ER luminal chaperone BiP ensure the correct direction of the translocation. (Rapoport, 2007)

1.5 Protein folding

It has been demonstrated that a third of all proteins coded by the human genome enter the ER to undergo protein folding and modification, which will allow these proteins to obtain their native structures and functions (Braakman and Bulleid, 2011, Braakman and Hebert, 2013). The nascent polypeptide chains are translocated into the ER with only correctly folded proteins transported to Golgi apparatus to be delivered to the cell surface or other cellular destinations. Misfolded proteins are retained in the ER and after being identified by the ER

quality control system, they will be retranslocated back to the cytosol to be degraded by the proteasome in a process called ER-associated degradation (ERAD). To ensure the efficiency of the protein folding and modification, the ER is highly specialised and it contains several chaperones, folding enzymes and co-chaperones to fulfil different tasks, like folding, assembly, modification, quality control and recycling (Braakman and Bulleid, 2011).

The protein folding process has two types: co-translational folding as protein folding process can occur during the synthesis process on ribosome-translocon complex, and post-translational folding which happens when the nascent polypeptide chain is released from ribosomes and fully translocated into ER lumen (Figure 1-8) (Ellgaard et al., 2016, Braakman and Hebert, 2013). It is worth noting that protein folding is a continuous process and there is no clear termination time point (Braakman and Bulleid, 2011).

Proteins folding begins once there is sufficient space (Braakman and Bulleid, 2011, Kleizen and Braakman, 2004). It has been demonstrated that the translocon complex can provide enough space for the formation of an α-helix, but the folding will be fully finished in the ER lumen (Woolhead et al., 2004). The newly synthesising polypeptide chain is surrounded by chaperones and folding enzymes in the ER lumen once it exits the translocon. The rate of co-translational folding is relatively slow because of the limited space of the protective environment which is shielded by the folding factors. The environment can separate nascent chains from each other to avoid the aggregation. Due to the rate of formation of the majority of secondary structures being faster than the rate of translation, the translational rate (4-5 residues/s in eukaryotic cells) can influence the rate of co-translational folding (Braakman et al., 1991).

In eukaryotic cells, post-translational folding predominates over co-translational folding (Ellgaard et al., 2016). This is due to the fact that it only takes ~ 2 min to synthesize an ~ 50-kDa protein (Influenza virus hemagglutinin (HA)), whereas the average half-time for protein folding is around 30 to 60 min (Braakman et al., 1991). In addition, a half of known structures of single-domain proteins and a lot of multidomain proteins have N- and C- proximity. This kind of folding cannot be completed until translation is fully terminated and the C-terminus of the nascent chain is released from the ribosome and translocon complex.

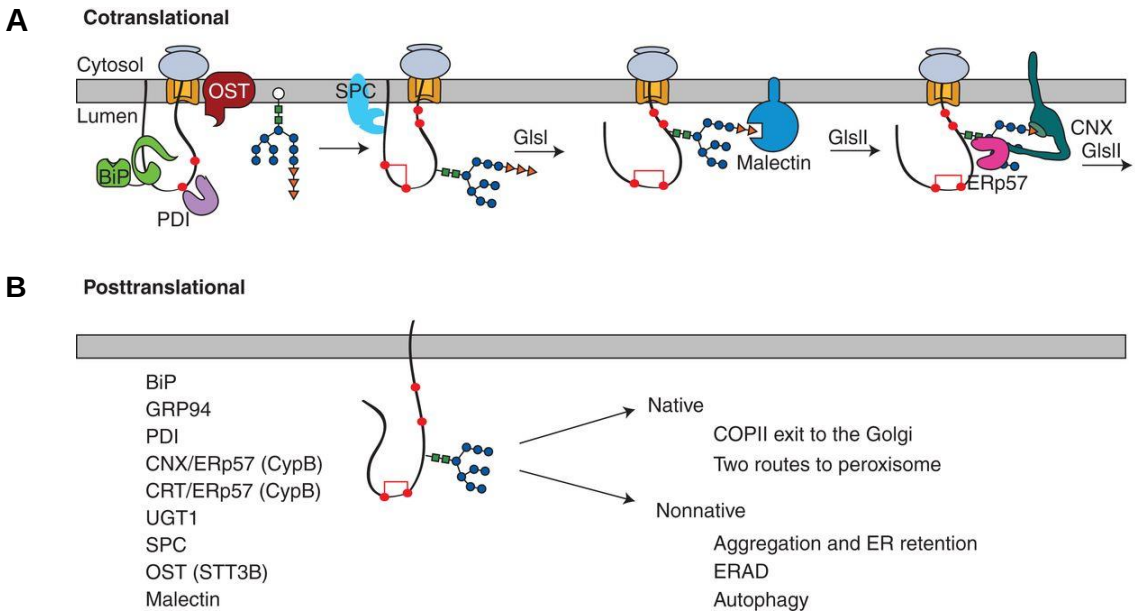

Figure 1-8 Co- and post-translational folding. **A**. The nascent polypeptide chain is synthesising by the ribosome (grey) and it is translocated into the ER lumen by Sec61 channel (orange) with the aid of BiP (green). Disulfides form with the assistance of PDI (purple). The glycans (three structure) is added to the Asn site on the newly synthesised polypeptide chain catalysed by oligosaccharyl transferase (OST). The N- terminal signal peptide is cleaved by signal sequence peptidase complex (SPC) (light blue). The terminal glucose residue (orange triangle) is removed from the N-linked glycan by the Glucosidase I (GlsI) and the nascent chain is bound to the membrane localised lectin, malectin (dark blue). The second glucose is removed by Glucosidase II (GlsII). The monoglucosylated glycan structure is bound to calnexin (CNX, green), a lectin chaperone associated with the oxidoreductase ERp57 (pink) until the last glucose is removed by Glucosidase II (GlsII). **B**. Co- and post- translational folding factors. These factors are involved in protein maturation and ER quality control processes. Calreticulin (CRT) is a soluble paralogue of calnexin, UGT1 is an UDP-glucuronosyltransferase. (Braakman and Hebert, 2013)

Protein folding during and after translation needs assistance from folding factors including folding enzymes and chaperones in the ER lumen. They work or are assumed to work (because of their homology with known folding factors) in complexes to affect the reactions during protein folding. Based on the folding steps that they catalyse and the intermediate they formed during protein folding, the protein folding factors are classified into different types: chaperones or co-chaperones (mainly heat shock proteins), peptidyl prolyl cis/trans isomerases (PPIases), oxidoreductases, and glycan-binding proteins (Braakman and Bulleid, 2011, Englander and Mayne, 2014). Some folding factors are multifunctional leading to overlapping functions between different folding factors. For instance, BiP is involved in translocation (Rapoport, 2007), regulation of unfolded protein

response (UPR) (Bertolotti et al., 2000) and stabilisation of folding intermediates (Fourie et al., 1994). In addition, PDI can catalyse the insertion of disulfide bonds (Bulleid and Ellgaard, 2011) and reduction of non-native disulfide bonds in misfolded proteins (Coe and Michalak, 2010). This overlapping function of protein folding factors ensures that the protein folding proceeds normally when one enzyme cannot function.

1.6 Protein modification

Protein modifications which can change the physical features of the polypeptide chain happen to the nascent polypeptide chain from the beginning of translation until the protein obtains its native structure and leaves the ER (Braakman and Bulleid, 2011, Braakman and Hebert, 2013). The well-known modifications include disulfide bond formation, N-linked glycosylation, proline hydroxylation. These modifications are crucial for protein folding, and the folding of the polypeptide chain can influence the modification.

1.6.1 N-linked glycosylation

In eukaryotic cells, N-linked glycosylation occurs when a block of 14 sugars, is co- or post-translationally added to a N-X-S/T sequon (N indicates Asparagine, S indicates Serine, T indicates Threonine, X can be any amino acid residue except proline) in the nascent polypeptide chain in the ER lumen (Helenius and Aebi, 2001, Ellgaard et al., 2016). The core of the glycan ($Glc_3Man_9GlcNAc_2$) is composed of three branches and is the precursor for glycosylation in the ER. The biogenesis of N-linked glycans includes three main steps: the synthesis of lipid-linked precursor, the core glycan is added to the asparagine residue in nascent polypeptide chain which is catalysed by the oligosaccharyltransferase (OST) enzyme complex, and the trimming of three glucose by glucosidase I and II and the removing of the terminal mannose by mannosidases in ER (Figure 1-9) (Helenius and Aebi, 2001, Aebi, 2013, Schwarz and Aebi, 2011). The glycans in the ER are relatively simple and homologous but they become more heterogenous after further modification in the Golgi apparatus.

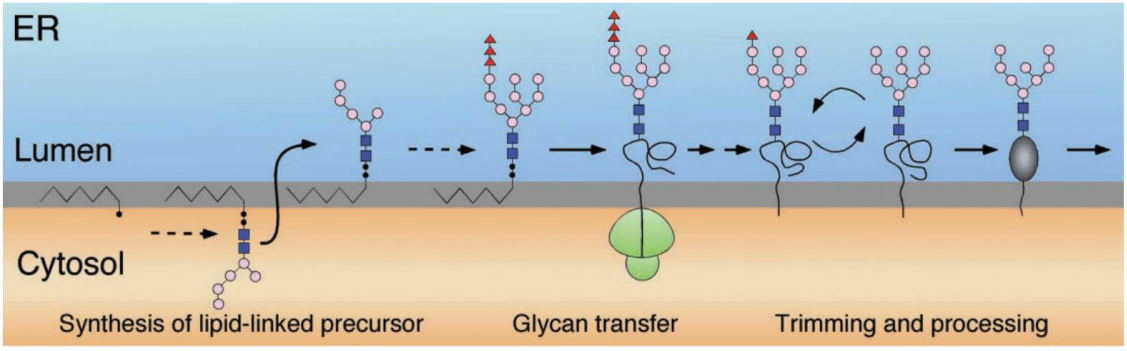

Figure 1-9 Schematic of N-linked glycosylation. The biogenesis of N-linked glycans includes three main steps: the synthesis of lipid-linked precursor, the core of glycan is added to the asparagine residue in nascent polypeptide chain which is catalysed by the oligosaccharyltransferase (OST) enzyme complex, and the trimming of three glucose residues by glucosidase I and II and the removal of the terminal mannose by mannosidases in ER. Triangle indicates glucose, circle indicate mannose, and square indicates N-acetyglucosamine (Helenius and Aebi, 2001)

Glycosylation has a significant effect on protein folding (Aebi, 2013). The addition of the glycan can stabilise the native structure of proteins by preventing the misfolding and aggregation of the nascent polypeptide chains. In addition, proteins with glycans are targeted to the calnexin/calreticulin (CNX/CRT) cycle. The interaction of CNX/CRT with a thiol oxidoreductase, ERp57, promotes protein folding: the correctly folded protein can leave ER while the misfolded protein enters another CNX/CRT cycle and is retained in the ER lumen. The misfolded glycoprotein is finally degraded by ERAD system also controlled by the N-linked glycan structure.

1.6.2 Disulfide bond formation and isomerisation

Disulfide bonds play important roles (Berkmen, 2012). First, disulfide bonds are essential for the stabilisation of protein structure and function of proteins. Second, disulfide bonds are important in the signalling of the redox environment by conformation change, like roGFP proteins. Third, disulfide bonds have functions in catalysis, like the disulfide bonds in oxidoreductases which can oxidise, reduce or isomerise their substrate proteins by accepting or donating electrons. Efficient disulfide bond formation commonly occurs in highly specialized compartments: the periplasm in bacterial (Collet and Bardwell, 2002), the mitochondria (Herrmann and Köhl, 2007) and the ER in eukaryotes (Tu et al., 2000).

a) In prokaryotes

The prokaryotic mechanisms of disulfide bond formation and isomerisation are relatively better characterised than eukaryotic (Berkmen, 2012).

In *E. coli*, the proteins containing disulfide bonds are secreted from the cytoplasm to the periplasm where disulfide bonds are formed, reduced and isomerised with the help of the Dsb system (Figure 1-10). Disulfide formation in the substrate protein is catalysed by DsbA protein via disulfide exchange with the oxidised active sites (CXXC) in DsbA (Bardwell et al., 1993). After the disulfide bond exchange with the substrate protein, the reduced DsbA is reoxidised by membrane protein DsbB to its active oxidised state (Kadokura et al., 2003). The electrons are finally donated by DsbB to ubiquinone (UQ) or menaquinone (MQ) during aerobic or anaerobic respiration. Because the DsbA tends to co-translationally oxidise adjacent cysteines in growing polypeptide chain (Kadokura et al., 2004), proteins which do not need consecutive disulfides bonds are misfolded. These mis-folded proteins will be degraded or isomerised to their native state.

Any non-native disulfide bonds formed during the oxidation process are corrected to their oxidised state by DsbC (Figure 1-10) (Shevchik et al., 1994). The reduced state of the active site in DsbC is maintained by the membrane protein DsbD to which the electron is ultimately received from cytoplasmic NADPH via thioredoxin (Trx) (Rietsch et al., 1997).

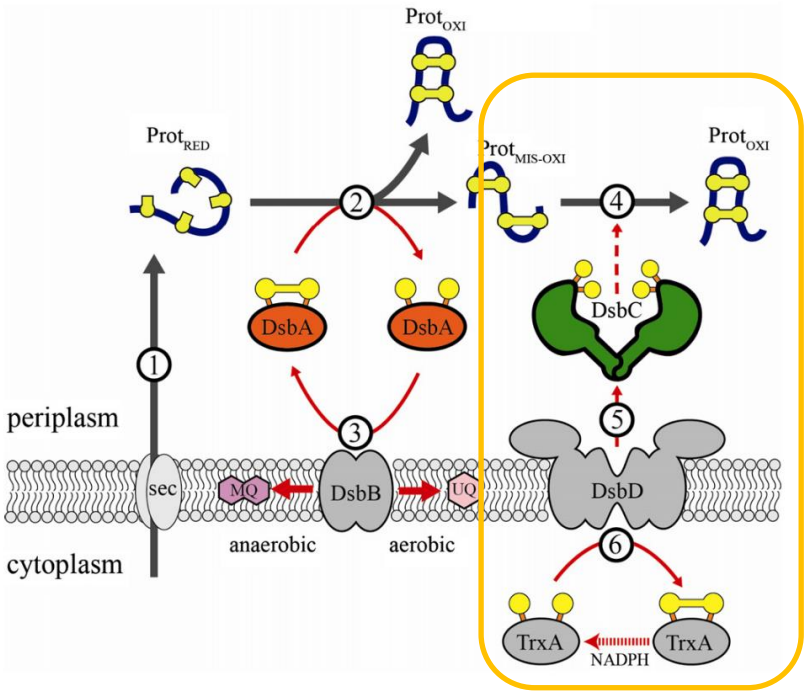

Figure 1-10 Disulfide bond formation and isomerisation in bacterial periplasm. Disulfide formation process (①②③); Disulfide isomerisation process (④⑤⑥), in yellow box. ① Translation, Sec, translocon Sec61; ② Disulfide formation by the disulfide shuttle with DsbA, Prot $_{RED}$, reduced state of protein, Prot $_{OXI}$, oxidised protein with correct disulfide bonds, Prot $_{MIS-OXI}$, protein containing non-native disulfide bonds; ③ Reoxidisation of DsbA by DsbB, MQ, menaquinone, UQ, ubiquinone; ④ Isomerisation of the non-native disulfide bond by DsbC; ⑤ The reduced state of DsbC is maintained by membrane protein DsbD; ⑥ DsbD accepts the electron from the ultimate electron donor, cytoplasmic NADPH, via a cytoplasmic thioredoxin (TrxA system). The protein containing non-native disulfide bonds (Prot $_{MIS-OXI}$). Disulfide formation process (①②③); Disulfide isomerisation process④⑤⑥. (Berkmen, 2012)

b) In mammalian cells

In mammalian cells, disulfide bonds are formed between two free cysteine and they can be formed in both ER and mitochondrial intermembrane space (IMS) but in different mechanisms (Riemer et al., 2009b).

The introduction of disulfide bond in IMS rely on two important proteins mitochondrial intermembrane space import and assembly protein 40 (MIA40) (Chacinska et al., 2004) and FAD-linked sulfhydryl oxidase ERV1 (ERV1) (Mesecke et al., 2005). In this MIA40-Erv1 oxidation system, the oxidised MIA40 can insert disulfide bond into the polypeptide chain and then will be reoxidised by the Erv1 which can pass the electron to FAD (Mordas and Tokatlidis, 2015).

Unlike mitochondria, the ER is highly specialised for disulfide bond formation and reduction in two important aspects: the redox buffer consisted by reduced tripeptide, glutathione (γ-L-glutamyl-L-cysteinylglycine) (GSH) and its oxidised form (GSSG) which directly or indirectly involved in the disulfide bond formation and isomerisation process (Chakravarthi et al., 2006) and enzymes which facilitate disulfide formation and isomerisation, like PDI (Ellgaard and Ruddock, 2005). In the ER, disulfide bonds are inserted by a disulfide exchange mechanism with the oxidised form of PDI (Figure 1-11). The introduction of disulfide bonds potentially results in either native or non-native linkages. We can find native disulfide bonds in the final correct structure of proteins whereas the non-native disulfide need to be removed before the protein can fold correctly or be targeted for degradation. The reduced form of PDI can isomerise the non-native disulfide bonds by disulfide exchange with substrate protein (Figure 1-11) (Bulleid and Ellgaard, 2011). The disulfide formation pathways are relatively more well-characterised than the pathway for disulfide isomerisation (Bulleid and Ellgaard, 2011).

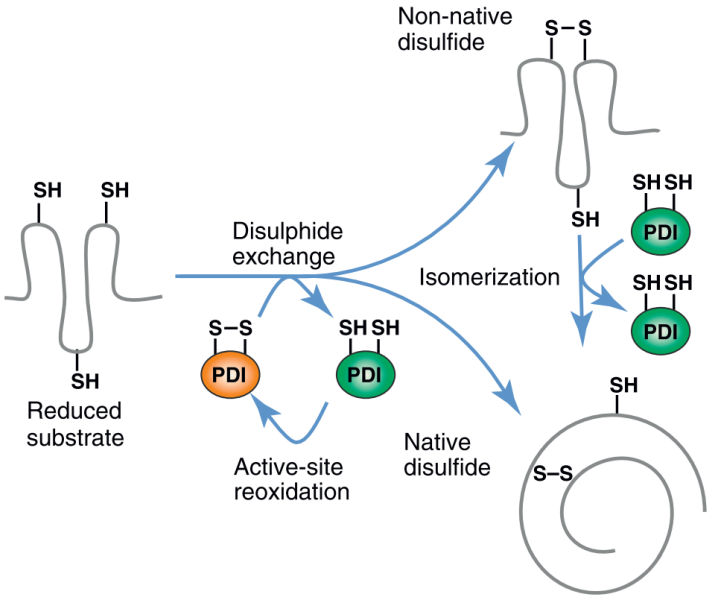

Figure 1-11 Disulfide formation and isomerisation. The disulfide bonds are inserted by disulfide exchange with the oxidised form of PDI. The introduction of disulfide bonds may result in native or non-native disulfides. The reduced form of PDI can isomerise the non-native to native disulfide. (Bulleid and Ellgaard, 2011)

Each PDI member contains one or more thioredoxin domains (CXXC) where the disulfide bonds are shuttled from the oxidised form of the CXXC motif to the dithiol in the substrate proteins. The disulfide transfer from the PDI to their client

protiens will reduce the active sites of the CXXC motif which have to be oxidised later for the next disulfide exchange with the client proteins in the future. At least 5 pathways were identified as the potential pathways which contribute to the *in vivo* disulfide formation in ER (Figure 1-12) (Bulleid and Ellgaard, 2011). These pathways are named by their key enzyme(s): ERO1 pathway (Frand and Kaiser, 1999, Tu and Weissman, 2004), peroxiredoxin (PRDX) 4 pathway (Tavender et al., 2010, Zito et al., 2010), glutathione peroxidase (GPX) 7 and GPX8 (Nguyen et al., 2011), quiescin sulfhydryl oxidase (QSOX) (Kodali and Thorpe, 2010), and vitamin K epoxide reductase (VKOR) pathway (Schulman et al., 2010).

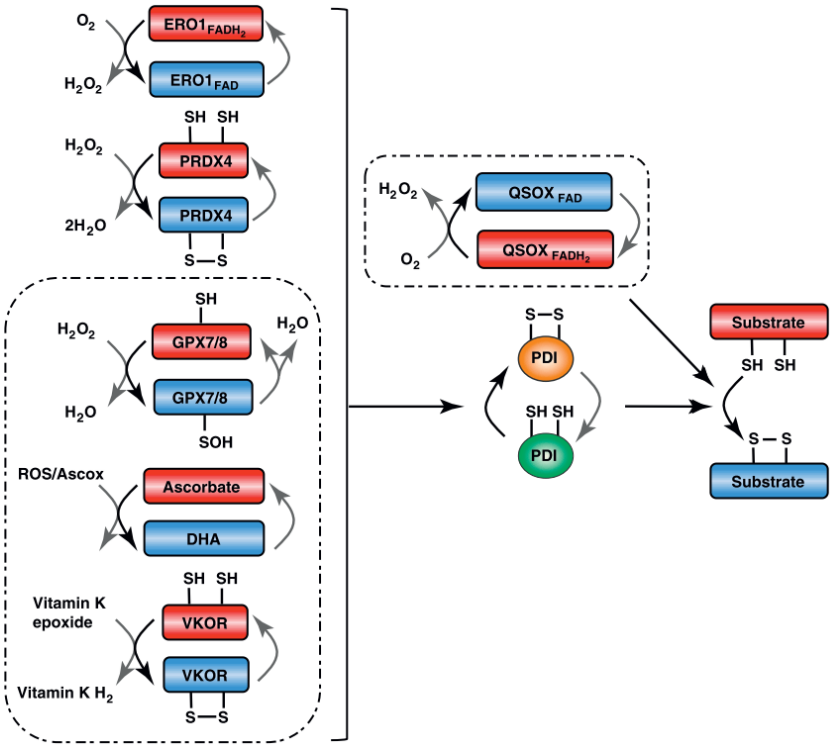

Figure 1-12 Disulfide formation pathways *in vivo*. The insertion of disulfide bonds is catalysed by PDI family. After the disulfide exchange with the substrate protein, the active sites of CXXC motif are reduced. The reduced active sites need to be reoxidised to catalyse further disulfide formation reactions. Several potential pathways, ERO1 pathway, PRDX 4 pathway, GPX 7/8 pathway, and VKOR pathway, have been identified as the potential disulfide bond formation pathways. ERO1 and QSOX sulfhydryl oxidases that introduced disulfide bond to the substrate protein via the oxidation $FADH_2$ and the electron was finally passed to the O_2 (QSOX can directly introduce disulfide bond into the substrate not via PDI). PRDX4 result in disulfide bonds by the oxidation of sulfenic acid coupling with the metabolisation of H_2O_2 (Tavender and Bulleid, 2010). GPX7/8 can also oxidise PDI by reducing the H_2O_2. DHA can accept electrons to produce ascorbate. VKOR participate the formation of disulfide via the reduction of vitamin K. In the dash box, the enzymes are hypothesised to contribute for the disulfide formation process with *in vitro* experiments, but which did not show *in vivo* evidence (Bulleid and Ellgaard, 2011). By 2012, *in vivo* evidence showed that the VKOR

contribute disulfide formation (Rutkevich and Williams, 2012). The reduced form is shown in blue and oxidised form is indicated in red color.

Like what happened in prokaryotes, non-native disulfide bonds that are contained in proteins in mammalian cells can prevent correct folding and post-translational modification processes leading to misfolding and protein aggregation. They must be reduced/isomerised to allow correct native-disulfides to be formed again (Kosuri et al., 2012). In bacterial periplasm, the non-native disulfide is isomerised by the DsbCD system (Figure 1-10). There must be similar systems in the ER ensuring the reduction and isomerisation of the non-native disulfide bonds.

It has been shown that PDI family members can reduce or isomerise the non-native disulfides by dithiol-disulfide exchange with client protein in the ER. PDI member is characterised by the presence of Trx homologous domain and at least 17 PDI family members have been identified (Ellgaard and Ruddock, 2005, Kozlov et al., 2010). One PDI family member, ERp57, is required for the correct folding of glycoproteins (Jessop et al., 2007). Another PDI member, ERdj5, has been shown to promote the degradation of proteins with non-native disulfide bonds (Ushioda et al., 2008). This indicates that other PDI family members are likely to be involved in the reduction pathway of non-native disulfides. The reduction function is dependent on the reduced state of the active sites of PDI family member. How the PDIs are reduced after the reduction of substrates is still to be addressed. It is not clear whether the electron is delivered from cytosol or ER lumen.

Two hypotheses are raised based on the link between the reduction of the disulfide bonds inside the ER lumen with the cytosolic electron donor NADPH by a reduced and oxidised glutathione system (GSH and GSSG) or a cytosolic thioredoxin/ thioredoxin reductase (Trx/TrxR) system (Figure 1-13) (Bulleid and van Lith, 2014). In the hypothetic reductive pathway constituted by glutathione and glutathione reductase, the reduction of the active sites in PDI are coupled with the oxidisation of GSH. It is unknown how the GSH is recycled from GSSG in the ER lumen. It is possibly directly reduced by an ER-localised glutathione reductase or the GSSG is reduced by a cytosolic GSH reductase and then transported back to the ER lumen (Figure 1-13 A). In the hypothetic reduction model of PDI mediated by thioredoxin reductase (TrxR), the reduction of the

active sites in PDI is driven by an ER-localised or a cytosolic thioredoxin reductase (Figure 1-13 B). The ER-localised TrxR and the membrane protein which can shuttle electrons from the cytosol to ER lumen is unknown. Recently, a study in our group demonstrated that the addition of G6P can recycle NADPH which is required for the reduction of Trx by TrxR and the robust cytosolic Trx/TrxR pathway is necessary for the correct disulfide bond formation suggesting a link between the cytosolic electron donor and the ER electron acceptor (Poet et al., 2017). However, how the electron is transferred into the ER is unknown. Whether other components are needed in this reductive pathway and whether a membrane protein which can transfer the electron from the cytosol into the ER lumen remain to be addressed.

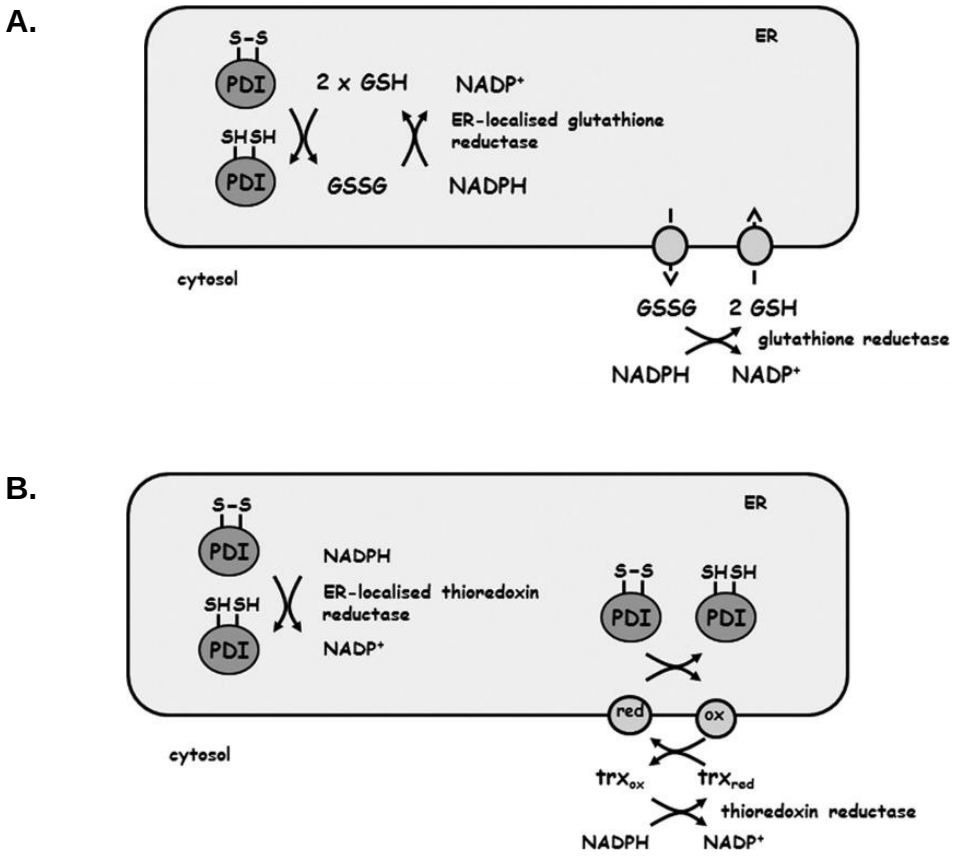

Figure 1-13 Potential ER reductive pathways of non-native disulfide bonds. **A**. Hypothetic reduction model of PDI by glutathione (GSH). GSSG, oxidised glutathione. **B**. Hypothetic reduction model of PDI mediated by thioredoxin reductase (TrxR). (Bulleid and van Lith, 2014)

1.7 Protein disulfide isomerase

Protein disulfide isomerase (PDI) is a soluble 55-kDa ER-localised proteins which has been considered a multifunctional enzyme (Parakh and Atkin, 2015).

PDI contain four domains: a, b, b', and a' domain (Pirneskoski et al., 2001) plus an signal peptide, an acidic C terminal extension c and an ER retention sequence (K/H)DEL (Norgaard et al., 2001). The a and a' domains are thioredoxin (Trx) homologues which have catalytic motif sites CXXC. Through thiol change, they can act as simple thiol: disulfide oxidoreductases. The b and b' domains do not have Trx-like catalytic motifs. Thus, they cannot catalyse disulfide exchange reactions like a and a' domains, but these two domains are the sites where substrate proteins bind. The full function of PDI needs the cooperation of all domains (Darby et al., 1998).

PDI are multifunctional enzymes (Wilson et al., 1998). They can catalyse the formation, reduction and isomerisation of disulfide bond in the ER compartment, which is critical for the efficient and correct folding of secreted and membrane proteins in the mammalian cells (Zheng and Gilbert, 2001). PDI can act as one subunit of prolyl 4-hydroxylases (P4H) which is essential for collagen synthesis (Kivirikko and Myllyharju, 1998) and PDI can associate with the M subunit to form an heterodimer, microsomal triglyceride transfer protein (MTP) that is responsible for lipid transfer (Hussain et al., 2012, Wetterau et al., 1990). In addition, the PDI is also a molecular chaperone. It was suggested that the PDI participates in protein preparation for ERAD as an redox state dependent chaperone (Molinari et al., 2002).

1.7.1 ERp57

ERp57, also named as glucose-regulated protein 58 (GRP58), ER-60, Q2, ERp58, ERp61, and 1,25D3-MARRS, is a multifunctional member of PDI family in the ER (Turano et al., 2011). This protein is coded by the PDIA3 gene which localised on chromosome 15. It contains 505 amino acids and the structure of ERp57 can be divided into four domains: a domain, b domain, b' domain and a' domain (Pirneskoski et al., 2001). The a and a' domain have thioredoxin (Trx) homologous

sequence with CXXC active site motifs. As these are redox active sites, the ERp57 has oxidoreductase function. The b and b' domains do not contain trx-like redox active sites, thus they cannot catalyse redox reactions. The four domains in ERp57 form a U-shape conformation where the a and a' domains come close to each other in order to interact with substrate proteins and the b and b'domain can bind with the calreticulin or its membrane-bound homologoue calnexin to facilitate the function of a and a' domains (Pirneskoski et al., 2001).

ERp57 is involved in glycosylated protein folding and quality control process in the ER in association with calreticulin or calnexin (Oliver et al., 1997, Frasconi et al., 2012). The ERp57 can promote the formation of disulfide bonds and also isomerise the misformed disulfide bonds (Oliver et al., 1997, Bulleid, 2009). It was also demonstrated that the ERp57 participitates in the assemble of major histocompatibility complex class 1 (MHC1) where it forms a complex with tapsin to ensure fidelity of peptide loading (Peaper et al., 2005). Besides, this protein can play a role as a chaperone in prevention of protein aggregation (Castillo et al., 2015). To ensure its normal function, the redox state of ERp57 should be regulated. In intact Hela cells, the ERp57 is mostly in a reduced form (Mezghrani et al., 2001). After catalysing disulfide bond reduction, it remains unclear how the cell reduces the oxidised ERp57 in the ER.

1.7.2 ERdj5

ERdj5 is the largest PDI family member and is particularly abundant in cells optimised for secretion (Adams et al., 2019, Cunnea et al., 2003). ER stress can induce the transcription of ERdj5. ERdj5 contains, a N-terminal DnaJ domain that can interact with BiP via adenosine triphosphate (ATP)-dependent cycle; 6 thioredoxin domains, 4 with redox active CXXC motifs; and a C-terminal ER retention KDEL motif (Figure 1-14 Domains of mouse ERdj5.Figure 1-14) (Ushioda et al., 2008, Hagiwara et al., 2011). The six thioredoxin domains in ERdj5 are divided into two cluster and the thioredoxin domain 3 and 4 in the C-terminal cluster are responsible for the reductase function (Hagiwara et al., 2011).

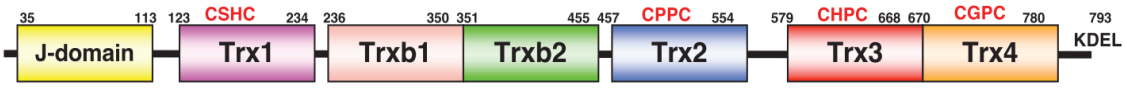

Figure 1-14 Domains of mouse ERdj5. It contains thioredoxin domains with active redox sites (CXXC motifs), a DnaJ domain and a C-terminal KDEL motif. (Hagiwara et al., 2011)

Envidence showed that ERdj5 can reduce several other PDI family members and it can not be reduced by the PDI members (Riemer et al., 2009a), because ERdj5 has one Trx domain which is lower than the other PDI family member suggesting that the ERdj5 function as a reductase (Hagiwara et al., 2011).In addition, ERdj5 can prevent multimer formation and reduce non-native disulfide bonds in misfolded glycosylated proteins recognised by ER degradation-enhancing a-mannosidase-like protein 1 (EDEM1) (Htm1/Mnl1p in yeast) and facilitate the retrotranslocation of the ERAD substrate proteins in association with the chaperone BiP in an ATP-dependent manner (Ushioda et al., 2008, Hagiwara et al., 2011). A remaining question is how ERdj5 receives its reducing power.

1.8 ER quality control system

In mammalian cells, secreted proteins and membrane proteins need to enter the ER lumen to attain their correct folding and modification to obtain their native function. Because misfolded proteins will disrupt protein homeostasis and form aggregates which could have cytotoxic effects on cells, there is an ER quality control system to evaluate and determine the structural integrity of proteins (Hurtley and Helenius, 1989, Adams et al., 2019). The proteins with native structure will pass the quality control system and be transported to the Golgi apparatus or other cellular destinations. The ER can also recognise misfolded proteins and try to retain and repair them in the ER lumen. If not, the proteins with non-native structures will be delivered back to the cytosol and degraded by the cytosolic ubiquitin-proteasome system (McCaffrey and Braakman, 2016).

The ER quality control is supported by many different ER localised factors. They are divided into three main groups (Adams et al., 2019). First category is the classical molecular chaperone systems, including different heat shock families (Hsps), like Hsp 70 (also named BiP and GRP 78) (Schlecht et al., 2011, McCaffrey

and Braakman, 2016). It has been shown that ATP-dependent BiP can prevent the misfolding of nascent polypeptide during translocation and is required to regulate the unfolded protein response (UPR) (Johnson et al., 2013). The second category is the glycan-dependent molecular chaperone systems, such as glycoprotein glucosyltransferase 1 (UGGT1) (Sousa and Parodi, 1995), calnexin and calreticulin. These group of factors facilitate the quality control of glycosylated proteins and decide on the retention or exportation of glycoproteins (Caramelo and Parodi, 2015). The third category is thiol-dependent oxidoreductases including different PDI family members (more than 20 members) like ERp57, ERdj5, and ERp44 (Anelli et al., 2003). PDIs catalyse the oxidation, reduction, and isomerisation of disulfide bonds via the catalytic CXXC motif sites to promote proper folding of the substrate protein. The various factors work together to maintain protein homeostasis in ER.

The accumulation of proteins which fail to obtain their native structure in the ER membrane and ER lumen (misfolded and mutated proteins) can break protein homeostasis and cause ER stress that can result in cell death. The clearance of these harmful proteins is achieved by the ERAD pathway (Olzmann et al., 2013). ERAD is a complicated process which can be divided into different steps: recognition, retrotranslocation, ubiquitylation, and degradation (Figure 1-15) (Olzmann et al., 2013, Ruggiano et al., 2014). The misfolded proteins are first recognised as ERAD substrates by molecular chaperones and lectins and subsequentially retrotranslocated to the cytoplasm. The cytosolic side of the membrane protein and misfolded secreted proteins are ubiquitinylated, by the attachment of ubiquitin (a 76 amino acids proteins) (Figure 1-15). The ubiquitination is catalysed by a membrane-associated ubiquitin ligase (also named E3 ligase) via an ATP-dependent process. These substrate proteins are then released in the cytoplasm and degraded by the proteasome.

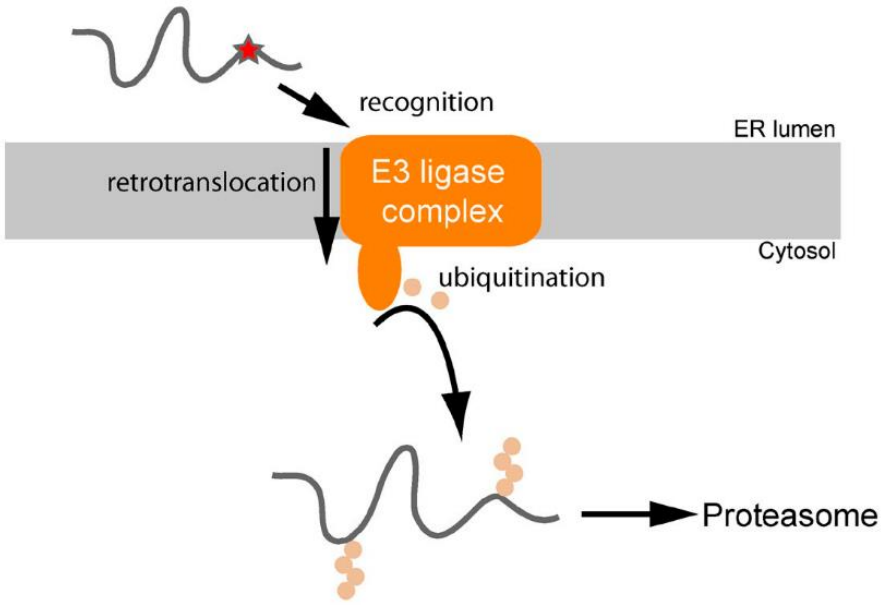

Figure 1-15 Key Steps in ERAD. ERAD is a complicated process which can be divided into different steps: recognition, retrotranslocation, ubiquitylation, and degradation. The different steps in ERAD process are coordinated by the ubiquitin ligase complex (also called E3 ligase complex). (Ruggiano et al., 2014)

1.9 Membrane transport

The ER is formed by a continuous lipid bilayer membrane which relates to the nuclear envelope. Thus, the ER lumen is completely enclosed and disconnected with the cytosol. However, cytosolic processes are essential for numerous enzyme activities in the luminal of the ER, such as the metabolism of carbohydrate and steroid, biotransformation, and protein folding and modification (Csala et al., 2007).

The ER membrane is selectively permeable (Figure 1-16) (Bruce Alberts, 1994, Yeagle, 2016). Different molecules pass the membrane at different speeds. Water can cross the membrane through a specific water channel called aquaporins by passive diffusion (Stillwell, 2013). Some small molecules, like O_2, and CO_2, can pass the membrane directly at a high speed (simple diffusion). Larger molecules, such as glucose, can cross the membrane with the facilitation of a transporter protein at a slower speed (passive or active transport) and some large proteins cannot pass through the membrane at all. The transport rate of certain substrates is the rate-limiting step for certain enzyme activities in the ER lumen. Hence, it

is important to identify the ER membrane protein involved in the transportation process. Only a limited number of membrane proteins involved in the transportation process are identified. Most membrane proteins that facilitate molecule transport are yet to be identified with better and more developed technologies. Based on the previous research in our group, it was shown that the ultimate electron donor of the disulfide formation in the ER is cytosolic NADPH indicating a pathway linking the cytosol and ER lumen (Poet et al., 2017). We assumed that an ER membrane protein is likely involved in the ER reductive pathway for the transportation of the electron.

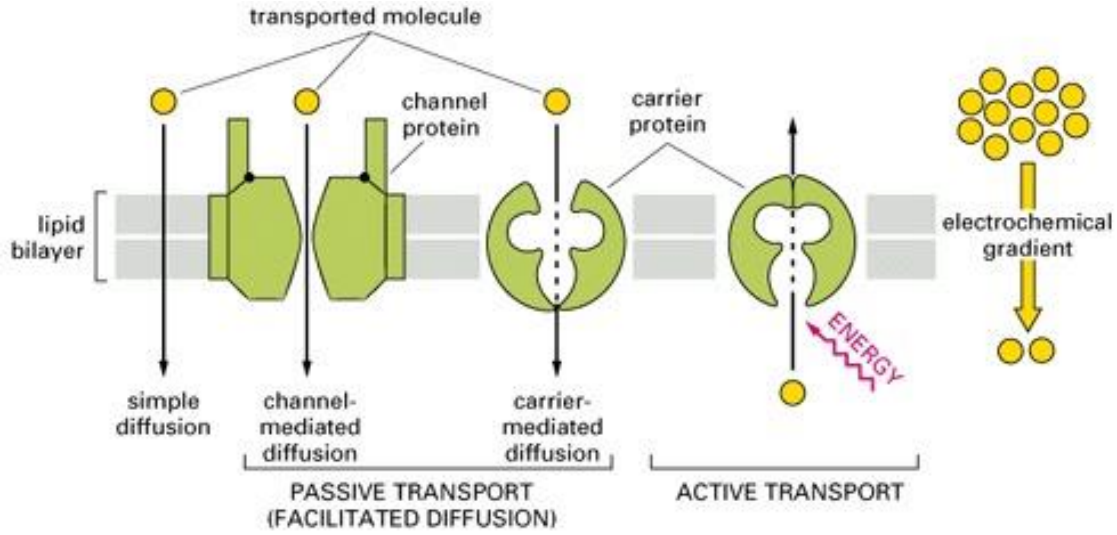

Figure 1-16 Different membrane transport. A molecule can cross the lipid bilayer membrane by simple diffusion or by diffusion in the absence or the presence of facilitation of the channel or carrier proteins following the electrochemical gradient (passive transport). On the contrary, the transport of a molecule against the electrochemical gradient needs energy and carrier protein (active transport). (Bruce Alberts, 1994)

1.9.1 Lipase maturation factor 1

Lipase maturation factor 1 (LMF1) is an ER membrane-bound protein (Doolittle et al., 2010). It has been shown that LMF1 is essential for folding and assembly of lipases, such as lipoprotein lipase (LPL), hepatic lipase (HL) and endothelial lipase (EL). Instead of playing a role at the transcription level, LMF1 is involved in the post-translational maturation process of these secreted lipases. The mutation of LMF1 results in the deficiency of lipase (LPL, HL and EL) and disrupts lipid homeostasis in mice and humans (Peterfy, 2012).

The LMF1 contains 5 transmembrane segments and 6 domains (Figure 1-17) (Doolittle et al., 2010). N-terminal domain, loop B domain and loop D domain are in the cytoplasm. The loop A, loop C and C-terminal domain are in the ER lumen. The function of each domain in LMF1 has not been clearly clarified except loop C domain and the C-terminal domain. The highly conserved loop C domain (CLD) can specifically bind with homodimer lipases like LPL, HL and EL rather than pancreatic lipase (PL), a monomer lipase. The C-terminal domain was demonstrated to play a critical role in lipase maturation. The mutations at the CLD, Y439X and W464X sites cause significant activity loss of LMF1 in lipase maturation that can result in severe human hypertriglyceridemia (Peterfy et al., 2007, Cefalu et al., 2009). A recent study suggests that the LMF1 plays a critical role in the ER redox state homeostasis and reduction of non-native disulfides (Roberts et al., 2018). It is unknown if the LMF1 can shuttle electrons from the cytosol to facilitate reduction of non-native disulfide bonds in the ER lumen.

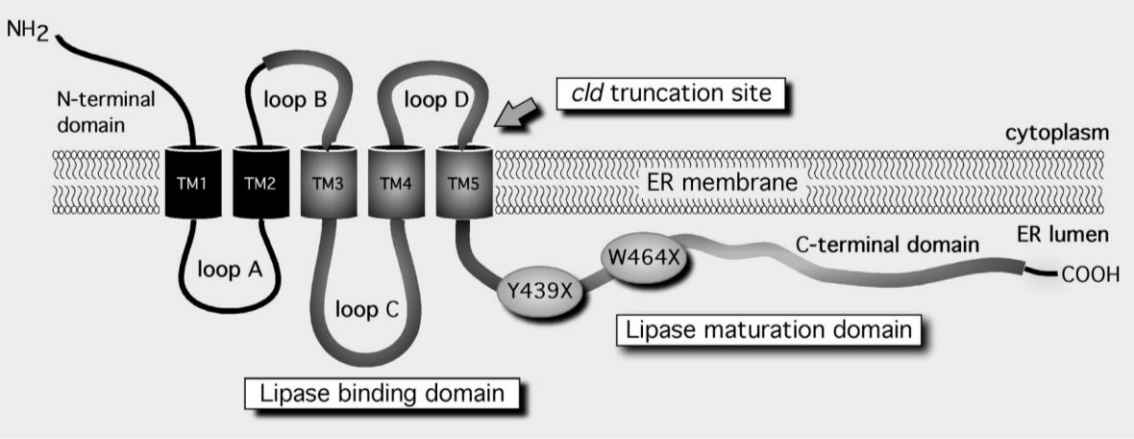

Figure 1-17 Structure of ER transmembrane protein, LMF1. There are five transmembrane segments in LMF1 that divide the protein into six domains. The loop C domain is the binding site of homodimer lipases like LPL, HL and EL. The C-terminal domain is where the lipases achieved their post-translational maturation. The mutation of *cld*, Y439X and W464X can cause the failure of the lipase maturation. (Doolittle et al., 2010)

1.9.2 Selenoprotein N

In the human proteome, there are 25 selenoproteins (Kryukov et al., 2003). The rare amino acid selenocysteine (Sec) is added to the selenoproteins co-translationally in response to a stop codon (UGA codon) (Schweizer and Fradejas-Villar, 2016). The mRNA of selenoproteins in bacteria contains a selenocysteine

insertion sequence (SECIS) element following the UGA codon in the opening reading frame, whereas, in eukaryotes, the SECIS element is localised in 3' untranslated region (UTR) and the addition of the Sec needs SECIS-binding proteins. The known selenoproteins, like glutathione peroxidase 1 (GPx1), thioredoxin reductases (TrxR) and methionine sulfoxide reductase (MsrB1), have been found in oxidoreductase reactions that are essential for redox state homeostasis and antioxidation. The selenoproteins are either directly or indirectly related to calcium homeostasis and ER Stress (Pitts and Hoffmann, 2018).

Selenoprotein N (SEPN1) is a member of selenoprotein family, that is encoded by *SEPN1* gene. This protein is a 70 kDa ER resident transmembrane glycosylated protein which contains one Sec (Petit et al., 2003). The SEPN contains a redox active motif (S-C-U-G) which is similar with the redox active motif CXXC in TrxR. It suggests that the SEPN can potentially act as a oxidoreductase (Pitts and Hoffmann, 2018). The mutation of SEPN1 results in muscular dystrophy that suggests its critical role in maintaining the redox state in the skeletal cell (Moghadaszadeh et al., 2001). It is shown that the SEPN1 is also involved in ER redox as an ERO1 inhibitor and calcium homeostasis with interaction with ER calcium sarcoplasmic reticulum Ca^{2+} ATPase (SERCA2) import pump (Marino et al., 2015). SEPN1 is another potential candidate ER membrane protein that links the cytosol and ER lumen reductive pathway for non-native disulfide bond reduction.

1.10 Green fluorescence protein

The green fluorescence protein (GFP) which was first found in a jellyfish, *Aequorea Victoria*, (Johnson et al., 1962, Shimomura et al., 1962) and there are now hundreds of GFP variants that have been developed (Pedelacq, 2019). Currently, they are widely used as a reporter and protein labels, such as pH indicator (Miesenböck et al., 1998, Hanson et al., 2002), calcium indicators (Mank and Griesbeck, 2008) and redox sensitive GFPs (Meyer and Dick, 2010) in biological studies.

The wild type *Aequorea victoria* GFP (AvGFP) protein consists of 238 amino acids that form an 11–stranded barrel structure (also called ß-can) surrounding a central

helix (Figure 1-18 A) (Weichsel et al., 1996, Pedelacq, 2019). Around 9–13 residues are located in each ß-can strand (Figure 1-18 B). The cyclisation, dehydration, and oxidation of the amino acid residues, Ser 65, Tyr 66, and Gly 67, within the central helix results in the chromophore. The correct folding is essential for the fluorescence properties. The emission of fluorescence of AvGFP is at 525 nm. The excitation spectrum of AvGFP shows two peaks at 396 – 398 nm (maximum excitation peak) and 476–478 nm (lower secondary peak). The maximum peak corresponds to the neutral state of Tyr 66 in the chromophore whereas the secondary peak results from the deprotonated anionic state of Tyr 66 in the chromophore.

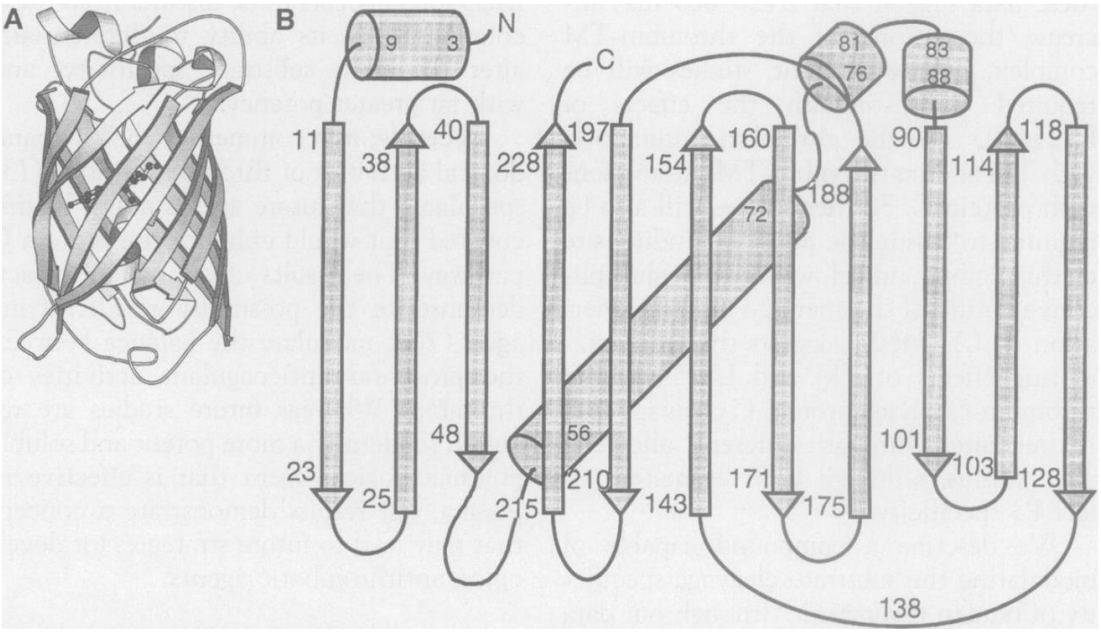

Figure 1-18 Schematic structure of AvGFP. A. The key feature of the AvGFP structure is 11-stranded - barrel wrapped around a single central helix that contains a chromophore (representing by a ball and stick model). **B**. The fold of AvGFP. The numbers indicate the beginning and ending residues in the secondary structure. N, indicating N-terminus of AvGFP; C, indicating COOH-terminus of AvGFP. (Weichsel et al., 1996)

In order to overcome the weak brightness and to optimise the excitation efficiency, different mutations, such as S65T, F64L, are incorporated into the AvGFP (Cormack et al., 1996). This GFP variant is converted to human codons which can encode the enhanced – GFP (eGFP) that have a much higher fluorescence intensity that the wild type AvGFP. To solve the solubility and overcome the folding defects when the GFP was fused to other proteins, superfolder GFP (sfGFP) is engineered by incorporating folding mutations, like

S30R which has been found to have a significant role on the stabilisation of the GFP structure and decrease the influence of fusion proteins on GFP correctly folding (Pédelacq et al., 2006). These sfGFPs can be expressed in pro- and eukaryotes and provide the possibility for diverse applications in mammalian cells.

Redox–sensitive GFP (roGFP) are GFP variants that are engineered with cysteines on adjacent strands that can or can not form a disulfide bond which modify the properties of the GFP fluorescence. Depending on the redox potential of the disulfide bonds in roGFP, it can be used to monitor the redox state change in living mammalian cells, such as in the cytosol (Ostergaard et al., 2001), the mitochondria (Hu et al., 2008), the ER (van Lith et al., 2011) and the later stages of the secretory pathway (Austin et al., 2005). Because of the more oxidising environment in the ER lumen, the disulfides need to have a higher reduction potential than that in the cytosol and mitochondria. My colleagues engineered one roGFP variant which can monitor the redox status change in real time based on the GFP variant (roGFP1-iL) (van Lith et al., 2011) which has a more similar disulfide reduction potential suitable for the use in the ER lumen (Lohman and Remington, 2008). To ensure ER-localisation in mammalian cells, a signal peptide from ERp57, was fused to the N-terminal of the roGFP1-iL and the ER retrieval sequence (KDEL) was incorporated to the C-terminal of the roGFP1-iL (van Lith et al., 2011). One of the known two cysteines (C49 and C71) that can independently form dimers by an interchain disulfide in roGFP1-iL is mutated to Ser (C49S), which allows roGFP1-iL-KDEL to respond to the redox state change in the ER lumen in real-time. To obtain a more stable and brighter roGFP variant, ER-SFGFP-iE, superfolder mutations (Pédelacq et al., 2006) were incorporated into the roGFP1-iL-KDEL. In addition, the ER-SFGFP-iE is human codon optimised for more efficient expression. Herein, ER-SFGFP-iE was used to monitor the microsomal redox status in our experiments.

1.11 Project Aims

Based on the work carried out previously, we have an unknown connection between the ultimate electron donor (NADPH) in the cytosol and the final acceptor in the ER. While the initial and final steps in the pathway are identified, we do not know the number of intermediate steps or the identity of a putative disulfide

transporter in the ER membrane. The gaps in our knowledge are indicated by question marks (Figure 1-19). Based on the different locations in cells, the knowledge gap is divided into three questions:

1. Are there additional components needed in the cytosolic reduction pathway?
2. What is the putative disulfide transporter in the ER membrane?
3. Which components are involved in the conversion of non-native to native disulfides in the ER?

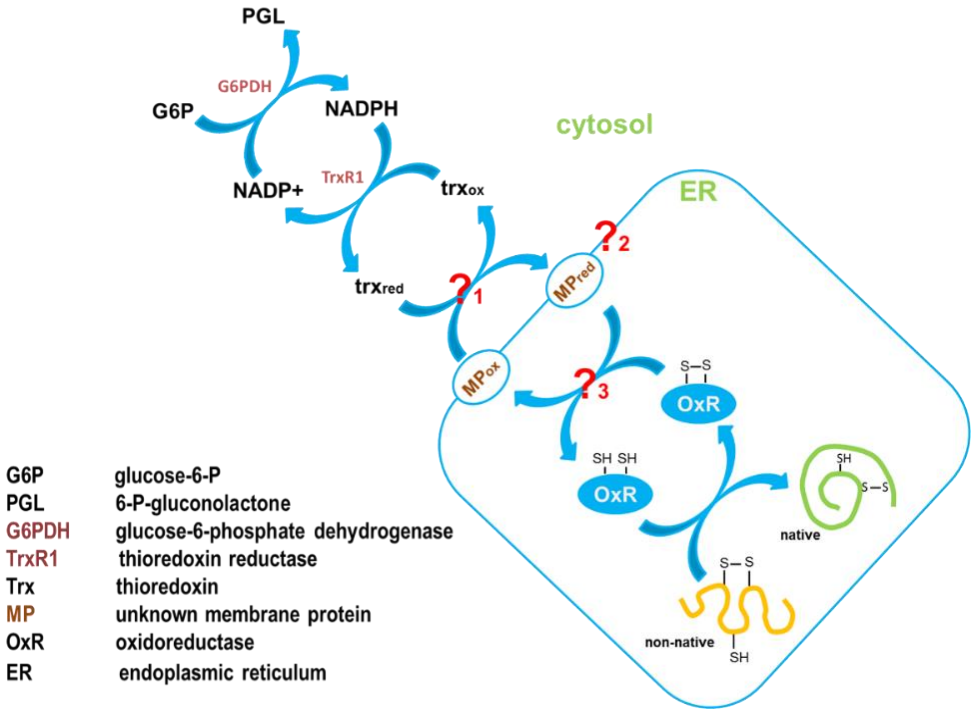

Figure 1-19 Hypothetical disulfide reductive pathway between thioredoxin in the cytosol and PDI in the ER. The potential connections between the electron donor (NADPH) in the cytosol and the ultimate electron acceptor in the ER are depicted. While the initial and final steps in the pathway are identified we do not know the number of intermediate steps or the identity of a putative disulfide transporter in the ER membrane. The gaps in our knowledge are indicated by question marks.

The goal of our research is to address the ER reductive pathway for disulfide reduction which is driven by the cytosolic ultimate donor NADPH via a robust cytosolic Trx/TrxR pathway. The three aims in each chapter to achieve this goal are as followed:

1. Reconstitute a cytosolic Trx/TrxR system using purified components and assess if these are the minimal components that are required for the reduction of proteins within a microsomal membrane system.

2. Evaluate if the minimal cytosolic Trx/TrxR system can reduce the oxidised ER-localised ERp57, a member of PDI, that plays a critical role in the reduction of disulfide in glycoprotein.

3. Develop a post-translational folding assay using RRL can be used to analyse the ability of the purified components to reduce disulfide bonds in the ER.

Chapter 2 Materials and Methods

2.1 Cell lines

The HT1080 cell line, a fibrosarcoma cell line, and Hela cell line was cultured in 75m^2 filter capped flasks and in Dulbecco's Modified Eagle Medium (DMEM) (Gibco) at 37^oC under 5% CO_2. HT1080 cell lines which stably over expressed V5-tagged ERp57 and roGFP were cultured as above in presence of antibiotic G-418 sulfate (Promega). The HEK 293 wild type and HEK 293 LMF1 KO cell lines are gifts from Saskia B Neher's lab (Roberts et al., 2018) and the Hela wild cell line and Hela SEPN1 KO cell lines are obtained from Ester Zito (Varone et al., 2019).

2.2 Reagents

If not specifically mentioned, chemicals were purchased from Sigma-Aldrich.

2.3 Preparation of SP cells

SP-cells were prepared as described previously (Wilson, Allen et al., 1995). The sub-confluent cells were rinsed twice with 10 ml PBS (Gibco) to remove the medium which inhibits trypsin. Trypsin solution (2 ml) (prewarmed to RT) was added into the flask and incubated for at 37 ^oC for 3 min to detach the cells. KHM buffer (8 ml) (20 mM HEPES buffer pH 7.2, including 110 mM KOAc, 2 mM MgOAc) was used to resuspend the cells and soybean trypsin inhibitor (final concentration 100 µg/ml) was added into the solution to inactivate the trypsin. The cell suspension was then transferred to a 15 ml tube tube which was pre-cooled on the ice. The cells were pelleted by centrifugation at 250 ×g at 4 ^oC for 3 min. The pellet was resuspended in 6 ml KHM buffer including 40 µg/ml digitonin (Calbiochem) and incubated on ice for 5 min to permeabilise the plasma membrane. The volume was made up to 14 ml and the cells were pelleted by centrifugation as above. The cells were resuspended in 14 ml ice-cold HEPES buffer (KOAc 50 mM, HEPES 20 mM, pH 7.2) and incubated on ice for 10 min. After centrifugation as above, the cell pellet was resuspended in 1 ml KHM buffer and 10 µl of cell suspension was transferred into an eppendorf tube which contained 10 µl Trypan Blue (Sigma). The SP cells were counted and checked for

permeabilization using a Cell Counter (Countess II FL). SP cells were pelleted by centrifugation as above and resuspended in KHM buffer containing $CaCl_2$ (5 mM) and treated with *Stapylocossus aureus* nuclease (Calbiochem) (final concentration 150 U/ml) at RT for 12 min to remove the endogenous mRNA. A final concentration 4.5 mM of ethylene glycol-bis(2-aminoethylether)-N,N,N′,N′-tetraacetic acid (EGTA, Sigma) was added into the solution to inactivate the nuclease. SP cells were pelleted by centrifugation as above and resuspended in 100 µl KHM buffer ready for the translation reactions or determination of the redox state experiments. For ERp57 redox state determination experiments, the nuclease treatment was not included during the preparation. In certain experiments, the SP cells were prepared from cells expressing V5-tagged ERp57.

2.4 Preparation of Adam 10 disintegrin domain DNA

The human Adam10 construct codes for residues 456 – 550 and contains the human - ß2M signal sequence residues (1-20). The generation of this construct and its transcription and translation were as described previously (Robinson et al., 2020). The plasmid DNA was used as a template for polymerase chain reaction (PCR) using a forward primer that adds a T7 promoter and a reverse primer that adds five methionine codons but lacks a stop codon. A reaction mixture (49 µl) (DNA template (50 – 100 ng), 5 µl 10 × Accubuffer (Bioline), 2 µl $MaCl_2$ (50 mM), 2 µl dNTPmix (100 mM), 2 µl forward primer (10 mM), 2 µl reverse primer (10 mM), distilled H_2O up to 49 µl) in the absence of ACCUZYME DNA polymerase (Bioline) was set up to do a hot-start PCR in order to obtain a more specific amplification of DNA. After the initial denaturation at 95 ^oC for 2 min, the DNA polymerase was added into the PCR reactions. The PCR cycle conditions in each cycle were as followed: denaturation at 95 ^oC for 30 s, annealing at 72 ^oC for 1 min, and extension at 72 ^oC for 1 min. To obtain sufficient target DNA, the PCR was carried out x 29 cycles. The DNA was precipitated by the addition of 0.1 volume NaAcetate (300 mM, pH 5.0) and 3 volumes ethanol absolute and the tube was centrifuged at 14,800 rpm for 10 min to isolate the DNA. The pellet was washed by 200 µl 70% ethanol and dried at RT for 5-10 min. The DNA was redisolved in 50 µl distilled water. The solution (2 µl) was mixed with 3 µl water and 1 µl 5 × Gel Loading Dye (Biolab). The samples were run on a 1% agarose gel which was dissolved in 1 × TAE buffer (40 mM Tris Base, 1.74 glacial acetic acid, 12.7 mM

ethylenediaminetetraacetic acid (EDTA). The gel was scanned in Azure c600 (Cambridge Bioscience) to obtain the image.

2.5 Transcription

RNase Zap™ (Invitrogen) was used to destroy RNases on the bench where a 50 µl of transcription system was set up. The reaction system for transcription were as followed: DNA template (5 – 10 µg), 5 µl 10 × transcription buffer (Promega), 2 µl DTT (100 mM), 6 µl 4 nucleotide mix (each at 25mM) (Biolabs), 1 µl RNasin (Promega), 2 µl T7 or SP6 RNA polymerase (Promega), distilled H_2O up to 50 µl. The transcription was carried out in a water bath at 37 °C for 2 h. The RNA was precipitated, and the quality of RNA was checked as described for DNA (2.4).

2.6 Translation

Translation reaction was carried out in the Flexi® Rabbit Reticulocyte Lysate (RRL) System (Promega). Each 25 µl translation reaction system contained 16.5 µl RRL (Promega), 1 µl RNA template, ~10^5 SP cells or 1 µl microsomes (50 unit/ µl), 20 mM amino acids minus methionine (Promega), 40 mM KCl, and 0.5 µl EasyTag™ EXPRESS ^{35}S Protein Labelling Mix (PerkinElmer). In certain experiment, RRL were treated with TrxR inhibitor, auranofin (AF) (20 µM), at RT for 15 min. The translation was carried out in the absence or presence of 5 mM glucose 6-phosphate (G6P) at 30 °C in water bath for different times depending on RNA template (15 min for Adam 10 disintegrin domain and 60 min for ß1-integrin). A final concentration of 25 mM N-ethylmaleimide (NEM, Thermo Scientific) was added to terminate the reaction by blocking free thiols in translation products, while NEM was not added to translations which were subsequently used in post-translational assays later.

2.7 Post-translational folding assay

The translation products translated in the absence of G6P were used to carry out a post-translational folding assay with the purified cytosolic components, such as NADPH, G6P, G6PDH, Trx, TrxR. SP cells or microsomes were pelleted by centrifugation at 14,800 rpm (cells for 30 s, microsomes for 10 min). KHM buffer

(HEPES buffer (20 mM, pH 7.5) for microsomes) was used to wash the pellet to remove the excess RRL. Post translational folding assays were carried out in fresh RRL (treated or not treated with AF as above), cell extract or KHM buffer, with or without 5 mM G6P or the reconstituted Trx/TrxR system (1 mM NADPH, 25 μM human Trx, 16.25 nM human TrxR (IMCO) or 600 nM yeast TrxR (purified by Jana Rudolf), 1.25 mM G6P, 10 mU G6PDH) in the absence or presence of Trx. The post-translational reactions were stopped by the addition of NEM (final concentration 25 mM). After centrifugation, the pellet was ready for immunoisolation.

2.8 Immunoisolation

The translation product was washed with KHM buffer (SP cells) or HEPES buffer (microsomes) to remove RRL or other background proteins. After centrifugation, the pellet was resuspended in 1 ml immunoprecipitation (IP) buffer (50 mM Tris-HCl pH7.5, 1% Triton X-10, 150 mM NaCl, 2 mM EDTA, 0.5 mM PMSF, 0.02% Na-azide) containing 50 μl 10% recombinant Protein A Sepharose FF Resin (PAS) (Generon). The solution was incubated on a roller at 4 ºC for at least 30 min. The beads were centrifuged at 14,800 rpm for 30 s. The supernatant was then transferred into a new tube contained 50 μl 10% PAS. A specific antibody, such as JB1A (Merck) and 9EG7 (BD Biosciences) for ß1-integirn and anti-V5 antibody (Invitrogen) for Adam 10 disintegrin domain, was added into the supernatant. The solution was incubated on roller at 4 ºC overnight. The beads were pelleted by centrifugation as above followed by three times washing using 1ml IP buffer. The target protein was eluted from the beads by 5 min boiling at 105 ºC with 35 μl 4 × SDS-PAGE loading buffer (200 mM Tris/HCl pH 6.8, containing 40% glycerol, 8% SDS, 0-4% bromophenol blue). The samples were separated by SDS-PAGE under reducing or non-reducing condition. The gel was fixed for 30 min in 10% acetic acid/10% methanol and then washed three times using distilled water. The gel was laid on wet filter paper and then dried at 80 ºC for 1 h. The dried gel was exposed to a phosphorimage plate or BioMax MR film (Kodak). A FLA-7000 bioimager (Fujifilm) was used to scan the plate to obtain the image.

2.9 Preparation of competent cells

Competent cells were prepared from *E. coli* XL-1 or BL21-DE3. One colony from an agar plate of XL-1 or BL-21 was picked and cultured in 10 ml LB (not containing any antibiotic) at 37 °C overnight. All bacterial culture was transferred into 500 ml LB and cultured for another 2.5-3 h at 37 °C, 180 × g until the OD_{600} reached 0.5. The solution was cooled down on ice for 15 min. The bacteria were pelleted in 10 × 50 ml tubes by centrifuge at 3,000 × g, 4 °C for 10 min. The supernatant was discarded while the pellet was resuspended in 30 ml (3 ml in each 50 ml tube) Tfb1 buffer (RbCl 100 mM, $MnCl_2$-$4H_2O$ 50 mM, potassium acetate 30 mM, $CaCl_2$-$2H_2O$ 10 mM, 15% glycerol). The solution was transferred into one 50 ml tube and placed on ice for 15 min. The bacteria were centrifuged at 4,000 rpm at 4 °C for 10 min. The pellet was resuspended in 6 ml Tfb2 buffer (Mops 0.2 M, RbCl 10 mM, CaCl2-$2H_2O$ 75 mM, 15% Glycerol) and aliquoted into eppendorf tubes. The aliquots were frozen in liquid nitrogen and stored in - 80 °C freezer.

2.10 Transformation

The competent cells were thaw on ice for 20 - 30 min. DNA (usually 10 pg to 100 ng, around 1-50 µl) were added into 20 - 50 µl competent cells. The solution was mixed gently by flicking the bottom of eppendorf tube with fingers for 5 times and incubated on ice for 20-30 min. The mixture was heat shocked in water bath at 42 °C for 30 - 90 s (Usually 45 s was ideal, but the heat shock time also varied depending on the competent cells). The tube was immediately placed on ice and incubated for 2 min. A volume of 200-800 µl Luria Broth (LB) (bactotryptone 10 g, yeast extract 5 g and NaCl 10 g in per 1 L water) (without antibiotic) was added into the tube. The tube was incubated at 37 °C for 45-60 min at 225 rpm/min in an incubator shaker (Innova 4400). Appropriate volume (50-200 µl) of solution was pipetted to the LB agar plate (containing 15% agar) including antibiotic (ampicillin 100 µg/ml). The plates were dried, inverted and incubated at 37 °C overnight. After overnight culture, single colonies were selected and cultured overnight in liquid LB. The bacterial culture was preserved at -80 °C with 30% glycerol.

2.11 Expression of Trx

2.11.1 Small scale protein expression

A small scale of protein expression was carried out to investigate whether the transformation was successful. A transformed BL21-DE3 colony was picked from the agar plate with antibiotic and cultured overnight in 5 ml LB (containing 100 µg/ml Amp) at 37 ºC, 225 × g in a shaker incubator (Innova 4400). A volume of 50 µl overnight culture was added to 5 ml fresh LB (containing 100 µg/ml Amp) and cultured for 3-4 h until the OD_{600} reached 1. A volume of 1 ml bacterial culture was centrifuged at 18,000 × g for 10 min. The pellet was resuspended in SDS-loading buffer and boiled at 105 ºC for 5 min (for example, if the OD_{600}= 1, 100 µl SDS-loading buffer was used to resuspend the pellet). This sample was loaded on the gel as the uninduced control of protein expression. The remaining bacterial culture was induced by the addition of isopropyl ß-D-1-thiogalactopyranoside (IPTG) (final concentration 2 mM) for 3 - 4 h. Another 1 ml solution was measured at 600 nm, centrifuged, and resuspended in SDS-loading buffer as above. The samples were loaded on a 15% SDS-PAGE gel (running conditions, 300 V, 25 mA, 2 h). Coomassie staining was carried out to visualize the protein.

2.11.2 Large scale protein expression

A colony was picked and cultured overnight in 10 ml LB in the presence of 100 µg/ml Amp at 37 ºC. Bacterial culture (5 ml) was added to 500 ml fresh LB with antibiotic and cultured for 3-4 h until the OD_{600} reached 1. Before the addition of IPTG, a 1 ml of culture was collected and after centrifugation, the pellet was resuspended in SDS-loading buffer as a uninduced control. The remaining bacterial culture was incubated with 2 mM IPTG for another 3 - 4 h to allow protein expression. The OD_{600} of a 1ml bacterial culture after induction was measured and the bacteria was isolated by the centrifugation at 14,800 rpm for 10 min as a control for expression. The rest of bacterial culture was split into 250 ml flat bottom screw cap centrifuge bottles and centrifuged at 4 ºC, 3,000 × g for 15 min (Beckman, rotor JA17). The supernatant was discarded. The bacteria were pelleted and washed three times with PBS (40 ml/tube). The pellet was stored -20 ºC. Samples before and after induction were loaded on a 15% SDS-PAGE gel

(running conditions, 300 V, 25 mA, 2 h) under reducing conditions. Coomassie staining was carried out to visualize protein expression.

2.12 Colloidal Coomassie blue stain

After SDS-PAGE analysis, the gel was stained with Coomassie blue (10% phosphoric acid (H_3PO_4), 10% ammonium sulphate $(NH_4)_2SO_4$, 0.12% Coomassie G250 (brilliant blue), 20% Methanol) for at least 1 h. Gel was de-stained using distilled H_2O overnight and scanned to obtain image the next day.

2.13 Purification of Trx

2.13.1 His tag affinity chromatography

The bacteria pellet after induction by IPTG was thawed on ice and then resuspended in 20 ml His-Buffer A (50 mM Tris pH 7.5, 150 mM NaCl, 5 mM imidazole). The cells were disrupted three times in a French Press cell disrupter (Thermo) at 950 Psi. After centrifuged at 10,000 × g, 4 ^oC for 30 min, the supernatant was filtered through a Minisart® Syringe Filter (Pore Size, 0.45 μm) (Sartorius). The sample was then loaded to a HisTrap HP histidine-tagged protein purification column (5ml) (GE Healthcare) at 2 ml/min which was pre-equilibrated by His-Buffer A. After the sample was applied, His-Buffer A was used to remove unbound proteins (flow rate at 2 ml/min). The His-tagged protein was eluted (flow rate at 0.4 ml/min) from the column by a linear gradient of 5-500 mM imidazole which is a mixture of His-Buffer A and His-Buffer B (50 mM Tris pH7.5, 150 mM NaCl, 500 mM imidazole).

2.13.2 Gel filtration

The eluted samples from His tag affinity chromatography were concentrated to a final volume 1 ml at 3,500 rpm, 4 ^oC for 30-60 min using a Vivaspin Turbo 15 centrifugal concentrator (100,000 MWCO PES) (Sartorius) which was washed with 10 ml distilled water and equilibrated by 15 ml GFC buffer (20 mM Tris pH 7.5, 100 mM NaCl). The sample was applied (flow rate at 0.4 ml/min) in the equilibrated gel filtration column (Superdex 200 10/300) (GE Healthcare). The

column was washed (flow rate at 0.4 ml/min) by GFC buffer until the UV absorbance curve became flat. Purity of protein was analysed after gel filtration using SDS-PAGE (15% SDS gel) under reducing conditions with an Coomassie stained. The fractions containing target protein were collected and concentrated until the protein concentration reached 500 mM/ml. The protein concentration was measured at an absorbance of 280 nm (Cary 300 Bio UV-Vis, Varian). The absorbance of the solution was measured at 280 nm in water including 1% SDS. The concentration of proteins were calculated using the equation: $c = A / (e \times b)$ (A is the value of A_{280}, e is extinction coefficient of the protein, and the b is the path length (cm)). The aliquots of purified protein were frozen in liquid nitrogen and then stored -80 °C.

2.14 Preparation of the cell extract and the microsomes

2.14.1 Cell extract preparation

The cell extract was prepared as previously described (Mikami et al., 2006). Cells were cultured using cell culture roller bottles (1700 cm^2, filter screw cap) (Greniner Bio-one) in an CO_2 incubator (Galaxy S, Wolf laboratories) (5% CO_2) at 37 °C in DMEM. The confluent cells were detached from the roller bottles by incubation with 100 ml PBS containing 1 mM EDTA for 10 -15 min at 37 °C. These cells then were pelleted by centrifugation at 250 ×g for 3 min and washed three times with washing buffer (35 mM HEPES–KOH pH 7.5, 140 mM NaCl, and 11 mM glucose) to remove the remaining DMEM and EDTA thoroughly. After washed once in extraction buffer (20 mM HEPES–KOH pH 7.5, 135 mM potassium acetate, 30 mM KCl, and 1.65 mM magnesium acetate), the cells were harvested by centrifugation at 2000 × g for 3 min. An equal volume of extraction buffer (less extraction buffer could be used to obtain a more concentrated cell extract) was used to resuspend the cells. The cells were disrupted in a Mini-Bomb Cell disruption chamber (KONTES) using a nitrogen pressure of 1.0 MPa for 30 min on the ice. Cell homogenates were centrifuged at 6000 × g for 5 min at 4 °C and the post nuclear supernatant was retained. To pellet the membrane, the supernatant was centrifuged at 50,000 × g (Rotor TL100.3) (Optima™ Max-XP Ultracentrifuge, Beckman Coulter) for 15 min at 4 °C. The supernatant was removed to a new eppendorf tube. The aliquots of the supernatant were frozen in liquid nitrogen

and stored at -80 °C. The membrane was used to prepare microsomes. In some experiments, a half of cell extract was treated with PD-10 desalting columns (GE healthcare) to remove small molecular weight compounds.

2.14.2 Microsomes preparation

The membrane pellet was resuspended in buffer A (50 mM Tris-HCl pH7.4, 0.25 M Sucrose, 50 mM KCl, 6 mM MgOAc, 1mM EDTA) to give an A_{280} value of 50 units/µl (the absorbance was determined in water in the presence of 1% SDS). If needed, a nuclease treatment of microsomes was carried out by the incubation with *Stapylocossus aureus* nuclease (Calbiochem) (final concentration 150 U/ml) in the presence of $CaCl_2$ (5 mM) at RT for 12 min to remove the endogenous mRNA. The nuclease was inactivated by the addition of EGTA (final concentration 4.5 mM). Sucrose cushion buffer (50 mM HEPES-KOH pH 7.5, 100 mM KCl, 0.5 M Sucrose) was added to the thickwall polycarbonate tubes (Beckman Coulter) and nuclease treated microsomes were then layered over the sucrose cushion buffer. The microsomes were isolated by centrifugation at 60,000 × g (Rotor TL100.3) for 15 min at 4 °C. The microsomes were resuspended in Buffer A (50 mM Tris-HCl pH7.4, 0.25 M Sucrose, 50 mM KCl, 6 mM MgOAc, 1 mM EDTA) and aliquoted into eppendorf tubes (50 µl/tube). The microsomes aliquots were frozen in liquid nitrogen and stored -80 °C.

2.15 Protein concentration measurement

The Bio-Rad Protein Assay was used to measure total protein concentration of the cell extract or microsomes. The Dye Reagent concentrate (Bio-Rad) was diluted 5 times using distilled water (1 ml Dye reagent with 4 ml water). The diluted dye was filtered through a Minisart filter (pore size 0.2 µm, Sartorius) to remove particulates. Five dilutions of a bovine serum albumin (BSA) standard were prepared to generate a standard curve (BSA concentration range was from 0.05 mg/ml to 0.5 mg/ml). The BSA solutions and samples were normally assayed in triplicate. BSA dilutions and samples were pipetted into Greiner-Bio Cell 96 Well black Cell Culture Microplates (10 µl/well) (Greiner Bio). The samples were incubated with 200 µl diluted dye reagent at RT for at least 10 min. The absorbance was measured at 595 nm (SPECTROstar *Nano*, BMG LABTECH).

2.16 Measurement of changes of the redox state of roGFP in microsomes

Microsomes were pipetted into Dulbecco's phosphate-buffered saline (PBS) (1.5 µl microsomes in 48.5 PBS) in the absence or presence of 0.1% Triton X-100 (Thermo Fisher). The solution was added into a CELLSTAR™ 96 Well Polystyrene Flat Bottom Cell Culture Microplate (Greiner Bio-One) (final volume 50 µl/well) (three wells per condition). The emission fluorescence intensities at 525 nm of microsomes were measured at both excitations wavelengths, 390 nm and 460 nm, using PHERAstar® FS microplate reader (BMG LABTECH). After 10 min of measurement to obtain the baseline, DTT, diamide or varied concentrations of Tris-(2-Carboxyethyl)phosphine (TCEP) (Thermo) were injected into microplate wells. The emission fluorescence intensity at two different excitation wavelengths were continuously recorded for another 50 min.

In certain experiments, the same amount of microsomes were untreated or treated with DTT, diamide, immobilised TCEP Disulfide Reducing Gel (Thermo) which has been neutralised and washed twice with PBS to remove soluble TCEP, or the PBS that had been preincubated with TCEP beads for 60 min. After 60 min incubation, the TCEP beads were isolated by the centrifuge at 1,000 × g for 3 min. The supernatant of each sample which contained microsomes was then transferred into microplate wells to measure the emission fluorescence intensity at 525 nm at excitation wavelengths, 390 nm and 460 nm.

2.17 Western blot

SDS-PAGE was performed as above. Proteins were transferred from gel to nitrocellulose blotting membrane (AmershamTM ProtranTM 0.45 µm NC) (GE Heathcare) in transfer buffer (25 mM Tris pH 8.3, 0.192 M Glycine, 0.0013 M SDS, 10-20% Methanol). The transfer conditions were 300 V, 250 mA for 1 h, 300 V, 150 mA for 2 h, or 300 V, 25 mA for overnight. The membrane was blocked by incubating with 10 ml 3% w/v dried skimmed milk (Marvel) in TBST buffer (Tris-HCl pH 8.0, NaCl 150 mM, Tween-20 0.5%) at RT for 1-16 h (generally 1 h). The membrane was incubated in 5 ml TBST including primary antibody overnight at 4 ^{o}C or RT for 1 h (incubation time varied depending on the primary antibody). After

primary antibody incubation, membrane was washed three times using 10 ml TBST buffer for 5 min at RT. The transferred membrane was incubated in 5 ml TBST with sondary antibody in the dark at RT for 45-60 min. Three times of 5 min washing with TBST or water was carried out to rinse membrane to remove excess secondary antibody. The membrane was scanned by Li-Cor Odyssey 9260 Imager to obtain image. Quantification of gel intensity was by ImageJ (NIH, USA). Experiments were carried out three times. Values quoted are averages with error bars depicting standard deviation. The western blot antibody information was as followed: for ERp57 using R283 as primary antibody which is raised in rabbits against the IQEEKPKKKKKAQEDL peptide (lab owned) and goat Anti-Rabbit 800 secondary antibody as the secondary antibody (Thermo Fisher), for ERp57-V5 using anti-V5 antibody (Invitrogen) as primary antibody and goat anti-Mouse IgG (H+L) (DyLight 800) (Thermo Fisher) as secondary antibody, for Trx using Streptavidin Protein DyLight 800 (ThermoFisher).

2.18 Proteinase K treatment

SP cells or microsomes which were prepared as above were incubated on ice with 10 µg/ml or 20 µg/ml proteinase K (Roche) for 25 min in the presence of 10 mM $CaCl_2$. The proteinase K was inactivated by the addition of phenylmethanesulfonyl fluoride (PMSF) (freshly made, final concentration 0.5 mM). For SP cells, proteinase and PMSF was removed by washing twice with KHM buffer. For microsomes, the proteinase and PMSF was removed by sucrose cushion ultracentrifugation as previously describes (2.14.2).

2.19 Determination of the redox state of ER localised ERp57

The redox state of ERp57 in SP cells was determined as described previously (Jessop and Bulleid, 2004). SP cells were either untreated or treated with 10 mM diamide at RT for 10 min. Samples were washed twice with 500 µl KHM buffer to remove diamide. Oxidised SP cells were incubated at 30 ^{o}C for 60 min in KHM buffer with or without DTT or the purified reductive components (1 mM NADPH, 25 µM human Trx (expressed and purified as above), 16.25 nM human TrxR (IMCO) or 600 nM Yeast TrxR (expressed and purified by Jana Rudolf), 1.25 mM G6P, 10

U/ml G6PDH). The SP cells were pelleted by centrifugation at 14,800 × g for 1 min and then incubated with 500 µl PBS containing 25 mM NEM to block free thiols. The samples were washed twice using PBS (1 ml) to remove excess NEM. The SP cells were lysed on ice with lysis buffer (50 mM Tris-HCl containing 150 mM NaCl, 2 mM EDTA, 0.5 mM phenylmethylsulfonyl fluoride, and 1% (v/v) Triton X-100) for 10 min. The lysate was centrifuged at 14,800 × g at 4 ºC for 10 min. The supernatant was removed to a new tube and boiled with 2% (w/v) SDS (VWR chemicals) to denature the protein. Denatured samples were incubated at RT with 10 mM TCEP to break existing disulfide bonds followed by a 1 - 2 h incubation with 20 mM alkylating agent 4-acetamido-4'-maleimidylstilbene-2, 2'-disulfonic acid (AMS) (Invitrogen) in the dark to alkylate free thiols. The samples were separated by SDS-PAGE and a western blot performed with R283 antibody or anti-V5 antibody to detect different redox state of ERp57 or V5-tagged ERp57 respectively.

2.20 Determination of the redox state of Trx

Purified Trx (final concentration 25 µM) was incubated in KHM buffer at 30 ºC for 60 min in the absence or presence of 100 µM NADPH, 16.25 nM human TrxR (IMCO), 1.25 mM G6P, 1 U G6PDH (total reaction volume was 100 µl). The reaction was stopped by the addition of NEM (final concentration 10 µM). Samples were incubated with streptavidin agarose resin (Thermo) in immunoprecipitation (IP) buffer (50 mM Tris-HCl pH7.5, 1% Triton, 150 mM NaCl, 2 mM EDTA, 0.5 mM PMSF and 0.02% Na-azide) at 4 ºC for 60 min. The streptavidin beads were pelleted by centrifugation. The beads were washed three times with IP buffer to remove unbounded proteins. Trx was eluted from streptavidin beads by incubating at RT for 15 min with PBS buffer including 2% SDS (w/v) and 3 mM Biotin. The samples were then boiled at 105 ºC for 15 min and incubated with 10 mM TCEP at RT for 10 min to break existing disulfide bonds followed by a 1.5 h incubation with 20 mM AMS (Invitrogen) in the dark to alkylate free thiols. The samples were separated by SDS-PAGE and a western blot performed using Streptavidin Protein DyLight 800 (ThermoFisher). The oxidised Trx displayed a decrease in mobility because of the larger molecular weight of AMS than NEM.

2.21 Evaluation of the activity of G6PDH

G6PDH is a cytosolic enzyme which produces NADPH using NADP and G6P. The NADPH concentration can be observed by the absorbance at 340 nm. To check the activity of G6PDH which was used in the reconstituted cytosolic Trx/TrxR system, G6PDH (10 U/ml) was incubated in KHM buffer with 1.25 mM G6P and 100 µM NADP at 30 ^{o}C for 60 min. Samples in the absence of either G6PH, G6P or NADP were negative controls. All samples were measured absorbance at 340 nm at the end of incubation.

2.22 Measurement of TrxR activity

Thioredoxin reductase (TrxR) activity in the cell extracts was measured using an assay kit for mammalian Trx and TrxR (IMCO). Different concentrations (1.87 – 9.37 ng/ µl) of TrxR and diluted cell extract were added to the TE buffer (50 mM Tris-Cl, 20 mM EDTA, 1 mg/ml BSA) containing 10 µM Trx. In certain experiments, the reaction mixture was incubated at RT for 15 min with a TrxR inhibitor, such as AF, TRi1 or TRi2 (Stafford et al., 2018). A volume of 30 µl mixture was carefully transferred into CELLSTAR™ 96 Well Polystyrene Flat Bottom Cell Culture Microplate (Greiner Bio-One). A volume of 20 µl reaction mixture M+N (2 mM ß-NADPH, 210 mM HEPES pH 7.6, 790 µM insulin, 20 mM EDTA) was added into every well. The mixture was incubated in a PHMP Thermoshaker (Grant Bio) at 200 rpm, 37 ^{o}C for 30 min. At the end of incubation, the stop solution (8 M GuHCl in 0.2 M Tris-Cl pH 8.0, 1 mM DTNB) was added to terminate all reactions (200 µl/well) and release free TNB which was a yellow product and absorbed light at 412 nm. For accuracy, the TrxR activity was assayed in triplicate.

2.23 Concentration measurement of NADP and NADPH

NADP and NADPH concentrations in the cell extract and RRL were measured using NADP/NADPH-Glo™ Assay (Promega). The cell extract (50 µl) was incubated with an equal volume of base solution (0.2 N NaOH). For the measurement of NADP concentration, a half of the cell extract (50 µl) was incubated with 25 µl HCl (0.4 N) at 60^{o}C for 15 min to destroy the NADPH in the cell extract. The sample was incubated at RT for 10 min and then neutralized by the addition of 25 µl Trizma

base (0.5 M). To measure the concentration of NADPH, a half of the solution (50 µl) was heated at 60°C for 15 min to destroy NADP in cell extract. The sample was cooled down to RT for 10 min. An equal volume of HCl/Trizma (0.25 M Trizma base, 0.2 N HCl) was added into the base-treated samples. For accuracy, the concentration of NADP and NADPH was normally assayed in triplicate. A standard curve using variant concentration (0 - 500 nM) of NADP and NADPH was generated to quantitate the concentration of NADP and NADPH in the cell extract or RRL. After the acid and base treatment, samples were mixed with 25 µl NAD/NADH-Glo™ detection reagent (reconstituted luciferin detection reagent 1ml, reductase 5µl, reductase substrate 5µl, NADP cycling enzyme 5µl, and NADP cycling substrate 5µl) (Promega) and immediately transferred into Corning® 96 Well white Solid Polystyrene Microplate (Life Science). A PHERAstar® FS microplate reader (BMG LABTECH) was used to record the luminescence of each sample.

2.24 Concentration measurement of the GSSG and GSH

The measurement of oxidised glutathione (GSSG) and reduced glutathione (GSH) concentration in cell extract and RRL was measured as followed. For total concentration of GSSG and GSH assay, a volume of 20 µl of cell extract or RRL was added into 1 ml assay buffer (0.1M $NaPO_4$ buffer pH 7.5 including 1mM EDTA, 0.2mM NADPH, 0.2mM DTNB). The reaction mixture was warmed to 30 °C followed by the addition of 1 unit of GSH reductase to reduce all of the GSSG to GSH. Reduced GSH converts the DTNB to a yellow product TNB, the absorbance at 412 nm of TNB can indicate the concentration of GSH. The solution was pipetted into CELLSTAR™ 96 Well Polystyrene Flat Bottom Cell Culture Microplate (Greiner Bio-One). The absorbance at 412 nm was recoded for 1 h. For GSSG concentration measurement, a 100 µl of the cell extract was incubated with a 2 µl of 2-vinylpyridine in 100 mM Tris (pH 7) at 30 °C for 1 h to alkylate GSH. The GSSG in the cell extract were reduced by the GSH reductase and measured as above.

2.25 Sample preparation for Mass Spectrometry analysis

Samples were prepared and data was analysed by Sergio Lilla in our collaborate lab in the Beatson West of Scotland Cancer Centre as previously described (van der Reest et al., 2018).

2.25.1 Treatment of the microsomes

roGFP microsomes (final concentration 5 unit/µl) were incubated with the reconstituted Trx/TrxR pathway using cytosolic components (1 mM NADPH, 25 µM human Trx (expressed and purified as above), 16.25 nM human TrxR (IMCO), 1.25 mM G6P, 10 U/ml G6PDH) in the absence or presence of Trx for 0 or 60 min. Reactions were carried out in quadruplicate. After the incubation, samples were prepared for MS as followed.

2.25.2 Sample preparation for MS analysis

Samples were lysed in a buffer containing 4% SDS, 50 mM triethylammonium bicarbonate pH 8.5 and 55 mM unlabelled iodoacetamide (light IAA, $^{12}C_2H_4INO$) to alkylate free cysteine thiols. The lysates were briefly sonicated (15-30 s, three times/sample) in eppendorf tubes. The samples were then centrifuged at 16,000 g for 5 min at 4 °C. The supernatant was transferred to clean tubes and incubated at RT in the dark to allow complete labelling of free cysteine thiols with 55 mM unlabelled iodoacetamide (light IAA, $^{12}C_2H_4INO$). The protein concentration in each sample was determined by Bradford assay and samples were stored at −80 °C until further processing.

For each experiment replicate, 30 µg of protein extracts were reduced with 70 mM DTT followed by dilution 1:2 using 50 mM triethylammonium bicarbonate buffer pH 7.0. The newly generated free cysteine thiols were subsequently alkylated by stable-isotope labelled iodoacetamide (heavy IAA, $^{13}C_2D_2H_2INO$). Differentially alkylated proteins were precipitated using trichloroacetic acid (TCA). The pellets were washed with 50 µl of HEPES 200 mM and digested with endoproteinase Lys-C (ratio 1:33 enzyme:lysate) for 1 h, followed by a trypsin, overnight (ratio 1:33 enzyme:lysate).

The digested peptides from each experiment, and a pool sample, were differentially labelled using TMT10-plex reagent (Thermo Scientific). Each sample was labelled with 0.1 mg of TMT reagent dissolved in 50 µl of 100% anhydrous acetonitrile. The reaction was carried out at RT for 2 h. Fully labelled samples were mixed in equal amount and desalted using a 100 mg Sep Pak C18 reverse phase solid-phase extraction cartridges (Waters).

2.25.3 High pH peptide fractionation

TMT-labelled peptides were fractionated using high pH reverse phase chromatography on a C18 column (150 × 2.1 mm i.d. - Kinetex EVO (5 µm, 100 Å)) on a HPLC system (Agilent, LC 1260 Infinity II, Agilent). A two-step gradient was applied, from 1–28% B in 42 min, then from 28–46% B in 13 min to obtain a total of 21 fractions for MS analysis.

2.25.4 UHPLC-MS/MS analysis

Fractionated peptides were separated by nanoscale C18 reverse-phase liquid chromatography using an EASY-nLC II 1200 (Thermo Scientific) coupled to an Orbitrap Fusion Lumos mass spectrometer (Thermo Scientific). Elution was carried out using a binary gradient with buffer A (2% acetonitrile) and B (80% acetonitrile), both containing 0.1% formic acid. Samples were loaded with 6 µl of buffer A into a 50 cm fused silica emitter (New Objective) packed in-house with ReproSil-Pur C18-AQ, 1.9 µm resin (Dr Maisch GmbH). Packed emitter was kept at 50 °C by means of a column oven (Sonation) integrated into the nanoelectrospray ion source (Thermo Scientific). Peptides were eluted at a flow rate of 300 nl/min using different gradients optimised for three sets of fractions: 1–7, 8–15, and 16–21. Initial Percentage of buffer B (%B) was kept constant for 3 minutes, then a two-step gradient was used, all with 113 min for step one and 37 min for step two. The %B were changed as follows. For F1-7, %B was 2 at the start, 17 at step one, and 26 at step two. For F8-14, %B was 4 at the start, 23 at step one, and 35 at step two. For F15-21, %B was 6 at the start, 27 at step one, and 43 at step two. All gradients were followed by a washing step (95% B) of 10 min followed by a 5 min re-equilibration step at the initial %B of each gradient, for a total gradient time of 168 min. Eluting peptides were electrosprayed into the mass spectrometer using a nanoelectrospray ion source (Thermo Scientific). An Active Background Ion Reduction Device (ESI Source Solutions) was used to decrease air contaminants signal level. The Xcalibur software (Thermo Scientific) was used for data acquisition. A full scan over mass range of 350–1400 m/z was acquired at 60,000 resolution at 200 m/z, with a target value of 500,000 ions for a maximum injection time of 20 ms. Higher energy collisional dissociation fragmentation was performed on the 15 most intense ions, for a maximum injection time of 100 ms, or a target

value of 100,000 ions. Peptide fragments were analysed in the Orbitrap at 50,000 resolution.

2.25.5 MS Data Analysis

The MS Raw data were processed with MaxQuant software version 1.6.3.3 (Cox and Mann, 2008) and searched with Andromeda search engine (Cox et al., 2011), querying (Apweiler et al., 2010). First and main searches were performed with precursor mass tolerances of 20 ppm and 4.5 ppm, respectively, and MS/MS tolerance of 20 ppm. The minimum peptide length was set to six amino acids and specificity for trypsin cleavage was required, allowing up to two missed cleavage sites. MaxQuant was set to quantify on "Reporter ion MS2", and TMT10plex was chose as Isobaric label. Interference between TMT channels were corrected by MaxQuant using the correction factors provided by the manufacturer. The "Filter by PIF" option was activated and a "Reporter ion tolerance" of 0.003 Da was used. Modification by light (H(3)NOC(2)) and heavy (HNOCx(2)Hx(2)) iodoacetamide on cysteine residues (carbamidomethylation) were specified as variable, as well as methionine oxidation and N-terminal acetylation modifications, no fixed modifications were specified. The peptide, protein, and site false discovery rate (FDR) was set to 1 %. MaxQuant outputs were analysed with Perseus software version 1.6.2.3 (Cox and Mann, 2008). The MaxQuant output ModSpecPeptide.txt file was used for quantitation of cysteine-containing peptides oxidation, whereas ProteinGroup.txt file was used for protein quantitation analysis. The peptides.txt and Carbamidomethyl sites tables were concatenated with the main data table as source of additional peptides features. Peptides with Cys count lower than one were excluded from the analysis, together with Reverse and Potential Contaminant flagged peptides. From the ProteinGroups.txt file, Reverse and Potential Contaminant flagged proteins were removed, as well as protein groups identified with no unique peptides. The TMT corrected intensities of proteins and peptides were normalised to the median of all intensities measured in each replicate. Only cysteine-containing peptides uniquely assigned to one protein group within each replicate experiment, and robustly quantified in three out of three replicate experiments, were normalised to the total protein levels and included in the analysis. To determine significantly oxidised cysteine-containing

peptides, a Student t-test with a 5% FDR (permutation-based) was applied using normalised reporter ions Intensities.

Chapter 3 Reduction of ER proteins by the cytosolic reductive pathway requires facilitative membrane transport

3.1 Introduction

Green Florescent Protein (GFP) was first isolated from *Aequorea vitoria* after the extraction and purification of a bioluminescent protein, aequorin (Shimomura et al., 1962, Johnson et al., 1962). *In vivo*, GFPs emit fluorescence due to the energy from a luciferase-oxyluciferin excited-state complex (Ward and Cormier, 1976) or a Ca^{2+}-activated photoprotein (Prasher et al., 1992). The GFP was successfully expressed in different organisms (prokaryotic and eukaryotic), such as *Escherichia coli* and *Caenorhabditis elegans* (Chalfie et al., 1994). Because the expression of GFP did not require any jellyfish-specific enzymes and special substrates and cofactors were not needed for its emission of fluorescence, GFP was then broadly used as a marker for gene expression and protein localisation in living organisms (Chalfie et al., 1994, Harper et al., 1999).

Variants of GFP were engineered to enable to monitor the redox status in living organisms by introducing different mutations (Meyer and Dick, 2010). Redox sensitive GFP (roGFPs) became an indicator which allowed real time visualization of redox status in cells (Dooley et al., 2004). The two excitation peaks of roGFP result from different forms of the fluorophore, the neutral form and the anion form, that are dependent on the redox status (Hoseki et al., 2016).

Because roGFP was genetically coded, it can be targeted to specific organelles, such as the ER, by fusing it to organelle specific signal sequence. An efficient ER reporter of real-time redox changes in living mammalian cells, ER-SFGFP-iE, was generated in our group based on a superfold roGFP variant, roGFP1-iL, by incorporating new cysteines to form an intracellular disulfide bond (van Lith et al., 2011) (Figure 3-2). Under reducing conditions, the disulfide bonds are cleaved resulting in the decrease of the neutral form of roGFPs and the increase of the anion form of roGFPs. Under oxidising environment, the disulfide bond is formed that causes the increase of the neutral form and decrease of the anion form of

roGFPs. These neutral and anion forms of roGFP have different excitation peaks at 390 nm and 475 nm respectively. The emission fluorescence intensity at 525 nm then displays rapid and reversible ratio metric changes corresponding to redox state changes of cells *in vivo*. Under reduced conditions, a decrease of fluorescence at 390 nm excitation wavelength was observed while the fluorescence increased at 470 nm excitation wavelength. The oxidation of cells leads to the opposite emission of fluorescence following excitation at 390 and 470 nm (Figure 3-1). The cells which could stably express ER-SFGFP-iE were used to prepare ER derived microsomes, for the experiments described in this chapter.

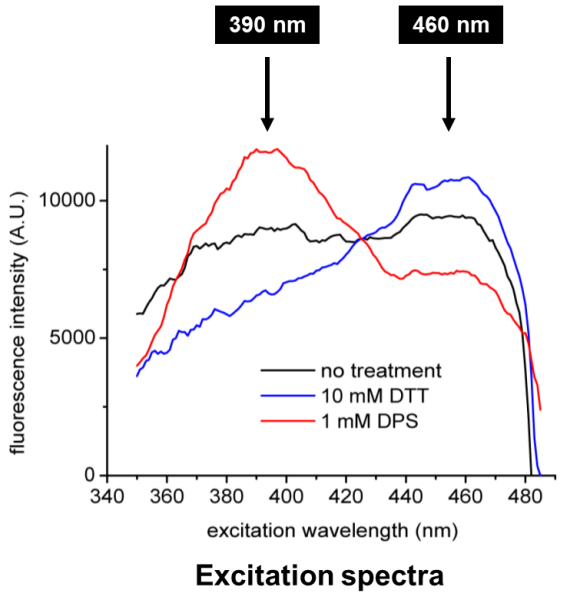

Figure 3-1 Excitation spectra of roGFP1-iL under no treatment, after reduction (DTT) or oxidation (diamide). Reduced roGFP had higher emission fluorescence intensity at 525 nm when it is excited at 460 nm while oxidised roGFP had higher emission fluorescence intensity at 525 nm when it is excited at 390 nm (van Lith et al., 2011).

Microsomes are ER derived vesicles with a diameter of 100 – 200 nm and isolated from homogenates of liver and other tissues(Claude, 1943, Kriechbaumer, 2018) or cultured cells (Sukhodub and Burchell, 2005) by differential centrifugation. Microsomes are composed of rough ER, smooth ER and ribosomes. Numerous enzyme activities are associated with the microsomal fraction. The microsomes can still carry out protein synthesis, protein translocation and glycosylation as happens in intact cells (Palade and Siekevitz, 1956, Sabatini, 2014). In this chapter, we prepared microsomes from a HT1080 cell line which stably

overexpresses roGFP to investigate how disulfide reduction occurs inside the ER lumen.

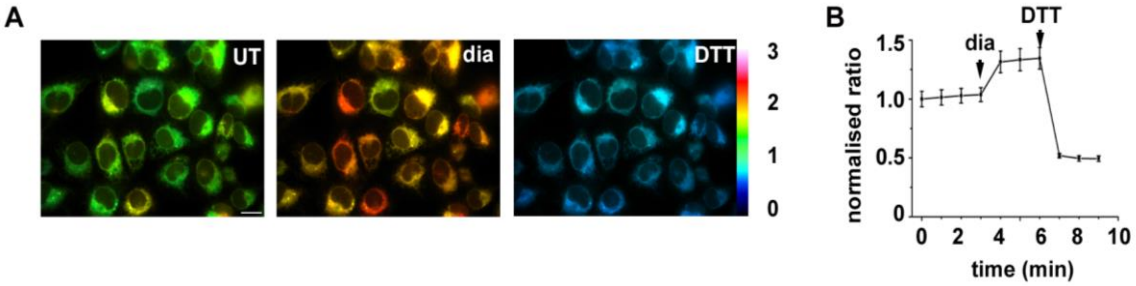

Figure 3-2 Stable cell-line expressing ER-SFGFP-iE was evaluated by live-cell imaging and was responsive to gross changes in redox conditions. A. Depicts fluorescent images of untreated, diamide or DTT-treated cells. Fluorescent ration changes are visualised using false colours with more reducing ratios in blue and more oxidising in red. **B.** Normalised fluorescent ratios of individual cells are averaged, and changes observed over time following the addition of 1 mM diamide followed by DTT (final concentration 10 mM).

The cell contains numerous intracellular organelles such as the nucleus, mitochondria, ER and Golgi apparatus each with its own set of enzymes and specialised functions. Synthesis and trafficking of secreted proteins are facilitated by the ER and Golgi apparatus. In the ER, the proteins undergo a series of modifications, like disulfide formation and reduction, glycosylation, to achieve its functional structure (Braakman and Hebert, 2013). It has previously been shown that the cytosolic Trx/TrxR pathway is necessary for correct disulfide bond formation in the ER (Poet et al., 2017). How the reducing equivalents that are generated in cytosol are transported across the ER membrane is still an open question. It has been demonstrated previously that a system for transfer of such reducing equivalents across an internal membrane does exist in prokaryotes (Berkmen, 2012). Various mechanisms are involved to ensure correct disulfide bond formation (Kadokura et al., 2003). DsbC is responsible for the isomerisation of the misfolded disulfide bonds (Shevchik et al., 1994). To maintain its isomersation function, DsbC is required to stay in a reduced state. A periplasmic membrane protein, DsbD, can receive reducing equivalents from the cytoplasmic NADPH via cytoplasmic Trx and then pass the electrons to the DsbC (Rietsch et al., 1997, Berkmen, 2012).

To address the role of mammalian cytosolic Trx in the reduction of disulfides within the ER lumen, mutants of Trx along with other cytosolic components were used to reconstitute the Trx/TrxR pathway. This approach makes use of the finding that mutant thiol-dependent oxidoreductases lacking the C-terminal cysteine of the CXXC active site motif form long-lived mixed disulfide intermediates with tarobtain proteins (Figure 3-3). Thus, substrate proteins remain covalently linked to the mutant oxidoreductase and become amenable to isolation and analysis (Figure 3-3A). Trx1 has 5 cysteines. Two (cysteines 32 and 35) are catalytic cysteines while another three (cysteines 62, 69 and 73) are non-catalytic (Figure 3-3B). To create Trx mutants, the second cysteine of the ^{32}CXXC^{35} motif was replaced by serine (C^{35}S) and all of the non-catalytic cysteines (C^{62}, C^{69} and C^{73}) were replaced with alanine because they may cause oxidative inactivation by either intra- or intermolecular disulfide bond formation. It was proven that Cys^{73} is easily accessed in the active site surface of Trx three-dimensional structure (Weichsel et al., 1996). It is possibly the active site Cys^{73} which forms disulfide bonds with glutathione in human T cell blasts (Casagrande et al., 2002). Subsequently, it was demonstrated that the Cys^{62} and Cys^{69} can form a non-native disulfide bond under oxidising conditions and the non-native disulfide bond resulted in the inhibition of TrxR activity (Watson et al., 2003). Trx1 mutant proteins Trx C-C, Trx C-S and S-S were produced and purified for future experiments. Three human Trx1 mutants (CC, CS, SS) will be used to reconstitute the Trx/TrxR pathway to investigate if the catalytic cysteines are playing a role in the electron transfer from the outside to the inside of ER derived microsomal membrane.

To investigate whether the minimal Trx/TrxR pathway could influence the redox state in the mamalian ER, we used purified cytosolic components, NADPH, G6PDH, G6P and Trx and TrxR, to reconstitute the cytosolic Trx/TrxR pathway. In this chapter, the reconstituted Trx/TrxR pathway and impermeable reducing agent TCEP were incubated with ER derived microsomes containing roGFPs to address the reduction pattern of ER localised proteins. Redox changes in the microsomes were measured with roGFP fluoressence at different excitation wavelengths. In order to investigate which membrane protein is involved in the electron-shuttling, we used an MS approach to analyse the reodox status of proteins in the microsomes before and after reconstitution with the Trx/TrxR pathway components. In the

next chapter, we will evaluate the impact of the reconstituted Trx/TrxR pathway on the ER localised PDI family member ERp57 which plays critical role in the disulfide isomerisation of glycoproteins.

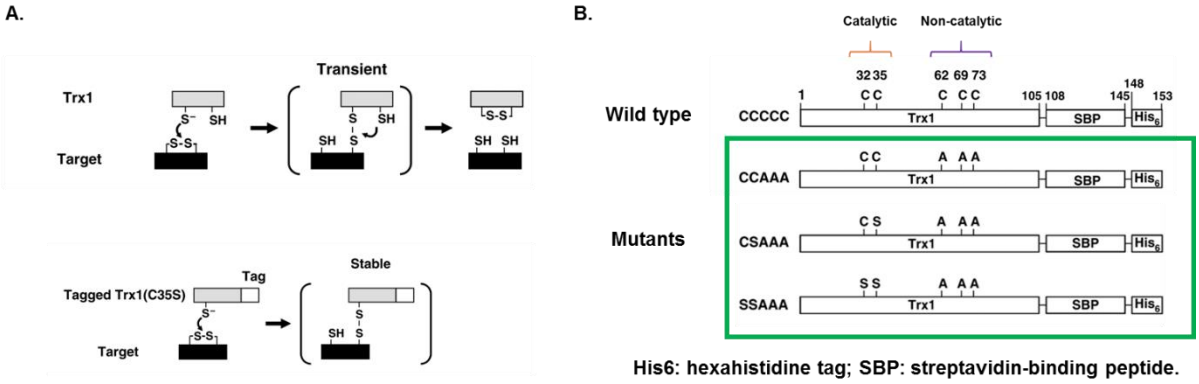

Figure 3-3 Catalytic mechanism of Trx and mutants of Trx. A. Catalytic mechanism of wild-type Trx1 (upper panel) and the principle of mutant Trx (lower panel). The mixed disulfide intermediate is normally resolved by cysteine-35. Replacement of cysteine-35 by serine (C35S) stabilizes the covalent intermediate. The affinity tag enables purification of resulting enzyme–substrate complexes. **B**. Schematic representation of wild type (CC) and mutants (CS and SS) of Trx. Catalytic (C32, C35) and structural cysteines (C62, C69, C73) are indicated. His6: hexahistidine tag; SBP: streptavidin-binding peptide **(Schwertassek et al., 2007a)**.

3.2 Results

3.2.1 The impermeable reducing agent TCEP can reduce microsomal roGFP

Microsomes prepared from a HT1080 cell line which overexpresses roGFP in the ER, were tested to ensure that the roGFP are still redox-sensitive. The same concentration of microsomes were left untreated or treated with the reducing or oxidising agents (Figure 3-4). The ratios of emission fluorescence intensities at 525 nm with excitation wavelength at 390 and 460 nm (ratio= 390nm/460nm) were calculated to indicate the redox state of roGFP microsomes. When microsomes were treated with a reducing agent (DTT), a significant decrease of ratio (390nm/460nm) was observed and oxidised microsomes with diamide gave an obvious increase of ratio (390nm/460nm). These results indicated that the prepared roGFP microsomes are sensitive to changes in redox conditions and we

can easily track the redox change of roGFP in the ER derived microsomes in real time.

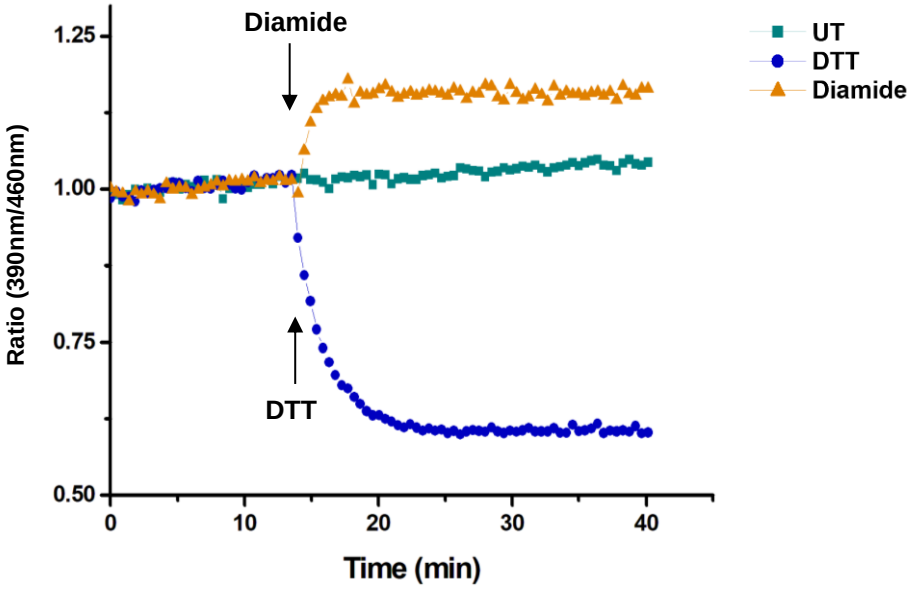

Figure 3-4 roGFP microsomes are sensitive to redox state changes. roGFP microsomes redox state were indicated by the emission fluorescence intensity (at 525 nm) at excitation wavelength 390nm divided by that at 460 nm (Ratio = 390nm/460nm). Untreated microsomes ratio (390nm/460nm) was normalised as value 1 (indicating by olive square). Microsome reduction by the reducing agent DTT (1 mM) (indicating by blue dot) led to a ratio (390nm/460nm) decrease while a ratio increase was caused by the oxidation by oxidising agent diamide (1 mM) (indicating by orange triangle).

To investigate if the membrane impermeable reductant TCEP can reduce roGFP in the microsomes, three samples (experimental replicates) were prepared in PBS in the absence or presence of 0.1 % (V/V) Triton™ X-100 which can permeabilise the membrane without denaturing the proteins. The emission fluorescence at two excitation wavelengths were recorded for 10 min to obtain the baseline. At 10 min, TCEP (final concentration 1 mM) was injected into the microplate wells. After the fluorescence emission saturated, Triton (final concentration 0.1%) was added at 40 min to a sample which was incubated in the absence of Triton.

Before addition of TCEP, the same ratios were observed in the presence or absence of Triton which indicated that the presence of Triton did not affect the redox state of roGFP (Figure 3-5A). At 10 min, TCEP was injected into the samples. A change to the roGFP redox status was observed in all three samples indicating reduction. The ratio values of roGFP in the presence of Triton (indicated by blue

triangle) decreased to a lower level than in the absence of Triton (indicated by grey square) which indicates more reduction happened in the presence of Triton than in the absence of Triton. In addition, the ratio change rate was faster in the presence of Triton than in the absence of Triton which indicates that the reduction of roGFP by TCEP was not due to the microsomes permeability of TCEP. If a fraction of the microsomes were permeable to TCEP then the rate of reduction of this fraction would be as rapid as the rate of reduction in the presence of Triton and then the rate would slowdown, a biphasic rate of reduction of roGFP would be observed. After the redox state became stable, Triton was added to the sample in which the microsomes were incubated in the absence of Triton. Immediately after the addition of Triton, the ratio value dropped significantly to the same ratio value as the microsomes were incubated with Triton from the beginning (indicated by red circle). The results demonstrated that the transfer of reducing equivalents from TCEP across the ER membrane occurred in the absence of Triton (Figure 3-5B and C). The results suggested that a membrane protein is possibly involved in the transducing reducing equivalents across the ER membrane, fulfilling an equivalent role to DsbD in the prokaryotic plasma membrane (Kadokura et al., 2003).

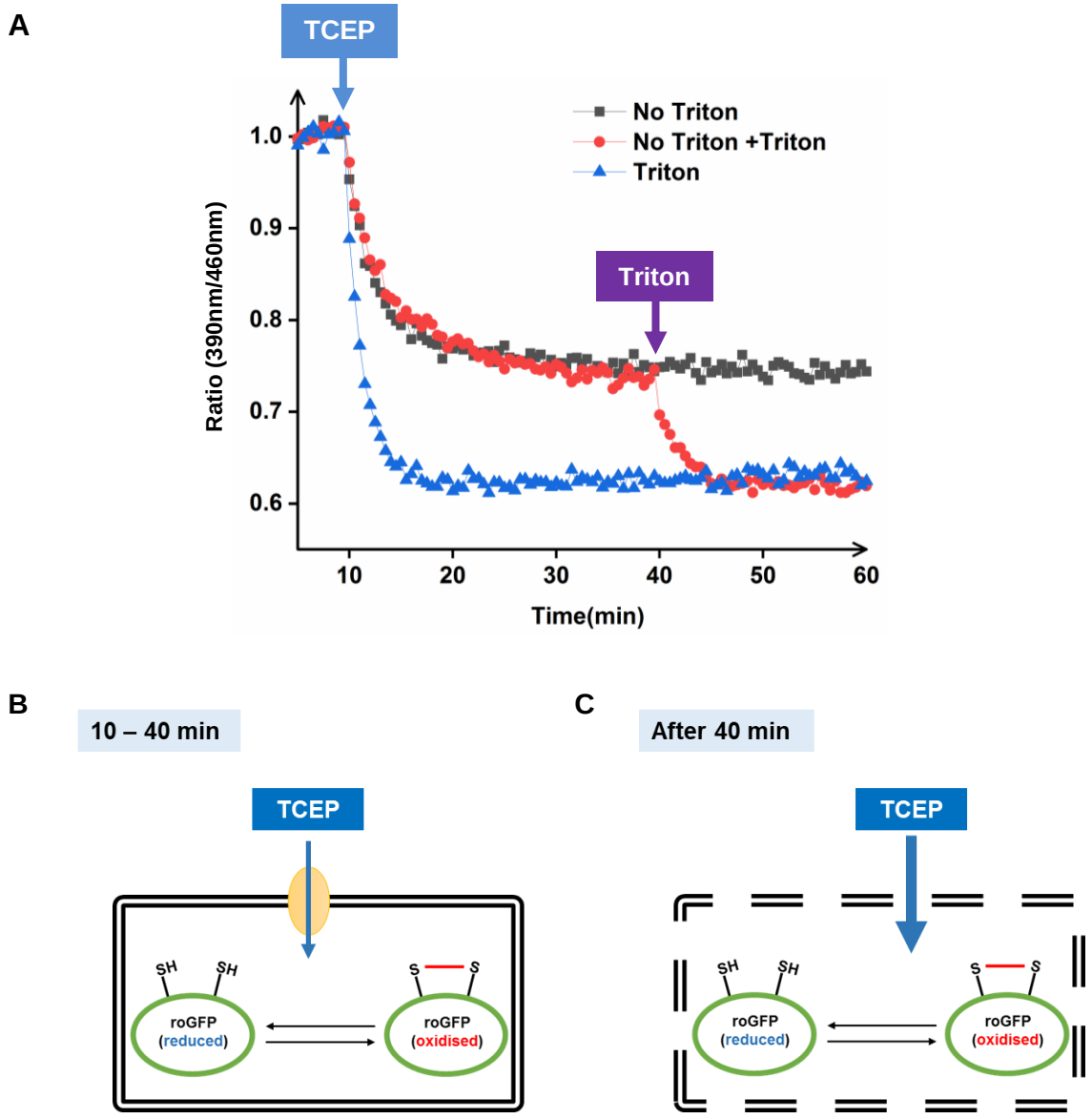

Figure 3-5 Addition of Triton resulted in further reduction of roGFP microsomes in the presence of TCEP. **A**. Ratio (390nm/460nm) change in the presence and absence of Triton. Emission fluoresence at 525 nm of three roGFP microsome samples at two different excition wavelengths 390 nm an 460 nm were recorded and caculated the ratio (390nm/460nm) to obtain the baseline (0 - 10 min). At 10 min, these three sample were treated with the same concentration of TCEP (1 mM) by injection into the microplate wells. Initially, one sample was treated with TCEP in the presence of 0.1% Triton™ X-100 (indicated by blue triangle) while the other two samples were treated with TCEP in the absence of Triton (indicated by grey squares and red circles). At 40 min, a sample incubated without Triton was injected with Triton (final concenrtation 0.1%) (indicated red circles). The emission of fluorescence was recorded. The ratio (390nm/460nm) was calculated and then normalised with baseline value (regarded as 1). **B.** Schematic diagram of TCEP reduction of roGFP microsomes before the addition of Triton (0-10 min). **C**. Schematic diagram of TCEP reduction of roGFP microsomes after the addition of Triton (10-40 min).

To further investigate the membrane permeability of TCEP, immobilised TCEP (TCEP beads) was used to reduce roGFP microsomes. TCEP was immobilized on agarose beads (TCEP beads) which ensured it cannot cross the microsomal membrane (Figure 3-6A). The TCEP beads were buffered to neutrality and washed with PBS to fully remove any soluble TCEP. The roGFP microsomes were either untreated or treated with the elution buffer from TCEP beads or TCEP beads. After incubation to allow the reduction progress, the TCEP beads were removed by centrifugation. The microsomes were transferred into 96-microplate wells and the fluorescence was measured at different excitation wavelengths to obtain the ratio which indicated the redox state of roGFP microsomes.

The results showed that the reduction of roGFP with TCEP beads is significant ($p=0.00001$), while the reductive effect of the wash buffer on roGFP is not significant ($p=0.03$) (Figure 3-6B). The result suggests that TCEP beads can reduce the roGFP inside of microsome without crossing the microsomal membrane supporting the requirement for a membrane protein to facilitate the reduction of microsomal roGFP.

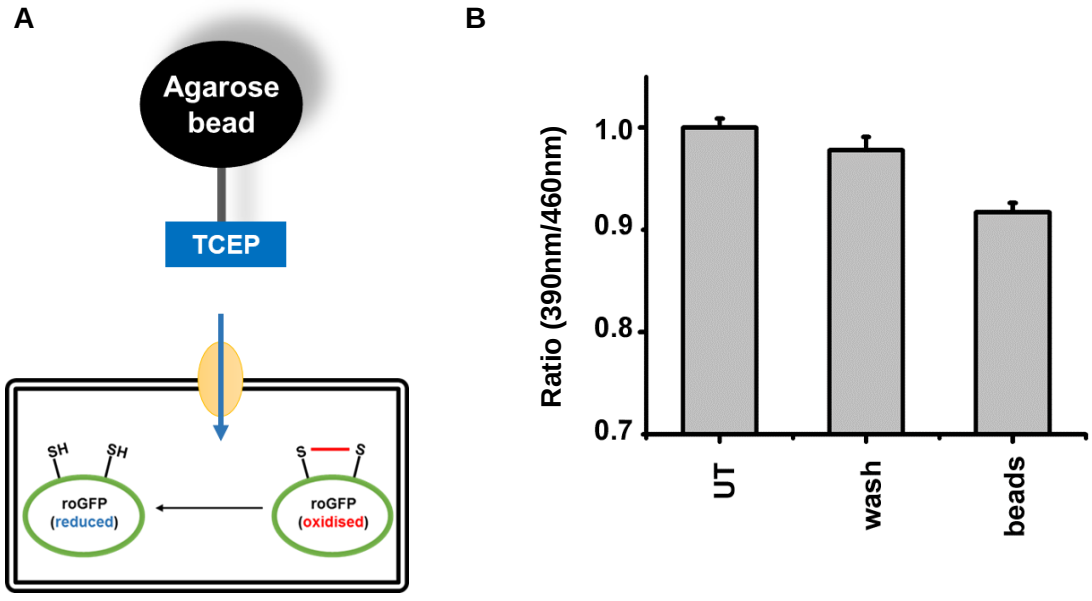

Figure 3-6 Reduction of roGFP microsomes by immobilized TCEP. A. Schematic diagram of reduction of roGFP in microsomes by immobilized TCEP disulfide reducing gel (TCEP beads). TCEP (Tris[2-carboxyethyl] phosphine hydrochloride) was immobilized on 4% crosslinked beaded agarose (indicating by grey oval circle) which ensures TCEP cannot cross microsomal membrane and can only reduce roGFP by acting via a membrane protein (indicating by yellow oval circle). **B**. Redox state of roGFP in untreated microsomes (UT) or microsomes treated with TCEP beads wash buffer

(wash) and TCEP beads (beads). The difference in ratio value between untreated and incubated with wash buffer is not significant (p=0.03) but there is a significant difference between untreated sample with the sample incubated with TCEP beads (p = 0.00001).

3.2.2 Microsomal roGFP was reduced by the membrane impermeable reducing agent TCEP via facilitated transport.

To address how the reducing agent TCEP can reduce the roGFP in microsomes, roGFP microsomes were treated with varied concentrations of TCEP in the absence or presence of 0.1% Triton™ X-100. The fluorescence intensities at different excitation wavelengths were recorded before and after the addition of TCEP. The ratios (390nm/460nm) were calculated and the rate of ratio change (**k**) was calculated by fitting the data to an exponential decay function ($y = -A(e^{-k\,(t-t0)}-1)+C$), where t_0 = the time of addition of TCEP, c = initial fluorescence ratio and A = difference in fluorescence ratio between t_0 and t.

The ratios (390nm/460nm) of roGFP microsomes treated with different concentrations of TCEP (0.2, 0.4, 0.6, 0.8, 1.0, 1.5 and 2 mM) were normalised to the ratio (390nm/460nm) of untreated roGFP microsomes (Figure 3-7A). It was noticed that the rate of ratio change increased with the increased concentration of TCEP (0-1 mM). However, when the microsomes incubated with concentrations of TCEP higher than 1 mM (1.5 and 2 mM), the rate of ratio change (k) reached saturation (Figure 3-7A). The k value increased as the concentration of TCEP increased. The rate of ratio changes in the absence of Triton appeared to exhibit a linear correlation with TCEP concentration when the final concentration of TCEP was lower than 1mM. However, the rate of change became saturated after treatment with higher TCEP concentration (1.5 mM and 2mM) (Figure 3-7B). The rate saturation indicates that the TCEP is transported across the membrane by a facilitated membrane transport process (Figure 3-7C).

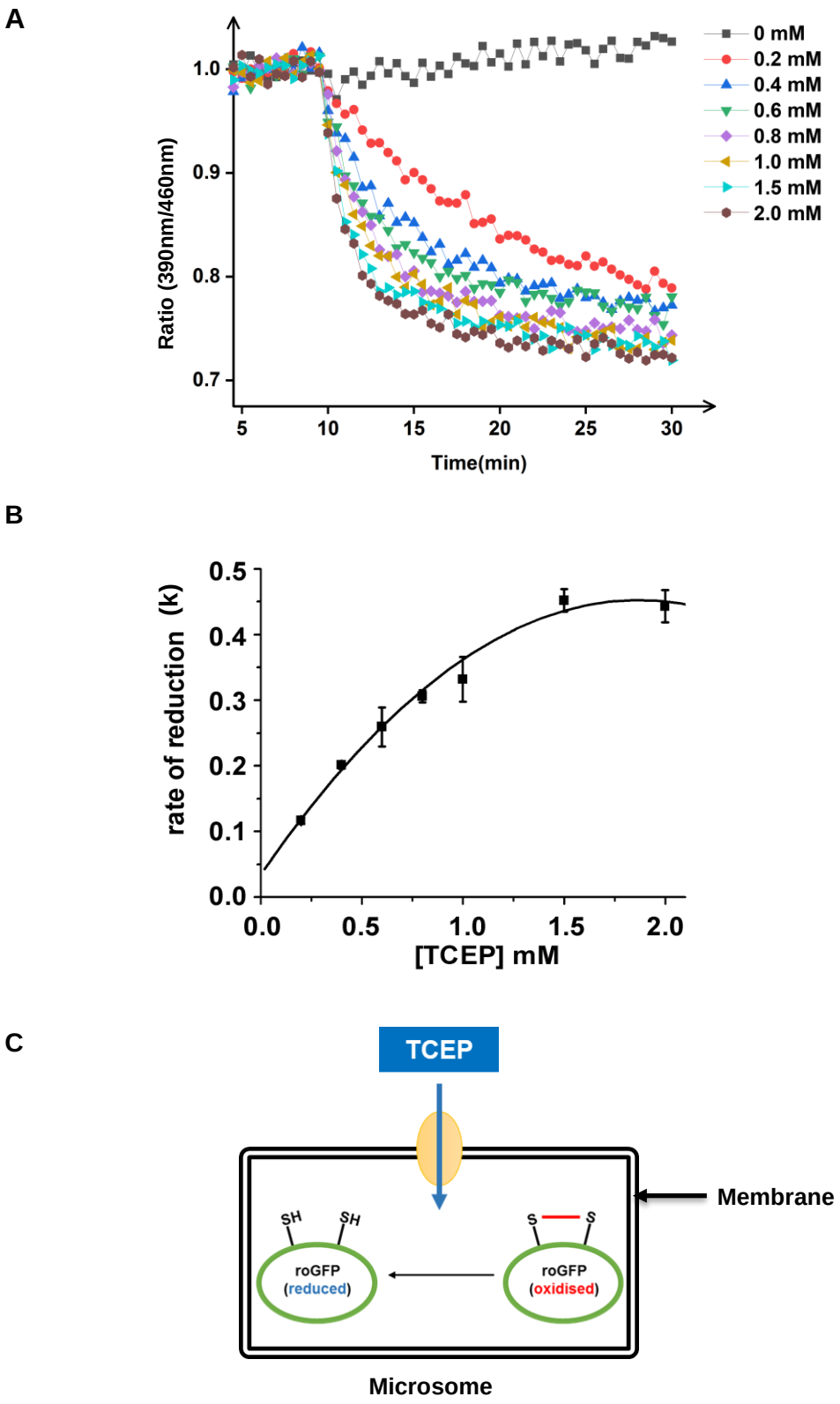

Figure 3-7 Reduction of roGFP microsomes by TCEP in the absence of Triton. A. roGFP microsomes were suspended in PBS. The fluorescence at different excitation wavelengths were recorded for 10 min to obtain a baseline. Different concentrations of TCEP (final concentrations 0, 0.2, 0.4, 0.6, 0.8, 1.0, 1.5 and 2 mM) were injected into each well. Emission fluorescence was continually recorded until the ratio reached saturation. Each sample at different concentrations of TCEP was performed in experimental triplicates. **B**. The rate of ratio change (indicated by **k**)

(390nm/460nm) was calculated and plotted vs TCEP concentration. **C**. Schematic diagram of TCEP reduction of roGFP in microsomes in the absence of Triton. In the absence of Triton, the microsome membrane was intact. The TCEP cannot cross the membrane by diffusion to reduce roGFPs in the lumen. This reduction process was facilitated by an unidentified membrane protein (indicated by yellow oval shape).

As a control, another group of microsomes were treated with different concentrations of TCEP (final concentrations 0, 0.2, 0.6, 1.0, 1.5 and 2 mM) in the presence of Triton™ X-100 which can permeabilise microsomes membrane allowing the reduction of roGFP by diffusion. In the presence of Triton, the rate of change (**k**) was calculated and analysed as above (Figure 3-8 A and B). Compared with roGFP microsomes in the absence of Triton, more significant reductions of redox state of roGFP microsomes were observed. Even that treated with the same concentration of TCEP, samples in the presence of Triton had a lower ratio indicating a more rapid reduction of roGFP. The ratio (390nm/460nm) of roGFP microsomes with 2 mM TCEP decrased to 0.72 in the absence of Triton while the ratio (390nm/460nm) decresed to 0.62 in the presence of Triton (Figure 3-8A). The rate of change (**k**) in the presence of Triton had a linear relationship to the concentration of TCEP and it was not saturable (Figure 3-8B) which is consistent with a diffusion-mediated process (Figure 3-8B). The results above indicate that after treatment with Triton, the membrane was solubilised and TCEP can directly reduce the roGFP by diffusion (Figure 3-8 C).

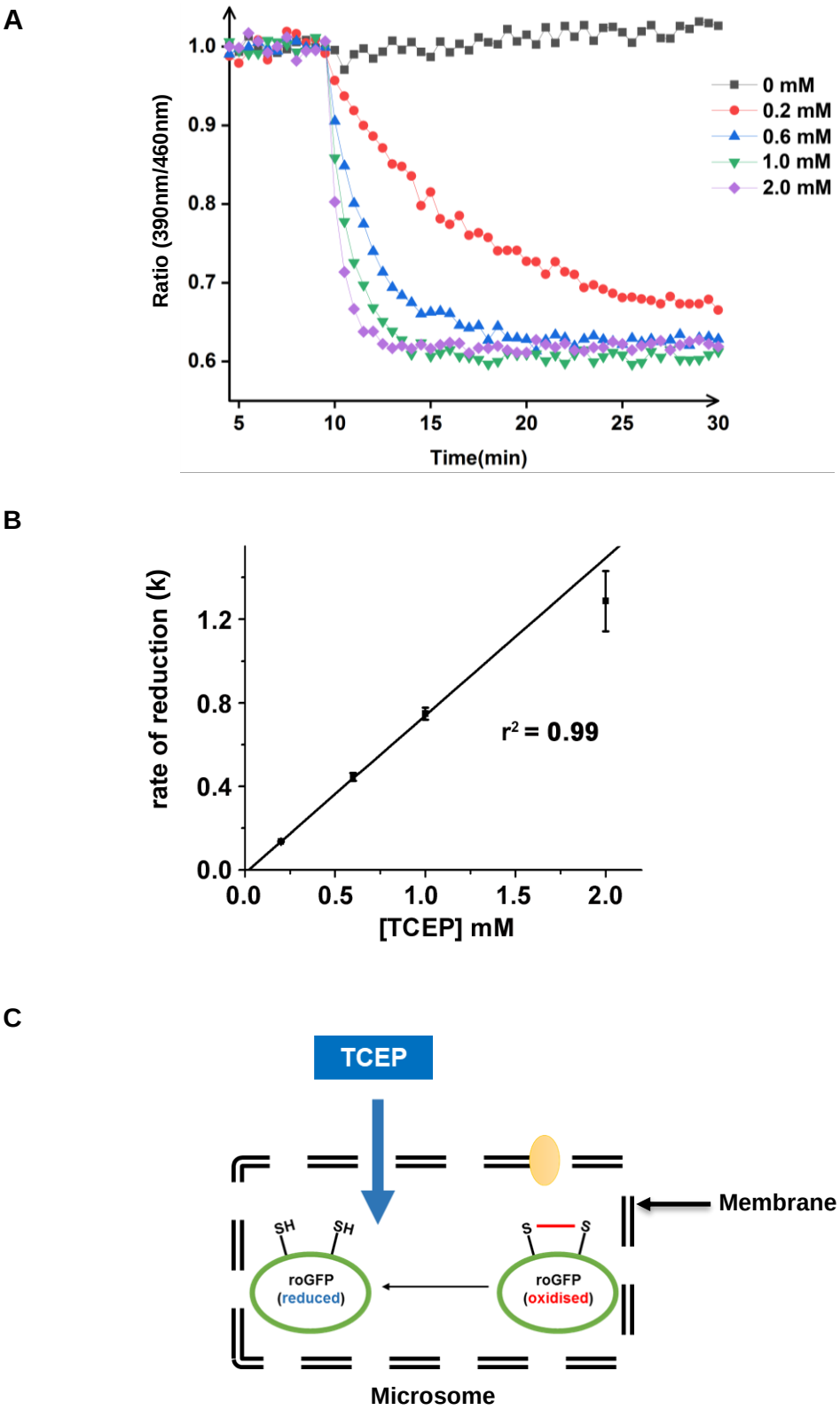

Figure 3-8 Reduction of roGFP microsomes by TCEP in the presence of 0.1% Triton™ X-100. **A**. roGFP microsomes were suspended in PBS in the presence of 0.1% Triton™ X-100 to permeabilise the microsome membrane without denaturing proteins. The experiment was carried out as above. **B**. The rate of ratio change (indicated by **k**) was calculated and analysed using Origin. **C**. Schematic diagram of TCEP reduction of roGFP in microsomes in the presence of Triton. In the

presence of Triton, the microsome membrane was permeabilised and the proteins in microsomes were exposed to TCEP. The TCEP can reduce solubilised roGFP by diffusion.

Our result above indicate that membrane proteins were involved in the reduction of roGFP in microsomes by the membrane impermeable TCEP. Integral membrane proteins may include cytosolic domains (indicated by yellow oval and brown square) or it only has ER lumen domain (indicated by red triangle) (Figure 3-9 A). To see whether a membrane protein was involved in the facilitated transport of TCEP, proteinase K, a serine protease, was used to cleave the regions of membrane proteins exposed to the outside of the microsomes (Figure 3-9 A).

Microsomes were untreated or incubated with proteinase K (final concentration 10 µg/ml and 20 µg/ml) in the presence of $CaCl_2$ (final concenrtation 10 mM) for 25 min. The proteinase K was then inactivited by a 5 min incubation with 0.5 mM PMSF. Microsomes were suspended in PBS in a 96-well microplate reader to measure the roGFP fluoresence. After obtaining a steady baseline, TCEP (final concentration 1 mM) was injected into each well. The fluoresence was continuously recorded until the signal became stable. The ratio was calculated and normalised using the ratio of roGFP in untreated microsomes (Figure 3-9B). After the addition of TCEP, the ratios of roGFP in microsomes treated with proteinase K decreased from 1 to 0.61 which is similar with the reduction in untreated microsomes (from 1 to 0.66), suggesting that the proteinase K treatment did not influence the reduction of roGFP in microsomes. This result indicates that the reduction of micrsomal roGFP by TCEP is not sensitive to proteinase K (Figure 3-9A).

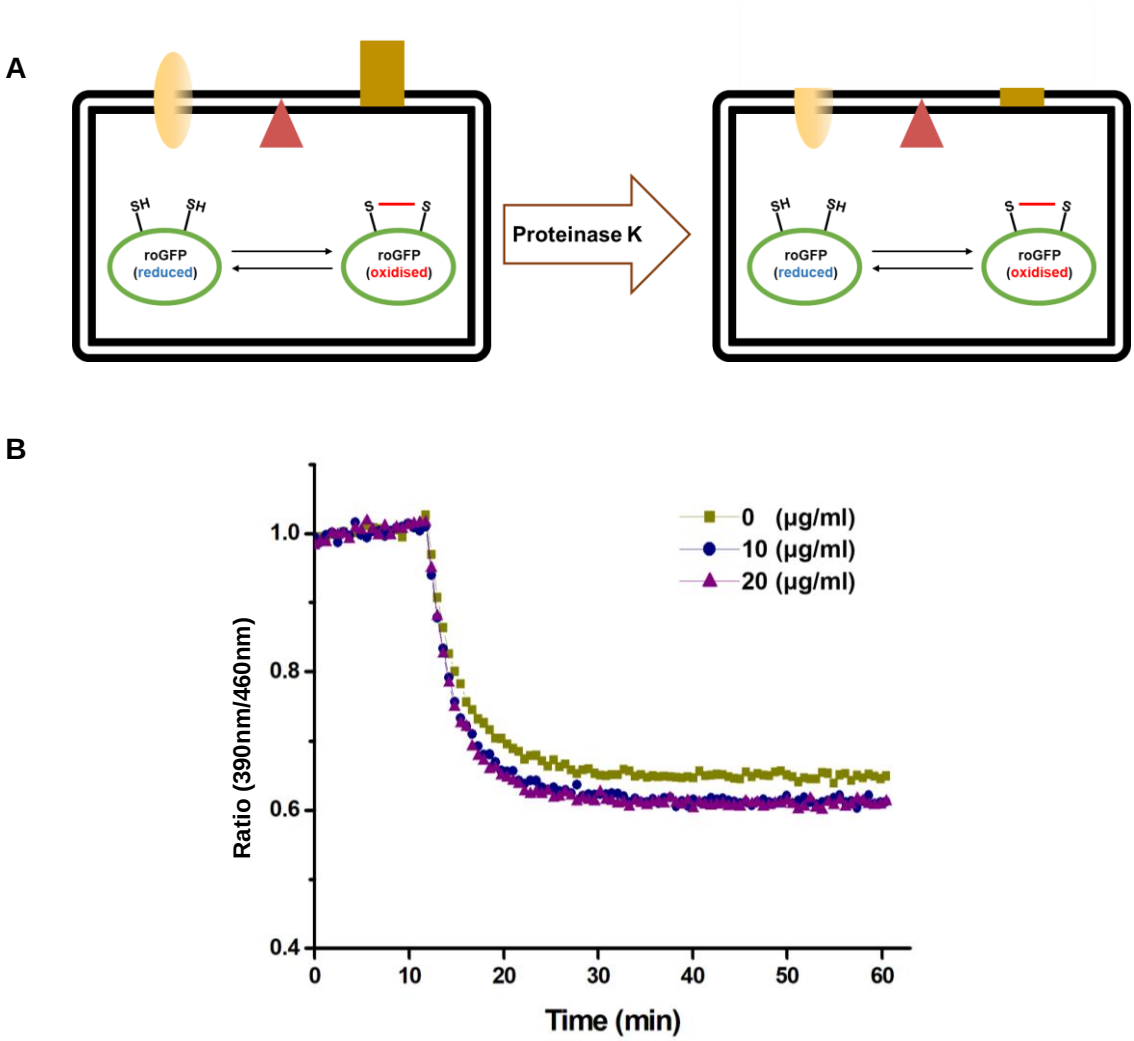

Figure 3-9 Reduction of roGFP in microsomes with and without Proteinase K treatment. A. Schematic diagram of proteinase K treatment of roGFP microsomes. Proteinase K treatment resulted in cleavage of microsomal proteins exposed to the outside of the membrane (yellow oval indicating transmembrane proteins; red triangle indicating membrane protein localised inside of the microsomes and brown square indicating membrane protein which were exposed to outside of membrane). **B**. Reduction of roGFP microsomes untreated or treated with proteinase K (two concentration 10 µg/ml and 20 µg/ml).

3.2.3 Reconstitution of the Trx/TrxR pathway

It has been demonstrated that cytosolic TrxR is required for correct disulfide formation in the ER (Poet et al., 2017). The Trx/TrxR pathway was essential for mammalian cells to transfer reducing equivalents from the cytosol to the ER. Here we addressed whether other cytosolic components were required for the transfer of reducing equivalents. A cytosolic Trx/TrxR pathway was reconstituted using purified components (G6P, G6PDH, NADPH, Trx and TrxR) to evaluate the minimal components required to facilitate reduction of microsomal roGFP. It is known that

the reduction of Trx is catalysed by TrxR using the reducing equivalents from NADPH (Holmgren and Bjornstedt, 1995, Arnér, 2009). To ensure the supply of NADPH in our reconstituted Trx/TrxR system, the addition of G6P and G6PDH can be used to recycle the oxidised NADPH ($NADP^+$) (Tian et al., 1998, Stanton, 2012) after donating the reducing equivalents to the Trx. Because of the presence of G6P and G6PDH which can continuously recycle NADPH, either commercial NADPH and $NADP^+$ can be used in our reconstituted Trx/TrxR system.

The cytosolic enzyme, G6PDH, can catalyses the conversion of G6P to PGL resulting in the reduction of NADP to NADPH that can be measured at 340 nm (Figure 3-10A) (Smolinski et al., 2019, Freeman and Willner, 2009). NADP, G6P and G6PDH were incubated together or the reaction was carried out in the absence of one component. During the incubation, the absorbance of NADPH at 340 nm was measured. It was noticed that no absorbance change at 340 nm was seen in samples in the absence of either NADP, G6P or G6PDH (Figure 3-10B). When all three components (NADP, G6P and G6PDH) were present, NADPH absorbance was observed. This result indicated that the G6PDH was active.

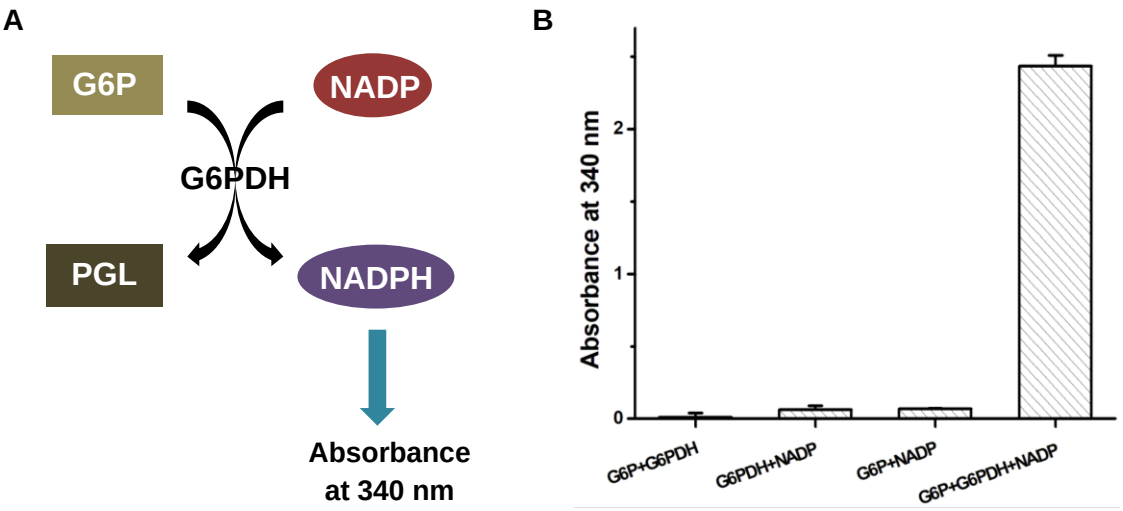

Figure 3-10 G6PDH and G6P assay. **A.** Schematic of G6PDH activity measurement. G6PDH is a cytosolic enzyme which catalyses the conversion of G6P to PGL resulting in the reduction of NADP to NADPH [2]. In order to test G6PDH activity, the experiment was designed to take advantage of the maximum absorbance NADPH at 340 nm. **B.** Absorbance of NADPH at 340 nm. NADP (100 µM), G6P (1.25 mM) and G6PDH (1 U/100 µl) were incubated in a complete reaction or reaction in the absence of one component (NADP, G6P or the enzyme G6PDH) at 30 °C. During incubation, the absorbance of NADPH at 340 nm was measured. The experiments were carried out in experimental triplicates.

In order to reconstitute the cytosolic Trx/TrxR pathway *in vitro*, human Trx (hTrx) mutants were expressed and purified (Figure 3-11). Small-scale protein expression was verified following induction of Trx expression with IPTG (Figure 3-12A). More protein at around 20 kDa was observed on the gel in the sample after IPTG induction indicating that hTrx C-C were successfully expressed (Figure 3-12A lane 1 before induction by IPTG, and lanes 2-3 after addition of IPTG). One of the colonies was used to carry out large scale of protein expression.

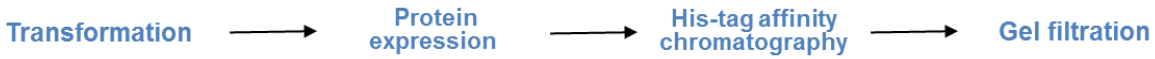

Figure 3-11 Workflow of protein induction and purification.

For large scale expression a 500 ml bacterial culture was initiated following 1/100 dilution of an overnight culture. After 3-4 hour culture, IPTG was added to induce protein expression. A portion of bacteria culture was kept to check the protein expression (Figure 3-12B). After addition of IPTG, a denser band at 20 kDa was observed (Figure 3-12B lanes 2 and 4) compared to the sample before induction by IPTG, indicating that the protein was being expressed after induction.

After induction, the bacteria were pelleted and lysed using a French press. The supernatant was collected after centrifugation and filtered through a 0.45 µm filter. The solution was loaded on a nickel agarose affinity chromatography column. Because of a poly-His-tag fused to its C-terminus, recombinant proteins hTrx CC were bound to the column and then eluted with imidazole buffer. Based on the UV absorption at 280 nm of elution buffer (Figure 3-12C), fractions were collected for analysis by SDS-PAGE under reducing condition (Figure 3-12D). The gel showed that hTrx CC was soluble (Figure 3-12D, lane 1) and hTrxCC was eluted by imidazole (Figure 3-12D, lanes 6 and 7). Some contaminating proteins were also eluted at this stage and appeared as some weak bands on Coomassie-stained gel. Hence, further purification was required.

Subsequently we used gel filtration to further purify hTrx and remove the contaminating proteins. The fractions from His-tag chromatography containing hTrx CC were gathered in one tube and concentrated to 1 ml. The sample was

loaded on an equilibrated gel filtration column. The proteins were separated based on the molecular size. Based on the UV absorption at 280 nm of elution buffer (Figure 3-12E), gel filtration fractions were analysed by SDS-PAGE under reducing conditions (Figure 3-12F). Most of the contaminants were removed at this stage. After gel filtration, fractions containing purified hTrx CC (Figure 3-12F lanes 3-5) were combined, concentrated, aliquoted and then stored at -80 ^{o}C for future assays.

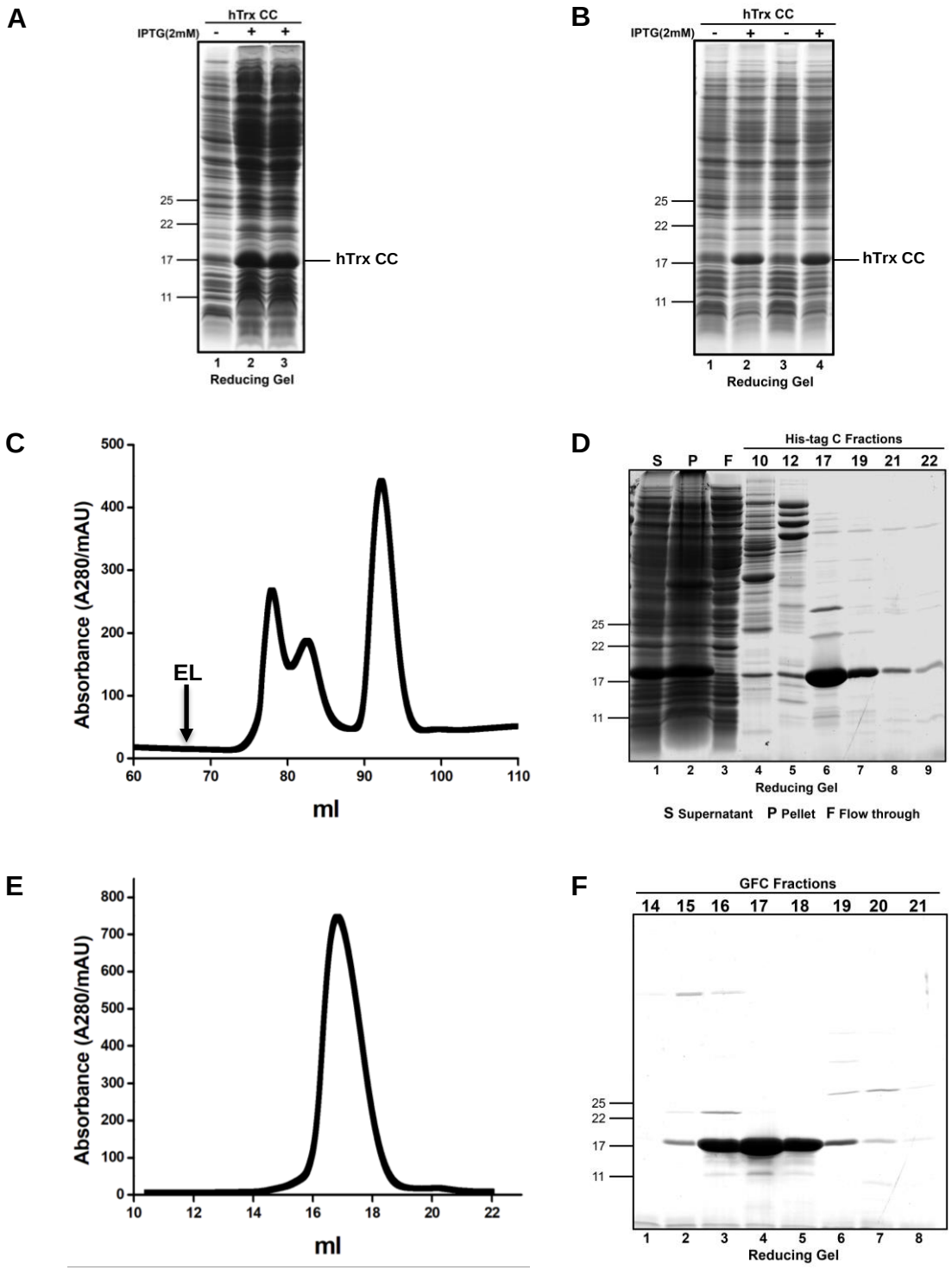

Figure 3-12 Protein expression and purification of hTrx CC. A. Small scale protein expression of two transformed colonies. Two transformed colonies were picked and cultured overnight with antibiotic (100 µg/ml ampicillin). Bacteria were inoculated (1:100) into fresh 5 ml LB with antibiotic. After 3 hours incubation, protein expression was induced by 4 hours incubation with IPTG (final concentration 2 mM). Bacteria before and after induction were analysed by SDS-PAGE under reducing conditions. The sample was visualized by Coomassie stain. A negative before addition of IPTG was regarded as control (lane 1). Both two colonies expressed hTrx CC (lanes 2 and 3). **B.** Large scale of protein expression of hTrx CC. Bacteria before (lanes 1 and 3) and after induction (lanes 2 and 4) were analysed by SDS-PAGE and visualized by Coomassie stain. **C**. His-tag chromatogram monitored at UV 280 nm of hTrx CC protein. EL, the start of elution with imidazole (range from 20 to 200 mM). **D.** SDS-PAGE analysis of various fractions of his-tag chromatography. S indicated supernatant (lane 1) and P indicated pellet (lane 2) after centrifuge of cell lysis. F indicated flow throw of nickel column (lane 3). His-tag C Fractions indicated the fractions from his-tag chromatography (lanes 4-9). **E**. Gel filtration chromatogram of hTrx CC protein. The solid line was recorded at UV absorbance of 280 nm. The single peak indicated target protein hTrx CC. **F**. SDS-PAGE analysis of various fractions of gel filtration chromatography. Based on the gel filtration chromatogram, fractions 14-21 were analysed by SDS-PAGE under reducing conditions. The majority of purified hTx CC was included in fractions 16-18 (lanes 3-5).

hTrx mutants (hTrx CS and SS) were also expressed and purified using the same protocol as above (figures not shown in thesis).

To test the quality of purified hTrx CC before the reconstitution of cytosolic Trx/TrxR pathway, the activity of purified Trx and TrxR (IMCO) were measured using an insulin reduction assay (Figure 3-13A) (Holmgren, 1979). This method is based on the reduction of insulin disulfides by reduced thioredoxin with thioredoxin reductase and NADPH as ultimate electron donor (Holmgren and Bjornstedt, 1995). At the end, DTNB can be reduced by reduced insulin and produce TNB, a yellow product that can be measured at 412 nm. Various concentrations of TrxR were used to make a standard curve (Figure 3-13B). Purified hTrx CC was used in these reactions. The TrxR activity increased linearly with the increasing concentrations of TrxR which indicated that the purified hTrx and TrxR are active and can be used to reconstitute the Trx/TrxR pathway.

A

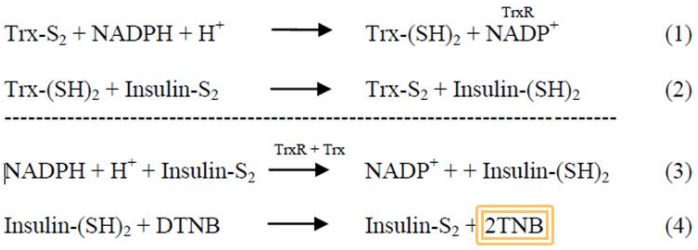

B

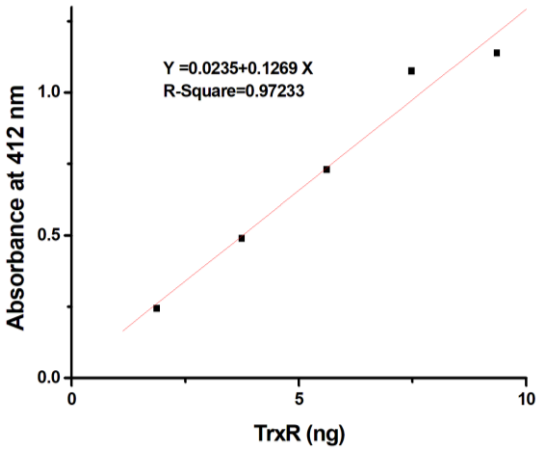

Figure 3-13 TrxR activity assay using purified Trx. A. Scheme of Trx and TrxR activity assay based on insulin assay (kTRX-01, IMCO). This method was based on the reduction of insulin disulfides by reduced thioredoxin (Trx) with thioredoxin reductase (TrxR) and NADPH as ultimate electron donor [5]. At the end, DTNB was reduced by reduced insulin to release TNB, a yellow product which can be measured at 412 nm. **B**. Standard curve of TrxR using insulin assays. Purified hTrx CC (50 µM) was used in this assay. NADPH concentration is 640 µg/ml.

3.2.4 A reconstituted Trx/TrxR pathway can reduce roGFP in microsomes

It had been demonstrated that roGFP in microsomes indicates the redox status of microsomes. We initially addressed whether a cytosolic reductive pathway composed of purified components (G6P, G6PDH, NADPH, Trx and TrxR) could reduce microsomal roGFP.

NADPH emits fluorescence at 460±50 nm when excited at 300 nm to 460 nm wavelengths (Figure 3-14) (Patterson et al., 2000, Chance et al., 1979). Because the redox state of roGFP microsomes was indicated by the ratio 390/460nm the

presence of NADPH would give background fluorescence. Therefore, the concentration of NADPH added was optimised to allow ratiometric roGFP analysis in the presence of the reconstituted pathway.

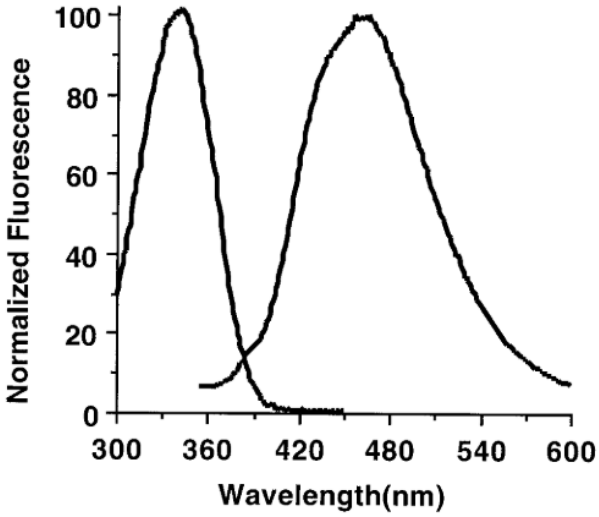

Figure 3-14 NADPH excitation and emission spectra. The excitation spectrum of NADPH was recorded from 300 nm to 460 nm wavelengths while detecting emission at 465 nm and its emission spectrum was recorded between 350 nm to 600 nm following excitation at 340 nm. (Patterson et al., 2000)

Equal quantities of microsomes were suspended in PBS in the presence of different concentrations of NADPH (0, 10, 50 and 100 μM). The emission fluorescence of roGFP in microsomes was obtained following excitation at 390 nm and 460 nm. The signal was observed for 10 min to obtain the baseline. At 10 min, diamide (final concentration 1 mM) was injected into each sample to oxidise the microsomes. DTT (final concentration 10 mM) was then injected into each sample to reduce the microsomes. The ratio (390 nm/460 nm) was calculated and normalised using the baseline ratio of roGFP microsomes in the absence of NADPH (Figure 3-15). From the line chart, the ratio was stable before addition of diamide. Larger ratio value of baseline was noticed with the increased NADPH concentration. After the injection of diamide, roGFP microsomes were oxidised and its ratio initially increased but then decreased in samples treated with 50 and 100 μM NADPH. Around 25 min, all ratio values were same. This effect at higher concentrations of NADPH is probably due to the oxidation of NADPH. After the injection of DTT (final concentration 10 mM), the ratio value decreased in all samples due to the reduction of roGFP. This result demonstrated that NADPH

gives a high background fluorescence at the higher concentrations which leads to an inaccurate measurement of the redox state of roGFP. Hence, a concentration of 10 or 50 μM NADPH was used to follow the reduction of roGFP microsomes by the reconstituted Trx/TrxR pathway.

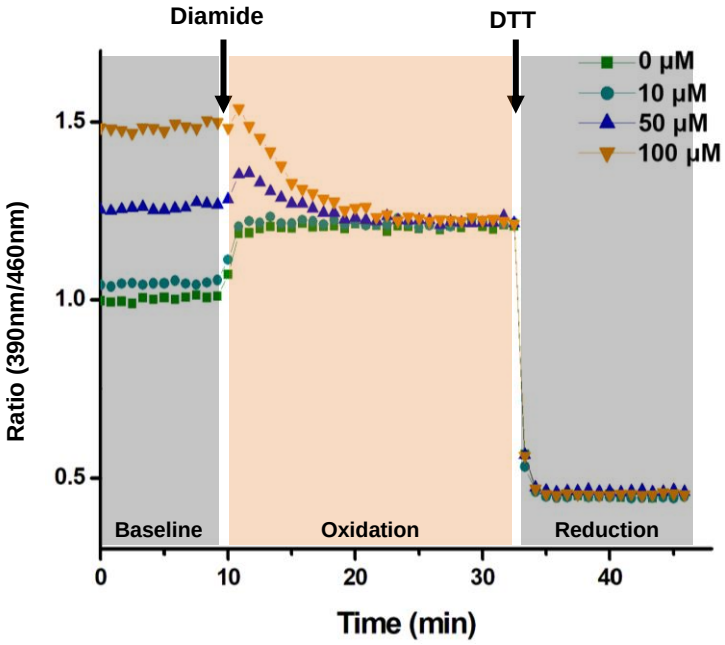

Figure 3-15 Optimisation of NADPH concentration during measurement redox state of roGFP microsomes. The same amount of microsomes was suspended in PBS in the presence of different concentrations of NADPH (0, 10, 50 and 100 μM). The emission fluorescence of roGFP in microsomes was obtained at excitation spectrum 390 nm and 460 nm. The signal was observed for 10 min to obtain a baseline. At 10 min, diamide (final concentration 1 mM) was injected into each sample to oxidise the microsomes. After the ratio reached saturation, DTT (final concentration 1 mM) was then injected into each sample to reduce the microsomes. The ratio (390 nm/460 nm) was calculated and normalised to the baseline ratio of roGFP before the addition of diamide.

To investigate if the minimal cytosolic components of cytosolic Trx/TrxR pathway can change the redox state of microsomal roGFP and whether this process is Trx-dependent, microsomes were incubated with the reconstituted Trx/TrxR pathway (Trx, TrxR, NADPH, G6P and G6PDH) using the wild type of Trx (CC) and active site mutants, Trx (CS) and Trx (SS) (Figure 3-16). Because Trx was assumed to be the protein which reacts with the membrane protein to transfer reducing equivalents to the inside of microsomes, roGFP microsomes were incubated in the absence of Trx to determine if the same reducing effect occurred. Each experiment was performed in experimental triplicate. During the incubation, the emmision fluoresence of roGFP was recorded. At the end of the experiment, the

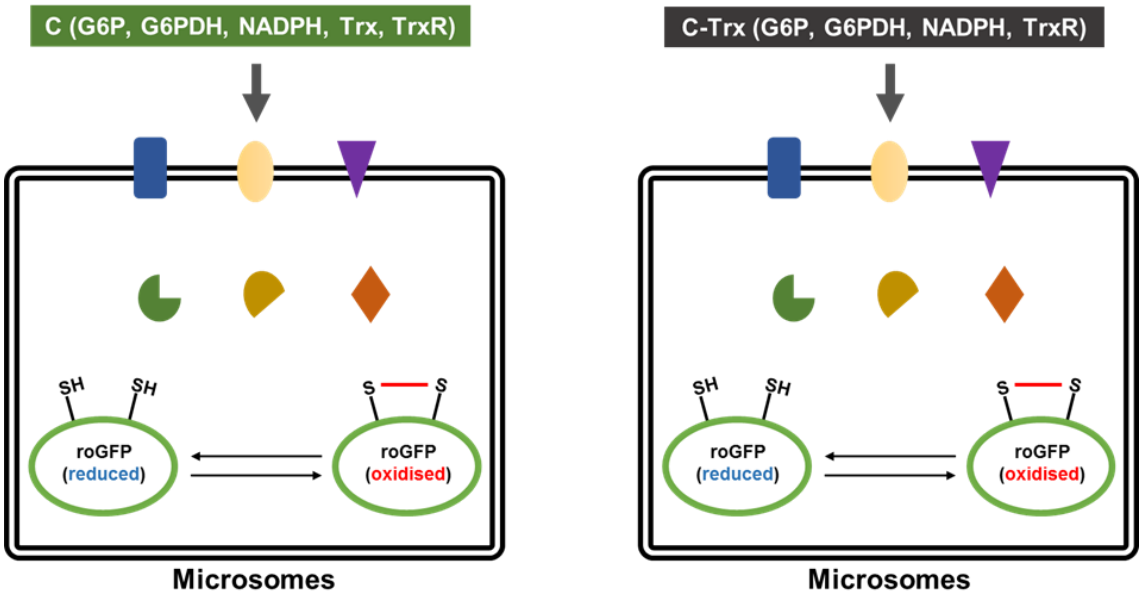

Figure 3-16 Sample preparation of roGFP microsomes. Two samples of roGFP microsomes were incubated at 30 °C with reconstituted Trx/TrxR pathway in the presence or absence of Trx using purified cytosol components (Trx, TrxR, NADPH, G6P and G6PDH). During the incubation, the emission of fluorescence of roGFP was recorded. The data was analysed to obtain a ratio value at 80 min.

ratio was calculated from each sample. The ratio value was normalised using the ratio value of roGFP microsomes treated in the absence of Trx (Figure 3-17, compare C(CC) and C-Trx). The result indicated that roGFP with the sample treated with the reconstituted Trx/TrxR pathway became more reduced than the sample treated with reconstituted Trx/TrxR pathway in the absence of Trx.

To confirm that the reducing equivalents generated outside of microsomes were passed via the Trx active site to the ER lumen, two enzymatically inactive Trx mutants, Trx (CS) and Trx (SS), were used to reconstitute the cytosolic TrxR pathway instead of wild type Trx (Figure 3-17). The ratio value at 80 min in the absence of Trx (C-Trx) was used to normalise the other three samples. The ratio value of the sample incubated with the reconstituted Trx/TrxR pathway using wild type Trx (CC) was 0.93 indicating the reduction of roGFP in microsomes. The ratio values from incubated with the reconstituted Trx/TrxR pathway using Trx mutants (CS and SS) were 1.01 and 1.00, indicating no reduction of roGFP occured. This result demonstrated that Trx was essential for transporting reducing equivalents from the outside of ER membrane to the inside.

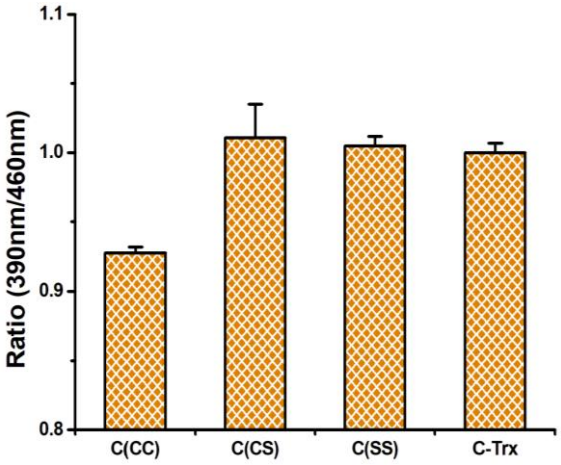

Figure 3-17 Reduction effect of the reconstituted Trx/TrxR pathway on roGFP microsomes. roGFP microsomes were incubated with reconstituted Trx/TrxR pathway using purified components (1.25 mM G6P, 1 U/100 µl G6PDH, 10 or 50 µM NADPH, 25 µM Trx and 16.25 nM TrxR) in the presence or absence of Trx. Each assay was performed in triplicate and repeated three times. During the incubation, the emission fluorescence of roGFP were recorded. At the end of the experiment, ratio was calculated and normalised with the ratio value of roGFP microsomes treated in the absence of Trx (C-Trx). C indicating complete reconstituted Trx/TrxR pathway. C(CC) indicated that the Trx with catalytic cysteine (CXXC) was used in the reconstitution of Trx/TrxR pathway. CS (CXXS) and SS (SXXS) indicated the active motif mutants.

3.2.5 Potential membrane proteins in microsomes are involved in ER reductive pathway

The experiments above showed that the reconstituted Trx/TrxR pathway using cytosolic components was able to partially reduce roGFP which was inside microsomes and the process was dependent on the catalytic cysteine of Trx. We considered if other membrane proteins and ER luminal proteins could be directly or indirectly reduced by the reconstituted Trx/TrxR pathway.

To investigate proteins influenced by the reconstituted Trx/TrxR pathway, redox proteomics were carried out (Figure 3-18A). roGFP microsomes were incubated with the reconstituted Trx/TrxR pathway in the absence or in the presence of Trx for 60 min. After incubation, the free thiols of microsomal proteins were blocked by light-iodoacetamide (IAA^L) under denaturing condition. Proteins were reduced by DTT and the free thiols which were released by reduction were then labelled by heavy-iodoacetamide (IAA^H). Each reaction was carried out in quadruplicate. Sample preparation data analysis for MS was carried out by our collaboration lab

(Sergio Lilla, Cancer Research UK Beatson Institute). The samples were prepared for liquid chromatography with tandem mass spectrometry (LC/MS/MS) by trypsin digestion followed by tandem mass tagging to enable quantification of the changes to the ratios of heavy to light peptides for each sample. The resulting data was analysed using Perseus software and presented as a volcano plot indicating the statistically significant changes to the heavy light ratios comparing the incubations +/- Trx1 (Figure 3-18B).

With the MS data analysis, the proteins whose redox state changed during treament with the Trx/TrxR pathway were identified (Table 3-1). The volcano plot results showed that the redox state of the majority of ER lumenal proteins (indicated by blue circles) became more reduced in the sample which was treated with the reconstitute Trx/TrxR pathway compared with that treated in the absence of Trx (Figure 3-18B). These results confirmed the important role of the Trx pathway in the reduction of ER proteins.

We analysed the location of proteins whose redox state changed because of the treatment with the Trx/TrxR pathway based on the information from UniProt (Figure 3-18C). They are localised to plasma membrane (PM), ER, nucleus, cytoplasm, mitochondria, lysosome, intermediate compartment, secreted pathway, and extracellular matrix (ECM). The proteins localised to the nucleus, cytosol or mitochondria which has been identified their redox status change because of the treatment with the Trx/TrxR pathway were possibly co-purified with the microsomes. The majority of proteins localised to the ER were reduced due to the incubation of the Trx/TrxR suggesting that the reducing power can be passed into the ER lumen by the cytosolic Trx/TrxR pathway. Notably, cysteine 131 of ERO1L, an endoplasmic reticulum oxidoreductase that is involved in the disulfide formation, was reduced by the Trx/TrxR pathway (Appenzeller-Herzog et al., 2008). In addition, the secreted proteins which need to form their disulfide bonds in the ER are also identified, indicating that their disulfide formation is also influenced by treatment with the Trx/TrxR pathway. The change of redox status change of several ER membrane proteins was also recognised, which suggested that they are maybe involved in the electron shuttling.

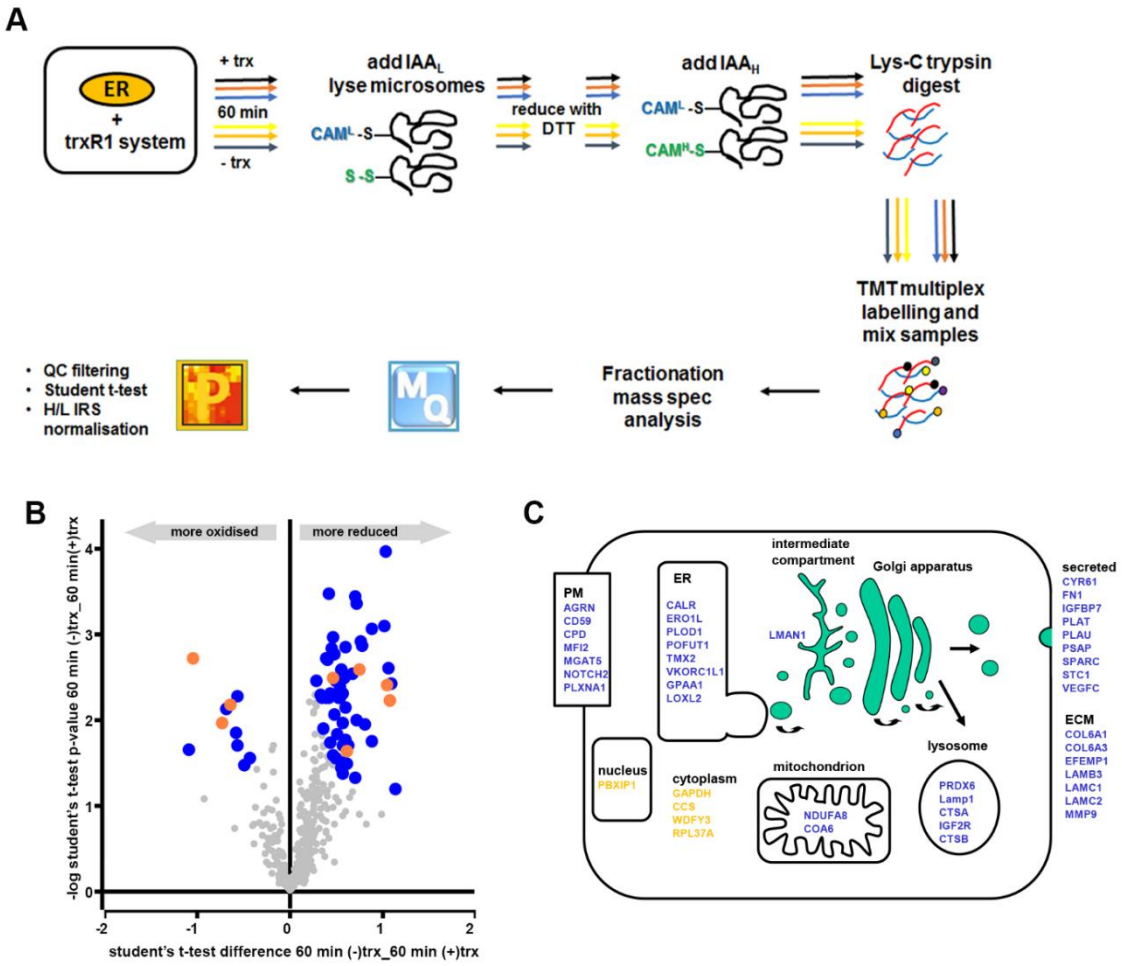

Figure 3-18 Mass Spectrometry (MS) analysis of microsome sample after incubation with reconstituted Trx/TrxR pathway in the absence or presence of Trx. A. Workflow of sample preparation and data analysis. Microsomes were incubated with the reconstituted Trx/TrxR pathway in the absence or presence of Trx for 60 min. The microsomes were then lysed in the presence of light iodoacetamide (IAA^L). The samples were subsequently reduced by DTT and released free thiols were labelled by heavy iodoacetamide (IAA^H). Following proteolytic digestion, the peptides are tandem mass tagged and fractionated prior to LC/MS/MS analysis. The data was analysed by MaxQuant and Perseus software. **B.** Volcano plot of redox state change of proteins. The blue circles indicate proteins which were in the ER while the orange circles indicate proteins which were localised to the cytosol. The redox state of proteins indicated by grey circles did not change significantly after incubation. **C.** Cartoon illustrating the final cellular location of proteins whose redox status changed significantly upon incubation of microsomes with the reconstituted Trx/TrxR pathway components. Proteins that enter the secretory pathway are in blue whereas those that do not enter the ER are in orange.

Table 3-1 List of proteins showing a significant change to their oxidised thiols along with information on their subcellular location, position and identity of the modified cysteine(s).

Location of cys modified	Gene name	protein location	type	Cysteine modified	More red/ox
cytosol	GAPDH	cytoplasm	soluble	152;156	Red
	CCS	cytoplasm	soluble	227	Red
	WDFY3	cytoplasm	soluble	952	Ox
	RPL37A	cytoplasm	soluble	39;42	Ox
	PBXIP1	nucleus	soluble	559;565	Ox
endomembrane system	COL6A1	ECM	soluble	745	Red
	COL6A3	ECM	soluble	1823;1824	Red
	EFEMP1	ECM	soluble	40;47	Red
	LAMB3	ECM	soluble	451;453;511;534;536	Red
	LAMC1	ECM	soluble	416;418;474;751;804;807;954;956	Ox
	LAMC2	ECM	soluble	28;30;53;56	Red
	MMP9	ECM	soluble	256	Red
	CALR	ER	soluble	105	Red
	ERO1L	ER	soluble	131	Red
	PLOD1	ER	soluble	267;270	Red
	POFUT1	ER	soluble	283	Red
	TMX2	ER	single-pass	59	Red
	GPAA1	ER	multi-pass	266	Red
	VKORC1L1	ER	multi-pass	50	Red

	LMAN1	ER/Golgi	single-pass	230	Red
	LOXL2	ER/secreted	soluble	395	Red
	PRDX6	lysosomal	soluble	47	Ox
	LAMP1	lysosomal	single-pass	338	Ox
	CTSA	lysosomal	soluble	239	Red
	IGF2R	lysosomal	soluble	1227	Red
	CTSB	lysosomal	soluble	211	Red
	KIDINS220	endosome	multi-pass	705	Red
	CD59	PM	GPI-anchored	70	Red
	CPD	PM	single-pass	309	Red
	MFI2	PM	GPI-anchored	199	Red
	MGAT5	PM	single-pass	338	Ox
	NOTCH2	PM	single-pass	1342;1346	Red
	PLXNA1	PM	single-pass	358	Red
	AGRN	PM/secreted	soluble	650	Red
	CYR61	secreted	soluble	337;314;317	Red
	ENDOD1	secreted	soluble	34	Red
	FN1	secreted	soluble	87;97;135;141;179;231;508	Red
	IGFBP7	secreted	soluble	156	Ox
	PLAT	secreted	soluble	419	Red

	PLAU	secreted	soluble	45	Red
	PSAP	secreted	soluble	42	Red
	SPARC	secreted	soluble	130	Red
	STC1	secreted	soluble	170	Red
	VEGFC	secreted	soluble	328	Red
mitochondrion	NDUFA8	mitochondrion	soluble	66	Red
	COA6	mitochondrion	soluble	44	Red
Unknown	NUMB	membrane	unknown	130;132	Ox
	DPY19L1	Unknown	multi-pass	647	Ox

Key: ECM; extracellular matrix, PM; plasma membrane, Ox; oxidised, Red; reduced.

3.3 Conclusion and discussion

GFP has been re-engineered to monitor redox status in living cells (Meyer and Dick, 2010). In my project, microsomes were prepared from a HT1080 cell line which stably overexpresses an ER localised roGFP (cell line was created by my colleague Marcel van Lith). It was proven that ER localised roGFP was a good indicator to monitor the real-time change of redox status of ER-derived microsomes. roGFP microsomes are a good tool to investigate the of impact of membrane impermeable reducing agent TCEP and reconstituted Trx/TrxR pathway on redox status inside microsomes.

Firstly, the membrane impermeable reducing agent TCEP was used to reduce microsomal roGFP to investigate how the reducing power outside the microsomal membrane was transported into the lumen. By using TCEP titrations in the presence or absence of Triton it was demonstrated that the reducing agent TCEP cannot cross microsomal membrane to directly reduce the microsomal roGFP. Membrane proteins were possibly facilitating the reduction of roGFP like the membrane protein, DsbD in *E. Coli* (Stewart et al., 1999). However, proteinase K treatment did not prevent the reduction of microsomal roGFP, which indicated

that the membrane protein that facilitated transportation of reducing power might not contain a cytosolic domain, or the reduction of the membrane protein by TCEP was not affected by proteinase K treatment.

It has been demonstrated previously in our group that cytosolic thioredoxin reductase 1 was required for correct disulfide formation in the ER (Poet et al., 2017). It was also showed that cytosolic NADPH was the ultimate electron donor for reduction in the ER. The role of other components needed to reduce non-native disulfides in the ER and which the reducing equivalents generated in cytosol are transferred into the ER, remain to be addressed. Here, we used known minimal cytosolic components in the Trx/TrxR pathway (G6P, G6PDH, NADPH, Trx and TrxR) to reconstitute the cytosolic reductive pathway. The microsomes were incubated with reconstituted Trx/TrxR pathway components in the presence or absence of Trx. roGFP was reduced after incubation with complete reconstituted Trx/TrxR pathway components whereas no reduction occurred in the absence of Trx. In addition, the reconstituted Trx/TrxR pathway using the Trx mutants, Trx CS and SS, was not able to reduce microsomal roGFP. The results demonstrate that the reduction of microsomal roGFP was dependent on the catalytic cysteines in either Trx motif (CXXC). We assumed that the reducing power which was generated by the reconstituted Trx/TrxR pathway was finally transported by the disulfide exchange between Trx and a membrane protein which contains redox-active cysteine residues as part of their active sites (Holmgren, 1989). Reduced Trx could reduce disulfide bonds within the membrane protein and then the roGFP was directly or non-directly reduced by this membrane protein. Based on this assumption, a Trx-trapping technique was considered to be used to potential trap this membrane protein in the future (Schwertassek et al., 2007b) . The catalytic cysteine can form a transient intermediate with its substrate protein by disulfide which is ususally resolved by Cys^{35}. The Trx mutant, Trx(CS), can not resolve the transient intermediate allowing us to trap and indentify the ER membrane proteins (Schwertassek et al., 2007b). It is possible to trap the membrane protein that is involved in the disulfide shuttling from the outside to the inside.

A proteomic experiment was carried out to identify proteins whose redox status was changed after incubation with the reconstituted Trx/TrxR pathway with or without Trx. The redox status of several peptides changed during the incubation with the complete reconstituted Trx/TrxR pathway. The analysis of protein

location showed that the majority of the corresponding proteins were located in the ER lumen. The results demonstrated that several thiols within endogenous proteins that were synthesised in the ER, including thiols that form structural and regulatory disulfides, can be reduced by the thioredoxin reduction system. Notably, ERO1L which mediates disulfide bond formation via PDI (Appenzeller-Herzog et al., 2010), was reduced during the incubation with the complete reconstituted Trx/TrxR pathway. *In vivo*, the ERO1 can reoxidise the PDI after they passed their disulfide to their substrate proteins. Furthermore, the regulatory Cys^{131} of ERO1 was identified by our proteomic experiment. It was previously shown that the Cys^{131} in ERO1 can compete with the free thiols in substrate proteins to form disulfide bond with the catalytic Cys^{94}, which is an feedback loop that play critical role in the reodx control in the ER (Appenzeller-Herzog et al., 2008, Baker et al., 2008). Due to the incubation with the Trx/TrxR system, more reduced PDI became substrates for ERO1 resulting in the release of the free thiol at Cys131. In addition, the reduction of microsomal proteins suggested that the reducing equivalents were transduced into the microsomal lumen. Because Trx in our recontituted Trx/TrxR pathway are ER membrane impermeable, it indicated the requirement for a membrane protein involved in the electron transport. The reduction of several microsomal membrane proteins due to the incubation with the Trx/TrxR complete system were also identified by the proteomic experiment, such as thioredoxin-related transmembrane protein 2 (TMX2), glycosylphosphatidylinositol anchor attachment 1 protein (GPAA1), vitamin K epoxide reductase complex subunit 1-like protein 1 (VKORC1L1), human lectin mannose-binding 1 (LMAN1). Whether they are the membrane proteins that are responsible for the transportation of reducing equivalents will be investigated in our future work.

Chapter 4 Trx/TrxR pathway can reduce ER localised ERp57 via a membrane protein

4.1 Introduction

Numerous enzymes are localised in ER to ensure the protein folding process. PDI are a family of enzymes which facilitate reduction, oxidation and isomerisation of disulfide bonds (Figure 4-1). It was demonstrated that a member of the PDI called ERdj5, which had previously been shown to have a role in ERAD (Ushioda et al., 2008), plays a crucial role in the reduction of non-native disulfides formed during productive folding (Oka et al., 2013). In addition, previous research suggests that another PDI, ERp57, has a specific role in the isomerisation of non-native disulfide bonds in specific glycoprotein substrates (Jessop et al., 2007).

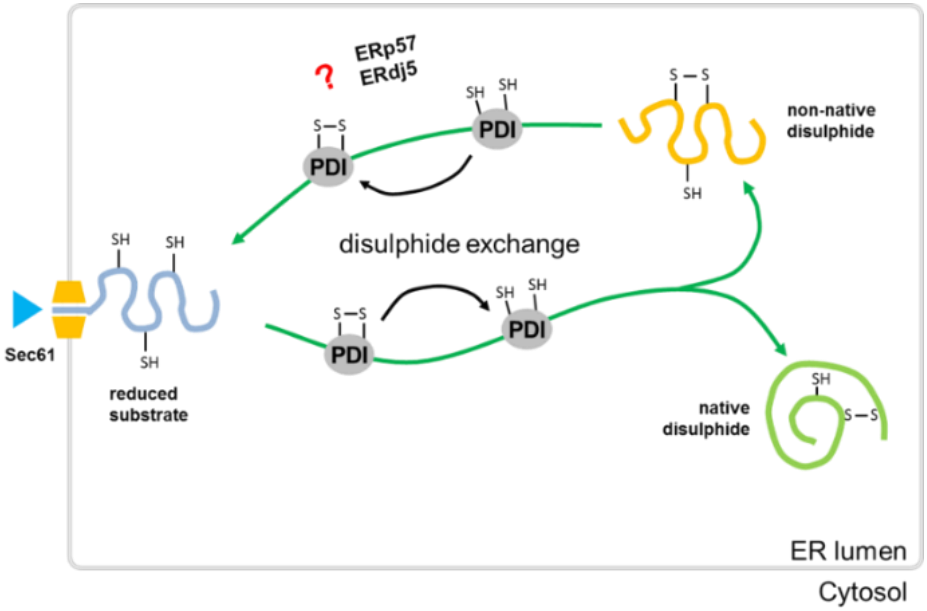

Figure 4-1 Disulfide formation and reduction. The insertion of disulfide bonds catalysed by PDI. Insertion of disulfide bonds could result in native disulfides, which can be found in the correctly folded and functional protein structure, and non-native disulfides which are not present in the native protein. It was demonstrated that ERp57 and ERdj5 play crucial role in reduction of non-native disulfide (Jessop et al., 2007, Oka et al., 2013). However, our understanding of reduction of non-native disulfides is still limited.

The ER protein ERp57 is one member of the PDI family (Oliver et al., 1999) with the alternate names ER-60, ERp60, ERp61, GRP58, P58, HIP-70, Q-2 or Pdia3 (Coe

and Michalak, 2010, Zapun et al., 1998). It is a 58-kDa thiol oxidoreductase which contains two thioredoxin-like active site motifs (CGHC) (Figure 4-2 A) (Tian et al., 2006, Bourdi et al., 1995, Coe and Michalak, 2010). ERp57 exhibits a variety of different functions. ERp57 was demonstrated to be part of the glycoprotein-specific quality control machinery in the ER lumen (Oliver et al., 1997) and it specifically interactes with newly synthesised glycoproteins to influence protein folding during calnexin/calreticulin cycle (Oliver et al., 1999). It also was shown that ERp57 plays a crucial role in isomerisation of non-native disulfide in a distinct set of secreted proteins (Jessop et al., 2007). Following the reduction of substrate protein, a PDI reductase like ERp57 become oxidised. To maintain the activity of ERp57 as a reductase, a reductive pathway is required to reduce the oxidised ERp57 in the ER.

It was shown that the redox state of ERp57 was not influenced by over-expression of Ero1-La suggesting specific pathways control oxidative protein folding in the ER (Mezghrani et al., 2001). After disulfide exchange with substrate protein, how ERp57 becomes reduced is to be addressed here. Our group found that a robust cytosolic Trx/TrxR pathway and cytosolic NADPH were essential for correct disulfide formation (Poet et al., 2017). To investigate if redox state of the ER can be maintained by cytosolic Trx/TrxR pathway, ERp57, was chosen to be a substrate to indicate the impact of the cytosolic Trx/TrxR pathway on its redox state. We optimised the assay to determine the redox status of endogenous ERp57 in a HT1080 cell line and a HT1080 cell line which stably overexpresses ERp57-V5 tagged protein. The effect of the reconstituted Trx/TrxR pathway on the redox status of ERp57 was determined.

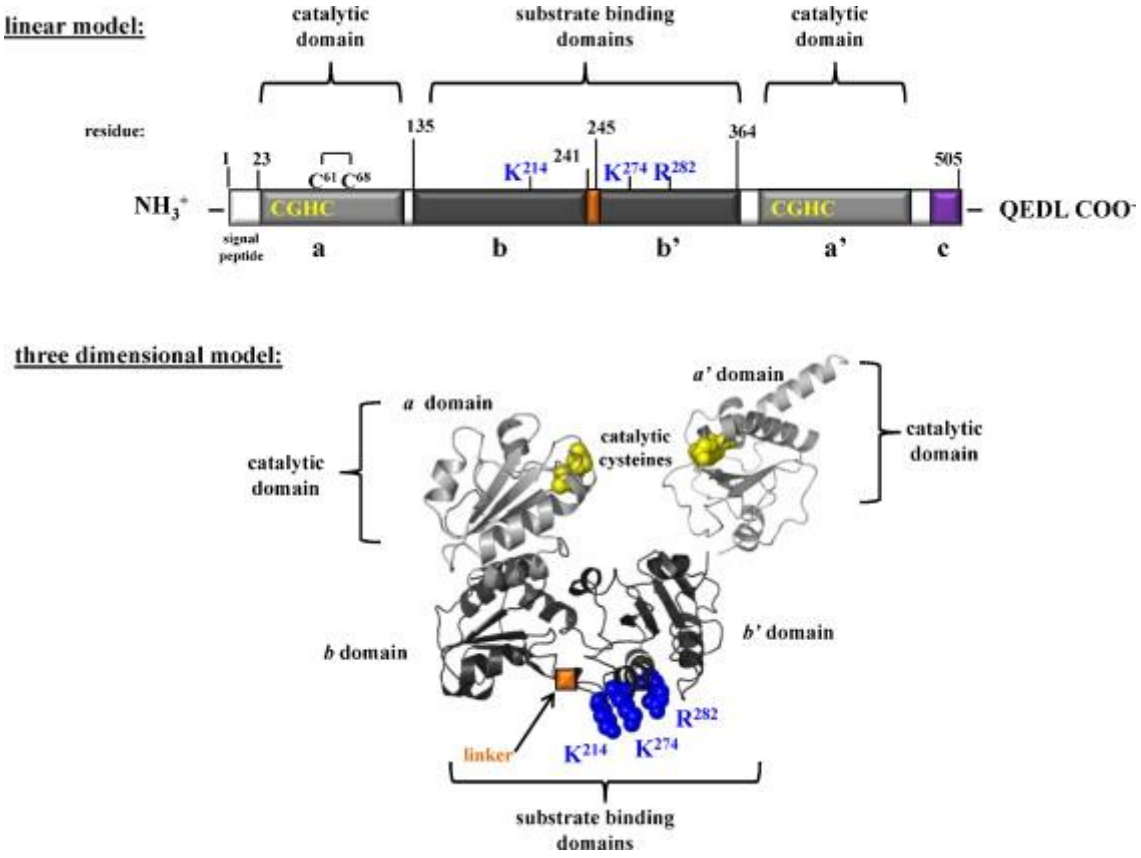

Figure 4-2 A linear representation of ERp57 and three-dimensional model of ERp57. The protein contains an N-terminal amino acid signal sequence and a C-terminal QDEL ER retention signal. In both the linear and three-dimensional model, the catalytic a and a' domains are shown in light grey while the substrate binding b and b' domains are shown in dark grey (Coe and Michalak, 2010). The yellow amino acids indicate the catalytic residues CGHC and the blue amino acids indicate residues involved in calnexin binding. In the linear model, the short linker between the b and b' domains is marked in orange and the basic C terminal is marked in purple. Three-dimensional model of the a b b' a' domains based on NMR studies of the a and a' domain of PDI (Tian et al., 2006) and the b and b' domains of ERp57 (Kozlov et al., 2006).

4.2 Results

4.2.1 Determining the redox state of ERp57

An important aspect of the project will be to determine the PDI family member responsible for catalysing the reduction of non-native disulfides within client proteins. To evaluate the process of reduction we will need to determine the redox status of the PDI family members which are most likely to be involved in this reductive step. It has previously been demonstrated that ERp57 is required

to catalyse the isomerisation of non-native disulfides both for correct folding and for reduction prior to degradation (Bulleid, 2009, Jessop et al., 2007).

To establish an assay for determining the redox status we sought to reproduce work carried out previously (Jessop and Bulleid, 2004, Oka et al., 2015). In live cells, ERp57 exists as a mixture of two redox states: oxidised and reduced. After treatment with NEM, the free thiols in reduced ERp57 can be alkylated with the membrane permeable alkylating reagent NEM, while the oxidised thiols within ERp57 will not be. The samples were denatured by boiling with 2% SDS and were reduced by TCEP to break the existing disulfide bond in oxidised ERp57. Newly reduced ERp57 was then alkylated with AMS which has a larger molecular weight than NEM. The samples modified with AMS have a slower mobility than the protein modified with NEM. Hence, the redox state of ERp57 in intact or SP cells can be identified by the different mobility on the gel (Figure 4-3A).

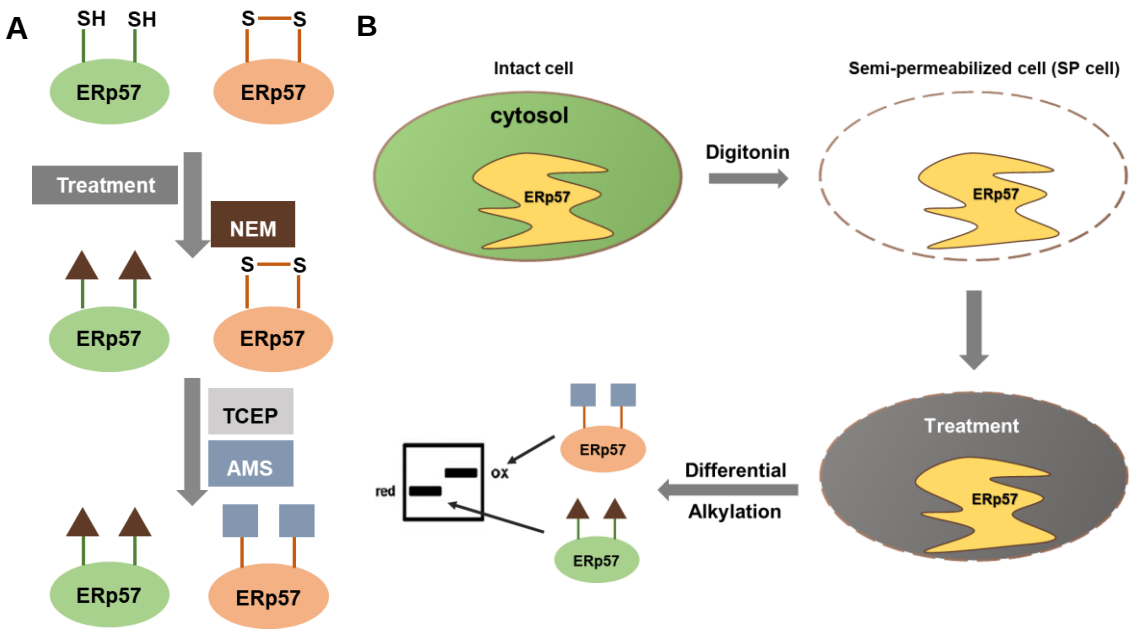

Figure 4-3 Determining the redox state of ERp57. A. Schematic diagram of the protocol for determining the redox state of ERp57. In intact or SP cells, there are two forms of ERp57, reduced form (green oval) and oxidised form (orange oval). The free thiols in reduced ERp57 will be blocked by alkylating agent NEM (molecular weight: 125.13) (brown triangle). After reduction by the reducing agent TCEP, existing disulfides in oxidised ERp57 were broken followed by the alkylation by another alkylating agent AMS (molecular weight: 466.4) (blue square) which has larger molecular weight than NEM. Different redox states of ERp57 will identified by the electrophoresis mobility shift on gel because of the different molecular weight between NEM and AMS. **B.** Schematic diagram of determination of ERp57 redox state in SP cells. SP cells were prepared from confluent flask of HT1080 cells. SP cells were untreated or treated with diamide or DTT in KHM buffer. Redox state

of ERp57 was then determined by differential alkylation which can be visualised on SDS-PAGE gel by the different mobility. Blue squares indicate alkylating agent AMS; brown triangles indicate smaller alkylating agent NEM.

To optimise the protocol for detection of ERp57, two antibodies (R282 and 283) and different blocking agents (milk and BSA) were tested in the western blot. HT1080 cells were lysed and the resulting lysate was denatured and separated by SDS-PAGE. The proteins were transferred from the gel to a nitrocellulose blotting membrane followed by blocking with different blocking agents, 3% BSA and milk. The membranes were incubated with different primary antibodies (R282 and 283). After incubation with rabbit 800 secondary antibody, the membranes were scanned by Li-Cor Odyssey 9260 Imager to obtain image (Figure 4-4A). The result shows that less background bands were observed using 3% milk (Figure 4-4A lanes 1, 2 and 5, 6) rather than using 3% BSA (Figure 4-4A lanes 3, 4 and 7,8) as blocking agent. More compact and clear bands revealed when using R283 (Figure 4-4A lanes 5 and 6). Blocking agent 3% milk and primary antibody, rabbit 283, would be used in later experiments.

To address the redox state of ERp57 in SP cells, the SP cells were untreated (UT), treated with DTT (DTT) or diamide (Dia) at room temperature. The samples were then treated with 25 mM NEM to block free thiols followed by 2 times KHM wash to remove excess NEM. Redox state of ERp57 was determined as above (Figure 4-3A). Samples were then separated by SDS-PAGE and visualised by western blot. Two bands and several background bands were observed in all three samples no matter if the sample were untreated, oxidised or reduced (Figure 4-4B lanes 1-3). To optimise the protocol, PBS was used instead of KHM buffer to remove excess NEM. Clearer bands were noticed. In untreated SP cells, two bands were observed: an upper band and a lower band (Figure 4-4B lane 4). The lower band migrated with the band in sample reduced by DTT (Figure 4-4B lane 5) indicating reduced form of ERp57. The upper band migrated at the same position with as the band in oxidised sample (Figure 4-4B lane 6) indicating oxidised form of ERp57. This result suggested that PBS buffer was better than KHM buffer in washing sample to remove excess NEM.

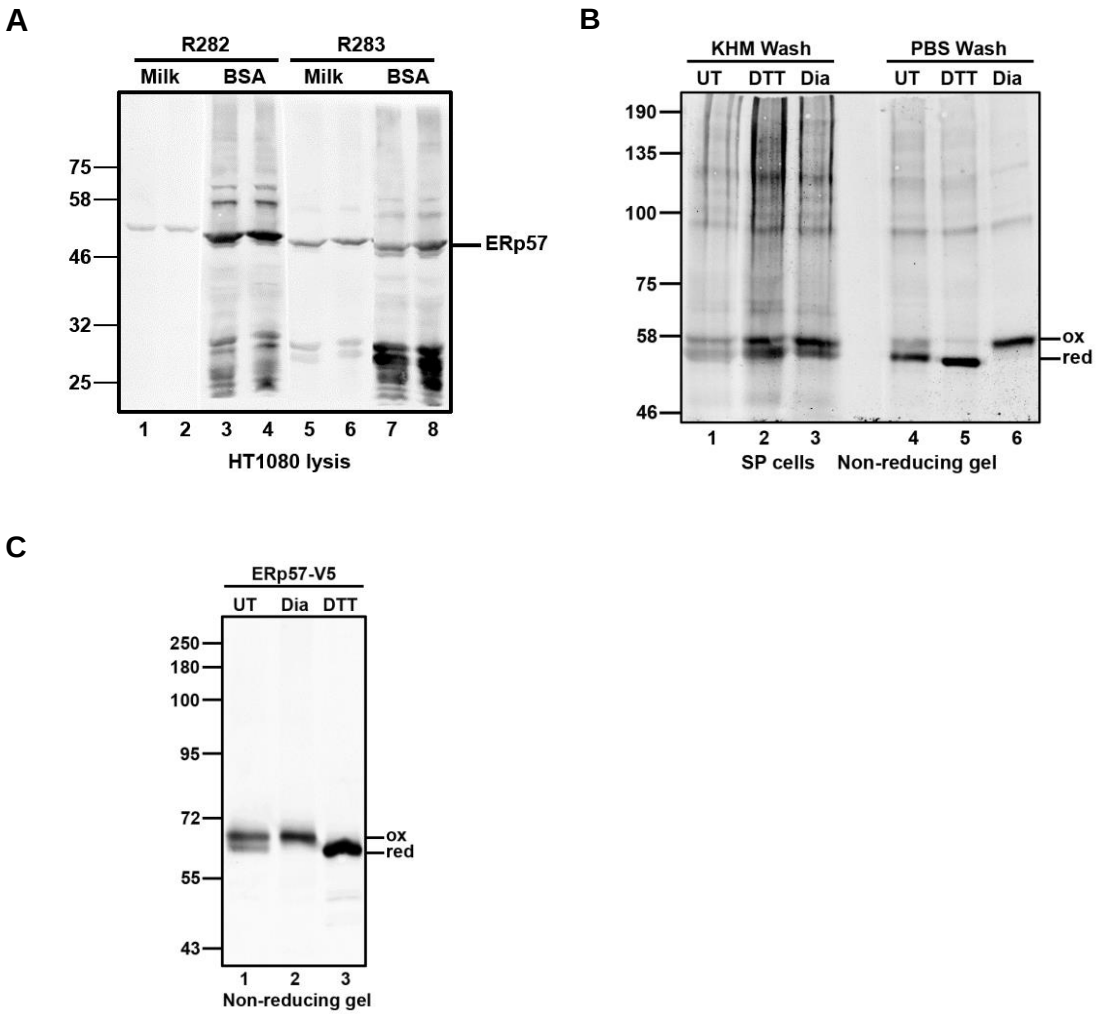

Figure 4-4 Optimisation of determination of ERp57 redox state. A. Optimisation of blocking agent (3 % BSA and milk) and primary antibody (R282 and R283) in western blot. HT1080 cell lysis were separated by SDS-PAGE. Proteins were then transferred to blotting membrane and cut into four pieces. The membranes were separately blocked using two different blocking agents (3 % BSA and milk) followed by incubation with primary antibody (R282 or R283). After incubated with secondary antibody, the membrane was scanned by Li-Cor Odyssey 9260 Imager to obtain the image. **B.** Comparison of KHM buffer wash and PBS wash. SP cells were prepared from confluent HT1080 cell flask. The SP cells were untreated (UT) and treated with DTT and diamide (Dia) at room temperature. After treatment, the sample were treated with 25 mM NEM in PBS to block free thiols. The excess NEM was removed by KHM or PBS washing. Reducing agent TCEP was used to break existing disulfide bonds in oxidised ERp57. The free thiols were then incubated with a larger alkylating agent AMS. The sample was separated by SDS-PAGE and western blot (3% milk, R383 primary antibody) was carried out to visualise the proteins. **Ox** indicating oxidised ERp57 and **red** indicating reduced form of ERp57. **C.** HT1080 cell line which can stably overexpress ERp57 including a V5 tag (ERp57-V5) which can be easily identified by anti-V5 antibody was used in the determination instead of untransfected HT1080 cell line.

Another option for determining the redox state of ERp57 was using HT1080 cell line which can stably overexpress a V5-tagged ERp57. ERp57-V5 can be easily identified by anti-V5 antibody. This cell line was created by my colleague Marie Ann Pringle. The determination of ERp57 was carried out as above. Anti-V5 antibody was used as the primary antibody in the western blot and then was incubated with Mouse 800 secondary antibody. Stronger bands and less background bands were observed (Figure 4-4C). It was noted that the reduced form ERp57 (lower band) (Figure 4-4C lane 3) can be distinguished from the oxidised form of ERp57 (higher band) (Figure 4-4C lane 2). There were two forms of ERp57 in untreated HT1080 ERp57-V5 SP cells which was consistent with HT1080 SP cell. The result demonstrated that the ERp57-taggged HT1080 cell line was a good cell line to study redox state change of ERp57.

4.2.2 The Trx/TrxR pathway can reduce oxidised ERp57

It has been demonstrated that ERp57 was required for the disulfide isomerisation of non-native disulfides both for correct folding and for reduction prior to degradation. We recently demonstrated that the reconstituted Trx/TrxR pathway was able to reduce roGFP in microsomes (chapter 3). We considered if the reconstituted Trx/TrxR pathway could change the redox state of ERp57.

In order to investigate if the reducing power is from cytosol, the redox status of ERp57 in the SP cells is determined in RRL, cell extract which was prepared from HT1080 cell line, the cell extract treated with PD-10 column that has been removed the cytosolic small molecules, and KHM buffer which has been used in SP cell preparation.

SP cells were prepared from confluent HT1080 cell flask which is not transfected. The SP cells were untreated (UT) and treated with DTT (DTT) or diamide (Dia) at room temperature as controls. Because it was demonstrated that the addition of G6P can promote correct disulfide bond formation, the other samples were incubated at 30^{o}C for 60 min in the absence or presence of G6P in KHM buffer or RRL in order to investigate if the addition of G6P can influence the redox status of ERp57 in SP cells. The sample were then treated with 25 mM NEM in PBS to block free thiols. The excess NEM was removed by two washes with PBS. The reducing agent TCEP was used to break existing disulfide bonds in oxidised ERp57.

The free thiols were then alkylated by a larger alkylating agent AMS. The sample was separated by SDS-PAGE and western blot was carried out to visualise the proteins as above. One upper band (ox) was observed in the oxidised sample (Figure 4-5A lane 1) while one lower (red) was noticed in the reduced SP cells (Figure 4-5A lane 2). Two bands showed in UT SP cells which indicated that there were two redox sates of ERp57: oxidised and reduced form (Figure 4-5A lane 3). Similar bands were observed in SP cells in the absence or presence of G6P (Figure 4-5A lanes 4 and 5). This result demonstrated that the incubation in KHM buffer did not change ERp57 redox state and the cytosolic component, G6P, cannot reduce ERp57 on its own. A compact lower band (indicating reduced form of ERp57) was observed in the sample which was incubated in RRL in the presence or absence of G6P (Figure 4-5A lanes 6 and 7). It demonstrated that there were reducing equivalents in RRL resulting the reduction of ERp57.

Since cell extract was prepared from the cell line which was also used to generated SP cells, the cell extract and the cell extract that was filtered through the PD-10 column to remove the small cytosolic molecules, were incubated with SP cells in order to determine if the reducing power originated in the cytosol. To make it easier to visualise the redox change after the incubation in cell extract, the SP cells were fully oxidised by 10 mM diamide in KHM buffer and the excess diamide was removed by KHM buffer washing before incubation in cell extract. One upper band (indicating oxidised ERp57) was observed in SP cells which were incubated in KHM buffer alone (Figure 4-5B lane 1). This indicated that the incubation in KHM buffer does not change the redox state of ERp57 which was consistent with the result we obtained previously. When the SP cells were incubated in cell extract (CE), one strong lower band (red) and a faint upper (ox) appeared indicating that cell extract reduced the oxidised ERp57 during the incubation (Figure 4-5B lanes 2 and 3). No reduced band occurred if the SP cells were incubated in the cell extract that was filtered through a PD-10 desalting column (GE Healthcare) (Figure 4-5B lane 4). This absence of reduction was possibly caused by the PD-10 desalting column removing small molecular components in the cytosol, such as G6P, NADPH and glutathione.

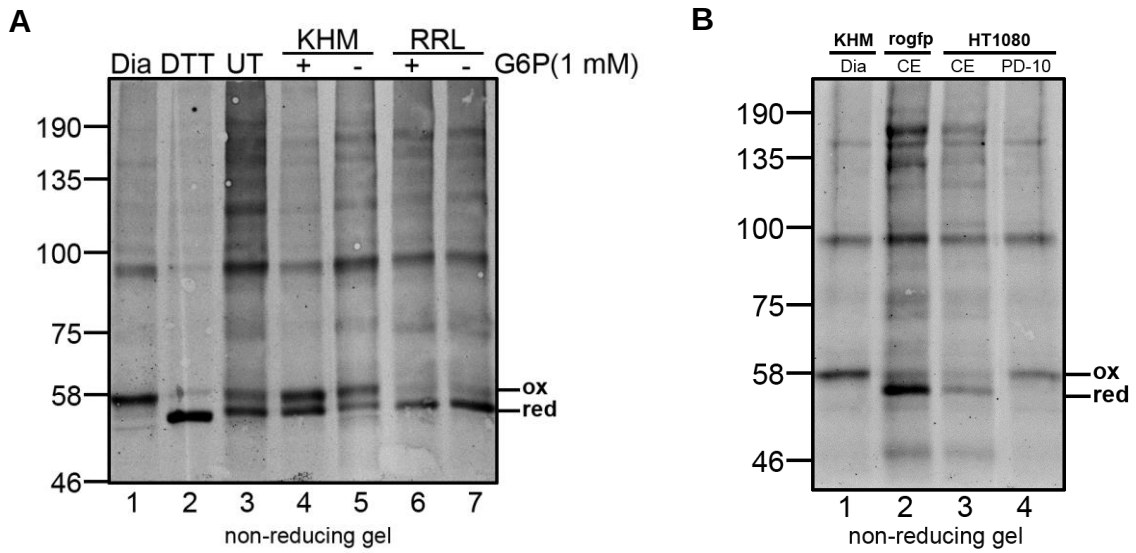

Figure 4-5 Incubation of SP cells in KHM buffer didn't change redox state of ERp57. A. SP cells were prepared from confluent untransfected HT1080 cell flask. The SP cells were untreated (UT) and treated with DTT (DTT) or diamide (Dia) at room temperature. The other samples were incubated at 30 ^{o}C for 60 min in the absence or presence of G6P in KHM buffer or RRL. After treatment, the sample were incubated with 25 mM NEM in PBS to block free thiols. The excess NEM was removed by 2 times PBS wash. Reducing agent TCEP was used to break existing disulfide bonds in oxidised ERp57. The free thiols were then reacted with a larger alkylating agent AMS. The sample was separated by SDS-PAGE and western blot was carried out to visualise the proteins. **Ox** indicating oxidised ERp57 and **red** indicating reduced form of ERp57. **B.** Cell extract from HT1080 cell line (HT1080 CE) and HT1080 cell line which expressed roGFP can reduce oxidised ERp57 (roGFP CE) while the cell extract which was filtered through a PD-10 column to remove small molecular components cannot reduce oxidised ERp57. SP cells were prepared from confluent HT1080 cell flask. All SP cells were first oxidised by 10 mM diamide. KHM buffer washing was used to remove excess diamide. The SP cells were incubated in KHM buffer, roGFP CE or HT1080 CE with or without filtration. The redox state was then determined by differential alkylation as above.

Based on the experiments result above, KHM buffer was chosen to be the buffer to reconstitute cytosolic Trx/TrxR pathway using purified components (1 mM NADPH, 25 μM human Trx (expressed and purified as above), 16.25 nM human TrxR (IMCO) or 600 nM Yeast TrxR (expressed and purified by Jana Rudolf), 1.25 mM G6P, 1 U G6PDH) to see if a reconsituted Trx/TrxR pathway can reduce ERp57.

SP cells were generated from HT1080 cell line and HT1080 ERp57-V5 cell line respectively. SP cells were first fully oxidised by diamide. Oxidised cells were then treated with DTT, complete Trx/TrxR pathway in the presence or absence of Trx, glutathione, or Trx alone. The redox status of ERp57 was determined by differential alkylation and a western blot was carried out to visulise proteins.

In the untreated samples, ERp57 appeared as two bands after AMS treatment where the upper band indicated oxidised ERp57 and the lower band indicated reduced ERp57 (Figure 4-6 A lane 7, B and C lane 6). A single upper band showed that the ERp57 was fully oxidised after diamide treatment (Figure 4-6 A lane 5, B and C lane 1). Two redox forms of ERp57 were observed in SP cells which had been incubated with complete Trx/TrxR system (Figure 4-6 A lane 1, B and C lane 3) indicating that reduction of oxidised ERp57 happened following incubation with the reconstituted Trx/TrxR pathway. In one sample the human TrxR (Ch) was replaced with yeast TrxR (Figure 4-6 B lane 4) and the reduction of ERp57 also occurred. However, no reduced band occurred in the sample which was treated with the reconstituted Trx/TxR system in the absence of Trx (Figure 4-6 A lane 2, B lane 5 and C lane 5). No ERp57 was reduced in sample which was treated with Trx alone (Figure 4-6 C lane 4). In addition, incubation with glutathione lead to reduction of ERp57 in SP cells (Figure 4-6 A lane 3 and 4). These results demonstrated that the reconstituted Trx/TrxR pathway outside of ER can reduce ERp57 inside the ER membrane and this reduction process was dependent on Trx. In addition, the addition of GSH can reduce the oxidized ERp57 and the reduction impact is more powerful than the Trx/TrxR pathway.

The results above demonstrate the importance of Trx in the reduction of ERp57. To investigate how Trx can reduce ERp57 in the ER, we determined the redox state of the Trx after incubation with the complete reconstituted Trx/TrxR pathway. The method for determination of Trx redox state was similar to the determination of ERp57 redox state i.e. by differential alkylation using NEM and AMS. Purified Trx was incubated in KHM buffer including or not including cytosolic components (NADPH, G6P, G6PDH and TrxR). After incubation, free thiols in Trx were blocked by NEM. Reducing agent was used to break existing disulfides and then AMS was used to alkylate the free thiols. Because of the different mobility on the gel, the reduced form of Trx (alkylated by NEM) ran faster on the gel while the oxidised form of Trx (alkylated by AMS) was slower. Two redox forms were observed when Trx was only incubated in KHM buffer (Figure 4-6D lane 1). The upper band indicated that there was oxidised Trx. Only one lower band was observed when Trx was incubated with other cytosolic components in TrxR pathway. This result indicated that the reduction of ERp57 in the ER requires fully reduced Trx. Because Trx was membrane impermeable, proteins localised to the ER membrane

might be involved in electron-shuttling from outside to inside of membrane after disulfide bond with the reduced Trx to further influence ER proteins like ERp57.

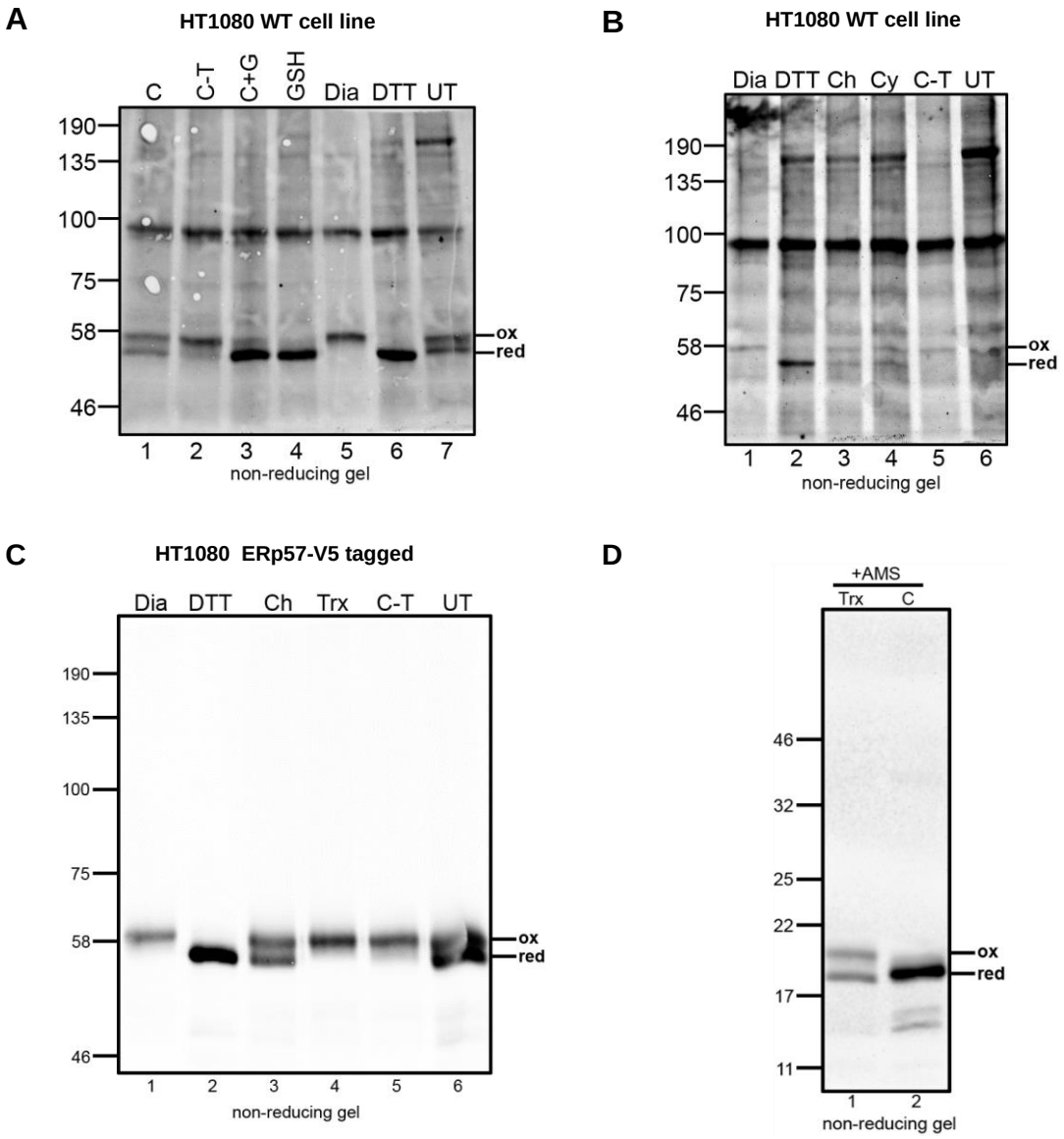

Figure 4-6 Reduction effect of reconstituted Trx/TrxR pathway on ERp57 redox state. A. SP cells were prepared from HT1080 wild type (WT) cell line. Sample were untreated (UT) (lane 7). SP cells in all other samples were first oxidised by incubation with 10 mM diamide. One portion of SP cells were kept as oxidised control (Dia) (lane 5) while one sample was then reduced by DTT as a reduced control (DTT) (lane 6). The sample were treated with the reconstituted Trx/TrxR pathway (C) (lane 1), reconstituted Trx/TrxR pathway in the absence of Trx (C-T) (lane 2), reconstituted Trx/TrxR pathway plus glutathione (C+GSH) (lane 3), or only GSH (lane 4). The determination of redox state was determined as above. Western blot was carried out using an anti-ERp57 (R283) as primary antibody. **B**. The sample were prepared as described above. Ch indicated the reconstituted Trx/TrxR pathway using human TrxR (lane 3), Cy indicated the reconstituted Trx/TrxR pathway using yeast TrxR (lane 4), and C-T indicated the complete system in the absence of Trx (lane 5). **C**. SP cell were generated from HT1080 cell line expressing ERp57-V5. Samples were prepared as above.

Trx indicated that the SP cells were only treated with purified Trx. Western blot was carried out using an anti-V5 antibody as primary antibody. **D**. Redox state of Trx in the absence or presence of reconstituted Trx/TrxR pathway in KHM buffer. The Trx was incubated in the absence (Trx) or presence (C) of other components of reconstituted Trx/TrxR pathway for 60 min. The NEM was then added to block free thiols in Trx. The Trx was then isolated using streptavidin agarose. PBS buffer including 2% SDS and 3 mM biotin was used to elute the Trx from streptavidin agarose. The Trx proteins were then reduced and not or alkylated by AMS. Samples were then separated by SDS-PAGE and visualised by western blot (antibody: Streptavidin Protein DyLight 800).

4.2.3 Trx/TrxR pathway using Trx mutants (CS, SS) failed to reduce oxidised ERp57

Results above suggested that the Trx/TrxR pathway can reduce ER localised ERp57 and this process was dependent on Trx. To address the role of Trx in the reduction process of ERp57 redox state, two Trx mutants (Trx C-S and Trx S-S) were used in the reconstituted Trx/TrxR pathway instead of wild Trx C-C.

SP cells were generated from HT1080 ERp57-V5 cell line and fully oxidised by diamide (Figure 4-7A). Oxidised SP cells were then treated with DTT, complete Trx/TrxR pathway using Trx wild type (CC) and two mutants (CS and SS). The redox status of ERp57 were determined by differential alkylation and a western blot using anti-V5 antibody was carried out to visuliazed proteins.

In untreated SP cells, two redox forms of ERp57 were observed (Figure 4-7B lane 6). Only the oxidised form of ERp57 was observed after the SP cells treated with diamide (lane 1). This showed that ERp57 was fully oxidised. A reduced band was observed when the SP cells were incubated with reconstituted Trx/TrxR pathway using wild type Trx (C-C) (lane 3). However, the incubation with reconstituted Trx/TrxR pathway using Trx mutants (C-S and S-S) failed to reduce oxidised ERp57 (lane 4 and 5). This result demonstrated that the catalytic cysteines of Trx are required for the reduction of ERp57.

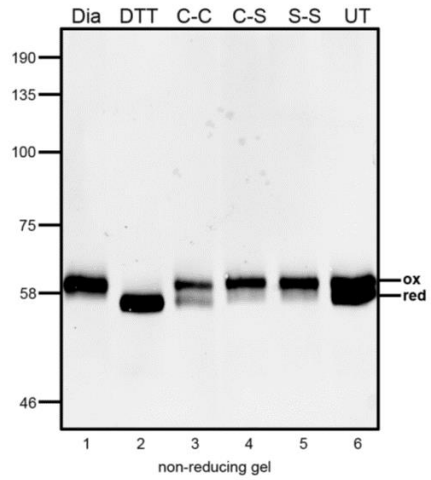

Figure 4-7 Catalytic cysteine was essential for reduction of ERp57. Reconstituted Trx/TrxR pathway using wild type Trx can reduce oxidised ERp57. Untreated (UT), diamide (Dia), dithiothreitol (DTT), reconstituted Trx/TrxR system using wild type Trx (C-C), reconstitute Trx/TrxR system using Trx mutants (C-S; S-S). Ox means oxidised form of ERp57; red indicating reduced form of ERp57.

4.2.4 A membrane protein is required for the reduction of ERp57 during incubation with the Trx/TrxR pathway

The previous results demonstrated that the cytosolic Trx/TrxR pathway (NADPH, G6P, G6PDH, Trx and TrxR) can reduce oxidised ERp57 which localised in the ER. It means that the reducing power generated by Trx/TrxR pathway which was outside of ER can be passed into ER lumen and then influenced ERp57 redox state. Catalytic cysteine of Trx might exchange disulfide to a membrane protein and then reduce ERp57 inside the ER membrane. How can the reducing power be transported into the ER? Are there any putative disulfide transporters in the ER membrane involved in this process? (Figure 4-8A).

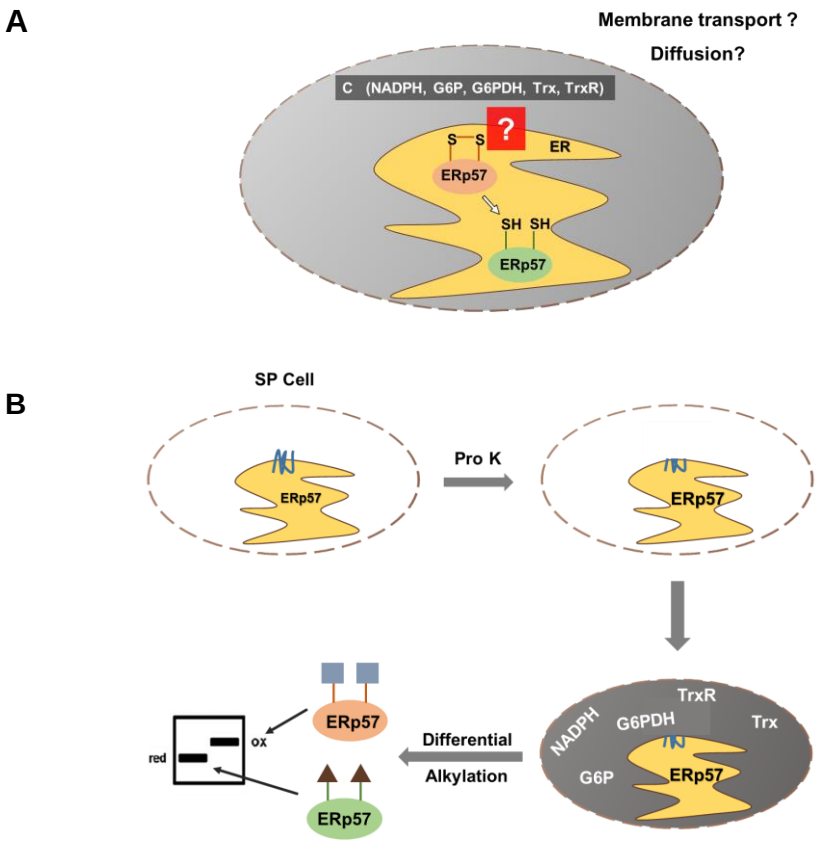

Figure 4-8 Influence of proteinase K treatment of SP cells on redox status of ERp57 in incubation with reconstituted Trx/TrxR pathway. A. It has been demonstrated that the cytosolic Trx/TrxR pathway (NADPH, G6P, G6PDH, Trx and TrxR) can reduce oxidised ERp57 localised to the ER. How is the reducing power transported into the ER? Are there any putative disulfide transporters in the ER membrane involved in this process? **B.** Schematic diagram of determination of redox state of ERp57 in SP cells treated by proteinase K (Pro K). SP cells were prepared from confluent cells which can stably overexpressing ERp57 including a V5 tag in ER. Cytosol was removed and intact ER was treated with proteinase K to digest membrane proteins. The SP cells were incubated with reconstituted Trx/TrxR pathway. The redox state of ERp57 was visualised by differential alkylation after SDS-PAGE gel and western blot. Ox means oxidised form of ERp57; red indicating reduced form of ERp57.

To investigate if membrane proteins are involved in the reduction process, a proteinase which can cleavage polypeptides was used to treated SP cells (Figure 4-8B). The experiment was carried out as previously with microsomes. The difference was that SP cells were treated with different concentrations (10 or 20 µg/ml) of proteinase K followed by inactivation by PMSF before oxidation of diamide. The SP cells were then incubated with the Trx/TrxR pathway. The redox status of ERp57 were then determined by differential alkylation. In untreated SP cells, ERp57 exists in two forms oxidised and reduced (Figure 4-9 lane 6). After

treated with the complete Trx/TrxR system, a reduced band was observed (lane 3) compared with the fully oxidised sample (lane 1). However, the incubation with the reconstituted Trx/TrxR pathway failed to reduce the oxidised ERp57 in samples which the SP cells were treated with proteinase K (lane 4 and 5). This result indicates that membrane proteins which have a protease-sensitive cytosolic domain were involved in the reduction of ERp57 via the Trx/TrxR pathway.

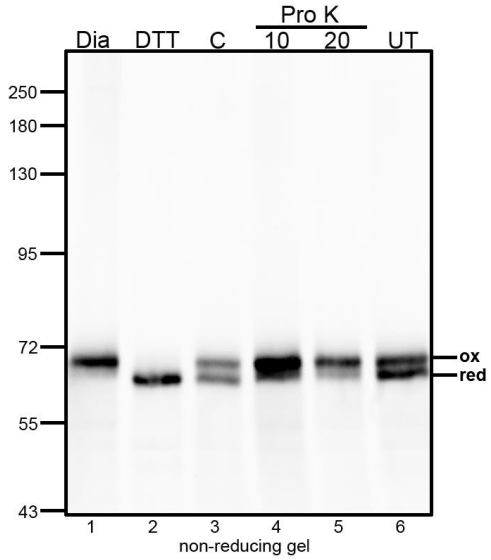

Figure 4-9 Proteinase K treatment could inhibit reduction of oxidised ERp57 by reconstituted Trx/TrxR pathway. SP cells were prepared from confluent cells which can stably overexpressing ERp57 including a V5 tag in ER. Cytosol was removed and intact ER was treated with Proteinase K to digest membrane protein. The oxidised SP cells were incubated in KHM buffer including DTT or the reconstituted Trx/TrxR pathway. The redox state of ERp57 was visualised by differential alkylation after SDS-PAGE gel and western blot. Untreated (UT); diamide (Dia); dithiothreitol (DTT); reconstituted Trx/TrxR system (C) using purified cytosolic components, NADPH, G6P, G6PDH, Trx and TrxR; Pro K means the SP cells were treated with proteinase K (10 µg/ml; 20 µg/ml). Ox means oxidised form of ERp57; red indicating reduced form of ERp57.

4.2.5 ERp57 was reduced by TCEP via a process that was not influenced by proteinase K treatment

In chapter 3, roGFP microsomes experiments showed that reducing agent TCEP reduced roGFP microsomes via membrane transport. Here, we used ERp57 as another reporter to investigate if reducing agent TCEP lead to reduction in the ER via membrane transport.

SP cells were generated from a HT1080 ERp57-V5 tagged cell line. Two groups of samples were untreated or treated with proteinase K. After inactivation by PMSF, the SP cells were untreated (UT), treated with diamide (Dia), DTT or TCEP. The redox status of ERp57 was determined by differential alkylation and a western blot was carried out with anti-V5 antibody (Figure 4-10). As before, there were two redox forms of ERp57 in the sample which was not treated (Figure 4-10 A and B lane 1): the reduced form (red) and oxidised form (ox) of ERp57. After oxidation, only one oxidised form was observed in the diamide treated sample indicating that the ERp57 was fully oxidised (Figure 4-10 A and B lane 2). In the reduced sample (DTT), only the reduced form of ERp57 was observed (Figure 4-10 A and B lane 3). In addition, ERp57 was reduced by the membrane impermeable reductant TCEP (Figure 4-10A lane 4). However, no difference in the ability of TCEP to reduce ERp57 was observed following proteinase K treatment of SP cells (Figure 4-10B lane 4). This result suggested that the reduction of any membrane protein involved by TCEP is not compromised by digestion of the cytosolic region.

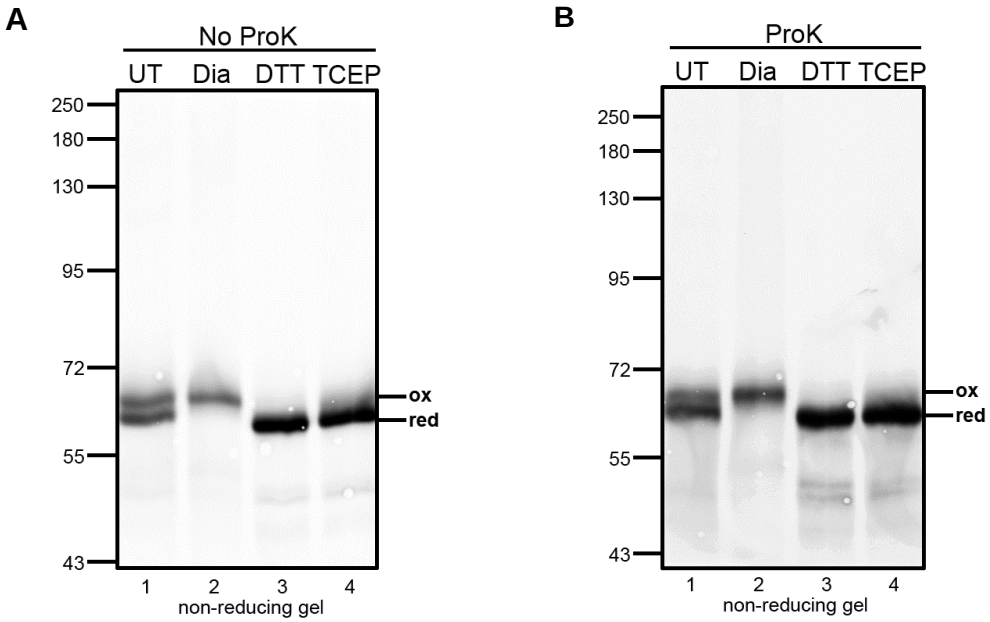

Figure 4-10 Proteinase K treament of SP cells does not prevent reduction of ERp57 by TCEP. SP cells were generated from HT1080 ERp57-V5 tagged cell line. Two group of samples were untreated (A) or treated (B) with proteinase K. After inactivation of the proteinase by PMSF, the SP cells were untreated (UT), treated with diamide, DTT or TCEP. Redox status of ERp57 was determined by differential alkylation and western blot was carried out with anti-V5 antibody.

4.3 Conclusion and Discussion

Previous work on the reduction of non-native disulfides in proteins entering the secretory pathway demonstrated a connection between the electron donor NADPH produced in the cytosol and the client protein within the ER (Poet et al., 2017). However, the intermediate steps in this pathway remain unknown. Based on the different locations in cells, the knowledge gap is divided into three questions: 1. Are there additional components needed in the cytosolic reduction pathway? 2. What is the putative disulfide transporter in the ER membrane? 3. Which components are involved in the conversion of non-native to native disulfides in the ER?

G6P, G6PDH, NADPH, Trx and TrxR were known as the minimal components in cytosolic Trx/TrxR pathway (Poet et al., 2017). We used purified components to reconstitute the cytosolic Trx/TrxR pathway. Inside the ER, we assumed that a member of the PDI family was involved in the reductive pathway in the lumen. The function of PDIs is driven by redox state. In the reduced state, it is able to bind and reduce substrate proteins while in the oxidised state, the substrate can be oxidised and released (Tsai et al., 2001). Hence, after disulfide exchange with client protein, it is necessary to reduce PDI so it can act as a reductase. One of PDI family members, ERp57, was shown to have a specific role in the isomerisation of non-native disulfide bonds in specific glycoprotein substrates (Jessop et al., 2007). ERp57 was chosen as an indicator of redox status to determine the impact of the Trx/TrxR pathway on the redox state of an ER luminal PDI. Determination of redox state of ERp57 in HT1080 WT or HT1080 which was transfected ERp57-V5 tagged protein was optimised based on a previously described approach (Oka et al., 2015).

Here we demonstrated that reconstituted Trx/TrxR using purified components (NADPH, G6P, G6PDH, Trx and TrxR) could reduce oxidised ERp57. This process is dependent on the catalytic cysteines of Trx. The Trx/TrxR pathway reconstituted by using Trx mutants was not able to reduce oxidised ERp57. This suggested that the reducing power generated outside of ER membrane was transferred into ER lumen depending on the disulfide bond exchange reaction between Trx and potential membrane protein. Our result also showed that the oxidised ERp57 can

be reduced with the incubation with GSH which is consistent with previous study (Jessop and Bulleid, 2004). It was demonstrated that GSH can directly reduce mammalian oxidoreductase in the ER to keep them in a reduce status in order to maintain their activity in the disulfide reduction and isomerisation. This indicates that there are possibly several mechanisms in mammalian cells that are responsible for the disulfide formation or isomerisation.

To investigate if membrane proteins are involved in reduction of oxidised ERp57, proteinase K was used to treat SP cells to digest the cytosolic domain of ER membrane proteins. The reduction of ERp57, which had been fully oxidised was prevented by the proteinase treatment. It showed that membrane proteins were involved in the reduction of ERp57. The cytosolic domain of membrane proteins were involved in disulfide exchange with reduced Trx and further passed the reducing power into ER lumen and directly or indirectly reduced ERp57. Recently, it was reported that an ER localised transmembrane protein lipase maturation factor 1 (LMF1) influenced the redox homeostasis in ER and could ensure the disulfide bond formation (Roberts et al., 2018). In LMF1 KO cell line, ER became more oxidised. Next, it is worth considering the possibility of LMF1 in the reductive pathway which connect the cytosol and ER. The key question in the future is how to identify the membrane protein involved in the reductive pathway.

Chapter 5 Developing a post-translational folding assay to evaluate the ability of purified components to rearrange disulfides

5.1 Introduction

In mammalian cells, a secreted protein needs to enter a nuclear contiguous intracellular organelle, the ER, to allow different modifications, such as signal peptide cleavage, N-Linked glycosylation, disulfide bond formation and proline hydroxylation to achieve its native and functional structure (Braakman and Bulleid, 2011). After modification, the protein has to pass the quality control in the ER and then the correctly folded proteins will be transported to its target location. Otherwise, the misfolded protein will be transported into the cytosol and degraded by the ER-associated protein degradation (ERAD) system. The whole journey is started with the recognition of a signal sequence, which is generally located in the N terminus of the protein sequence, by signal recognition particle (SRP) (High, 1995). The complex of ribosomes, nascent chain and SRP then bounds to the SRP receptor which is localised in ER membrane. The ribosome/nascent chain complex is directed to the Sec61 translocon and the newly synthesising nascent chain is translocated across the ER membrane and exposed to the ER lumen. Once the polypeptide chain is exposed to the various ER chaperones and folding enzymes in the ER lumen, folding begins. The rate of cotransl(oc)ational folding is limited by the rate of translation (generally 4-5 residues per seconds) (Braakman et al., 1991, Horwitz et al., 1969). Most formation of the secondary structure more rapid than translation. That is the reason that formation of the secondary structure happens on the nascent polypeptide chain. Modification may take place during or after the termination of translation and full translocation (Braakman and Bulleid, 2011).

Disulfide bonds are common linkages in secreted proteins and protein localised to the cell membrane. They are formed between free thiols of two cysteine residues and play crucial roles to support the structure, stability, and function of proteins (Fass, 2012). Disulfide bond formation is catalysed by the thiol disulfide exchange reaction with ER-localised PDI family members (Benham, 2012). Disulfide bonds

can form not only cotranslationally but also posttranslationally (Braakman and Hebert, 2013). The insertion of a disulfide can result in covalent linkages found in the native structure as well as those that are not, so called non-native disulfides. Such non-native disulfides which are formed between the incorrect cysteine residues need to be resolved for the polypeptide to form its native and functional conformation. The resolution of non-native disulfides is absolutely required for cells to be able to fold secreted proteins correctly and to remove misfolded proteins to alleviate cell stress. The question that how the non-native disulfide bonds are reduced, remains to be addressed. Based on the work carried out previously, we have an unknown connection between the ultimate electron donor (NADPH) in the cytosol and the final acceptor in the ER. NADPH is the ultimate electron donor for the resolution of non-native disulfides in the ER and the cytosolic TrxR pathway ensures the correct formation of native disulfide bonds (Poet et al., 2017).

To investigate if the known cytosolic components (G6P, G6PDH, NADPH, Trx and TrxR) are sufficient to reconstitute the reductive pathway for isomerisation of non-native disulfide bonds, we developed a post-translational folding assay. To develop the assay, we took advantage of the properties of a commercial translational system RRL with the addition of SP cells acting as an ER source. Translation of a model protein was carried out in a RRL translation system in the presence of ^{35}S-labelled Met and SP cells where the plasma membrane has been selectively permeabilised to release the cytosol but leaving the intracellular organelles, such as ER and Golgi apparatus intact. Reagents (eg. G6P) can be added to the translation system during or after translation followed by immunoisolation of the translation product. The reduction of non-native disulfide can be distinguished by different mobilities of reduced and disulfide bonded proteins following separation of the product by SDS-PAGE in the absence of added reducing agent. Different substrate proteins such as ß1-integrin (Poet et al., 2017), low-density lipoprotein receptor (LDLr) (Bulleid, 2009), tissue-type plasminogen activator (tPA) and Adam 10 disintegrin domain were compared to develop the post-translational folding assay. We demonstrated that the smallest substrate protein, Adam 10 disintegrin domain, is the most sensitive indicator for posttranslational isomerisation of non-native disulfide bonds. We also showed by using the post-translational folding assay, that the minimal cytosolic component

required for the reduction of non-native disulfide bonds in the ER is the Trx/TrxR pathway.

5.2 Results

5.2.1 Development of the post-translational folding assay

To determine whether we could restore the cytosolic reductive pathway to reduce disulfides, we first established a post-translational folding assay in the absence of added SP-cells.

Translations were carried out as described previously (Poet et al., 2017). We took advantage of a commercial translation system RRL without any reducing reagents containing all the cellular components essential for protein synthesis *in vitro*, such as tRNA, ribosomes, initiation factors, elongation factors and termination factors , to synthesis human ß1-integrin (Pelham and Jackson, 1976). The RNA template and ^{35}S-Met were added into RRL to allow radiolabelled protein synthesis (Figure 5-1). When the RNA template was translated without any addition, a mixture of proteins with different disulfide bonds (native and non-native disulfide bonds) was synthesised. After translation, G6P was added into the mixture to allow further incubation for different times. If G6P was able to reduce disulfide bonds, then we will get homogeneous reduced protein. The sample was then separated by SDS-PAGE. The gel was fixed, dried and exposed to phosphorimager plate overnight. The films were scanned by FLA-7000 bioimager to obtain result images.

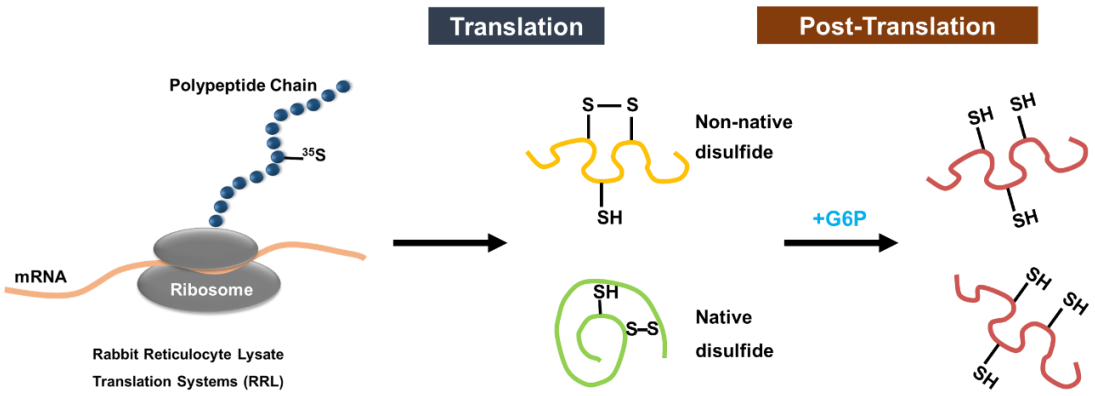

Figure 5-1 Schematic of the post-translational folding assay. Translation was carried out in RRL in the presence of ^{35}S-labelled met/cys in the absence of added SP-cells. Various disulfide bonds (native and non-native disulfide) maybe formed during translation in the absence of G6P. After translation is finished, G6P was added into the reaction system. If the G6P has ability to activate the reductive pathway, disulfides will be reduced.

Previous research showed that the addition of G6P could re-establish the reducing environment in the cytosol by driving glucose-6-phosphate dehydrogenase (G6PDH) to produce more NADPH (Poet et al., 2017). We repeated the experiment showing that only the reduced form of ß1-integrin was synthesised when translation is carried out in the presence of G6P (Figure 5-2 lane 2). In other samples, G6P was added into RRL and post-translationally incubated for various times. NEM was added into the reaction at different time points to block free thiols. Here, the oxidised ß1-integrin was gradually reduced becoming fully reduced after 40 min (Figure 5-2 lane 5-8).

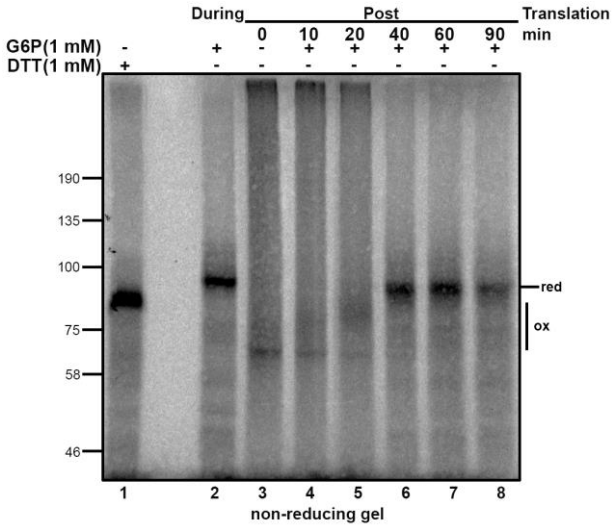

Figure 5-2 Time course of post-translational folding assay in cytosol. Translation of β1-integrin was carried out in RRL in the presence of ^{35}S-labelled Met and the absence of semi-permeabilized (SP) cells with (lane 2) or without G6P (1 mM). After translation, the samples were incubated in the presence (lane 2) or absence of G6P (lane 3) (1 mM). Following translation in the presence of G6P, samples were incubated for different times (10 - 90 min) after the addition of G6P. The alkylating agent NEM (5 mM) was used block free thiols to avoid disulfide bond change after the reaction ended. The sample was then separated by SDS-PAGE under non-reducing conditions. The gel was fixed, dried and exposed to phosphorimager plate overnight. The films were scanned using the FLA-7000 phosphorimager to obtain images. Note, the sample (lane 1) was translated in the absence of G6P, but it was run under reducing condition as a reduced control. Ox indicating oxidised form of proteins including different types of disulfide bond; red indicating that the proteins were fully reduced.

It has been demonstrated that the cytosolic reductive pathway drives the resolution of non-native disulfides formed within the ER and the inhibition of TrxR could prevent correct disulfide formation (Poet et al., 2017). To investigate if the TrxR is involved in the post-translational resolution of non-native disulfides into native disulfide, we planned to use the inhibitors of TrxR in the post-translational folding assay. The ability of AF and TRi1 (Stafford et al., 2018) to inhibit TrxR in our cell extract was tested before their application in the post-translational folding assay.

The classical way to determine the activity of the thioredoxin system is by using an insulin reduction assay (Holmgren, 1979). This method is based on the reduction of insulin disulfides by reduced thioredoxin with thioredoxin reductase and NADPH as ultimate electron donor (Holmgren and Bjornstedt, 1995). At the end of the reaction, DTNB can be reduced by the reduced insulin and produce TNB, a yellow product that can be measured at 412 nm. The absorbance at 412

nm indicated TrxR activity in the cell extract. Various concentrations of TrxR were used to make a standard curve which could indicate that the assay is working well (in chapter 3). In addition, the cell extract prepared from Hela cell line as described previously was tested for TrxR activity (Figure 5-3A). TrxR activity in the cell extract which was treated with PD-10 column to remove the small molecules like G6P was also tested. Without addition of Trx, no TrxR activity was observed (negative control). TrxR activity was not influenced by the DMSO solvent which was used to dissolve AF and TRi1 (Stafford et al., 2018). When the cell extract was treated with inhibitors (AF and TRi1), the TrxR activity was inhibited significantly. These results suggested that either AF or TRi1 could be used as a TrxR inhibitor in post-translational folding assay.

To determine if thioredoxin reductase (TrxR1) was involved in the post-translational reduction pathway, the translation system was untreated or treated with AF which can irreversibly inhibit the activity of TrxR1. The post-translational folding assay was carried out as described above. TrxR inhibitor AF was used to treat the reaction system before translation (Figure 5-3 lane 3) or after translation (Figure 5-3 lane 9). It was noticed that a diffuse band was presented when translation was carried out in the presence of G6P in RRL which was treated with AF (Figure 5-3 lane 1). This indicated that the AF treatment prevented the reduction of disulfide bonds during translation. No reduction was observed in sample which were post-translationally incubated in absence of G6P (Figure 5-3 lane 4), but reduction was observed in samples which were post-translationally incubated with G6P (Figure 5-3 lanes 5 - 8). This suggested the post-translational addition of G6P can promote the reduction of disulfide bonds. However, this reduction was stopped with AF (Figure 5-3 lane 9). These results demonstrated that addition of G6P and cytosolic thioredoxin reductase are required for the reduction of disulfide bonds in the cytosol after translation.

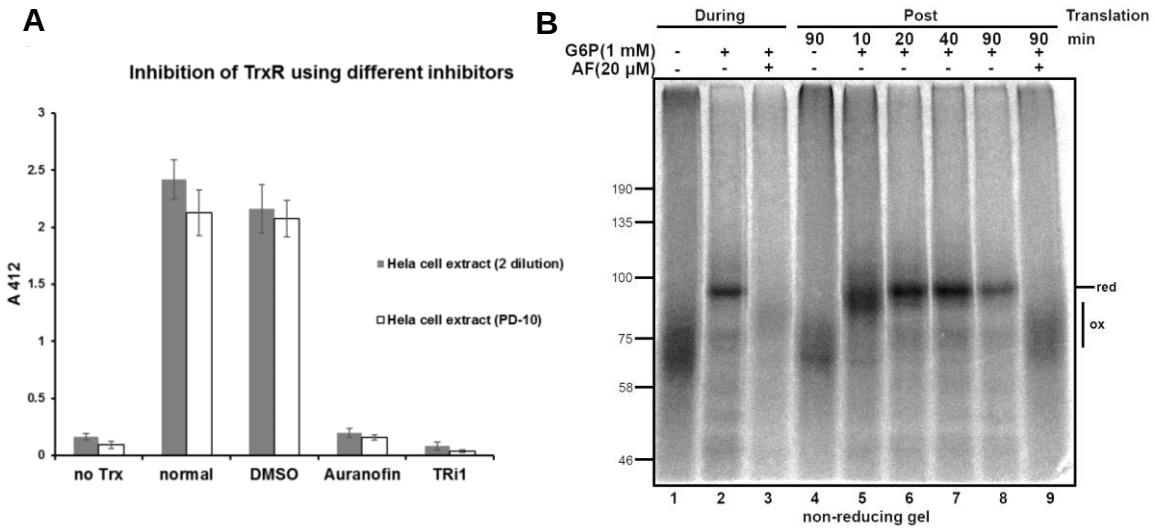

Figure 5-3 G6P and cytosolic thioredoxin reductase is required for the reduction of disulfides in the cytosol. A. Inhibition impact of AF and TRi1 on TrxR in Hela cell extract before or after PD-10 column treatment. To make sure the TrxR concentration was same in each lysate, the Hela cell extract was diluted so that the lysates had the same protein concentration. **B**. Translation of β1-integrin was carried out in RRL in the presence of ^{35}S - Met in the absence of SP cells without G6P (1 mM) (lane 1) or with (lane 2) in the absence (lane 2) or presence of AF (lane 3). After translation, the samples untreated or treated with TrxR inhibitor AF were incubated in the absence (lane 4) or presence of G6P (1 mM) for different times (10 - 90 min). The alkylating agent NEM (5 mM) was used block free thiols to avoid disulfide bond change after reaction ended. The sample was then separated by SDS-PAGE under non-reducing conditions. The gel was fixed, dried and exposed overnight. The films were scanned by FLA-7000 bioimager to obtain result images. The oxidised species was present when translated or post-translational incubated without G6P (lane 1 and 4). The presence of AF during translation and when added post-translation prevented the reduction of disulfide bonds (lane 3 and 9). Ox indicating oxidised form of proteins including different types of disulfide bond; red indicating that the proteins were fully reduced.

5.2.2 Development of post-translational folding assay in the ER

To investigate the reduction progress of non-native to native disulfides in the ER, SP cells were added to the RRL translation system (Wilson et al., 1995). Here, the SP cells acted as a source of ER which allowed the newly synthesised proteins to be translocated into the ER and undergo processes such as signal sequence cleavage, disulfide bond formation, and glycosylation.

The post-translational folding assay in the ER was developed based on the post-translational folding assay in cytosol (Figure 5-4A). The SP cells were added to the translational system to allow the translocation and protein folding to occur in

the ER. After translation, proteins with different kinds of disulfide bonds were synthesised in ER at the same time. G6P was then added to the translational system. If G6P was able to restore the reductive pathway then non-native disulfide bonds would be converted to native disulfide bonds. At the end of incubation, the alkylating agent NEM was added to prevent disulfide exchange. Two bands were observed in the sample which was translated in the presence of G6P (Figure 5-4B lane 1). The upper band indicated glycosylated β1-integrin (gly-β1) and the lower band was untranslocated β1-integrin (untrans). The sample which was translated in the absence of G6P separated as a smear on the gel indicating a mixture of glycosylated and untranslocated β1-integrin with various disulfide bonds (Figure 5-4B lane 2). When translation was carried out without G6P and then post-translationally incubated with G6P, a similar banding pattern was observed (Figure 5-4B lane 3). We were unable to directly identify the post-translational isomerisation of non-native to native disulfide bonds by the mobility shift on SDS-PAGE. It was necessary to optimise the protocol to distinguish different proteins containing non-native or native disulfide bonds by the SDS-PAGE.

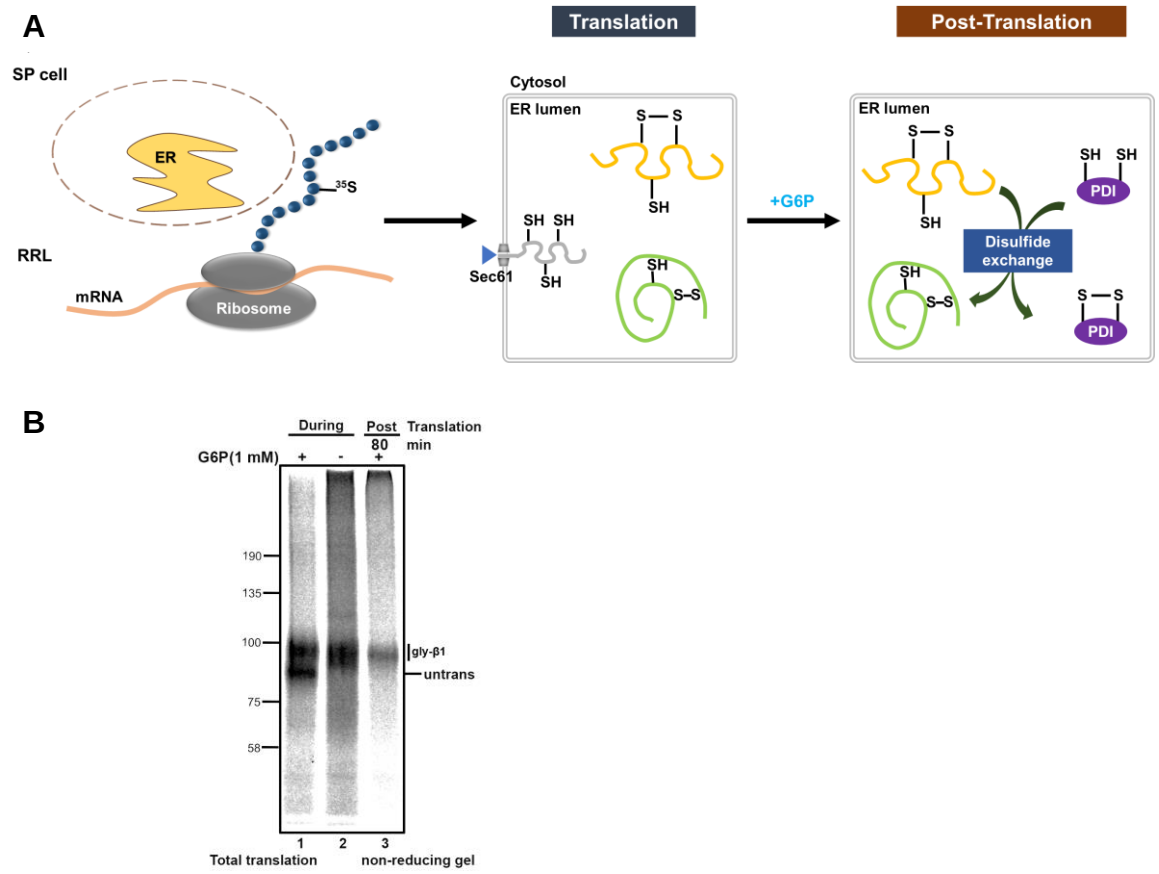

Figure 5-4 Schematic diagram of post translational folding assay in ER. A. Translation was carried out in RRL in the presence of radiolabeled ^{35}S Met. SP cells were added to RRL translation system as a source of ER. After translation, NEM was added to some samples to block disulfide exchange. In the other samples, the SP cells were post-translationally incubated with G6P. **B**. The translation was carried out with (lane 1) or without G6P (lane 2) (final concentration 1 mM) in the presence of SP cells. After translation in the absence of G6P, the reaction system was incubated in the presence of G6P (lane 3). The samples were separated by SDS-PAGE under non-reducing condition.

a) Optimisation of post-translational folding assay

Immunoprecipitation was used to optimise the post-translational folding assay in the ER (Figure 5-5). The post-translational folding assay was carried out as previously, SP cells were isolated from the translation mix by centrifugation and then lysed to release the ER components. The cell lysate was incubated with protein G beads for 30 mins to preclear proteins which could bind non-specifically to the protein G beads. After centrifugation, the supernatant was removed to a new tube and incubated overnight with ß1-integrin antibody (JB1A or 9EG7) (Lenter et al., 1993, Tiwari et al., 2011) in the presence of newly added protein G beads. The beads were isolated and washed three times to remove non-

specifically bound proteins. The proteins were eluted from the beads by boiling with SDS-loading buffer at 105 ºC. The proteins were separated by SDS-PAGE under non-reducing condition.

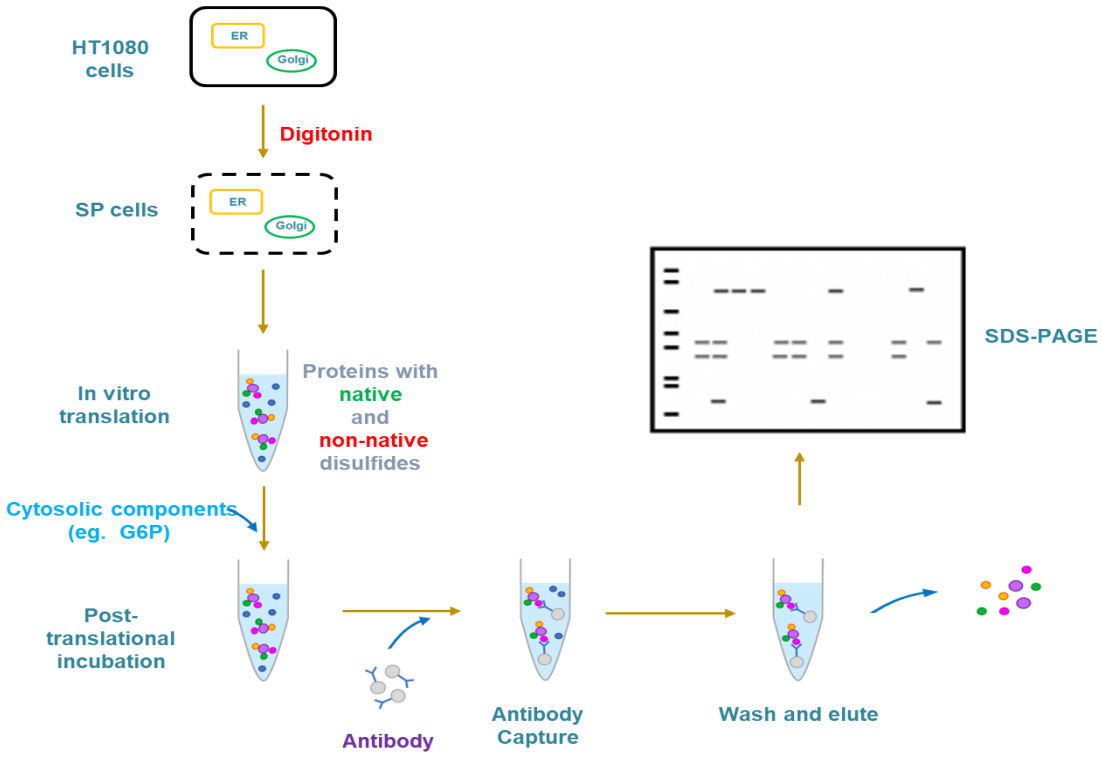

Figure 5-5 Workflow for the optimised post-translational folding assay in ER. Translation of β1-integrin was carried out in the presence of SP-cells in the RRL. After translation, the products were incubated in the absence or presence of 1mM G6P. An antibody that recognises all forms of β1-integrin (JB1A) or a conformational-specific antibody (9EG7) was used to isolate the protein before SDS-PAGE. Products were separated by SDS-PAGE under non-reducing conditions or non-reducing gel as indicated. The gel was fixed, dried and exposed to phosphorimager plate overnight. The films were scanned by FLA-7000 bioimager to obtain result images.

When G6P was included during translation, a more intense band was observed in the immunoprecipitates with the conformational antibody 9EG7, which can only recognise ß1-integrin with native disulfide, than when translation was carried out in the absence of G6P (Figure 5-6B, compares lane 1 and 2). This suggested that more proteins with native disulfide bonds were synthesised during translation with G6P. In contrast when translations were carried out with G6P in the presence of AF, a quite weak band was observed (Figure 5-6 B, lane 3). These results suggest that the addition of G6P during translation resulted in the formation of native disulfides but not if TrxR was inhibited by AF. An increase in signal was obtained following incubation post-translationally with G6P from 10 min indicating the post-

translational reduction of non-native disulfides (Figure 5-6B, lane 5 - 8). Similar distinct bands were also appeared after post-translational incubation in the presence of G6P even when the cells were treated with the TrxR inhibitor auranofin before this incubation (Figure 5-6, B, lane 9). This indicated that the inhibition of TrxR1 did not prevent the reduction of native-disulfides after translation. A band indicating protein with native disulfide bonds was observed in sample which were translated and post-translationally incubated in the absence of G6P indicating that, in this case, post-translational non-native disulfide reduction is independent of G6P addition (Figure 5A and B, lane 4). The results suggest that the post-translational reduction of non-native to native disulfides was independent of the involvement of Trx pathway driven by G6P in the RRL. It was difficult to determine if the addition of G6P after translation can result in the isomerisation of non-native to native disulfide bonds when using β1-integrin as substrate in this post-translational folding assay.

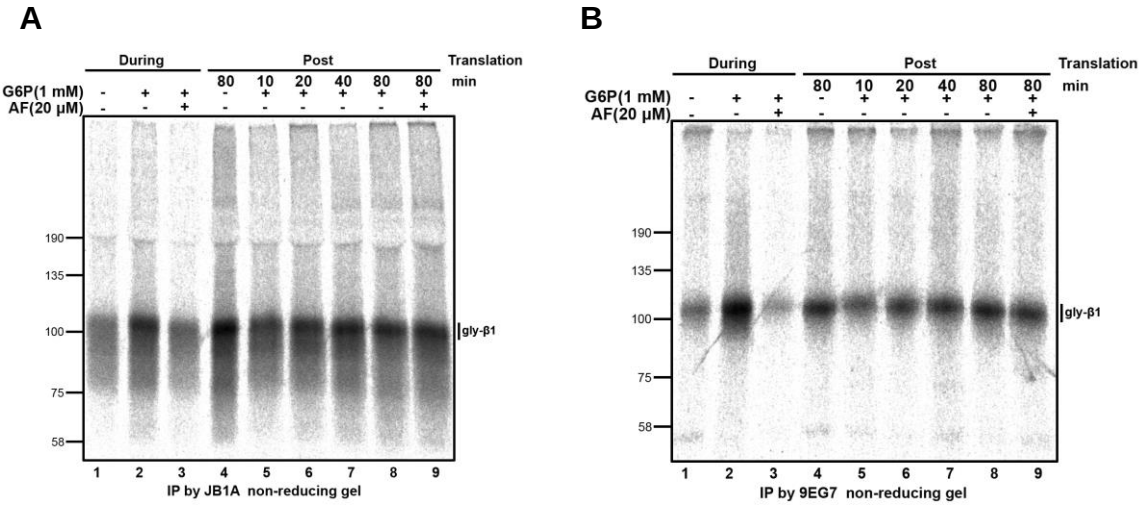

Figure 5-6 Post-translational non-native disulfide reduction in ER is independent of G6P in RRL. Translation of β1-integrin was carried out in the presence of HT1080 SP-cells. G6P (1 mM) was included either during translation or post-translationally in the absence or presence of 1mM G6P as indicated. Auranofin, inhibitor of TrxR, was used before or after translation as indicated to determine if the TrxR pathway was involved in the post-translational folding process. **A**. An antibody that recognises all forms of β1-integrin (JB1A) was used to isolate the protein before SDS-PAGE. **B**. A conformational-specific antibody (9EG7) was used to demonstrate the formation of native disulfides following the post-translational addition of G6P. Products were separated by SDS-PAGE under non-reducing conditions. The mobility of the glycosylated (gly-β1) protein is as indicated.

Besides β1-integrin, two other substrates such as the tissue-type plasminogen activator (tPA) (Bulleid et al., 1992) and low-density lipoprotein receptor (LDLr) (Oka et al., 2013) were tested to determine if they would be suitable to use in this post-translational folding assay (Figure 5-7). The translation of the tissue-type plasminogen activator (tPA) and low-density lipoprotein receptor (LDLr) was carried out with (lane 2) or without G6P (lane 3) (final concentration 1 mM) in the presence of SP cells as previously described. In one sample, the RRL was pretreated with TrxR inhibitor AF (lane 4). After translation in the absence of G6P, the reaction system was incubated in the absence (lane 5) or presence (lane 6) of the same concentration of G6P. Before the addition of G6P, the system was incubated with auranofin (lane 7). Unfortunately, it was difficult to tell if the disulfide bonds change during the post translational addition of G6P. The incubation with and without G6P after translation did not exhibit any differences in the banding pattern (lane 5-6).

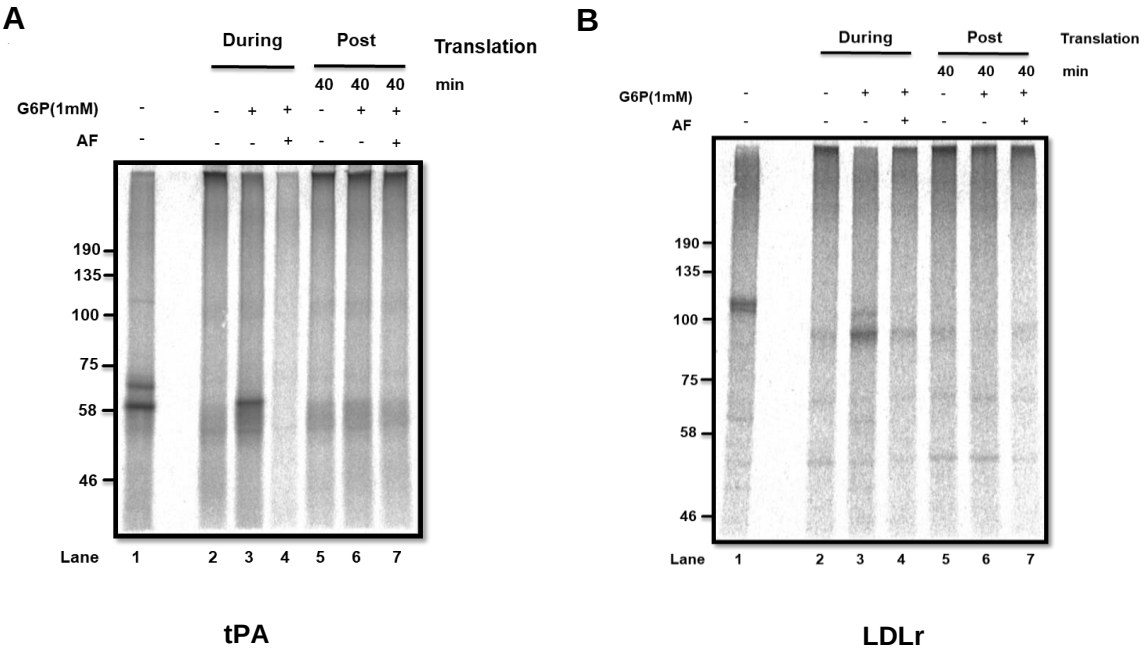

Figure 5-7 Test of substrate proteins for post-translational folding assay. The translation of the tissue-type plasminogen activator (tPA) and low-density lipoprotein receptor (LDLr) was carried out with (lane 2) or without G6P (lane 3) (final concentration 1 mM) in the presence of SP cells as previously described. In one sample, the RRL was pretreated with TrxR inhibitor AF (lane 4). After translation in the absence of G6P, the reaction system was incubated in the absence (lane 5) or presence (lane 6) of the same concentration of G6P. Before the addition of G6P, the system was incubated with auranofin (lane 7). One sample (lane 1) was separated under reducing condition. And the other samples (lane 2 - 7) were separated by SDS-PAGE under non-reducing condition.

b) Post-translational folding assay using substrate protein Adam 10 disintergin domain

To generate a suitable substrate to study the post-translational rearrangement of non-native disulfides in the ER, Adam 10 disintegrin domain was chosen because of its dense disulfide pattern, which has a high possibility of forming non-native disulfides (Figure 5-8C). A V5 epitope and a string of methionine residues (Met*5) was included at the C terminus to aid immunoprecipitation and boost the signal of the radiolabelled translation product (Figure 5-8A). As the substrate does not have a stop codon, the disintegrin domain is not released from the ribosome. The fact that the nascent chain remains attached to the ribosome means that 63 amino acids (plus 20 aa signal sequence) are exposed to the lumen of the ER as 63 amino acids are required to bridge the gap from the polypeptide translocation site through the ribosome tunnel and Sec61 translocon (Figure 5-8B) (Robinson et al., 2017).

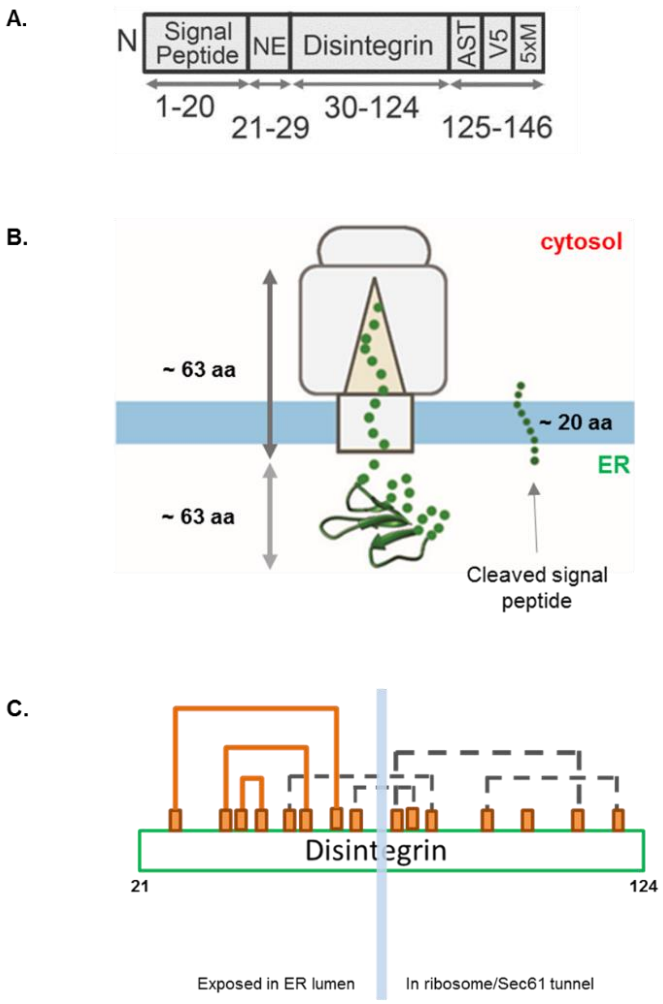

Figure 5-8 Schematic representation of Adam 10 disintegrin domain. **A**. Schematic representation of Adam 10 disintegrin domain and the organisation of key elements including the signal peptide, Neo-epitope tag (NE), Adam 10 disintegrin domain, V5 epitope (V5), methionine residues (Met5) (Robinson et al., 2020). **B**. Schematic representation of the stalled Adam disintegrin domain entering the ER. After the signal peptide (20 aa) is cleaved, 63 amino acids are exposed to ER lumen allowing disulfide formation and folding while 63 aa span the ribosome and Sec61. **C**. The native disulfides in stalled Adam 10 integrin. Orange lines indicate native disulfides in exposed nascent chain; Grey broken lines indicate native disulfides which cannot form because of the unexposed cysteines in the ribosome/ Sec61 tunnel.

PCR was used to amplify Adam 10 disintegrin domain to provide a transcript that encodes 146 aa including a signal peptide, Neo-epitope tag (NE), Adam 10 disintegrin domain, V5 epitope (V5), and methionine residues (Met5) (Figure 5-9A). The forward primer was used to add a T7 promoter onto the template while the reverse primer lacks a stop codon (Figure 5-9C). The transcript was constructed without a stop codon which makes it stall on the ribosome.

A.

ATGAGCAGATCTGTGGCCCTGGCTGTGCTGGCCCTGCTGTCTCTGTCTGGCCTGGAAGCCAttattc
cggtggaagaagaaaacccgGGGCAGCCTATCTGCGGCAACGGAATGGTGGAACAGGGCGAAGAGTGC
GACTGTGGCTACAGCGACCAGTGCAAGGACGAGTGCTGCTTCGATGCCAACCAGCCTGAGGGC
AGAAAGTGCAAGCTGAAGCCTGGCAAGCAGTGCAGCCCTAGCCAGGGACCTTGTTGCACAGCC
CAGTGTGCCTTCAAGAGCAAGAGCGAGAAGTGCCGCGACGACTCTGATTGTGCTAGAGAGGGC
ATCTGCAACGGCTTCACCGCTCTGTGTCCTGCCAGCGATCCTAAACCTGCCAGCACCGGCAAGC
CCATCCCCAACCCTCTGCTGGGCCTGGACAGCACCATGATGATGATGATGTCCGGCACCGCCAG
CGCCAGCTCTGCTGGATCTGGCGGCGGAGCCACAGCCAGCTCTACATCTGCTGGCGGCACAAG
CACCGGCTCTACAGGCGGATCTACAGCAGGCGCTGCTGGCGCAACAGGCGGAGGATCTACTGG
CGGAGCTGCCTCTACTGGAACAGCTGCTGGGGGCGGAGGCGGAGCTTCTTCTGGAACAGGCAC
AGGCGCCAGCGGCGCTACAGGCACCGGAACAACA

B.

Forward primer: GATGGCTAATACGACTCACTATAGGGTCAGGCCACCATGAGCAGATCTGTGGCCCTG

Reverse primer: CATCATCATCATCATGGTGCTGTC

C.

MSRSVALAVLALLSLSGLEAIIPVEEENPGQPICGNGMVEQGEECDCGYSDQCKDECCFDANQPEGRKCKLKPGK
QCSPSQGPCCTAQCAFKSKSEKCRDDSDCAREGICNGFTALCPASDPKPASTGKPIPNPLLGLDSTMMMMM

Figure 5-9 Full DNA sequence, primer information and amino acid information of Adam 10 disintegrin. **A**. DNA sequence of the full-length Adam 10 disintegrin template. **B**. Primers used to generate the DNA fragments. F: forward primer, adding a T7 promoter; R: Reverse primer, adding the 5x Met to generate translation intermediates protein 146 amino acids in length. **C**. Amino acid sequence of full-length Adam 10 disintegrin template. Blue: Beta-2-M signal sequence; red: Neo-epitope tag; Green: Disintegrin domain from ADAM10; Orange: V5 tag and 5x Met. (From Philip Robinson).

A co-translational assay was carried out to determine if we could distinguish changes to the disulfide bonding pattern of the Adam 10 disintegrin domain in the presence or absence of G6P. The RNA was also translated in the presence of DTT in RRL containing HT1080 SP cells which acted as an ER source to provide fully reduced protein. After the reaction, samples were immunoprecipitated using anti-V5 antibody and then analysed by SDS-PAGE. When the transcript was translated in the presence of DTT, two compact bands were noticed on the gel (Figure 5-10 A and B lane 1). The upper band (indicated by *) is reduced preprotein that was not translocated into the ER and the lower band (indicated by arrow) is the signal peptide cleaved protein. A faster migrating diffuse band was observed when translation was carried out in the absence of G6P suggesting the substrate formed different kinds of disulfides including native and non-native disulfides during the translation (Figure 5-10 lane 2). Several distinct bands were observed in the presence of G6P (Figure 5-10 lane 3). These results demonstrated that the addition of G6P is required for correct disulfide formation which is consistent with previous conclusions (Poet et al., 2017).

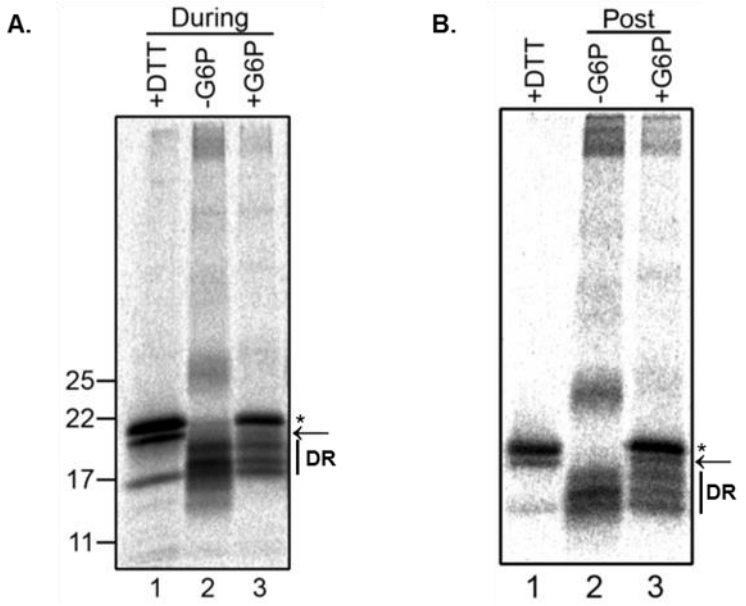

Figure 5-10 Co-translational and post-translational folding assay using Adam 10 disintegrin domain as a model protein. A. Adam 10 disintegrin domain was translated in the presence of DTT (lane 1) or absence of DTT and in the absence (lane 2) or presence of G6P (lane 3). **B**. Post-translational incubation of Adam 10 translation products in the absence (lane 2) or presence of G6P (lane 3). Autoradiographs of radiolabelled, immunoisolated translation product generated from stalled intermediate of Adam 10. Gels were run under non-reducing conditions. An example of preprotein (untranslocated) (*) and signal peptide cleavage (arrow) are highlighted in the samples. Disulfide bond rearrangement (DR).

To investigate if Adam 10 disintegrin domain is suitable as a model protein for disulfide rearrangement in the post-translational folding assay, the RNA template was translated in RRL with HT1080 SP cells in the absence of G6P. After the translation, the products were incubated in the absence and presence of G6P and then the products were immunoprecipitated using anti-V5 antibody and then analysed by SDS-PAGE. After translation, a diffuse band was observed when post-translationally incubated without the addition of G6P (Figure 5-10 lane 2) indicating that the products were Adam 10 disintegrin with different kinds of disulfides. However, after the addition of G6P at the end of translation, several distinct bands appeared (Figure 5-10 lane 3) suggesting that the addition of G6P facilitated the rearrangement of disulfides. The change in banding pattern before and after the addition of G6P was more noticeable than β1-integrin. Hence, we decided to use Adam 10 disintegrin domain as a model substrate for our post-translational folding assay.

5.2.3 The cytosolic Trx/TrxR pathway is required for post-translational disulfide rearrangement

We wondered if the Trx/TrxR pathway is also required for the post-translational disulfide rearrangements we observed after addition of G6P. To address this question, the TrxR inhibitor AF was used in the post-translational folding assay to see if the disulfide rearrangement after translation was prevented (Figure 5-11B).

A co-translational assay was carried out as a control (Figure 5-11C, lanes 1-3). The RNA was translated in the presence of DTT or in the absence or presence of G6P in RRL containing SP cells. After translation, samples were immunoprecipitated using anti-V5 antibody and then analysed by SDS-PAGE. Similar results (Figure 5-11, lane 1 - 3) were obtained to those seen previously (Figure 5-10).

A post-translational folding assay was carried out using TrxR inhibitor AF. As described above, the translation was performed in the absence of G6P in SP cells and after translation the products were incubated in the absence or presence of G6P. No disulfide reaarangement occurred in the absence of added G6P (Figure 5-11C, lane 4) as seen previously while several distinct bands were observed after incubation with G6P (Figure 5-11C, lane 5). However, in the presence of the TrxR inhibitor AF, the post-translational incubation with G6P did not lead disulfide rearrangement (Figure 5-11C, lane 7). Diffuse bands were observed when the

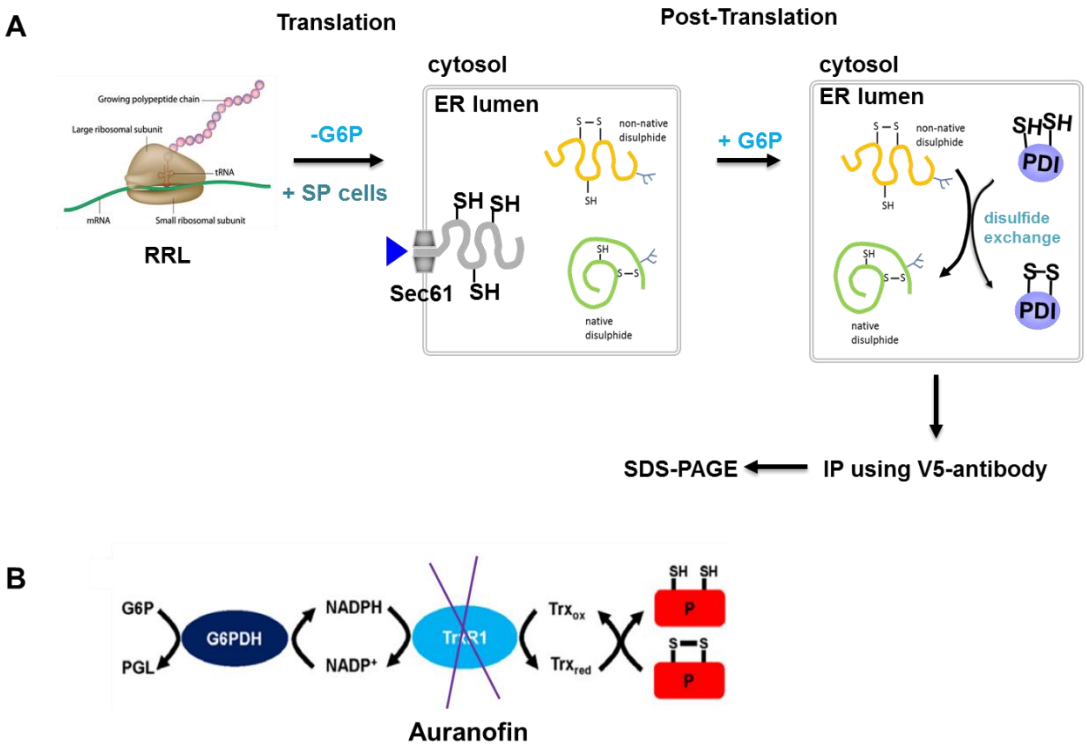

Figure 5-11 The cytosolic Trx/TrxR pathway is essential for post-translational disulfide rearrangement (DR). **A**. Schematic diagram of post translational folding assay using Adam 10 disintegrin domain as substrate. Translation was carried out in RRL in the presence of SP-cells. G6P was included either during translation or post-translationally. V5-antibody was used for immunoprecipitation and to remove background labelling. Products were separated by SDS-PAGE. **B**. Trx/TrxR reductive pathway in the cytosol. AF is an inhibitor of TrxR. Figure adapted from (Poet et al., 2017). **C**. Co- and post- translational folding assay of G6P in the presence or absence of TrxR inhibitor AF. Note * indicating preprotein which was not translocated into ER; arrow indicating signal peptide cleaved protein; DR indicating disulfide rearrangement.

translation products were post-translationally incubated in the absence or presence of G6P (Figure 5-11C, lane 6, 7). This result indicated that post-translational disulfide rearrangement in the ER was dependent on G6P and required the Trx/TrxR pathway to transfer reducing equivalent from the outside of ER into the ER lumen.

5.2.4 Reconstitution of the Trx/TrxR pathway using minimal cytosolic components leads to post-translationally disulfide bonds rearrangement

Experiments with TrxR inhibitor AF above showed that the cytosolic TrxR pathway is required for post-translational disulfide rearrangement in the ER. We already know the minimal components for cytosolic TrxR pathway (Trx, TrxR, NADPH, G6P and G6PDH) (Poet et al., 2017). It has been demonstrated that the reconstituting the Trx/TrxR pathway using these components can influence redox status of one PDI family member, ERp57, as well as the redox state of roGFP in the ER derived microsomes. Here we used the post-translational folding assay using Adam 10 disintegrin domain to investigate if the Trx/TrxR pathway cytosolic components were sufficient for the reduction of disulfide bonds after translation.

As described above, the RNA was translated in the absence of G6P in a RRL with SP cells. A co-translational assay was carried out as above as control (Figure 5-12B lane 1-3). For the post-translational folding assay, SP cells were washed in KHM buffer to remove RRL translation system and then were incubated in KHM buffer in the absence and presence of the Trx/TrxR pathway using purified cytosolic components (Trx, TrxR, NADPH, G6P and G6PDH). In one sample, SP cells were incubated in KHM buffer with TrxR, NADPH, G6P and G6PDH, in the absence of Trx. A diffuse banding pattern was observed prior to addition of the Trx/TrxR pathway as translation was carried out in the absence of G6P (Figure 5-12B, lane 4) while several distinct bands were observed after incubation with the Trx/TrxR pathway (Figure 5-12B, lane 5) which indicated that the Trx/TrxR pathway could lead to disulfide rearrangements. A diffuse banding pattern remained when the translation products were incubated with TrxR, NADPH, G6P and G6PDH (Figure 5-12B, lane 5, 6). This indicated that known minimal cytosolic components in the

cytosolic reductive pathway was sufficient for the rearrangement of disulfide post-translationally and that this process was dependent on the presence of Trx.

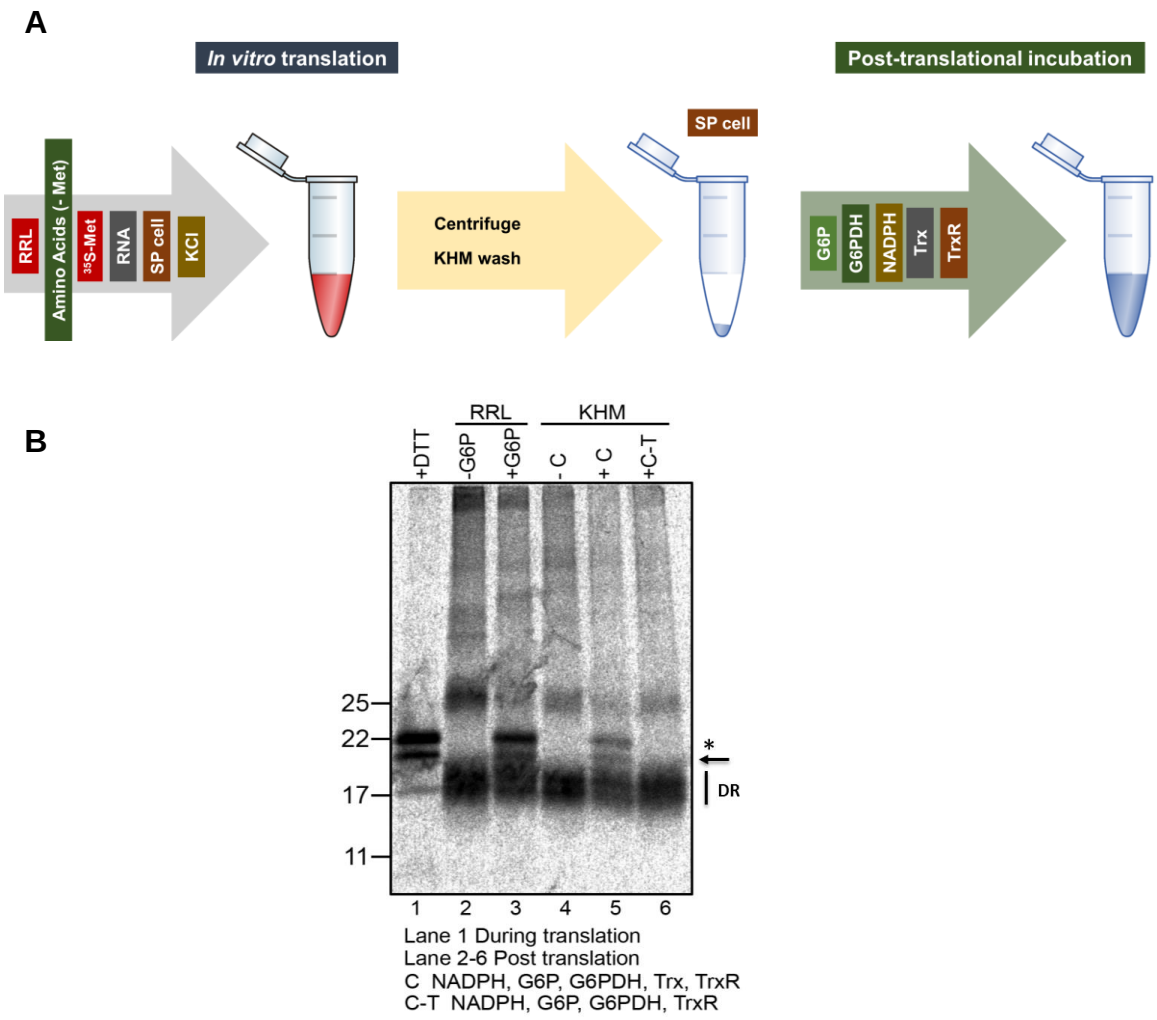

Figure 5-12 Reconstituted Trx/TrxR pathway lead to post-translational disulfide rearrangement. A. Workflow of post translational folding assay. Translation of Adam 10 disintegrin domain was carried out in RRL in the presence of radiolabeled ^{35}S Met. SP cells were added into RRL translation system acting as ER source. After translation, NEM was added to some samples to block the free thiols. In the other samples, the SP cells were pelted and washed with KHM buffer to remove RRL and then incubated in KHM buffer including or not including the Trx/TrxR system (C) using purified cytosolic components (Trx, TrxR, NADPH, G6P and G6PDH). One sample was incubated with reconstituted Trx/TrxR pathway in the absence of Trx (C-Trx). **B**. Translations were carried out in RRL as described above. Translations in the presence of DTT or in the absence of DTT and presence of G6P were stopped by addition of NEM (B, lanes 1-3). After translation, SP cells were pelleted and washed by KHM buffer to remove RRL and then incubated in KHM buffer (lane 4), in the presence of the Trx/TrxR system (C) (lane 5), or with TrxR, NADPH, G6P and G6PDH but without Trx (C-Trx) (lane 6). Note * indicating preprotein which was not translocated into the ER; arrow indicating signal peptide cleaved protein; DR indicating disulfide rearrangement.

5.2.5 Post-translational folding assay with TCEP

We previously demonstrated that the membrane impermeable reducing agent TCEP can reduce roGFP which localised in ER derived microsomes via membrane transport. We also showed that TCEP can reduce the PDI enzyme, ERp57. In both experiments, the reducing agent had a stronger reduction effect than the Trx/TrxR pathway. We also determined whether TCEP can rearrange disulfide bond after translation.

To investigate the effect of the reducing agent TCEP on post-translational disulfide exchange, a post-translational folding assay was carried out. As described above, the RNA template was translated in the absence of G6P in RRL with SP cells. In some samples, the SP cells were directly incubated in the absence (Figure 5-13 lane 1) or in the presence of G6P (final concentration 5 mM) (Figure 5-13 lane 2) or TCEP (final concentration 1 mM) (Figure 5-13 lane 3). To remove the effect from RRL, the SP cells were pelleted and washed with KHM buffer to remove the RRL or the other components in translation system. The SP cells were then resuspended in KHM buffer or cell extract in the absence or presence of TCEP (final concentration 1 mM) (Figure 5-13 lane 4-7). All the reactions were ended by the addition of alkylating agent. The Adam 10 disintegrin was immunoisolated using an anti-V5 antibody. The proteins were then separated by SDS-PAGE.

A mixture of proteins with different forms of disulfide bonds appeared when the SP cells were incubated in RRL (Figure 5-13 lane 1) indicating no reduction happened, which was consistent with previous results above. The addition of G6P into RRL promoted disulfide rearrangement in RRL which was showed by clear bands on the gel (Figure 5-13 lane 2). The same pattern of protein bands was observed after the addition of TCEP (Figure 5-13 lane 3). The disulfide rearrangement occurred in the sample which was only incubated in KHM buffer with TCEP. Compared with the sample incubated in KHM buffer, it suggested that the TCEP can lead to the reduction of disulfide bonds on its own and this reduction was independent of other components in cytosol. Some rearrangement of disulfides occurred when the SP cells were incubated in a cell extract which was prepared from HT1080 cell line (Figure 5-13 lane 6). The addition of TCEP into cell extract leads to disulfide rearrangement (Figure 5-13 lane 7). The results

demonstrated that a membrane impermeable reducing agent can lead to disulfide bonds on its own and the reduction process was not dependent on any other cytosolic components.

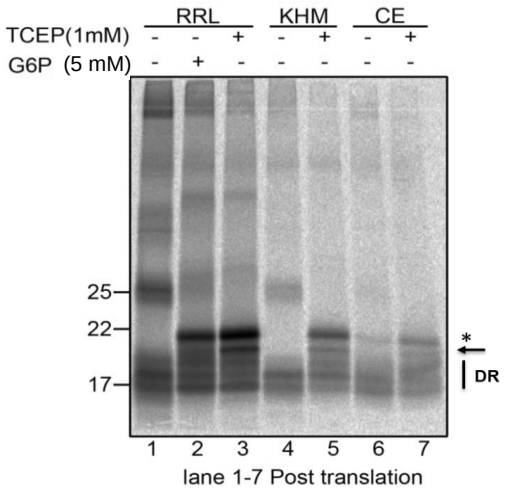

Figure 5-13 TCEP can lead to the disulfide rearrangement post-translationally. Translations were carried out in RRL as described above. After translation, the products were incubated in the absence (lane 1) or presence of G6P (5 mM) (lane 2) or TCEP (1 mM) (lane 3). In the other samples, the SP cells were centrifuged and washed by KHM buffer to remove RRL. The SP cells were resuspended in KHM buffer or a cell extract (CE) in the absence or presence of TCEP. The reactions were terminated by the addition of NEM to block free thiols. Products were separated by SDS-PAGE gel. Note * indicating preprotein which was not translocated into ER; arrow indicating signal peptide cleaved protein; DR indicating disulfide rearrangement.

5.2.6 Membrane protein, LMF1 and SEPN1, are not required for native disulfide bond formation of β1-integrin

It was shown previously (Peterfy et al., 2007) that LMF1, an ER localised membrane protein, is required for the protein folding and secretion of Lipoprotein lipase (LPL). Recently, it was demonstrated by proteomic and biochemical experiments that LMF1 interacts with ER localised PDI family members, like ERp72, ERp44 and ERdj5 as well as cytosolic protein Trx (Roberts et al., 2018) (Roberts et al., 2018) . All the proteins have been proven to play an important role in disulfide formation process. Another ER resident protein Selenoprotein N (SEPN1) is one of the selenocysteine-containing protein family. It is involved in maintaining of ER redox and calcium homeostasis (Marino et al., 2015). The function of LMF1 and SEPN1 is still not clearly known. We decided to test if they

are involved in the isomerisation of non-native disulfide bonds and if they could connect the reductive pathway in cytosol and the reduction of disulfide bonds in the ER. We obtained HEK 293 wild type and LMF1 KO cell lines (gift from Saskia B Neher) (Roberts et al., 2018) and Hela wild cell line and SEPN1 KO cell lines (gift from Ester Zito) (Varone et al., 2019).

A co-translational assay was first carried out to investigate if the LMF1 and SEPN1 was involved in the disulfide formation process. Translations were carried out in the absence or presence of G6P in RRL translation system including SP cells that were prepared from different cell lines (HEK 293 wild type and LMF1 KO cell line; Hela wild cell line and SEPN1 KO cell line). The NEM was added to the reaction to block free thiols and then the SP cells were isolated by centrifugation and washed once with KHM buffer to remove RRL. One portion of sample was boiled with SDS-loading buffer and directly run on the SDS-PAGE as total translation product (TT). The remaining part was immunoisolated with a conformation-specific antibody and then separated on SDS-PAGE.

Two clear bands were observed when the translation products were separated under reducing conditions (Figure 5-14 lanes 1 and 2). The lower band was untranslocated (untrans) ß1-integrin and the upper band was glycosylated ß1-integrin which was running slower than untranslocated ß1-integrin because of its glycosylation. When we used HEK 293 wild and LMF1 KO SP cells as ER source in translation system, a smear band was observed in the absence of G6P (Figure 5-14 A and B, lane 3), but two bands appeared when the translation was carried out in the presence of G6P (Figure 5-14 A and B, lane 4). This suggested that the native disulfide bonds formation requires the addition of G6P which was also demonstrated by the IP samples. More ß1-integrin with native disulfide bonds were observed in the samples that were translated in the presence of G6P (Figure 5-14 A and B lane 6). No difference was observed between the translations that were carried out with HEK 293 WT and LMF1 KO cell line (Figure 5-14 A and B). This result suggested that LMF1 was not essential for native disulfide bonds formation of ß1-integrin. Two bands were observed in samples which were translated with Hela WT or Hela SEPN1 KO SP cells in the absence of G6P (Figure 5-14 C and D lane 3) which indicated that native disulfide bond formation of ß1-integrin in the presence of Hela SP cells were not depend on addition of G6P. This was also demonstrated by the IP results (Figure 5-14 C and D lane 5). The same

amount of ß1-integrin was isolated by conformation specific antibody 9EG7 in both Hela wild and SEPN1 KO cell line. And in both total translation and IP samples, no difference was observed between WT and SEPN1 KO cell line (Figure 5-14 C and D). These results suggested that the formation of native disulfide bonds in ß1-integrin did not require the membrane proteins LMF1 or SEPN1 and this indicated the possibility of other membrane protein in the reductive pathway which ensures native disulfide bond formation.

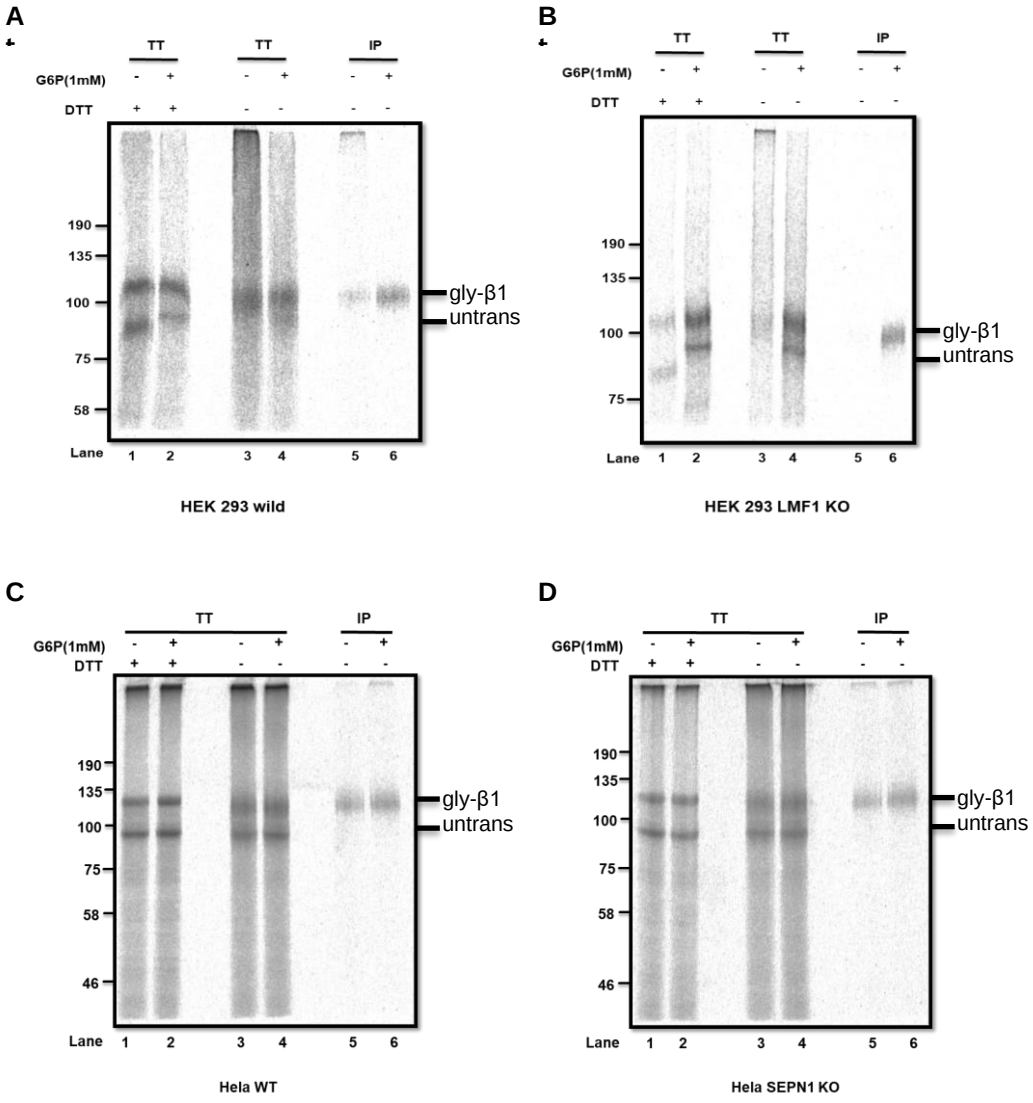

Figure 5-14 Membrane proteins, LMF1 and SEPN1, are not required for native disulfide bond formation within β1-integrin. SP cells were prepared from different cell lines (HEK 293 wild type and LMF1 KO cell line; Hela wild cell line and SEPN1 KO cell line). The β1-integrin was translated in the absence or presence of G6P (final concentration 1 mM) in RRL containing SP cells. During the translation, the products were radiolabelled by ^{35}S Met. The reactions were ended by the addition of alkylating NEM. The SP cells were isolated by centrifugation and washed once by KHM buffer to remove RRL. The SP cells was then resuspended in 40 µl KHM buffer. Two portions of 5 µl SP

cells were kept as total translation product (TT). The remaining part of samples were immunoprecipitated using conformational specific antibody 9EG7. All samples were separated by SDS-PAGE. One portion of total translation product was run on the gel under reducing condition (lanes 1 and 2). The rest of samples were under non-reducing condition.

5.3 Conclusion and Discussion

Previous work on the reduction of non-native disulfides in proteins entering the secretory pathway demonstrated a connection between the electron donor NADPH produced in the cytosol and client proteins within the ER (Poet et al., 2017). However, the intermediate steps in this pathway remain unknown. The post-translational folding assay which we have developed will be used to evaluate the ability of cytosolic components to resolve non-native disulfides in the ER lumen and will ultimately be used to identify the membrane protein involved.

We first developed the post-translational folding assay in RRL. The translation was carried out as described previously (Poet et al., 2017). We took advantage of a commercial translation system RRL containing all the cellular components essential for protein synthesis *in vitro*, such as tRNA, ribosomes, initiation factors, elongation factors and termination factors, to synthesis human ß1-integrin protein (Pelham and Jackson, 1976). The RNA template and ^{35}S-Met were added into RRL to allow radiolabelled proteins synthesis. When the RNA template was translated without any addition, a mixture of proteins including different disulfide bonds (native and non-native disulfide bonds) was synthesised. After translation, a cytosolic component eg. G6P can be added into the mixture to allow further incubation for different times. If the component can reduce disulfide bonds, then a homogeneous reduced protein will be observed on the SDS-PAGE gel. By using this system, we demonstrated that the post-translational addition of G6P in the cytosol leads to the reduction of disulfide bonds. The post-translational folding assay which was carried out with TrxR inhibitor AF demonstrated that the cytosolic reduction of protein disulfide bonds after translation needed the TrxR pathway in the cytosol.

The post-translational folding assay in the ER was carried out as above with SP cells acting as ER source. The SP cells were prepared from cultured confluent cells by the treatment with digitonin which selectively permeabilised the plasma

membrane to allow the removal of cytosolic components, but the ER membrane maintains its integrity because of its low cholesterol content (Wilson et al., 1995). Initially, the post-translational folding assay was not successful when it was performed in RRL with SP cells using β1-integrin as the substrate protein. After translation, the reduction of non-native disulfides in β1-integrin was independent of the component G6P added to the reaction system. This maybe caused by the particularity of RRL.

RRL Translation System has been used for characterising protein products from RNA transcripts and investigating transcriptional and translational control for over four decades, primarily due to the ability to reproducibly obtain large amounts of RRL that is highly efficient in protein translation (Jackson and Hunt, 1983, Walter and Blobel, 1983). Reticulocytes are made from immature red blood cells at the penultimate stage of differentiation. At this stage the red blood cells have lost their nucleus, but their protein synthesis (primarily of hemoglobin) continues robustly using pre-existing cellular components necessary for protein synthesis (tRNA, ribosomes, amino acids, initiation, elongation and termination factors) (Lodish and Desalu, 1973). After the reticulocytes are lysed, RRL is optimised further for mRNA translation supplemented with tRNA, creatine phosphate, creatine phosphokinase, DTT, potassium acetate, magnesium chloride or hemin (Pelham and Jackson, 1976). In addition, RRL may contain a variety of post-translational processing activities (Walter and Blobel, 1983, Krieg and Melton, 1984). The addition of canine pancreatic microsomal membranes to a standard translation reaction means core glycosylation can be examined. Hence, a more defined system to study the role of cytosolic components in the resolution of non-native disulfides within the ER maybe worth establishing. A cytosol extract from Hela cells or HT1080 cells containing all the cytosolic components probably could provide an alternative of RRL (Mikami et al., 2006).

As *in vitro* studies work best with smaller simpler proteins (Braakman and Bulleid, 2011), other substrate proteins, LDLr, tPA and Adam 10 disintegrin domain were considered as model substrate proteins to develop the post-translational folding assay in ER. We successfully developed the post-translational folding assay in the ER with Adam 10 disintegrin domain as the substrate protein.

We demonstrated the post-translational disulfide rearrangement needs the addition of G6P after translation and the process could be inhibited by TrxR inhibitor in RRL. It was previously demonstrated that the addition of G6P drove the generation of NADPH providing an electron donor for cytosolic TrxR1, which in turn reduces Trx1. A robust TrxR1 pathway was required to prevent the formation of non-native disulfides and allow correct disulfides to form within proteins entering the ER (Poet et al., 2017). Similarly, the addition of G6P in RRL after translation could encourage the disulfide rearrangement. This is maybe caused by the generation of NADPH which could provide electrons for the rearrangement in ER after depletion by translation reactions. Instead of adding G6P to RRL after translation, the SP cells were isolated from RRL and resuspended in a Hela cell extract. The disulfide rearrangement also occurred and this process was independent of addition of G6P in Hela cell extract. This indicated that the redox status of cytosol in Hela cell line was different from the HT1080 cell line and there were enough reducing equivalents in Hela cell extract which could provide enough reducing power for the disulfide reduction.

After the success of post-translational folding assay of G6P, we used this assay to evaluate the ability of reconstituted Trx/TrxR pathway using cytosolic components (Trx/TrxR/NADPH/G6PDH/G6P) to reduce disulfide bonds after translation. The result demonstrated that the reconstituted Trx/TrxR reductive pathway using purified components (NADPH, G6P, G6PDH, Trx and TrxR) can lead to the disulfide rearrangement of Adam 10 disintegrin domain in the ER after translation and the absence of Trx can prevent disulfide rearrangement. Because we isolated the SP cells from translational system and excess RRL was removed by KHM buffer wash. This excluded the possibility of the effects of other cytosolic components in the isomerisation of non-native disulfide bonds. The disulfide rearrangement still happened when the SP cells were only incubated with reconstituted Trx/TrxR pathway in KHM buffer. It proved that no additional components are needed in cytosolic reductive pathway. The post-translational folding assay also proved the equal effect of TCEP on the isomerisation of non-native disulfide bonds.

Current results of ß1-intergin translations using LMF1 and SEPN1 KO SP cells showed that the ER membrane proteins, LMF1 and SEPN1, were not required for native disulfide bond formation during translation. In the future, it would be

worth carrying out the post-translational folding assay using Adam 10 disintegrin domain as substrate to investigate if these two ER membrane proteins are necessary for the post-translational disulfide bonds rearrangement.

Chapter 6 Discussion

6.1 General discussion

6.1.1 The minimal components in the cytosolic Trx/TrxR pathway are sufficient for the ER reductive pathway

The Trx/TrxR system exists extensively in prokaryotes and eukaryotes and their structure and function have been well characterised (Holmgren et al., 1975, Sandalova et al., 2001, Collet and Messens, 2010). Mammalian Trx has approximately 25% sequence identity to Trx in *E. coli* (Eklund et al., 1991). In the Trx/TrxR system, the electrons from NADPH can flow to the substrate protein in an oxidised form via the catalytic cysteines of the Trx active site motif.

The Trx/TrxR system plays diverse and critical roles in mammalian cells. The Trx/TrxR system can regulate transcription by regulating the nuclear and cytoplasmic redox-sensitive transcription factors (Schenk et al., 1994, Hirota et al., 1999). Trx can also regulate apoptosis by binding with apoptosis signal-regulating kinase 1 (ASK1) (Saitoh et al., 1998). In *E.coli*, the electrons for reduction of non-native disulfide ultimately came from cytoplasmic NADPH via Trx/TrxR system (Rietsch et al., 1997). Hence, the mammalian Trx/TrxR were assumed to contribute to the reduction of incorrect disulfide in the ER (Bulleid and van Lith, 2014). A previous study emphasised the critical role of the mammalian cytosolic TrxR pathway in the correct disulfide formation in the ER (Poet et al., 2017). It was unknown whether additional cytosolic components are required for the reduction of non-native disulfide occurring in the ER.

To further investigate the effect of the cytosolic Trx/TrxR pathway, we successfully reconstituted the cytosolic Trx/TrxR pathway using minimal components (G6P, G6PDH, NADPH, Trx, and TrxR) (Figure 6-1). The concentration of each component is controlled as close as possible to the cell extract to reconstitute a Trx/TrxR pathway like that *in vivo*. Using a reconstituted Trx/TrxR system can eliminate the influence of numerous compounds in the cytosol on the redox change in the ER or microsomes to focus on the effect of Trx/TrxR pathway. We demonstrated that no additional cytosolic components are required for the

transduction of the reducing equivalents from the cytosolic Trx/TrxR system to the ER and the process is dependent on the catalytic cysteines in the Trx motif. We determined that the Trx was fully reduced in the presence of the reconstituted Trx/TrxR system. In terms of thermodynamic stability, the oxidised form of Trx is far more stable than its reduced form (Roos et al., 2007). The large difference in stability provides the driving force for the reduction of the substrate protein by Trx (Roos et al., 2007). This suggested that electrons are directly shuttled to the substrate protein in the ER from Trx which is itself reduced by TrxR.

Cytosolic Trx/TrxR pathway is not the only cytosolic reductive pathway contributing to the reduction of non-native disulfide bonds in the ER (Chakravarthi et al., 2006). To reduce the non-native disulfide in the ER, PDI needs to stay in a reduced form to donate electrons to the substrate proteins. In chapter 4, we noticed that incubation with GSH, that is required for redox homeostasis in the ER (Appenzeller-Herzog et al., 2010), can fully reduce oxidised ERp57 in the SP cells. This result is consistent with a previous study by Jessop (Jessop and Bulleid, 2004). They showed that cytosolic GSH is required for the ER reductive pathway by maintaining the ERp57 in a reduced state. However, there is no direct evidence of the effect of GSH on disulfide rearrangement after translation. It is worth investigating post-translational reduction of substrate proteins by GSH using our post-translational folding assay.

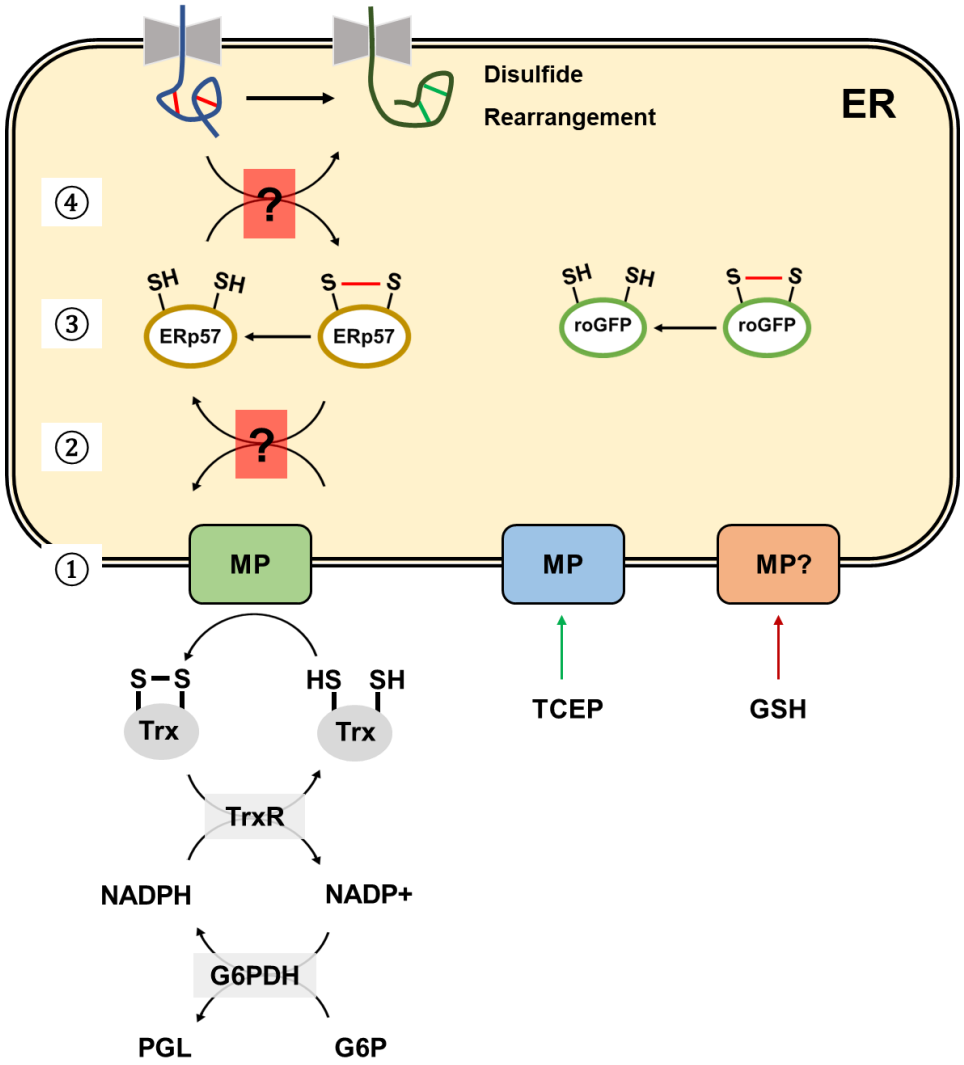

Figure 6-1 Schematic of the flow of the reducing equivalents from the outside of the ER to the ER lumen. Reducing equivalents can come from different sources, the reconstituted Trx/TrxR pathway, GSH and membrane impermeable reducing agent TCEP. Unknown membrane proteins (MP, indicated by squares) are involved in the transduction of reducing equivalents to the ER. It has been demonstrated the cytosolic Trx/TrxR pathway and TCEP can reduce ERp57, roGFP, and lead to the disulfide rearrangement in the ER, which is dependent of the interaction between Trx and a membrane protein. We also showed that the GSH can reduce ERp57. The questions remaining to address are: (1) Which membrane protein is involved in the transduction of reducing equivalents? (2) How does the ERp57 accept electrons from membrane proteins? (3) Can other PDI family members accept electrons from the cytosolic Trx/TrxR pathway? (4) How are non-native disulfides reduced?

6.1.2 A membrane protein is involved in the ER reductive pathway

Cytosolic Trx/TrxR pathway exists in all living cells including prokaryotics and eukaryotics (Holmgren and Bjornstedt, 1995, Arner et al., 1999). It plays a central role in redox balance (Cardenas-Rodriguez and Tokatlidis, 2017) and signal

transduction (Monteiro et al., 2017) at the cellular level. In bacteria, it was demonstrated that the electrons can flow from the cytosolic Trx/TrxR system to periplasmic DsbC via a membrane protein DsbD and then finally to the substrate proteins (Cho and Beckwith, 2009, Chung et al., 2000, Rietsch et al., 1997). A previous study showed the link between the cytosolic Trx/TrxR pathway and the correct disulfide formation in the ER in mammalian cells (Poet et al., 2017). However, we do not know if there is a membrane protein in the ER which functions like DsbD that can shuttle the electrons.

We demonstrated the cytosolic Trx/TrxR pathway can reduce diverse proteins in the ER derived microsomes, ERp57 in the ER, and can reduce the non-native disulfides in the SP cells. These results further confirm that reducing equivalents generated by the cytosolic pathway can cross the ER membrane. Later, we took advantage of proteinase K and SP cells to prove that the digestion of the ER membrane protein prevents the reduction of fully oxidised ERp57 suggesting the existence of a membrane protein facilitating the electron shuttling. In addition, the reconstituted Trx/TrxR pathway using Trx catalytic cysteine mutants indicated that the membrane protein can be reduced by receiving the electrons from the reduced form of Trx (Holmgren and Bjornstedt, 1995, Holmgren, 1995). Our study confirms the existence of a membrane protein like prokaryotic DsbD in the ER membrane which can shuttle electrons and highlights the potential catalytic mechanism. In the future, we will focus on investigating the membrane protein which is the substrate of reduced Trx.

We initially used a membrane reducing agent TCEP to replace the reconstituted Trx/TrxR pathway. It demonstrated that TCEP can also reduce ERp57, non-native disulfides and roGFP via a membrane protein. However, when the microsomes or SP cells were treated with the proteinase K, the reducing equivalents can still cross the microsome or SP cells, which is different from the Trx/TrxR pathway. This suggested the membrane protein which is required for the TCEP reductive pathway is not protease sensitive. A different catalytic mechanism is required for the TCEP and its membrane substrate protein.

Apart from cytosolic Trx/TrxR pathway, GSH is suspected as another reducing equivalents source for the ER reductive pathway (Jessop and Bulleid, 2004, Bulleid and van Lith, 2014). Herein using the ERp57 as the redox indicator, we showed

that the electron from GSH can cross the ER membrane, supporting the hypothesis. A previous study by Alise Ponsero showed in *S. cerevisiae* that GSH is imported into the ER lumen through the Sec61 channel by facilitated diffusion and the transport process is regulated by BiP (Ponsero et al., 2017). Whether Sec61 is required for the GSH dependent ER reductive pathway in mammalian cells remains to be addressed. It is worthwhile to evaluate this possibility using our roGFP microsomes, ERp57-V5 in SP cells and post-translationally folding assay.

6.1.3 The redox balance in the ER is tightly maintained by the oxidative and reductive pathway

In chapter 4, the results indicated that the Trx/TrxR pathway can reduce fully oxidised ERp57, a PDI family member. However, a redox change of PDI is not observed in the microsomal lumen after incubation with the reconstituted Trx/TrxR pathway in chapter 3. These results suggested that the redox status of PDI is in balance.

It known that the PDI can catalyse the oxidisation, reduction, and isomerisation of disulfide bonds (Darby et al., 1998, Ellgaard and Ruddock, 2005). The oxidation function required the oxidised form of PDI while the reduction and isomerisation functions need PDI in the reduced form (Bulleid and Ellgaard, 2011). The balance between the reduced form and oxidised form needs to be tightly regulated to ensure the normal functions of PDI. The oxidised formed of PDI is maintained by several pathways, like ERO1 (Cabibbo et al., 2000, Pagani et al., 2000), VKOR1 (Schulman et al., 2010), and so on. We consider that if the microsomal PDI was reduced by reducing equivalents from reconstituted Trx/TrxR pathway, the electrons were accepted by ERO1 and VKOR1 meaning there would be no change is the redox status of PDI. This is supported by the MS result showing that ERO1 and VKOR are reduced in microsomes treated with complete Trx/TrxR pathway (in chapter 4).

The limitation of our MS experiment is that it begins with microsomes in which the redox state is in balance which causes difficulty in observing the change of redox state of ER localised proteins in the presence and in the absence of Trx. In chapter 4, we determined that ERp57 is partially reduced and oxidised in untreated

HT1080 SP cells. It is hard to observe the reduction effect of Trx/TrxR pathway on the ERp57 in untreated SP cells. But if we first fully oxidised the SP cells, the redox state of ERp57 was restored (partially reduced and oxidised) after the incubation with complete Trx/TrxR pathway while the ERp57 was still in a fully oxidised state in the absence of Trx. We can consider using fully oxidised microsomes in the future to amplify the effect of reconstituted Trx/TrxR on the microsome membrane protein and microsomal lumen proteins. This approach would improve the possibility to identify the membrane proteins and ER localised proteins involved in the ER reductive pathway.

6.1.4 The ER reductive pathway

RRL is a commonly used mammalian cell free translation system (Pelham and Jackson, 1976). The commercial RRL has been universally used in protein folding and modifications (Carlson et al., 2012). Recently, the RRL with SP cells was applied to investigate *in vitro* disulfide formation in the ER (Poet et al., 2017). Based on this mammalian translation system, we developed a post-translational folding assay using a stalled substrate protein (Robinson et al., 2020) which can evaluate the reductive ability of cytosolic components on the newly synthesised polypeptide chain after translation. We demonstrated that the reconstituted Trx/TrxR pathway can reduce non-native disulfides and leads to disulfide rearrangement in the nascent chain. In addition, through a proteomic analysis in chapter 3, a lot of secreted proteins became more reduced compared to the sample in the absence of Trx.

PDI can catalyse the reduction of disulfides. We chose one PDI family member, ERp57 which is essential for the folding of glycosylated protein (Jessop et al., 2007), as an indicator. The result showed the fully oxidised ERp57 in SP cells can be reduced by the complete Trx/TrxR pathway suggesting the ER-localised PDI can receive electrons from the Trx/TrxR pathway. Whether other PDI family members can receive electrons from the Trx/TrxR pathway is worth testing, for example ERdj5 that already shows its importance in removing non-native disulfides (Oka et al., 2013, Ushioda et al., 2008).

We demonstrated the link between cytosolic Trx/TrxR pathway and the redox state of diverse substrate proteins in the ER lumen and the connection between

cytosolic Trx/TrxR pathway and ERp57 (Figure 6-1). How ERp57 accepts electrons from the membrane protein, whether additional components are required in this process, whether other PDI is involved in the reductive pathway, and how the nascent chain is reduced are still puzzles to address. These can be our research focus in the future.

6.2 Future experiments

6.2.1 Membrane protein involved in Trx/TrxR-dependent reductive pathway

Components of the cytosolic Trx/TrxR pathway that are required for the ER reductive pathway have been clarified. We also demonstrated that a membrane protein is necessary for the reduction in the ER. However, we have not identified the membrane protein.

a) Trapping membrane proteins using Trx mutants

Based on our study, the ER membrane protein which is involved in the ER reductive pathway is assumed accepting electrons from reduced Trx (Figure 6-2) (Holmgren, 1995). If we consider the membrane protein is the substrate protein of Trx, different methods can be used to trap Trx substrates complexes (Collet and Messens, 2010). As described previously in chapter 3, the Cys^{35} in Trx active motif is required to dissociate the transient intermediate during the disulfide exchange with substrate proteins (Schwertassek et al., 2007a). Mutation of Cys^{35} (replace by serine) can stop the dissociation process allowing Trx and substrate protein to stay in the transient intermediate. We already purify the different Trx mutants (CC, CS, and SS) in chapter 3. It will provide us an opportunity to trap the membrane protein.

To identify the ER membrane protein, we will use the ER derived microsomes as the material rather than intact cells which have diverse intracellular organelles. These microsomes will be incubated with reconstituted Trx/TrxR pathway using the Trx mutants (CC, CS, and SS), so that the reconstituted system can keep the Trx mutants in reduced state. The incubation will be ended with the incubation

with NEM blocking the free thiols followed by the lysing of the microsomes. The Trx can be immunoisolated by streptavidin beads due to the streptavidin tag. The samples will be separated by SDS-PAGE and visualized by the antibody, Streptavidin Protein DyLight 800, we will expect that diverse bands occur in the sample incubated with Trx CC and CS and more intense bands will be observed in CS sample due to the Cys^{35} mutation. Only a single band should be observed in the sample treated with TrxSS, because both catalytic Cys are mutated. The protein bands occurring in the CS sample but not the SS sample will be analysed by the MS to identify the membrane protein.

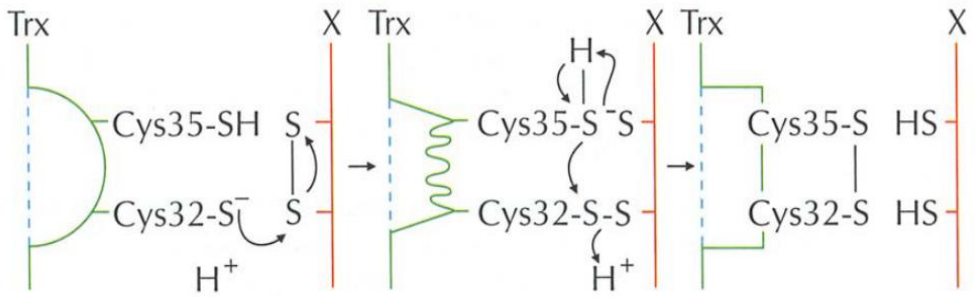

Figure 6-2 Potential catalytic mechanism of membrane protein by the reduced form of Trx. The membrane protein potentially received electrons by nuleophilic attack from Cys^{32} in the reduced Trx (Trx-$(SH)_2$) forming a transient intermediate. Another electron was then donated from Cys^{35}. In the end the Trx become oxidised and the membrane protein becomes reduced. (Holmgren, 1995)

b) Homologous analysis with prokaryotic membrane protein DsbD

In prokaryotes, the reductive pathway has been clearly clarified (Berkmen, 2012). The cytosolic membrane protein DsbD (Missiakas et al., 1995, Katzen and Beckwith, 2000) can keep protein disulfide isomerase DsbC (Rietsch et al., 1996) in reduced status using reducing equivalents providing by the cytosolic Trx/TrxR system. We have demonstrated that in mammalian cells the cytosolic Trx/TrxR system can also provide the reducing equivalents to the ER and the process is Trx-dependent. We assume that the ER membrane protein involved in the reductive pathway may have a certain similarity with DsbD. Maybe we can try to find ER membrane protein in mammalian cells which have a homologous sequence with DsbD using bioinformatics.

c) Proteomic analyse by MS

In chapter 3, we showed our reconstituted Trx/TrxR pathway can reduce ER-localised protein. In addition, some membrane proteins were also identified by the MS. However, the ERp57 redox state did not show large differences. We assumed that in the untreated microsomes the redox state of membrane proteins and redox state of ER-localised proteins are still in balance. We can consider optimising the MS protocol to investigate which proteins are involved in the Trx/TrxR dependent ER reductive pathway. Like the determination of redox state of ERp57, oxidation with diamide can be applied in the protocol. However, it is hard to thoroughly remove diamide from microsomes by centrifugation.

To obtain oxidised microsomes, we can treat the confluent HT1080 cells which can stably overexpress roGFP before preparation of microsomes. The redox status of roGFP microsomes will be evaluated by the ratio (390nm/460nm). The same portion of microsomes will be incubated with reconstituted Trx/TrxR pathway in the absence and presence of Trx. The redox state of proteins will be evaluated by MS as described previously in chapter 2. We expect that more membrane protein and ER-localised proteins will be observed than that in untreated in microsomes.

6.2.2 Membrane protein involved in GSH-dependent pathway

GSH is produced in the cytosol but GSH is also required in other intracellular organelles, like the mitochondria (Meredith and Reed, 1982) and the ER (Hwang et al., 1992). A lot of evidence has shown that GSH can be transport crossing the ER membranes (Molteni et al., 2004, Chakravarthi et al., 2006). Our experimental result in chapter 4 also supports that GSH can across the ER membrane and lead to the reduction of PDI. However, there is limited information about how the GSH crosses the ER membrane. Recently a study found a new function of Sec61 channel, facilitating GSH diffusion to the ER and the study also showed that in *S. cerevisiae* the transportation of GSH crossing the ER membrane is regulated by the ERO1 and BiP (Ponsero et al., 2017). We think it is worth investigating if the Sec61 is involved in the GSH-dependent ER reductive pathway.

To confirm the importance of Sec61 in GSH transportation, we can consider using mycolactone, an exotoxin which can block the Sec61 channel (Baron et al., 2016, McKenna et al., 2017), in our post-translational folding assay and ERp57-V5 redox state determination.

The translations are carried out in the absence of G6P and remove the excess RRL with KHM washing. The SP cells will be untreated or treated with mycolactone followed by the post-translation incubation with or without GSH. The products will be separated by SDS-PAGE. If the reduction is observed in the SP cells untreated with mycolactone but no reduction observed in the sample treated with mycolactone, the result will suggest that the Sec61 are involved in the GSH dependent reductive pathway. If reduction occurs in both the untreated and treated sample with mycolactone, perhaps there are other membrane proteins involved in the GSH transportation.

Determination of the redox state of ERp57-V5 can be used in the evaluation of the role of Sec61. The SP cells are generated from the HT1080 ERp57-V5 cell line, after full oxidation, the SP cells are treated with or without mycolactone. Then the SP cells will be incubated with GSH. The redox state of ERp57 will be visualised by differential alkylation. If no reduction occurs in the SP cells treated with mycolactone, it will demonstrate that the GSH is transported across the ER membrane by Sec61 channel.

6.2.3 Evaluation the role of the membrane protein in the ER reductive pathway

In chapter 3 we already screened several ER membrane proteins, TMX2, GPAA1, VKORC1L1, and LMAN1, whose redox state can be influenced by the complete Trx/TrxR system. In addition, if we succeed to identify more membrane protein using Trx trapping and proteomic analyse, it is necessary to have an assay to evaluate if the proteins are involved in the ER reductive pathway. In chapter 5, we developed a post-translational folding assay using a stalled substrate. We can take advantage of this assay.

Based on the identified protein, we can create KO cell line using CRISPR-Cas9 (Sander and Joung, 2014). SP cells can be prepared from the wild type and KO

cell line. The translation of Adam 10 will be carried out in the absence of G6P in RRL with two different kinds of SP cells. The SP cells will be isolated by centrifugation and washed with KHM buffer to remove excess RRL. Sample will be incubated with the reconstituted Trx/TrxR system in the absence and presence of Trx. The NEM would be used to stop the reaction. The protein will be immunoisolated and separated by SDS-PAGE. Different band patterns will be observed in samples which are translated with the wild type. If diffused bands occur in the samples which are translated with the KO cell line. The result would suggest the KO protein is required in the ER reductive pathway.

6.2.4 The influence of Trx/TrxR on the redox status of other PDI family members

In chapter 4 we demonstrated that cytosolic Trx/TrxR pathway can reduce ERp57. It is worth investigating whether other PDIs are involved in the Trx/TrxR dependent ER reductive pathway. A previous study proved that ERdj5 is also involved in the reduction of non-native disulfide (Oka et al., 2013, Ushioda et al., 2008).

To investigate if the ERdj5 is involved in the Trx/TrxR dependent ER reductive pathway, an ERdj5-V5 tagged cell line can be used to generate SP cells. After fully oxidised by diamide, the SP cells will be incubated with reconstituted Trx/TrxR pathway in the absence and presence of Trx. The redox state will be determined by differential alkylation and visualised by the western blot. If the ERdj5 is reduced due to the incubation with the complete Trx/TrxR system, the result will suggest that the ERdj5 is also involved in the Trx/TrxR dependent reductive pathway. In a similar way, the role of other PDI in the ER reductive pathway can be demonstrated using this assay. If there is a good quality antibody which can recognise the PDI, we can directly determine the redox state in wild type cell line rather than V5-tagged cell line.

In my thesis, we have demonstrated that the cytosolic reductive pathway is required for the reduction of ER-localised proteins and the reduction of non-native disulfide using a reconstituted Trx/TrxR pathway. We suggested that a membrane protein is required for the ER reductive pathway and indicated the possible

mechanism of electron shuttling via an ER membrane protein using Trx mutants. In summary the work presented in my thesis provides further information on the ER reductive pathway enabling future work to focus on identifying membrane proteins involved in electron transfer and to expand the number of PDI family members involved in the reduction of the non-native disulfides.

List of References

ADAM, S. A., MARR, R. S. & GERACE, L. 1990. Nuclear protein import in permeabilized mammalian cells requires soluble cytoplasmic factors. *J Cell Biol,* 111**,** 807-16.

ADAMS, B. M., OSTER, M. E. & HEBERT, D. N. 2019. Protein Quality Control in the Endoplasmic Reticulum. *Protein Journal,* 38**,** 317-329.

AEBI, M. 2013. N-linked protein glycosylation in the ER. *Biochimica Et Biophysica Acta-Molecular Cell Research,* 1833**,** 2430-2437.

AITS, S., JAATTELA, M. & NYLANDSTED, J. 2015. Methods for the quantification of lysosomal membrane permeabilization: A hallmark of lysosomal cell death. *Lysosomes and Lysosomal Diseases,* 126**,** 261-285.

ALKALAEVA, E. Z., PISAREV, A. V., FROLOVA, L. Y., KISSELEV, L. L. & PESTOVA, T. V. 2006. In vitro reconstitution of eukaryotic translation reveals cooperativity between release factors eRF1 and eRF3. *Cell,* 125**,** 1125-1136.

ANELLI, T., ALESSIO, M., BACHI, A., BERGAMELLI, L., BERTOLI, G., CAMERINI, S., MEZGHRANI, A., RUFFATO, E., SIMMEN, T. & SITIA, R. 2003. Thiol-mediated protein retention in the endoplasmic reticulum: the role of ERp44. *Embo Journal,* 22**,** 5015-5022.

APPENZELLER-HERZOG, C., RIEMER, J., CHRISTENSEN, B., SØRENSEN, E. S. & ELLGAARD, L. 2008. A novel disulphide switch mechanism in Ero1alpha balances ER oxidation in human cells. *The EMBO journal,* 27**,** 2977-2987.

APPENZELLER-HERZOG, C., RIEMER, J., ZITO, E., CHIN, K. T., RON, D., SPIESS, M. & ELLGAARD, L. 2010. Disulphide production by Ero1alpha-PDI relay is rapid and effectively regulated. *EMBO J,* 29**,** 3318-29.

APWEILER, R., MARTIN, M. J., O'DONOVAN, C., MAGRANE, M., ALAM-FARUQUE, Y., ANTUNES, R., BARRELL, D., BELY, B., BINGLEY, M., BINNS, D., BOWER, L., BROWNE, P., CHAN, W. M., DIMMER, E., EBERHARDT, R., FEDOTOV, A., FOULGER, R., GARAVELLI, J., HUNTLEY, R., JACOBSEN, J., KLEEN, M., LAIHO, K., LEINONEN, R., LEGGE, D., LIN, Q., LIU, W. D., LUO, J., ORCHARD, S., PATIENT, S., POGGIOLI, D., PRUESS, M., CORBETT, M., DI MARTINO, G., DONNELLY, M., VAN RENSBURG, P., BAIROCH, A., BOUGUELERET, L., XENARIOS, I., ALTAIRAC, S., AUCHINCLOSS, A., ARGOUD-PUY, G., AXELSEN, K., BARATIN, D., BLATTER, M. C., BOECKMANN, B., BOLLEMAN, J., BOLLONDI, L., BOUTET, E., QUINTAJE, S. B., BREUZA, L., BRIDGE, A., DECASTRO, E., CIAPINA, L., CORAL, D., COUDERT, E., CUSIN, I., DELBARD, G., DOCHE, M., DORNEVIL, D., ROGGLI, P. D., DUVAUD, S., ESTREICHER, A., FAMIGLIETTI, L., FEUERMANN, M., GEHANT, S., FARRIOL-MATHIS, N., FERRO, S., GASTEIGER, E., GATEAU, A., GERRITSEN, V., GOS, A., GRUAZ-GUMOWSKI, N., HINZ, U., HULO, C., HULO, N., JAMES, J., JIMENEZ, S., JUNGO, F., KAPPLER, T., KELLER, G., LACHAIZE, C., LANE-GUERMONPREZ, L., LANGENDIJK-GENEVAUX, P., LARA, V., LEMERCIER, P., LIEBERHERR, D., LIMA, T. D., MANGOLD, V., MARTIN, X., MASSON, P., MOINAT, M., MORGAT, A., MOTTAZ, A., PAESANO, S., PEDRUZZI, I., PILBOUT, S., PILLET, V., POUX, S., POZZATO, M., REDASCHI, N., et al. 2010. The Universal Protein Resource (UniProt) in 2010. *Nucleic Acids Research,* 38**,** D142-D148.

ARNER, E. S., ZHONG, L. & HOLMGREN, A. 1999. Preparation and assay of mammalian thioredoxin and thioredoxin reductase. *Methods Enzymol,* 300, 226-39.

ARNÉR, E. S. J. 2009. Focus on mammalian thioredoxin reductases — Important selenoproteins with versatile functions. *Biochimica et Biophysica Acta (BBA) - General Subjects,* 1790, 495-526.

AUSTIN, C. D., WEN, X., GAZZARD, L., NELSON, C., SCHELLER, R. H. & SCALES, S. J. 2005. Oxidizing potential of endosomes and lysosomes limits intracellular cleavage of disulfide-based antibody-drug conjugates. *Proc Natl Acad Sci U S A,* 102, 17987-92.

BAKER, K. M., CHAKRAVARTHI, S., LANGTON, K. P., SHEPPARD, A. M., LU, H. & BULLEID, N. J. 2008. Low reduction potential of Ero1alpha regulatory disulphides ensures tight control of substrate oxidation. *The EMBO journal,* 27, 2988-2997.

BARDWELL, J. C., LEE, J. O., JANDER, G., MARTIN, N., BELIN, D. & BECKWITH, J. 1993. A pathway for disulfide bond formation in vivo. *Proc Natl Acad Sci U S A,* 90, 1038-42.

BARON, L., PAATERO, A. O., MOREL, J.-D., IMPENS, F., GUENIN-MACÉ, L., SAINT-AURET, S., BLANCHARD, N., DILLMANN, R., NIANG, F., PELLEGRINI, S., TAUNTON, J., PAAVILAINEN, V. O. & DEMANGEL, C. 2016. Mycolactone subverts immunity by selectively blocking the Sec61 translocon. *The Journal of experimental medicine,* 213, 2885-2896.

BENHAM, A. M. 2012. The protein disulfide isomerase family: key players in health and disease. *Antioxid Redox Signal,* 16, 781-9.

BERINGER, M. & RODNINA, M. V. 2007. The ribosomal peptidyl transferase. *Molecular Cell,* 26, 311-321.

BERKMEN, M. 2012. Production of disulfide-bonded proteins in Escherichia coli. *Protein Expression and Purification,* 82, 240-251.

BERTOLOTTI, A., ZHANG, Y. H., HENDERSHOT, L. M., HARDING, H. P. & RON, D. 2000. Dynamic interaction of BiP and ER stress transducers in the unfolded-protein response. *Nature Cell Biology,* 2, 326-332.

BOURDI, M., DEMADY, D., MARTIN, J. L., JABBOUR, S. K., MARTIN, B. M., GEORGE, J. W. & POHL, L. R. 1995. Cdna Cloning and Baculovirus Expression of the Human Liver Endoplasmic-Reticulum P58 - Characterization as a Protein Disulfide-Isomerase Isoform, but Not as a Protease or a Carnitine Acyltransferase. *Archives of Biochemistry and Biophysics,* 323, 397-403.

BRAAKMAN, I. 2006. Protein folding in the endoplasmic reticulum. *European Journal of Cell Biology,* 85, 22-22.

BRAAKMAN, I. & BULLEID, N. J. 2011. Protein Folding and Modification in the Mammalian Endoplasmic Reticulum. *Annual Review of Biochemistry, Vol 80,* 80, 71-99.

BRAAKMAN, I. & HEBERT, D. N. 2013. Protein Folding in the Endoplasmic Reticulum. *Cold Spring Harbor Perspectives in Biology,* 5.

BRAAKMAN, I., HOOVERLITTY, H., WAGNER, K. R. & HELENIUS, A. 1991. Folding of Influenza Hemagglutinin in the Endoplasmic-Reticulum. *Journal of Cell Biology,* 114, 401-411.

BRUCE ALBERTS, D. B., JULIAN LEWIS, MARTIN RAFF, KEITH ROBERTS, JAMES D. WATSON 1994. Molecular Biology of the Cell.

BULLEID, J.-L. B. A. N. J. 2009. ERp57 is involved in the oxidative folding of the low-density lipoprotein receptor in the endoplasmic reticulum. *Bioscience Horizons,* 2.

BULLEID, N. J., BASSELDUBY, R. S., FREEDMAN, R. B., SAMBROOK, J. F. & GETHING, M. J. H. 1992. Cell-Free Synthesis of Enzymatically Active Tissue-Type Plasminogen-Activator - Protein Folding Determines the Extent of N-Linked Glycosylation. *Biochemical Journal,* 286**,** 275-280.

BULLEID, N. J. & ELLGAARD, L. 2011. Multiple ways to make disulfides. *Trends in Biochemical Sciences,* 36**,** 485-492.

BULLEID, N. J. & VAN LITH, M. 2014. Redox regulation in the endoplasmic reticulum. *Biochemical Society Transactions,* 42**,** 905-908.

CABIBBO, A., PAGANI, M., FABBRI, M., ROCCHI, M., FARMERY, M. R., BULLEID, N. J. & SITIA, R. 2000. ERO1-L, a Human Protein That Favors Disulfide Bond Formation in the Endoplasmic Reticulum. 275**,** 4827-4833.

CARAMELO, J. J. & PARODI, A. J. 2015. A sweet code for glycoprotein folding. *Febs Letters,* 589**,** 3379-3387.

CARDENAS-RODRIGUEZ, M. & TOKATLIDIS, K. 2017. Cytosolic redox components regulate protein homeostasis via additional localisation in the mitochondrial intermembrane space. *FEBS letters,* 591**,** 2661-2670.

CARLSON, E. D., GAN, R., HODGMAN, C. E. & JEWETT, M. C. 2012. Cell-free protein synthesis: applications come of age. *Biotechnol Adv,* 30**,** 1185-94.

CASAGRANDE, S., BONETTO, V., FRATELLI, M., GIANAZZA, E., EBERINI, I., MASSIGNAN, T., SALMONA, M., CHANG, G., HOLMGREN, A. & GHEZZI, P. 2002. Glutathionylation of human thioredoxin: A possible crosstalk between the glutathione and thioredoxin systems. *Proceedings of the National Academy of Sciences of the United States of America,* 99**,** 9745-9749.

CASTILLO, V., ONATE, M., WOEHLBIER, U., ROZAS, P., ANDREU, C., MEDINAS, D., VALDES, P., OSORIO, F., MERCADO, G., VIDAL, R. L., KERR, B., COURT, F. A. & HETZ, C. 2015. Functional Role of the Disulfide Isomerase ERp57 in Axonal Regeneration. *PLoS One,* 10**,** e0136620.

CEFALU, A. B., NOTO, D., ARPI, M. L., YIN, F., SPINA, R., HILDEN, H., BARBAGALLO, C. M., CARROCCIO, A., TARUGI, P., SQUATRITO, S., VIGNERI, R., TASKINEN, M. R., PETERFY, M. & AVERNA, M. R. 2009. Novel LMF1 nonsense mutation in a patient with severe hypertriglyceridemia. *J Clin Endocrinol Metab,* 94**,** 4584-90.

CHACINSKA, A., PFANNSCHMIDT, S., WIEDEMANN, N., KOZJAK, V., SANJUÁN SZKLARZ, L. K., SCHULZE-SPECKING, A., TRUSCOTT, K. N., GUIARD, B., MEISINGER, C. & PFANNER, N. 2004. Essential role of Mia40 in import and assembly of mitochondrial intermembrane space proteins. *The EMBO journal,* 23**,** 3735-3746.

CHAKRAVARTHI, S., JESSOP, C. E. & BULLEID, N. J. 2006. The role of glutathione in disulphide bond formation and endoplasmic-reticulum-generated oxidative stress. *EMBO Rep,* 7**,** 271-5.

CHALFIE, M., TU, Y., EUSKIRCHEN, G., WARD, W. W. & PRASHER, D. C. 1994. Green Fluorescent Protein as a Marker for Gene-Expression. *Science,* 263**,** 802-805.

CHANCE, B., SCHOENER, B., OSHINO, R., ITSHAK, F. & NAKASE, Y. 1979. Oxidation-reduction ratio studies of mitochondria in freeze-trapped samples. NADH and flavoprotein fluorescence signals. *J Biol Chem,* 254**,** 4764-71.

CHO, S. H. & BECKWITH, J. 2009. Two snapshots of electron transport across the membrane: insights into the structure and function of DsbD. *J Biol Chem,* 284**,** 11416-24.

CHONG, S. 2014. Overview of cell-free protein synthesis: historic landmarks, commercial systems, and expanding applications. *Curr Protoc Mol Biol,* 108**,** 16 30 1-11.

CHUNG, J., CHEN, T. & MISSIAKAS, D. 2000. Transfer of electrons across the cytoplasmic membrane by DsbD, a membrane protein involved in thiol-disulphide exchange and protein folding in the bacterial periplasm. *Molecular Microbiology,* 35**,** 1099-1109.

CLAUDE, A. 1943. The constitution of protoplasm. *Science,* 97**,** 451-456.

COE, H. & MICHALAK, M. 2010. ERp57, a multifunctional endoplasmic reticulum resident oxidoreductase. *International Journal of Biochemistry & Cell Biology,* 42**,** 796-799.

COLLET, J.-F. & BARDWELL, J. C. A. 2002. Oxidative protein folding in bacteria. 44**,** 1-8.

COLLET, J.-F. & MESSENS, J. 2010. Structure, Function, and Mechanism of Thioredoxin Proteins. *Antioxidants & Redox Signaling,* 13**,** 1205-1216.

CORMACK, B. P., VALDIVIA, R. H. & FALKOW, S. 1996. FACS-optimized mutants of the green fluorescent protein (GFP). *Gene,* 173**,** 33-38.

COX, J. & MANN, M. 2008. MaxQuant enables high peptide identification rates, individualized p.p.b.-range mass accuracies and proteome-wide protein quantification. *Nat Biotechnol,* 26**,** 1367-72.

COX, J., NEUHAUSER, N., MICHALSKI, A., SCHELTEMA, R. A., OLSEN, J. V. & MANN, M. 2011. Andromeda: A Peptide Search Engine Integrated into the MaxQuant Environment. *Journal of Proteome Research,* 10**,** 1794-1805.

CSALA, M., MARCOLONGO, P., LIZAK, B., SENESI, S., MARGITTAI, E., FULCERI, R., MAGYAR, J. E., BENEDETTI, A. & BANHEGYI, G. 2007. Transport and transporters in the endoplasmic reticulum. *Biochim Biophys Acta,* 1768**,** 1325-41.

CUNNEA, P. M., MIRANDA-VIZUETE, A., BERTOLI, G., SIMMEN, T., DAMDIMOPOULOS, A. E., HERMANN, S., LEINONEN, S., HUIKKO, M. P., GUSTAFSSON, J. A., SITIA, R. & SPYROU, G. 2003. ERdj5, an endoplasmic reticulum (ER)-resident protein containing DnaJ and thioredoxin domains, is expressed in secretory cells or following ER stress. *J Biol Chem,* 278**,** 1059-66.

DARBY, N. J., PENKA, E. & VINCENTELLI, R. 1998. The multi-domain structure of protein disulfide isomerase is essential for high catalytic efficiency. *Journal of Molecular Biology,* 276**,** 239-247.

DESHAIES, R. J., SANDERS, S. L., FELDHEIM, D. A. & SCHEKMAN, R. 1991. Assembly of yeast Sec proteins involved in translocation into the endoplasmic reticulum into a membrane-bound multisubunit complex. *Nature,* 349**,** 806-808.

DEVER, T. E. & GREEN, R. 2012. The Elongation, Termination, and Recycling Phases of Translation in Eukaryotes. *Cold Spring Harbor Perspectives in Biology,* 4.

DOOLEY, C. T., DORE, T. M., HANSON, G. T., JACKSON, W. C., REMINGTON, S. J. & TSIEN, R. Y. 2004. Imaging dynamic redox changes in mammalian cells with green fluorescent protein indicators. *J Biol Chem,* 279**,** 22284-93.

DOOLITTLE, M. H., EHRHARDT, N. & PETERFY, M. 2010. Lipase maturation factor 1: structure and role in lipase folding and assembly. *Curr Opin Lipidol,* 21**,** 198-203.

EKLUND, H., GLEASON, F. K. & HOLMGREN, A. 1991. Structural and functional relations among thioredoxins of different species. *Proteins,* 11**,** 13-28.

ELLGAARD, L., MCCAUL, N., CHATSISVILI, A. & BRAAKMAN, I. 2016. Co- and Post-Translational Protein Folding in the ER. *Traffic,* 17**,** 615-38.

ELLGAARD, L. & RUDDOCK, L. W. 2005. The human protein disulphide isomerase family: substrate interactions and functional properties. *Embo Reports,* 6**,** 28-32.

ENGLANDER, S. W. & MAYNE, L. 2014. The nature of protein folding pathways. *Proceedings of the National Academy of Sciences,* 111**,** 15873.

ENGLISH, A. R. & VOELTZ, G. K. 2013. Endoplasmic Reticulum Structure and Interconnections with Other Organelles. *Cold Spring Harbor Perspectives in Biology,* 5.

FASS, D. 2012. Disulfide Bonding in Protein Biophysics. *Annual Review of Biophysics, Vol 41,* 41**,** 63-79.

FOURIE, A. M., SAMBROOK, J. F. & GETHING, M. J. H. 1994. Common and Divergent Peptide Binding Specificities of Hsp70 Molecular Chaperones. *Journal of Biological Chemistry,* 269**,** 30470-30478.

FRAND, A. R. & KAISER, C. A. 1999. Ero1p oxidizes protein disulfide isomerase in a pathway for disulfide bond formation in the endoplasmic reticulum. *Molecular Cell,* 4**,** 469-477.

FRASCONI, M., CHICHIARELLI, S., GAUCCI, E., MAZZEI, F., GRILLO, C., CHINAZZI, A. & ALTIERI, F. 2012. Interaction of ERp57 with calreticulin: Analysis of complex formation and effects of vancomycin. *Biophysical Chemistry,* 160**,** 46-53.

FREEMAN, R. & WILLNER, I. 2009. NAD(+)/NADH-Sensitive Quantum Dots: Applications To Probe NAD(+)-Dependent Enzymes and To Sense the RDX Explosive. *Nano Letters,* 9**,** 322-326.

FROLOVA, L., LEGOFF, X., ZHOURAVLEVA, G., DAVYDOVA, E., PHILIPPE, M. & KISSELEV, L. 1996. Eukaryotic polypeptide chain release factor eRF3 is an eRF1- and ribosome-dependent guanosine triphosphatase. *Rna-a Publication of the Rna Society,* 2**,** 334-341.

HAGIWARA, M., MAEGAWA, K., SUZUKI, M., USHIODA, R., ARAKI, K., MATSUMOTO, Y., HOSEKI, J., NAGATA, K. & INABA, K. 2011. Structural

Basis of an ERAD Pathway Mediated by the ER-Resident Protein Disulfide Reductase ERdj5. *Molecular Cell,* 41**,** 432-444.

HALIC, M. & BECKMANN, R. 2005. The signal recognition particle and its interactions during protein targeting. *Current Opinion in Structural Biology,* 15**,** 116-125.

HANSON, G. T., MCANANEY, T. B., PARK, E. S., RENDELL, M. E. P., YARBROUGH, D. K., CHU, S. Y., XI, L. X., BOXER, S. G., MONTROSE, M. H. & REMINGTON, S. J. 2002. Green fluorescent protein variants as ratiometric dual emission pH sensors. 1. Structural characterization and preliminary application. *Biochemistry,* 41**,** 15477-15488.

HARPER, B. K., MABON, S. A., LEFFEL, S. M., HALFHILL, M. D., RICHARDS, H. A., MOYER, K. A. & STEWART, C. N. 1999. Green fluorescent protein as a marker for expression of a second gene in transgenic plants. *Nature Biotechnology,* 17**,** 1125-1129.

HEGDE, R. S. & LINGAPPA, V. R. 1999. Regulation of protein biogenesis at the endoplasmic reticulum membrane. *Trends in Cell Biology,* 9**,** 132-137.

HELENIUS, A. & AEBI, M. 2001. Intracellular functions of N-linked glycans. *Science,* 291**,** 2364-2369.

HERRMANN, J. M. & KÖHL, R. 2007. Catch me if you can! Oxidative protein trapping in the intermembrane space of mitochondria. *J Cell Biol,* 176**,** 559-63.

HIGH, S. 1995. Protein Translocation at the Membrane of the Endoplasmic-Reticulum. *Progress in Biophysics & Molecular Biology,* 63**,** 233-250.

HIROTA, K., MURATA, M., SACHI, Y., NAKAMURA, H., TAKEUCHI, J., MORI, K. & YODOI, J. 1999. Distinct Roles of Thioredoxin in the Cytoplasm and in the Nucleus: A TWO-STEP MECHANISM OF REDOX REGULATION OF TRANSCRIPTION FACTOR NF-κB. *Journal of Biological Chemistry,* 274**,** 27891-27897.

HOLMGREN, A. 1979. Thioredoxin Catalyzes the Reduction of Insulin Disulfides by Dithiothreitol and Dihydrolipoamide. *Journal of Biological Chemistry,* 254**,** 9627-9632.

HOLMGREN, A. 1989. Thioredoxin and Glutaredoxin Systems. *Journal of Biological Chemistry,* 264**,** 13963-13966.

HOLMGREN, A. 1995. Thioredoxin structure and mechanism: conformational changes on oxidation of the active-site sulfhydryls to a disulfide. *Structure,* 3**,** 239-43.

HOLMGREN, A. & BJORNSTEDT, M. 1995. Thioredoxin and Thioredoxin Reductase. *Biothiols, Pt B,* 252**,** 199-208.

HOLMGREN, A., SÖDERBERG, B. O., EKLUND, H. & BRÄNDÉN, C. I. 1975. Three-dimensional structure of Escherichia coli thioredoxin-S2 to 2.8 A resolution. *Proc Natl Acad Sci U S A,* 72**,** 2305-9.

HORWITZ, M. S., SCHARFF, M. D. & MAIZEL, J. V., JR. 1969. Synthesis and assembly of adenovirus 2. I. Polypeptide synthesis, assembly of capsomeres, and morphogenesis of the virion. *Virology,* 39**,** 682-94.

HOSEKI, J., OISHI, A., FUJIMURA, T. & SAKAI, Y. 2016. Development of a stable ERroGFP variant suitable for monitoring redox dynamics in the ER. *Bioscience Reports,* 36.

HU, J., DONG, L. & OUTTEN, C. E. 2008. The redox environment in the mitochondrial intermembrane space is maintained separately from the cytosol and matrix. *J Biol Chem,* 283**,** 29126-34.

HURTLEY, S. M. & HELENIUS, A. 1989. Protein Oligomerization in the Endoplasmic-Reticulum. *Annual Review of Cell Biology,* 5**,** 277-307.

HUSSAIN, M. M., RAVA, P., WALSH, M., RANA, M. & IQBAL, J. 2012. Multiple functions of microsomal triglyceride transfer protein. *Nutrition & metabolism,* 9**,** 14-14.

HWANG, C., SINSKEY, A. J. & LODISH, H. F. 1992. Oxidized Redox State of Glutathione in the Endoplasmic Reticulum. *Science,* 257**,** 1496-1502.

IKONEN, E. 2018. Mechanisms of cellular cholesterol compartmentalization: recent insights. *Current Opinion in Cell Biology,* 53**,** 77-83.

JACKSON, R. J., HELLEN, C. U. T. & PESTOVA, T. V. 2010. The mechanism of eukaryotic translation initiation and principles of its regulation. *Nature Reviews Molecular Cell Biology,* 11**,** 113-127.

JACKSON, R. J. & HUNT, T. 1983. Preparation and Use of Nuclease-Treated Rabbit Reticulocyte Lysates for the Translation of Eukaryotic Messenger-Rna. *Methods in Enzymology,* 96**,** 50-74.

JESSOP, C. E. & BULLEID, N. J. 2004. Glutathione directly reduces an oxidoreductase in the endoplasmic reticulum of mammalian cells. *J Biol Chem,* 279**,** 55341-7.

JESSOP, C. E., CHAKRAVARTHI, S., GARBI, N., HAMMERLING, G. J., LOVELL, S. & BULLEID, N. J. 2007. ERp57 is essential for efficient folding of glycoproteins sharing common structural domains. *EMBO J,* 26**,** 28-40.

JOHNSON, F. H., GERSHMAN, L. C., WATERS, J. R., REYNOLDS, G. T., SAIGA, Y. & SHIMOMURA, O. 1962. Quantum Efficiency of Cypridina Luminescence, with a Note on That of Aequorea. *Journal of Cellular and Comparative Physiology,* 60**,** 85-&.

JOHNSON, N., POWIS, K. & HIGH, S. 2013. Post-translational translocation into the endoplasmic reticulum. *Biochimica Et Biophysica Acta-Molecular Cell Research,* 1833**,** 2403-2409.

KADOKURA, H., KATZEN, F. & BECKWITH, J. 2003. Protein disulfide bond formation in prokaryotes. *Annu Rev Biochem,* 72**,** 111-35.

KADOKURA, H., TIAN, H. P., ZANDER, T., BARDWELL, J. C. A. & BECKWITH, J. 2004. Snapshots of DsbA in action: Detection of proteins in the process of oxidative folding. *Science,* 303**,** 534-537.

KATZEN, F. & BECKWITH, J. 2000. Transmembrane Electron Transfer by the Membrane Protein DsbD Occurs via a Disulfide Bond Cascade. *Cell,* 103**,** 769-779.

KATZEN, F., CHANG, G. & KUDLICKI, W. 2005. The past, present and future of cell-free protein synthesis. *Trends Biotechnol,* 23**,** 150-6.

KIVIRIKKO, K. I. & MYLLYHARJU, J. 1998. Prolyl 4-hydroxylases and their protein disulfide isomerase subunit. *Matrix Biology,* 16**,** 357-368.

KLEIZEN, B. & BRAAKMAN, I. 2004. Protein folding and quality control in the endoplasmic reticulum. *Current Opinion in Cell Biology,* 16**,** 343-349.

KODALI, V. K. & THORPE, C. 2010. Oxidative Protein Folding and the Quiescin-Sulfhydryl Oxidase Family of Flavoproteins. *Antioxidants & Redox Signaling,* 13**,** 1217-1230.

KOSURI, P., ALEGRE-CEBOLLADA, J., FENG, J., KAPLAN, A., INGLES-PRIETO, A., BADILLA, C. L., STOCKWELL, B. R., SANCHEZ-RUIZ, J. M., HOLMGREN, A. & FERNANDEZ, J. M. 2012. Protein Folding Drives Disulfide Formation. *Cell,* 151**,** 794-806.

KOZLOV, G., MAATTANEN, P., SCHRAG, J. D., POLLOCK, S., CYGLER, M., NAGAR, B., THOMAS, D. Y. & GEHRING, K. 2006. Crystal structure of the bb ' domains of the protein disulfide isomerase ERp57. *Structure,* 14**,** 1331-1339.

KOZLOV, G., MÄÄTTÄNEN, P., THOMAS, D. Y. & GEHRING, K. 2010. A structural overview of the PDI family of proteins. *Febs j,* 277**,** 3924-36.

KRIECHBAUMER, V. 2018. ER Microsome Preparation in Arabidopsis thaliana. *Methods Mol Biol,* 1691**,** 117-123.

KRIEG, P. A. & MELTON, D. A. 1984. Functional messenger RNAs are produced by SP6 in vitro transcription of cloned cDNAs. *Nucleic Acids Res,* 12**,** 7057-70.

KRYUKOV, G. V., CASTELLANO, S., NOVOSELOV, S. V., LOBANOV, A. V., ZEHTAB, O., GUIGO, R. & GLADYSHEV, V. N. 2003. Characterization of mammalian selenoproteomes. *Science,* 300**,** 1439-43.

LANGE, Y., YE, J., RIGNEY, M. & STECK, T. L. 1999. Regulation of endoplasmic reticulum cholesterol by plasma membrane cholesterol. *J Lipid Res,* 40**,** 2264-70.

LENTER, M., UHLIG, H., HAMANN, A., JENO, P., IMHOF, B. & VESTWEBER, D. 1993. A Monoclonal-Antibody against an Activation Epitope on Mouse Integrin Chain-Beta(1) Blocks Adhesion of Lymphocytes to the Endothelial Integrin-Alpha(6)Beta(1). *Proceedings of the National Academy of Sciences of the United States of America,* 90**,** 9051-9055.

LIN, J. H., WALTER, P. & YEN, T. S. B. 2008. Endoplasmic reticulum stress in disease pathogenesis. *Annual Review of Pathology-Mechanisms of Disease,* 3**,** 399-425.

LISCUM, L. & MUNN, N. J. 1999. Intracellular cholesterol transport. *Biochimica et Biophysica Acta (BBA) - Molecular and Cell Biology of Lipids,* 1438**,** 19-37.

LITVINOV, D. Y., SAVUSHKIN, E. V. & DERGUNOV, A. D. 2018. Intracellular and Plasma Membrane Events in Cholesterol Transport and Homeostasis. *Journal of Lipids,* 2018**,** 3965054.

LODISH, H. F. & DESALU, O. 1973. Regulation of synthesis of non-globin proteins in cell-free extracts of rabbit reticulocytes. *J Biol Chem,* 248**,** 3420-7.

LOHMAN, J. R. & REMINGTON, S. J. 2008. Development of a Family of Redox-Sensitive Green Fluorescent Protein Indicators for Use in Relatively Oxidizing Subcellular Environments. *Biochemistry,* 47**,** 8678-8688.

LUIRINK, J. & SINNING, I. 2004. SRP-mediated protein targeting: structure and function revisited. *Biochimica et Biophysica Acta (BBA) - Molecular Cell Research,* 1694**,** 17-35.

MANK, M. & GRIESBECK, O. 2008. Genetically Encoded Calcium Indicators. *Chemical Reviews,* 108**,** 1550-1564.

MARINO, M., STOILOVA, T., GIORGI, C., BACHI, A., CATTANEO, A., AURICCHIO, A., PINTON, P. & ZITO, E. 2015. SEPN1, an endoplasmic reticulum-localized selenoprotein linked to skeletal muscle pathology, counteracts hyperoxidation by means of redox-regulating SERCA2 pump activity. *Human Molecular Genetics,* 24**,** 1843-1855.

MATLACK, K. E. S., MISSELWITZ, B., PLATH, K. & RAPOPORT, T. A. 1999. BiP Acts as a Molecular Ratchet during Posttranslational Transport of Prepro-α Factor across the ER Membrane. *Cell,* 97**,** 553-564.

MCCAFFREY, K. & BRAAKMAN, I. 2016. Protein quality control at the endoplasmic reticulum. *Proteostasis,* 60**,** 227-235.

MCKENNA, M., SIMMONDS, R. E. & HIGH, S. 2017. Mycolactone reveals the substrate-driven complexity of Sec61-dependent transmembrane protein biogenesis. *Journal of Cell Science,* 130**,** 1307.

MEREDITH, M. J. & REED, D. J. 1982. Status of the mitochondrial pool of glutathione in the isolated hepatocyte. *J Biol Chem,* 257**,** 3747-53.

MESECKE, N., TERZIYSKA, N., KOZANY, C., BAUMANN, F., NEUPERT, W., HELL, K. & HERRMANN, J. M. 2005. A disulfide relay system in the intermembrane space of mitochondria that mediates protein import. *Cell,* 121**,** 1059-69.

MEYER, A. J. & DICK, T. P. 2010. Fluorescent Protein-Based Redox Probes. *Antioxidants & Redox Signaling,* 13**,** 621-650.

MEZGHRANI, A., FASSIO, A., BENHAM, A., SIMMEN, T., BRAAKMAN, I. & SITIA, R. 2001. Manipulation of oxidative protein folding and PDI redox state in mammalian cells. *Embo Journal,* 20**,** 6288-6296.

MIESENBÖCK, G., DE ANGELIS, D. A. & ROTHMAN, J. E. 1998. Visualizing secretion and synaptic transmission with pH-sensitive green fluorescent proteins. *Nature,* 394**,** 192-195.

MIKAMI, S., MASUTANI, M., SONENBERG, N., YOKOYAMA, S. & IMATAKA, H. 2006. An efficient mammalian cell-free translation system supplemented with translation factors. *Protein Expr Purif,* 46**,** 348-57.

MISSIAKAS, D., SCHWAGER, F. & RAINA, S. 1995. Identification and characterization of a new disulfide isomerase-like protein (DsbD) in Escherichia coli. *Embo j,* 14**,** 3415-24.

MOGHADASZADEH, B., PETIT, N., JAILLARD, C., BROCKINGTON, M., QUIJANO ROY, S., MERLINI, L., ROMERO, N., ESTOURNET, B., DESGUERRE, I., CHAIGNE, D., MUNTONI, F., TOPALOGLU, H. & GUICHENEY, P. 2001. Mutations in SEPN1 cause congenital muscular dystrophy with spinal rigidity and restrictive respiratory syndrome. *Nat Genet,* 29**,** 17-8.

MOLINARI, M., GALLI, C., PICCALUGA, V., PIEREN, M. & PAGANETTI, P. 2002. Sequential assistance of molecular chaperones and transient formation of covalent complexes during protein degradation from the ER. *J Cell Biol,* 158**,** 247-57.

MOLTENI, S. N., FASSIO, A., CIRIOLO, M. R., FILOMENI, G., PASQUALETTO, E., FAGIOLI, C. & SITIA, R. 2004. Glutathione limits Ero1-dependent oxidation in the endoplasmic reticulum. *J Biol Chem,* 279**,** 32667-73.

MONTEIRO, H. P., OGATA, F. T. & STERN, A. 2017. Thioredoxin promotes survival signaling events under nitrosative/oxidative stress associated with cancer development. *Biomedical journal,* 40**,** 189-199.

MORDAS, A. & TOKATLIDIS, K. 2015. The MIA pathway: a key regulator of mitochondrial oxidative protein folding and biogenesis. *Accounts of chemical research,* 48**,** 2191-2199.

NG, D. T., BROWN, J. D. & WALTER, P. 1996. Signal sequences specify the targeting route to the endoplasmic reticulum membrane. *Journal of Cell Biology,* 134**,** 269-278.

NGUYEN, V. D., SAARANEN, M. J., KARALA, A. R., LAPPI, A. K., WANG, L., RAYKHEL, I. B., ALANEN, H. I., SALO, K. E. H., WANG, C. C. & RUDDOCK, L. W. 2011. Two Endoplasmic Reticulum PDI Peroxidases Increase the Efficiency of the Use of Peroxide during Disulfide Bond Formation. *Journal of Molecular Biology,* 406**,** 503-515.

NIRENBERG, M. & MATTHAEI, J. H. 1961. Dependence of Cell-Free Protein Synthesis in E Coli Upon Naturally Occurring or Synthetic Polyribonucleotides. *Proceedings of the National Academy of Sciences of the United States of America,* 47**,** 1588-&.

NORGAARD, P., WESTPHAL, V., TACHIBANA, C., ALSOE, L., HOLST, B. & WINTHER, J. R. 2001. Functional differences in yeast protein disulfide isomerases. *Journal of Cell Biology,* 152**,** 553-562.

NURENBERG-GOLOUB, E., HEINEMANN, H., GEROVAC, M. & TAMPE, R. 2018. Ribosome recycling is coordinated by processive events in two asymmetric ATP sites of ABCE1. *Life Science Alliance,* 1.

NURENBERG, E. & TAMPE, R. 2013. Tying up loose ends: ribosome recycling in eukaryotes and archaea. *Trends in Biochemical Sciences,* 38**,** 64-74.

OKA, O. B., PRINGLE, M. A., SCHOPP, I. M., BRAAKMAN, I. & BULLEID, N. J. 2013. ERdj5 is the ER reductase that catalyzes the removal of non-native disulfides and correct folding of the LDL receptor. *Mol Cell,* 50**,** 793-804.

OKA, O. B., YEOH, H. Y. & BULLEID, N. J. 2015. Thiol-disulfide exchange between the PDI family of oxidoreductases negates the requirement for an oxidase or reductase for each enzyme. *Biochem J,* 469**,** 279-88.

OLIVER, J. D., RODERICK, H. L., LLEWELLYN, D. H. & HIGH, S. 1999. ERp57 functions as a subunit of specific complexes formed with the ER lectins calreticulin and calnexin. *Molecular Biology of the Cell,* 10**,** 2573-2582.

OLIVER, J. D., VANDERWAL, F. J., BULLEID, N. J. & HIGH, S. 1997. Interaction of the thiol-dependent reductase ERp57 with nascent glycoproteins. *Science,* 275**,** 86-88.

OLZMANN, J. A., KOPITO, R. R. & CHRISTIANSON, J. C. 2013. The Mammalian Endoplasmic Reticulum-Associated Degradation System. *Cold Spring Harbor Perspectives in Biology,* 5.

OSTERGAARD, H., HENRIKSEN, A., HANSEN, F. G. & WINTHER, J. R. 2001. Shedding light on disulfide bond formation: engineering a redox switch in green fluorescent protein. *The EMBO journal,* 20**,** 5853-5862.

PAGANI, M., FABBRI, M., BENEDETTI, C., FASSIO, A., PILATI, S., BULLEID, N. J., CABIBBO, A. & SITIA, R. 2000. Endoplasmic reticulum oxidoreductin 1-lbeta (ERO1-Lbeta), a human gene induced in the course of the unfolded protein response. *J Biol Chem,* 275**,** 23685-92.

PALADE, G. E. & SIEKEVITZ, P. 1956. Liver microsomes; an integrated morphological and biochemical study. *J Biophys Biochem Cytol,* 2**,** 171-200.

PANZNER, S., DREIER, L., HARTMANN, E., KOSTKA, S. & RAPOPORT, T. A. 1995. Posttranslational protein transport in yeast reconstituted with a purified complex of Sec proteins and Kar2p. *Cell,* 81**,** 561-70.

PARAKH, S. & ATKIN, J. D. 2015. Novel roles for protein disulphide isomerase in disease states: a double edged sword? *Front Cell Dev Biol,* 3**,** 30.

PATTERSON, G. H., KNOBEL, S. M., ARKHAMMAR, P., THASTRUP, O. & PISTON, D. W. 2000. Separation of the glucose-stimulated cytoplasmic and mitochondrial NAD(P)H responses in pancreatic islet beta cells. *Proc Natl Acad Sci U S A,* 97**,** 5203-7.

PEAPER, D. R., WEARSCH, P. A. & CRESSWELL, P. 2005. Tapasin and ERp57 form a stable disulfide-linked dimer within the MHC class I peptide-loading complex. *Embo Journal,* 24**,** 3613-3623.

PÉDELACQ, J.-D., CABANTOUS, S., TRAN, T., TERWILLIGER, T. C. & WALDO, G. S. 2006. Engineering and characterization of a superfolder green fluorescent protein. *Nature Biotechnology,* 24**,** 79-88.

PEDELACQ, J.-D. C., S. 2019. Development and Applications of Superfolder and Split Fluorescent Protein Detection Systems in Biology. *International Journal of Molecular Sciences,* 20(14)**,** 3479.

PELHAM, H. R. & JACKSON, R. J. 1976. An efficient mRNA-dependent translation system from reticulocyte lysates. *Eur J Biochem,* 67**,** 247-56.

PETERFY, M. 2012. Lipase maturation factor 1: a lipase chaperone involved in lipid metabolism. *Biochim Biophys Acta,* 1821**,** 790-4.

PETERFY, M., BEN-ZEEV, O., MAO, H. Z., WEISSGLAS-VOLKOV, D., AOUIZERAT, B. E., PULLINGER, C. R., FROST, P. H., KANE, J. P., MALLOY, M. J., REUE, K., PAJUKANTA, P. & DOOLITTLE, M. H. 2007. Mutations in LMF1 cause combined lipase deficiency and severe hypertriglyceridemia. *Nat Genet,* 39**,** 1483-7.

PETIT, N., LESCURE, A., REDERSTORFF, M., KROL, A., MOGHADASZADEH, B., WEWER, U. M. & GUICHENEY, P. 2003. Selenoprotein N: an endoplasmic reticulum glycoprotein with an early developmental expression pattern. *Human Molecular Genetics,* 12**,** 1045-1053.

PIRNESKOSKI, A., RUDDOCK, L. W., KLAPPA, P., FREEDMAN, R. B., KIVIRIKKO, K. I. & KOIVUNEN, P. 2001. Domains b ' and a ' of protein disulfide isomerase fulfill the minimum requirement for function as a subunit of prolyl 4-hydroxylase - The N-terminal domains a and b enhance this function and can be substituted in part by those of ERp57. *Journal of Biological Chemistry,* 276**,** 11287-11293.

PITTS, M. W. & HOFFMANN, P. R. 2018. Endoplasmic reticulum-resident selenoproteins as regulators of calcium signaling and homeostasis. *Cell Calcium,* 70**,** 76-86.

PLUTNER, H., DAVIDSON, H. W., SARASTE, J. & BALCH, W. E. 1992. Morphological analysis of protein transport from the ER to Golgi membranes in digitonin-permeabilized cells: role of the P58 containing compartment. *J Cell Biol,* 119**,** 1097-116.

POET, G. J., OKA, O. B., VAN LITH, M., CAO, Z., ROBINSON, P. J., PRINGLE, M. A., ARNER, E. S. & BULLEID, N. J. 2017. Cytosolic thioredoxin reductase 1 is required for correct disulfide formation in the ER. *EMBO J,* 36**,** 693-702.

PONSERO, A. J., IGBARIA, A., DARCH, M. A., MILED, S., OUTTEN, C. E., WINTHER, J. R., PALAIS, G., D'AUTRÉAUX, B., DELAUNAY-MOISAN, A. & TOLEDANO, M. B. 2017. Endoplasmic Reticulum Transport of Glutathione by Sec61 Is Regulated by Ero1 and Bip. *Molecular cell,* 67**,** 962-973.e5.

PRASHER, D. C., ECKENRODE, V. K., WARD, W. W., PRENDERGAST, F. G. & CORMIER, M. J. 1992. Primary structure of the Aequorea victoria green-fluorescent protein. *Gene,* 111**,** 229-33.

PUHKA, M., JOENSUU, M., VIHINEN, H., BELEVICH, I. & JOKITALO, E. 2012. Progressive sheet-to-tubule transformation is a general mechanism for endoplasmic reticulum partitioning in dividing mammalian cells. *Molecular Biology of the Cell,* 23**,** 2424-2432.

RAPOPORT, T. A. 2007. Protein translocation across the eukaryotic endoplasmic reticulum and bacterial plasma membranes. *Nature,* 450**,** 663-669.

RAPOPORT, T. A., LI, L. & PARK, E. 2017. Structural and Mechanistic Insights into Protein Translocation. *Annual Review of Cell and Developmental Biology, Vol 33,* 33**,** 369-390.

RIEMER, J., APPENZELLER-HERZOG, C., JOHANSSON, L., BODENMILLER, B., HARTMANN-PETERSEN, R. & ELLGAARD, L. 2009a. A luminal flavoprotein in endoplasmic reticulum-associated degradation. *Proceedings of the National Academy of Sciences,* 106**,** 14831.

RIEMER, J., BULLEID, N. & HERRMANN, J. M. 2009b. Disulfide Formation in the ER and Mitochondria: Two Solutions to a Common Process. *Science,* 324**,** 1284.

RIETSCH, A., BELIN, D., MARTIN, N. & BECKWITH, J. 1996. An in vivo pathway for disulfide bond isomerization in Escherichia coli. *Proc Natl Acad Sci U S A,* 93**,** 13048-53.

RIETSCH, A., BESSETTE, P., GEORGIOU, G. & BECKWITH, J. 1997. Reduction of the periplasmic disulfide bond isomerase, DsbC, occurs by passage of electrons from cytoplasmic thioredoxin. *Journal of Bacteriology,* 179**,** 6602-6608.

ROBERTS, B. E. & PATERSON, B. M. 1973. Efficient Translation of Tobacco Mosaic-Virus Rna and Rabbit Globin-9s Rna in a Cell-Free System from Commercial Wheat-Germ. *Proceedings of the National Academy of Sciences of the United States of America,* 70**,** 2330-2334.

ROBERTS, B. S., BABILONIA-ROSA, M. A., BROADWELL, L. J., WU, M. J. & NEHER, S. B. 2018. Lipase maturation factor 1 affects redox homeostasis in the endoplasmic reticulum. *EMBO J,* 37.

ROBINSON, P. J., KANEMURA, S., CAO, X. & BULLEID, N. J. 2020. Protein secondary structure determines the temporal relationship between folding and disulfide formation. 295**,** 2438-2448.

ROBINSON, P. J., PRINGLE, M. A., WOOLHEAD, C. A. & BULLEID, N. J. 2017. Folding of a single domain protein entering the endoplasmic reticulum precedes disulfide formation. *Journal of Biological Chemistry,* 292**,** 6978-6986.

ROOS, G., GARCIA-PINO, A., VAN BELLE, K., BROSENS, E., WAHNI, K., VANDENBUSSCHE, G., WYNS, L., LORIS, R. & MESSENS, J. 2007. The Conserved Active Site Proline Determines the Reducing Power of Staphylococcus aureus Thioredoxin. *Journal of Molecular Biology,* 368**,** 800-811.

ROSENBLUM, G. & COOPERMAN, B. S. 2014. Engine out of the chassis: Cell-free protein synthesis and its uses. *Febs Letters,* 588**,** 261-268.

RUGGIANO, A., FORESTI, O. & CARVALHO, P. 2014. Quality control: ER-associated degradation: protein quality control and beyond. *J Cell Biol,* 204**,** 869-79.

RUTKEVICH, L. A. & WILLIAMS, D. B. 2012. Vitamin K epoxide reductase contributes to protein disulfide formation and redox homeostasis within the endoplasmic reticulum. *Molecular biology of the cell,* 23**,** 2017-2027.

SABATINI, D. D. 2014. Subcellular fractionation of rough microsomes. *Cold Spring Harb Protoc,* 2014**,** 932-4.

SAITOH, M., NISHITOH, H., FUJII, M., TAKEDA, K., TOBIUME, K., SAWADA, Y., KAWABATA, M., MIYAZONO, K. & ICHIJO, H. 1998. Mammalian thioredoxin is a direct inhibitor of apoptosis signal-regulating kinase (ASK) 1. *Embo j,* 17**,** 2596-606.

SANDALOVA, T., ZHONG, L., LINDQVIST, Y., HOLMGREN, A. & SCHNEIDER, G. 2001. Three-dimensional structure of a mammalian thioredoxin reductase: implications for mechanism and evolution of a selenocysteine-dependent enzyme. *Proceedings of the National Academy of Sciences of the United States of America,* 98**,** 9533-9538.

SANDER, J. D. & JOUNG, J. K. 2014. CRISPR-Cas systems for editing, regulating and targeting genomes. *Nature Biotechnology,* 32**,** 347-355.

SCHENK, H., KLEIN, M., ERDBRÜGGER, W., DRÖGE, W. & SCHULZE-OSTHOFF, K. 1994. Distinct effects of thioredoxin and antioxidants on the activation of transcription factors NF-kappa B and AP-1. *Proc Natl Acad Sci U S A,* 91**,** 1672-6.

SCHLECHT, R., ERBSE, A. H., BUKAU, B. & MAYER, M. P. 2011. Mechanics of Hsp70 chaperones enables differential interaction with client proteins. *Nature Structural & Molecular Biology,* 18**,** 345-U135.

SCHULLER, A. P. & GREEN, R. 2018. Roadblocks and resolutions in eukaryotic translation. *Nature Reviews Molecular Cell Biology,* 19**,** 526-541.

SCHULMAN, S., WANG, B., LI, W. K. & RAPOPORT, T. A. 2010. Vitamin K epoxide reductase prefers ER membrane-anchored thioredoxin-like redox partners. *Proceedings of the National Academy of Sciences of the United States of America,* 107**,** 15027-15032.

SCHWARZ, D. S. & BLOWER, M. D. 2016. The endoplasmic reticulum: structure, function and response to cellular signaling. *Cellular and Molecular Life Sciences,* 73**,** 79-94.

SCHWARZ, F. & AEBI, M. 2011. Mechanisms and principles of N-linked protein glycosylation. *Current Opinion in Structural Biology,* 21**,** 576-582.

SCHWEIZER, U. & FRADEJAS-VILLAR, N. 2016. Why 21? The significance of selenoproteins for human health revealed by inborn errors of metabolism. *FASEB J,* 30**,** 3669-3681.

SCHWERTASSEK, U., BALMER, Y., GUTSCHER, M., WEINGARTEN, L., PREUSS, M., ENGELHARD, J., WINKLER, M. & DICK, T. P. 2007a. Selective redox regulation of cytokine receptor signaling by extracellular thioredoxin-1. *EMBO J,* 26**,** 3086-97.

SCHWERTASSEK, U., WEINGARTEN, L. & DICK, T. P. 2007b. Identification of redox-active cell-surface proteins by mechanism-based kinetic trapping. *Sci STKE,* 2007**,** pl8.

SHEVCHIK, V. E., CONDEMINE, G. & ROBERTBAUDOUY, J. 1994. Characterization of Dsbc, a Periplasmic Protein of Erwinia-Chrysanthemi and Escherichia-Coli with Disulfide-Isomerase Activity. *Embo Journal,* 13**,** 2007-2012.

SHIMOMURA, O., JOHNSON, F. H. & SAIGA, Y. 1962. Extraction, purification and properties of aequorin, a bioluminescent protein from the luminous hydromedusan, Aequorea. *J Cell Comp Physiol,* 59**,** 223-39.

SITIA, R. & BRAAKMAN, I. 2003. Quality control in the endoplasmic reticulum protein factory. *Nature,* 426**,** 891-894.

SMOLINSKI, M. B., GREEN, S. R. & STOREY, K. B. 2019. Glucose-6-phosphate dehydrogenase is posttranslationally regulated in the larvae of the freeze-tolerant gall fly, Eurosta solidaginis, in response to freezing. *Archives of Insect Biochemistry and Physiology*.

SOUSA, M. & PARODI, A. J. 1995. The Molecular-Basis for the Recognition of Misfolded Glycoproteins by the Udp-Glc-Glycoprotein Glucosyltransferase. *Embo Journal,* 14**,** 4196-4203.

STAFFORD, W. C., PENG, X. X., OLOFSSON, M. H., ZHANG, X. N., LUCI, D. K., LU, L., CHENG, Q., TRESAUGUES, L., DEXHEIMER, T. S., COUSSENS, N. P., AUGSTEN, M., AHLZEN, H. S. M., ORWAR, O., OSTMAN, A., STONE-ELANDER, S., MALONEY, D. J., JADHAV, A., SIMEONOV, A., LINDER, S. & ARNER, E. S. J. 2018. Irreversible inhibition of cytosolic thioredoxin reductase 1 as a mechanistic basis for anticancer therapy. *Science Translational Medicine,* 10.

STANTON, R. C. 2012. Glucose-6-phosphate dehydrogenase, NADPH, and cell survival. *IUBMB Life,* 64**,** 362-9.

STEWART, E. J., KATZEN, F. & BECKWITH, J. 1999. Six conserved cysteines of the membrane protein DsbD are required for the transfer of electrons from the cytoplasm to the periplasm of Escherichia coli. *Embo Journal,* 18**,** 5963-5971.

STILLWELL, W. 2013. Chapter 14 - Membrane Transport. *In:* STILLWELL, W. (ed.) *An Introduction to Biological Membranes*. San Diego: Elsevier.

SUKHODUB, A. L. & BURCHELL, A. 2005. Preparation of intact microsomes from cultured mammalian H4IIE cells. *J Pharmacol Toxicol Methods,* 52**,** 330-4.

TAVENDER, T. J. & BULLEID, N. J. 2010. Peroxiredoxin IV protects cells from oxidative stress by removing H2O2 produced during disulphide formation. *J Cell Sci,* 123**,** 2672-9.

TAVENDER, T. J., SPRINGATE, J. J. & BULLEID, N. J. 2010. Recycling of peroxiredoxin IV provides a novel pathway for disulphide formation in the endoplasmic reticulum. *Embo Journal,* 29**,** 4185-4197.

TIAN, G., XIANG, S., NOIVA, R., LENNARZ, W. J. & SCHINDELIN, H. 2006. The crystal structure of yeast protein disulfide isomerase suggests cooperativity between its active sites. *Cell,* 124**,** 61-73.

TIAN, W. N., BRAUNSTEIN, L. D., PANG, J. D., STUHLMEIER, K. M., XI, Q. C., TIAN, X. N. & STANTON, R. C. 1998. Importance of glucose-6-phosphate dehydrogenase activity for cell growth. *Journal of Biological Chemistry,* 273**,** 10609-10617.

TIWARI, S., ASKARI, J. A., HUMPHRIES, M. J. & BULLEID, N. J. 2011. Divalent cations regulate the folding and activation status of integrins during their intracellular trafficking. *J Cell Sci,* 124**,** 1672-80.

TSAI, B., RODIGHIERO, C., LENCER, W. I. & RAPOPORT, T. A. 2001. Protein disulfide isomerase acts as a redox-dependent chaperone to unfold cholera toxin. *Cell,* 104**,** 937-948.

TU, B. P., HO-SCHLEYER, S. C., TRAVERS, K. J. & WEISSMAN, J. S. 2000. Biochemical basis of oxidative protein folding in the endoplasmic reticulum. *Science,* 290**,** 1571-4.

TU, B. P. & WEISSMAN, J. S. 2004. Oxidative protein folding in eukaryotes: mechanisms and consequences. *Journal of Cell Biology,* 164**,** 341-346.

TURANO, C., GAUCCI, E., GRILLO, C. & CHICHIARELLI, S. 2011. ERp57/GRP58: a protein with multiple functions. *Cell Mol Biol Lett,* 16**,** 539-63.

USHIODA, R., HOSEKI, J., ARAKI, K., JANSEN, G., THOMAS, D. Y. & NAGATA, K. 2008. ERdj5 is required as a disulfide reductase for degradation of misfolded proteins in the ER. *Science,* 321**,** 569-572.

VAN DER REEST, J., LILLA, S., ZHENG, L., ZANIVAN, S. & GOTTLIEB, E. 2018. Proteome-wide analysis of cysteine oxidation reveals metabolic sensitivity to redox stress. *Nature Communications,* 9.

VAN LITH, M., TIWARI, S., PEDIANI, J., MILLIGAN, G. & BULLEID, N. J. 2011. Real-time monitoring of redox changes in the mammalian endoplasmic reticulum. *Journal of Cell Science,* 124**,** 2349-2356.

VARONE, E., POZZER, D., DI MODICA, S., CHERNORUDSKIY, A., NOGARA, L., BARALDO, M., CINQUANTA, M., FUMAGALLI, S., VILLAR-QUILES, R. N., DE SIMONI, M.-G., BLAAUW, B., FERREIRO, A. & ZITO, E. 2019. SELENON (SEPN1) protects skeletal muscle from saturated fatty acid-induced ER stress and insulin resistance. *Redox Biology,* 24**,** 101176.

WALTER, P. & BLOBEL, G. 1983. Preparation of microsomal membranes for cotranslational protein translocation. *Methods Enzymol,* 96**,** 84-93.

WARD, W. W. & CORMIER, M. J. 1976. In vitro energy transfer in Renilla bioluminescence. *The Journal of Physical Chemistry,* 80**,** 2289-2291.

WATSON, W. H., POHL, J., MONTFORT, W. R., STUCHLIK, O., REED, M. S., POWIS, G. & JONES, D. P. 2003. Redox potential of human thioredoxin 1 and identification of a second dithiol/disulfide motif. *Journal of Biological Chemistry,* 278**,** 33408-33415.

WEICHSEL, A., GASDASKA, J. R., POWIS, G. & MONTFORT, W. R. 1996. Crystal structures of reduced, oxidized, and mutated human thioredoxins: Evidence for a regulatory homodimer. *Structure,* 4**,** 735-751.

WEST, M., ZUREK, N., HOENGER, A. & VOELTZ, G. K. 2011. A 3D analysis of yeast ER structure reveals how ER domains are organized by membrane curvature. *Journal of Cell Biology,* 193**,** 333-346.

WETTERAU, J. R., COMBS, K. A., SPINNER, S. N. & JOINER, B. J. 1990. Protein disulfide isomerase is a component of the microsomal triglyceride transfer protein complex. 265**,** 9801-9807.

WILSON, R., ALLEN, A. J., OLIVER, J., BROOKMAN, J. L., HIGH, S. & BULLEID, N. J. 1995. The translocation, folding, assembly and redox-dependent degradation of secretory and membrane proteins in semi-permeabilized mammalian cells. *Biochem J,* 307 (Pt 3)**,** 679-87.

WILSON, R., LEES, J. F. & BULLEID, N. J. 1998. Protein disulfide isomerase acts as a molecular chaperone during the assembly of procollagen. *Journal of Biological Chemistry,* 273**,** 9637-9643.

WOOLHEAD, C. A., MCCORMICK, P. J. & JOHNSON, A. E. 2004. Nascent membrane and secretory proteins differ in FRET-detected folding far inside the ribosome and in their exposure to ribosomal proteins. *Cell,* 116**,** 725-736.

YAMADA, T., MATSUMOTO, M., KANDA, S. & TERAYAMA, H. 1960. Distribution of protein-bound aminoazo dyes in the rat liver microsome. *Nature,* 187**,** 943.

YEAGLE, P. L. 2016. *The Membranes of Cells*, Elsevier Science.

ZAPUN, A., DARBY, N. J., TESSIER, D. C., MICHALAK, M., BERGERON, J. J. M. & THOMAS, D. Y. 1998. Enhanced catalysis of ribonuclease B folding by the interaction of calnexin or calreticulin with ERp57. *Journal of Biological Chemistry,* 273**,** 6009-6012.

ZHENG, J. & GILBERT, H. F. 2001. Discrimination between native and non-native disulfides by protein-disulfide isomerase. *Journal of Biological Chemistry,* 276**,** 15747-15752.

ZIMMERMANN, R., EYRISCH, S., AHMAD, M. & HELMS, V. 2011. Protein translocation across the ER membrane. *Biochimica Et Biophysica Acta-Biomembranes,* 1808**,** 912-924.

ZITO, E., MELO, E. P., YANG, Y., WAHLANDER, A., NEUBERT, T. A. & RON, D. 2010. Oxidative Protein Folding by an Endoplasmic Reticulum-Localized Peroxiredoxin. *Molecular Cell,* 40**,** 787-797.

Appendices

CAO, X., LILLA, S., CAO, Z., PRINGLE, M. A., OKA, O. B. V., ROBINSON, P. J., SZMAJA, T., VAN LITH, M., ZANIVAN, S. & BULLEID, N. J. 2020. The mammalian cytosolic thioredoxin reductase pathway acts via a membrane protein to reduce ER-localised proteins. *Journal of Cell Science,* 133**,** jcs241976.

© 2020. Published by The Company of Biologists Ltd | Journal of Cell Science (2020) 133, jcs241976. doi:10.1242/jcs.241976

RESEARCH ARTICLE

The mammalian cytosolic thioredoxin reductase pathway acts via a membrane protein to reduce ER-localised proteins

Xiaofei Cao[1], Sergio Lilla[2], Zhenbo Cao[1], Marie Anne Pringle[1], Ojore B. V. Oka[1], Philip J. Robinson[1], Tomasz Szmaja[1], Marcel van Lith[1], Sara Zanivan[2,3] and Neil J. Bulleid[1,*]

ABSTRACT

Folding of proteins entering the mammalian secretory pathway requires the insertion of the correct disulfides. Disulfide formation involves both an oxidative pathway for their insertion and a reductive pathway to remove incorrectly formed disulfides. Reduction of these disulfides is crucial for correct folding and degradation of misfolded proteins. Previously, we showed that the reductive pathway is driven by NADPH generated in the cytosol. Here, by reconstituting the pathway using purified proteins and ER microsomal membranes, we demonstrate that the thioredoxin reductase system provides the minimal cytosolic components required for reducing proteins within the ER lumen. In particular, saturation of the pathway and its protease sensitivity demonstrates the requirement for a membrane protein to shuttle electrons from the cytosol to the ER. These results provide compelling evidence for the crucial role of the cytosol in regulating ER redox homeostasis, ensuring correct protein folding and facilitating the degradation of misfolded ER proteins.

KEY WORDS: Disulfide formation, Endoplasmic reticulum, Protein folding, Thioredoxin pathway

INTRODUCTION

Proteins entering the secretory pathway undergo several modifications that are unique to the ER, including glycosylation and disulfide formation (Braakman and Bulleid, 2011). The consequence of these modifications is often increased stability of the protein fold in preparation for secretion into the extracellular milieu. Failure to fulfil the correct modification can lead to protein misfolding and disease (Wang and Kaufman, 2016). Correct protein disulfide formation requires resident ER proteins to catalyse both disulfide formation and reduction (Ellgaard et al., 2018). Disulfide formation is catalysed primarily by Ero1, which oxidises members of the protein disulfide isomerase (PDI) family by coupling the reduction of oxygen to the introduction of a disulfide (Sevier et al., 2007). PDI then exchanges its disulfide with substrate proteins during and following their translocation into the ER lumen (Chen et al., 1995). During this process, disulfides might form that are not present in the final native structure (Jansens et al., 2002). Such non-native disulfides need to be removed to allow correct folding or to facilitate protein degradation (Ushioda et al., 2008). Hence, there is a requirement for both an oxidative and reductive pathway in the ER to ensure that correct native disulfides are formed or for proteins to be targeted for degradation (Bulleid and Ellgaard, 2011). In addition to the reduction of structural disulfides, there is also a requirement for a reductive pathway to recycle enzymes such as methionine sulfoxide reductase (Cao et al., 2018), vitamin K epoxide reductase (Rishavy et al., 2011), peroxiredoxin IV (Tavender et al., 2010) and formyl glycine generating enzyme (Dierks et al., 2005), which contain active site thiols that become oxidised during catalysis.

Despite our understanding of the various pathways to introduce disulfides, our knowledge of the reductive pathway is limited. Members of the PDI family such as ERdj5 are likely to catalyse the initial stage in the reduction of non-native disulfides (Jessop et al., 2007; Oka et al., 2013; Ushioda et al., 2008). ERdj5 has a relatively low reduction potential, making it an efficient reductase (Hagiwara et al., 2011). ERdj5 is recruited to substrate proteins via its interaction with BiP (Cunnea et al., 2003; Hagiwara et al., 2011; Oliver et al., 1997). Following the reduction of substrates, the PDI reductases become oxidised so there is a requirement for their enzymatic reduction to maintain activity. Within the cytosol, the main disulfide reductase, thioredoxin-1 (Trx1), is maintained in a reduced state by the action of cytosolic thioredoxin reductase 1 (TrxR1) with potential contributions from both the glutathione reductase (GR) and glutaredoxin (Grx) pathways (Lillig and Holmgren, 2007). Both the Trx1 and glutathione (GSH) pathways require NADPH as ultimate electron donor to maintain their reductase activity within the cytosol. However, there are no known equivalent pathways present within the ER for the reduction of disulfides in the thioredoxin domains within the PDI family. We recently showed that the regeneration of NADPH within the cytosol is required to ensure correct disulfide formation in the ER lumen (Poet et al., 2017), raising the possibility that the cytosolic reductive pathways are responsible for ensuring correct disulfide formation in the ER lumen. How the reducing equivalents generated in the cytosol are transferred to the ER lumen remains unknown, but a system for the transfer of such equivalents does exist in prokaryotes. There, disulfide formation and reduction within the periplasmic space is catalysed by DsbA and DsbC, which are structurally homologous to Trx1 (Kadokura et al., 2003). Disulfide formation is coupled to the electron transport chain via a membrane protein called DsbB, allowing *de novo* disulfide formation in the disulfide exchange protein DsbA. To remove incorrectly oxidised periplasmic thiols, the cytosolic thioredoxin reductase pathway via thioredoxin reduces the membrane protein DsbD, which transfers electrons across the membrane to reduce DsbC that then catalyses disulfide reduction.

[1]Institute of Molecular, Cell and Systems Biology, College of Medical Veterinary and Life Sciences, Davidson Building, University of Glasgow, Glasgow, G12 8QQ, UK. [2]Cancer Research UK Beatson Institute, Glasgow, G61 1BD, UK. [3]Institute of Cancer Sciences, University of Glasgow, Glasgow, G61 1QH, UK.

*Author for correspondence (neil.bulleid@glasgow.ac.uk)

X.C., 0000-0002-8118-0917; S.L., 0000-0003-3142-7640; Z.C., 0000-0002-1863-4357; M.A.P., 0000-0002-1358-4610; O.B.V.O., 0000-0003-3482-115X; P.J.R., 0000-0003-2576-5010; M.v.L., 0000-0003-0225-5501; S.Z., 0000-0002-9880-9099; N.J.B., 0000-0002-9839-5279

Handling Editor: David Stephens
Received 20 November 2019; Accepted 10 March 2020

Journal of Cell Science (2020) 133, jcs241976. doi:10.1242/jcs.241976

A role for GSH in the reduction of protein thiols has been suggested based on its role as a redox buffer (Chakravarthi et al., 2006). This role is thought to be required to maintain redox balance after large fluctuations in either reducing or oxidising conditions (Appenzeller-Herzog et al., 2010; Jessop and Bulleid, 2004; Molteni et al., 2004). A recent report identifying Sec61 as a GSH transporter provides a possible route for its transfer into the ER (Ponsero et al., 2017). However, the GSH requirement for the formation of the correct disulfides in proteins is less clear. Depletion of ER GSH either by inhibition of GSH synthase or by targeting GSH-degrading enzymes does not prevent correct disulfide formation in proteins containing complex disulfides, such as tissue-type plasminogen activator or the low-density lipoprotein receptor (Chakravarthi and Bulleid, 2004; Tsunoda et al., 2014). The relative roles of the thioredoxin and GSH pathways in maintaining ER redox poise and in reducing oxidised thiols remain undefined (Bulleid and Ellgaard, 2011; Ellgaard et al., 2018).

To evaluate the requirement for the reduction of disulfides within the ER, we reconstituted the pathway using purified cytosolic components and microsomal vesicles or semi-permeabilised (SP) cells as a source of ER. Using a redox-sensitive green fluorescent protein (roGFP) as a readout (van Lith et al., 2011), we established the minimum requirements for disulfide reduction and demonstrated that the transfer of reducing equivalents across the ER membrane requires a membrane protein. In addition, we showed that the resolution of non-native to native disulfides can be driven solely by the thioredoxin pathway. Our results highlight the similarity between the pathways for reduction of disulfides in the bacterial periplasm and the mammalian ER.

RESULTS

The reduction of ER-localised disulfides requires an ER membrane component

To follow the reduction of disulfide bonds within the ER lumen, we created a HT1080 stable cell line expressing a version of roGFP that can act as a reporter of disulfide formation within the ER of mammalian cells. To improve the folding and stability of roGFP, we included the superfolder mutations as described previously (Hoseki et al., 2016), but using an ER targeted roGFP1-iE rather than roGFP1-iL. The resulting cell line demonstrated bright ER-localised fluorescence that was responsive to changes in both oxidation and reduction, making it an ideal reporter for changes in ER redox state (Fig. 1A,B). In addition, there was an absence of light-induced fluorescence changes, an effect that compromised the use of the roGFP1-iL variant (van Lith et al., 2011). The variant of roGFP was designated ER-SFGFP-iE. We isolated microsomal vesicles from the ER-SFGFP1-iE cell line and were able to follow changes to ER redox status over time using a plate reader (Fig. 1C). We established that the microsomes were sensitive to both reduction with dithiothreitol (DTT) and oxidation with diamide, indicating that the reporter was neither fully oxidised nor reduced following isolation. Reduction with membrane-permeable DTT was rapid, reaching completion within 10 min. When the membrane-impermeable reducing agent tris-(2-carboxyethyl)phosphine (TCEP) was added to microsomes containing ER-SFGFP-iE, reduction still occurred but much slower than if the microsomes were solubilised prior to TCEP addition (Fig. 1D, blue versus black). Reduction in intact microsomes did not reach completion unless detergent was added to solubilise the ER membrane (see from 35 min in Fig. 1D). To ensure the TCEP was not directly reducing ER-SFGFP-iE, we carried out a similar experiment but used TCEP immobilised on agarose beads. ER-SFGFP-iE was reduced significantly (P=0.00001) by immobilised TCEP agarose beads but not by buffer pre-incubated with TCEP beads (P=0.03) (Fig. 1E). These results strongly suggest the indirect reduction of ER-SFGFP-iE by TCEP when the microsomal membrane is intact.

The lack of full reduction of ER-SFGFP-iE by TCEP suggests that the reaction had reached saturation. To evaluate this possibility further we determined the rate of reduction with a range of TCEP concentrations (Fig. 1F,G). The results show that the rate of reduction does indeed reach saturation at concentrations of TCEP over 1 mM, suggesting a facilitated process. To show that TCEP can reduce ER-SFGFP-iE directly and fully we determined the rate of reduction with a range of TCEP concentrations after solubilising the ER membrane (Fig. 1H,I). Under these conditions the rate did not reach saturation, suggesting a diffusion-limited process. These results with the membrane-impermeable reducing agent suggest the indirect reduction of an ER-localised disulfide mediated via an ER membrane component.

The thioredoxin reduction pathway is sufficient to reduce ER-localised proteins via a membrane protein

To evaluate the cytosolic components required to ensure reduction of ER-localised disulfides, we attempted to reconstitute the pathway with purified components. We reasoned that a source of NADPH would be required as well as TrxR1 and Trx1. To ensure efficient recycling of NADPH, we included glucose 6 phosphate (G6P) as well as G6P dehydrogenase. To demonstrate that the system could maintain Trx1 in its reduced state, we determined the redox status of purified Trx1 before and after incubation with the recycling system. Redox status was evaluated following modification with 4-acetamido-4′-malemidylstilbene-2,2′-disulfonic acid (AMS), which increases the protein mass and thus slows its electrophoretic mobility. Prior to incubation, Trx1 was present as a mixture of both reduced and oxidised protein (Fig. 2A, lane 1). After incubation with TrxR1 and the NADPH recycling system, Trx1 was fully reduced (Fig. 2A, lane 2). When our microsomes containing ER-SFGFP-iE were incubated with the TrxR1 reduction system, roGFP became more reduced, an effect that was dependent on the inclusion of Trx1 as no reduction occurred in the presence of TrxR1 and the NADPH recycling system alone (Fig. 2B, C-Trx). No reduction of roGFP was observed when active site mutants of Trx1 (CXXS or SXXS) were used in place of wild-type protein (CXXC). These results demonstrate that the minimal requirement for reduction of ER-localised roGFP is the thioredoxin reduction system and that disulfide exchange is mediated through the Trx1 CXXC active site motif. As the reduction was Trx1 dependent and Trx1 is membrane impermeable, it is highly likely that an ER membrane component is required to transfer the reducing equivalents from Trx1 to roGFP.

The experiments with roGFP provide us with a useful way to follow reduction of a specific disulfide within the ER lumen by components added outside the vesicles; however, this protein is not normally present in the ER. Hence, we evaluated the redox status of ERp57, a member of the PDI family, to determine whether the thioredoxin reduction system could also reduce an endogenous ER protein that has previously been shown to be required for the correct folding of glycoproteins (Jessop et al., 2007).

We used the approach described for AMS (Jessop and Bulleid, 2004) to probe the redox status of ERp57 in SP cells isolated from a cell line stably transfected with V5-tagged ERp57 (Jessop et al., 2007). Samples were either untreated or treated with the oxidising agent diamide, with the reducing agent DTT or with the membrane-impermeable TCEP (Fig. 3Ai,ii). Treatment with *N*-ethylmaleimide (NEM) blocks any free thiols and subsequent reduction, and alkylation with AMS reduces the mobility of the protein. Proteins

Journal of Cell Science (2020) 133, jcs241976. doi:10.1242/jcs.241976

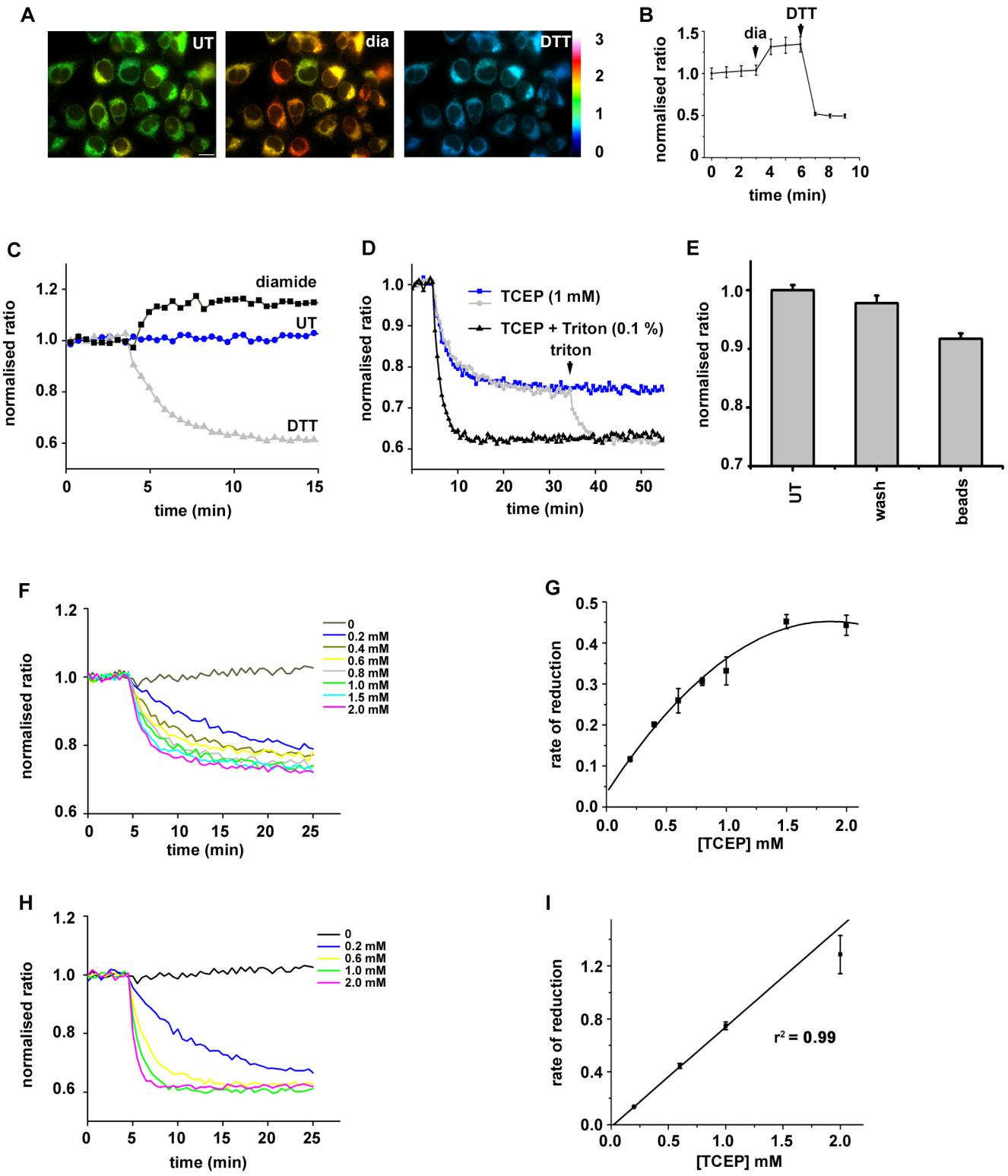

Fig. 1. See next page for legend.

that contain disulfides in the original SP cells, therefore, show reduced mobility on SDS-PAGE. Following this procedure, ERp57 in untreated SP cells migrated as two species representing the oxidised and reduced forms, by comparison with the diamide- or DTT-treated samples (Fig. 3Ai, lanes 1-3). After incubation with TCEP most of the ER-localised ERp57 was reduced, although not completely (Fig. 3Ai, lane 4), a result that mirrors the incomplete reduction of roGFP and demonstrates that TCEP can substitute for a cytosolic reduction system.

To evaluate the ability of the thioredoxin pathway to reduce ER-localised ERp57, we first fully oxidised SP cells with diamide, removed diamide by re-isolating the SP cells and incubated them with the complete TrxR1 reduction system, just recombinant Trx1 or the reduction system without Trx1 (Fig. 3Bi,ii). Partial reduction

Journal of Cell Science (2020) 133, jcs241976. doi:10.1242/jcs.241976

Fig. 1. Reduction of ER-localised disulfides by TCEP requires a membrane component. A stable cell-line expressing ER-SFGFP-iE was evaluated by live-cell imaging and was responsive to gross changes in redox conditions. (A) Fluorescent images of untreated, diamide- (1 mM) or DTT-treated (10 mM) cells. Fluorescence ratio changes are visualised using false colours, with a more reducing ratio in blue and a more oxidising in yellow. (B) Normalised fluorescent ratios of individual cells (*n*=37) are averaged (mean±s.d.) and changes observed over time by the sequential addition of diamide (1 mM) and DTT (10 mM). (C) Normalised fluorescence ratio changes in microsomal membranes isolated from the cell line expressing ER-SFGFP-iE, followed using a plate reader. An increase in ratio is seen following diamide (1 mM) addition whereas a decrease is seen following DTT (1 mM) addition. The ER-SFGFP-iE in untreated cells is, therefore, neither fully oxidised nor reduced. The experiment was repeated four times (*n*=5). (D) Changes in normalised fluorescence ratio following the addition of impermeable TCEP in the absence (blue) or presence (black) of Triton X-100. After 35 min, Triton X-100 (0.1% v/v) was added to solubilise the intact microsomes. Note the slower rate of reduction and the lack of full reduction with TCEP unless the membranes are solubilised. The experiment was repeated twice (*n*=3). (E) ER-SFGFP-iE is reduced by TCEP immobilised on agarose beads, further confirming that the reduction is not direct. The experiment was carried out in triplicate with average (mean±s.d.) indicated for untreated (UT), buffer preincubated with TCEP beads (wash) and TCEP beads (beads). (F-I) The change in normalised fluorescent ratio was followed at various TCEP concentrations as indicated either without (F) or with (H) detergent solubilisation of microsomes. The rate of reduction at each TECP concentration was calculated in triplicate with the average (mean±s.d.) plotted versus the TCEP concentration (G,I).

of fully oxidised ERp57 occurred in the presence of the complete system (Fig. 3Bi, lane 3) but did not occur with just Trx1 alone (Fig. 3Bi, lane 4) indicating a requirement for the recycling system. The reduction of ERp57 was dependent on Trx1 (Fig. 3Bi, lane 5) as was the case with roGFP. In addition, the active site mutants of Trx1 lacking one or both cysteines within the CXXC motif were unable to reduce ERp57 (Fig. 3Ci,ii; lanes 4 and 5). These results demonstrate that ER-localised ERp57 can be reduced following oxidation by the cytosolic reduction pathway and that this reduction is dependent on thioredoxin.

To further characterise the membrane component required for reduction, we carried out a proteinase K digestion of our SP cells prior to assay for ERp57 reduction (Fig. 3Di,ii). We surmised that if a membrane protein was involved then the transfer of reducing equivalents across the membrane might be sensitive to proteolysis. Proteinase K digestion prevented the reduction of oxidised ERp57 by the reconstituted reduction system (Fig. 3Di, lane 4), suggesting the requirement for a membrane protein whose cytosolic domain is sensitive to digestion. We also determined whether the reduction of ERp57 by TCEP was sensitive to proteinase K treatment of the SP cells (Fig. 3Ei,ii). TCEP was still able to reduce oxidised ERp57 (Fig. 3Ei, lane 4), suggesting that either the membrane protein involved can be reduced efficiently by TCEP without its protease-sensitive cytosolic domain or that TCEP acts via a component separate from the thioredoxin-dependent pathway.

The thioredoxin reduction pathway is sufficient to reduce non-native disulfides in nascent chains exposed to the ER lumen

We previously demonstrated that non-native disulfides formed during the synthesis of β1 integrin require a cytosolic reductive pathway to ensure their isomerisation to the correct disulfides (Poet et al., 2017). To evaluate the ability of our reconstituted pathway to isomerise non-native disulfides, we generated stalled translocation intermediates of a protein that forms non-native disulfides following *in vitro* translation in the presence of SP cells (Robinson et al., 2020). By isolating SP cells containing these intermediates, we were then able to follow the rearrangement of disulfides post-translationally in the presence or absence of a TrxR1 reduction system (Fig. 4A). We generated a stalled translocation intermediate of the disintegrin domain of ADAM10 by translating an RNA transcript lacking a stop codon. The length of the synthesised chain is sufficient to allow exposure of several cysteine residues in the ER lumen (Fig. 4B) that have the potential to form disulfides. Translations were performed using a rabbit reticulocyte lysate supplemented with SP cells to study folding in the ER (Wilson et al., 1995). All samples were treated with NEM on completion to irreversibly modify thiols and freeze the disulfide status of the samples for downstream processing. When translations were carried out in the presence of a reducing agent (DTT) and the samples separated under non-reducing conditions, two products of approximately 18 and 20 kDa were synthesised (Fig. 4C, lane 1). These products correspond to the translocated, signal sequence cleaved chain and untranslocated preprotein (Robinson et al., 2020). When the translations were carried out in the absence of added G6P and a post-translational incubation carried out in the absence of G6P, a diffuse pattern emerged with the translation products forming both intra- and interchain disulfides (Fig. 4C, lane 2). When G6P was added post-translationally and samples incubated for 60 min, more distinct products were formed indicative of discrete disulfide-bonded species (Fig. 4C, lane 3). When SP cells were

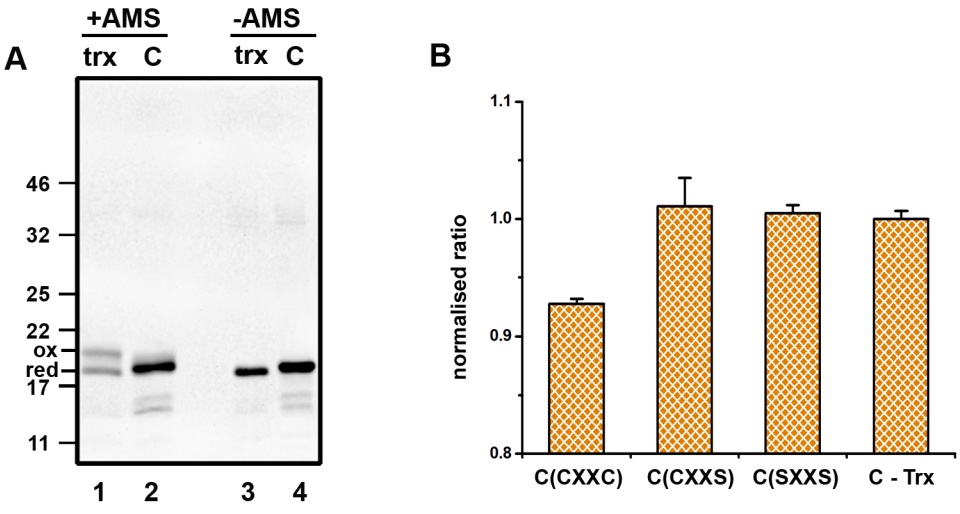

Fig. 2. Thioredoxin-dependent reduction of ER-localised disulfides. (A) The redox status of Trx1 (trx) was determined by AMS differential alkylation either before (lane 1) or after (lane 2) incubation with TrxR1 and a NADPH recycling system (C). Samples not treated with AMS are shown in lanes 3 and 4. The experiment was carried out once. (B) The normalised fluorescence ratio of ER-SFGFP-iE was measured following incubation with the reduction system without Trx1 (C-Trx) or with the TrxR1 system containing wild-type Trx1 (CXXC) or active site mutants CXXS or SXXS. The experiment was repeated twice (*n*=3) with the average (mean±s.d.) presented.

Journal of Cell Science (2020) 133, jcs241976. doi:10.1242/jcs.241976

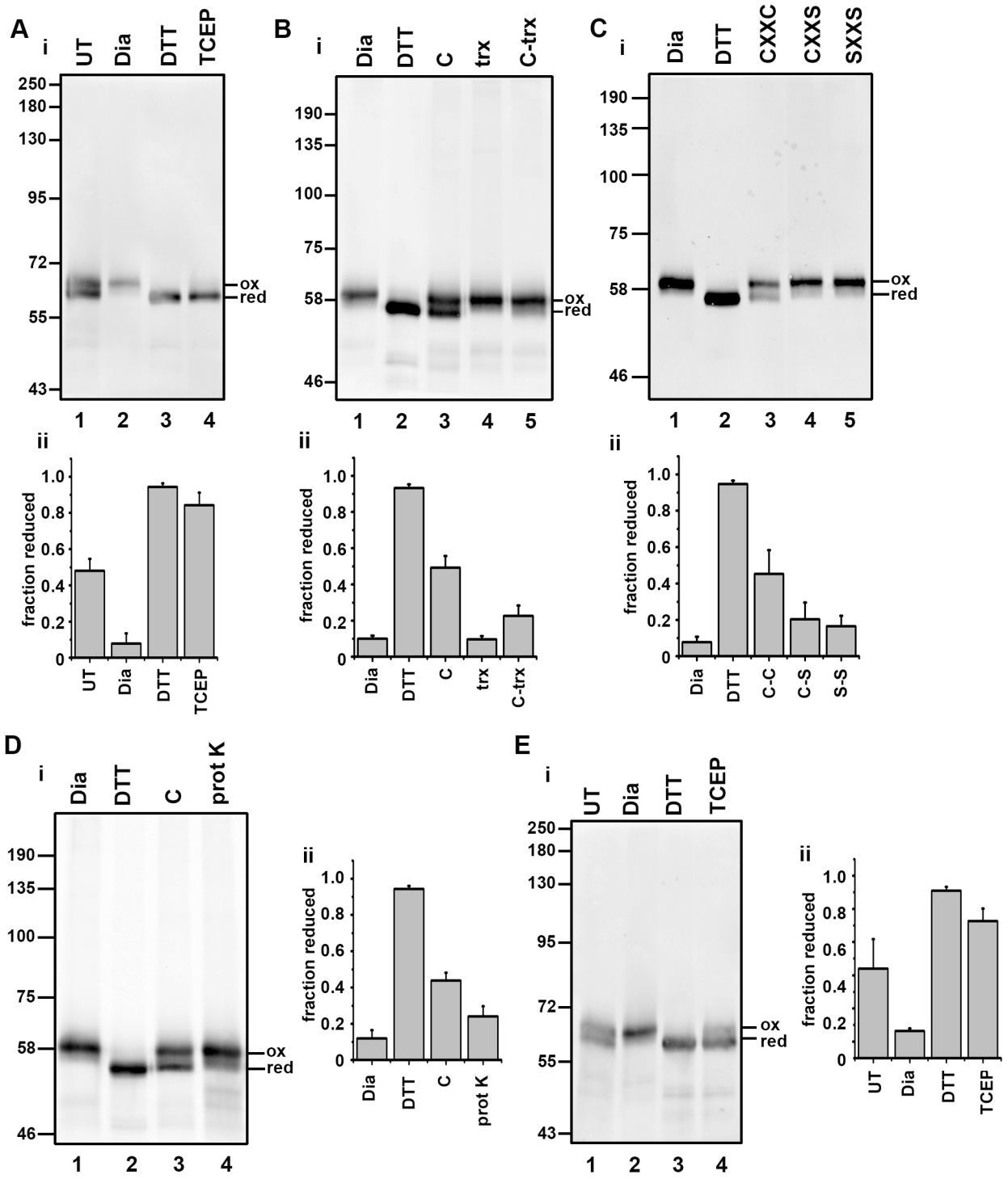

Fig. 3. See next page for legend.

isolated from translations carried out in the absence of G6P and incubated in buffer alone, no change to the banding pattern was observed (Fig. 4C, lane 4). However, when the TrxR1 reduction system was added to the isolated SP cells, rearrangement of disulfides was observed and resulted in more distinct disulfide-bonded species (Fig. 4C, lane 5). This change to the banding pattern to more discrete disulfide-bonded species did not occur when the isolated SP cells were incubated in the TrxR1 reductive pathway lacking Trx1 (Fig. 4C, lane 6). We also demonstrated that TCEP could substitute for G6P when added to translations or to isolated SP cells post-translationally, giving rise to discrete disulfide-bonded species (Fig. 4D, lanes 3 and 5). We have previously shown that the disulfide-bonded products formed from this ADAM10 construct are present in nascent chains translocated into the ER lumen (Robinson et al., 2020). Taken together, these results show that a source of non-membrane-permeable reducing agent can resolve the non-native disulfides formed in nascent chains within the ER lumen.

Journal of Cell Science (2020) 133, jcs241976. doi:10.1242/jcs.241976

Fig. 3. Thioredoxin-dependent reduction of ERp57 requires a membrane protein. (A) The redox status of ER-localised ERp57 was determined following differential alkylation with AMS. (Ai) In untreated SP cells, ERp57 exists as a mixture of reduced and oxidised forms (lane 1) and becomes fully oxidised (lane 2) or fully reduced (lane 3) following the addition of diamide (Dia) or DTT, respectively. Partial reduction of ERp57 also occurs following incubation of fully oxidised ERp57 with the membrane-impermeable reductant TCEP (lane 4). (Aii) Quantification of the fraction reduced in untreated SP cells (UT), SP cells treated with diamide, DTT or TCEP. The experiment was repeated twice (n=3). (B) Thioredoxin-dependent reduction of ER-localised ERp57. (Bi) SP cells were treated with diamide before incubation with either the complete TrxR1 reduction system (C; lane 3) or without (C–trx; lane 5) or with Trx1 alone (trx; lane 4). ERp57 was partially reduced only by the complete system. (Bii) Quantification of the fraction reduced in SP cells treated as for Bi. The experiment was repeated twice (n=3). (C) The reduction of ERp57 by the TrxR1 system needs Trx1 with an intact active site. (Ci) Neither of the active site mutants CXXS (lane 4) or SXXS (lane 5) can substitute for wild-type (CXXC) Trx1. (Cii) Quantification of the fraction reduced in SP cells treated as for Ci. The experiment was repeated twice (n=3). (Di) The reduction of ER-localised ERp57 by the TrxR1 system is sensitive to prior treatment of the SP cells with proteinase K (lane 4). (Dii) Quantification of the fraction reduced in SP cells treated with diamide, DTT or a TrxR1 reduction system either before (C) or after (protK) treatment of the SP cells with proteinase K. The experiment was repeated twice (n=3). (Ei) SP cells were treated with proteinase K in the absence of further treatment (UT) or after treatment with diamide, DTT or TCEP. The reduction of ER-localised ERp57 by TCEP is not prevented by prior treatment of the SP cells with proteinase K (lane 4). (Eii) Quantification of the fraction reduced in SP cells treated as for Ei. The experiment was repeated twice (n=3). All graphs show mean values; error bars indicate s.d.

The thioredoxin reduction pathway reduces disulfides in several secretory and ER resident proteins

The experiments with roGFP and ERp57 are dependent on the reduction of a reversible disulfide that is solvent accessible in the final protein structure. To determine whether our reconstituted reductive system could reduce other disulfides within secretory or membrane proteins, we carried out redox proteomics. Essentially, microsomes were incubated with the TrxR1 system in either the presence or absence of Trx1 for 60 min and the reversibly oxidised thiol groups labelled with heavy iodoacetamide. The samples were prepared for liquid chromatography with tandem mass spectrometry (LC/MS/MS) analysis by trypsin digestion followed by tandem mass tagging to enable quantification of the changes in the cysteine oxidation levels between experimental conditions. The resulting data were analysed by Perseus software and are presented as a volcano plot indicating the statistically significant changes to the reversibly oxidised cysteine residues upon incubation with Trx1 (Fig. 5A). The redox status of several peptides changed during the incubation; specifically, there was a subset of cysteines whose oxidised status decreased (became more reduced) in the reactions containing Trx1, with the majority of the corresponding proteins being located in the ER lumen (Fig. 5A, blue circles). Notably, the regulatory cysteine (Cys131) in Ero1α was reduced (Appenzeller-Herzog et al., 2008; Baker et al., 2008) as was the cysteine involved in recycling VKORC1L1 (Cys50) (Tie et al., 2014). Changes to the redox status of a few cytosolic and mitochondrial proteins also occurred (Fig. 5A, orange circles), which probably co-purified with our microsomal vesicles. The identity of all the proteins identified whose redox status changed along with their ultimate subcellular location is as illustrated (Fig. 5B) or detailed separately (Table 1). The results demonstrate that several thiols within endogenous proteins that are synthesised at the ER, including thiols that form structural and regulatory disulfides, can be reduced by the thioredoxin reduction system. The target proteins were localised to the ER lumen and the TrxR1 reduction system was membrane impermeable, illustrating the requirement to transfer reducing equivalents across the membrane.

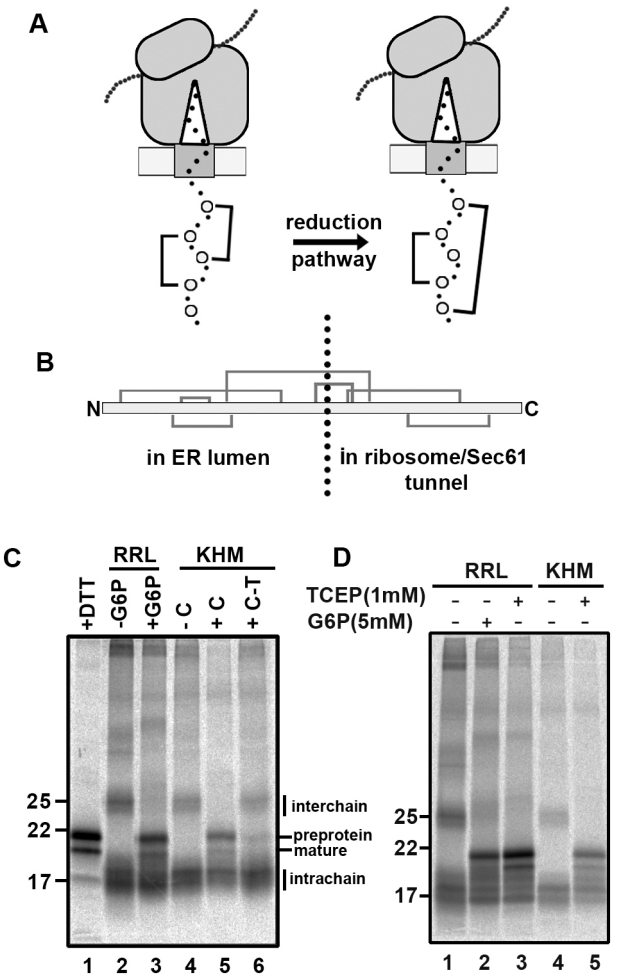

Fig. 4. Thioredoxin-dependent post-translational rearrangement of ER-localised nascent chain disulfides. (A) Cartoon depicting the rearrangement of nascent chain disulfides in a stalled translocation intermediate following the addition of a cytosol-localised reduction system. (B) Schematic of the disulfide pattern within the disintegrin domain of ADAM10. The stalled intermediate used in subsequent experiments has the indicated disulfide-forming cysteines in the ER lumen. (C) Translations carried out in the presence of DTT (5 mM) gave rise to distinct translation products that migrate with the sizes of the pre-protein and mature protein as indicated (lane 1). Translations were carried out in the absence of added G6P and SP cells subsequently incubated post-translationally in a reticulocyte lysate (RRL) in the absence (lane 2) or presence (lane 3) of G6P. SP cells were isolated from the translations and resuspended in KHM buffer alone (–C) (lane 4). Note the rearrangement of nascent chain disulfides when the TrxR1 system is included in the incubation (lane 5) (+C) and the dependence of this rearrangement on the presence of Trx1 (lane 6) (C-T). The experiment was repeated once (n=2). (D) Similarly to the TrxR1 system, TCEP brings about the rearrangement of nascent chain disulfides when added to SP cells post-translationally either in the presence of RRL (lane 3) or in KHM buffer alone (lane 5). The experiment was repeated once (n=2).

DISCUSSION

Our previous work provided the first indication that a cytosolic reductive pathway was required to ensure correct disulfide formation within the ER (Poet et al., 2017). Here, we demonstrate that the thioredoxin pathway is sufficient to provide the reducing equivalents to ensure the reduction of regulatory and non-native

Journal of Cell Science (2020) 133, jcs241976. doi:10.1242/jcs.241976

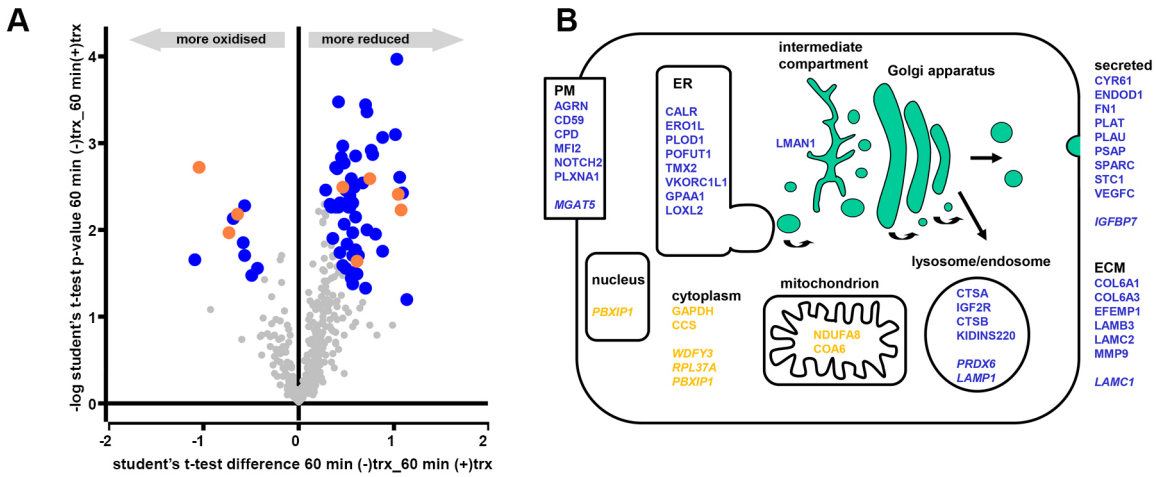

Fig. 5. Evaluation of the changes in the redox status of microsomal proteins following incubation with the TrxR1 system. (A) Volcano plot depicting proteins with significant changes to their redox status where the modified cysteine is localised to the ER (blue) or the cytosol (orange). Proteins identified by mass spectrometry whose redox status does not change significantly are also indicated (grey). (B) Cartoon illustrating the final cellular location of proteins whose redox status changes significantly upon incubation of microsomes with the TrxR1 system. Proteins that enter the secretory pathway are in blue whereas those that do not enter the ER are in yellow. Proteins that become more reduced are in normal text and those that become more oxidised are in italics. Note that PBXIP1 associates with the cytoskeleton and is mainly in the cytosol but it does shuttle to the nucleus to act in addition to its role as a soluble transcription factor (Abramovich et al., 2002).

disulfides within ER proteins. We have successfully reconstituted the reduction of ER disulfides using a microsomal system in the presence of purified components to demonstrate that the thioredoxin pathway can drive the reduction of disulfides in several ER-localised soluble and membrane proteins. In addition, we show that the pathway is sufficient to facilitate the reduction of disulfides formed in nascent chains entering the ER lumen but does not prevent disulfide re-formation, a requirement for correct isomerisation of non-native to native disulfides. Importantly, we show that a membrane protein is required to facilitate the transfer of reductant across the ER membrane, presumably via a disulfide exchange mechanism as demonstrated for the transfer of disulfides across the bacterial plasma membrane by DsbD (Cho et al., 2007).

The absolute requirement for the presence of thioredoxin in our reconstituted system rules out a role for an NADPH-dependent ER-localised reductase. Previously, it has been postulated that an ER glutathione or thioredoxin reductase could utilise the ER pool of NADPH to drive the reduction of disulfides (Bulleid and Ellgaard, 2011). As there is an ER-localised hexose 6-phosphate dehydrogenase (Lavery et al., 2006), G6P might enter the ER via the G6P-transporter, be metabolised to phosphogluconolactone and in the process regenerate the ER pool of NADPH. Hence, the G6P effect we previously observed during our *in vitro* translations might be the result of a process independent of the thioredoxin pathway. This is clearly not the case for the reduction of roGFP, ERp57, disulfides in nascent chains and the range of proteins identified from the redox proteomics whose redox state change depends on the presence of thioredoxin.

The reductive pathway driven by cytosolic thioredoxin is versatile in terms of its target disulfides in the ER lumen. These disulfides included those present within folded proteins such as roGFP, in proteins undergoing folding during translocation and in proteins that require reduction to maintain their activity. Such versatility suggests a broad substrate specificity of the terminal enzyme involved in catalysing reduction. Changes to the redox status of ERp57 would suggest that this member of the PDI family could act as a reductase, as suggested previously for newly synthesised glycoproteins (Jessop et al., 2007) to which it is targeted via its interaction with calnexin or calreticulin (Oliver et al., 1997). It is also likely that ERdj5 is reduced by the cytosolic reductive pathway and targeted to substrate proteins through its interaction with BiP (Cunnea et al., 2003). Our identification of one of the regulatory disulfides within Ero1α (Baker et al., 2008) as a target for the cytosolic reductive pathway suggests that this disulfide can be reduced by one of the PDI family members, as demonstrated previously using purified proteins (Shepherd et al., 2014). Whether the ER membrane protein responsible for transfer of reducing equivalents directly reduces the PDI reductase remains to be established.

The role of thioredoxin as reductant of the ER membrane protein can be replaced with the membrane-impermeable reducing agent TCEP. However, in contrast to thioredoxin-mediated process, reduction of ER proteins via TCEP was shown to be insensitive to protease digestion, suggesting that this reagent can reduce the ER membrane protein in the absence of a protease-sensitive cytosolic domain. This result probably reflects the different requirements for reduction of the membrane protein disulfide by thioredoxin and TCEP. The mechanism underlying recognition and reduction of substrates by thioredoxin is not completely understood given its wide range of substrate specificity. However, it has been demonstrated that noncovalent interactions prior to disulfide reduction are important, with recognition being due to the conformational restriction afforded by the oxidised substrate (Palde and Carroll, 2015). Hence, the proteolytic digestion of a protein domain or loop might prevent thioredoxin interacting with the membrane protein, thereby inhibiting activity. A chemical reductant such as TCEP has no requirement for such noncovalent interactions and only requires the target disulfide to be solvent accessible.

The identity of the membrane protein involved in connecting the cytosolic thioredoxin couple with the ER remains unknown. One resident ER membrane protein whose depletion leads to a more oxidising ER and a specific defect in correct disulfide formation in lipoprotein lipase is lipase maturation factor 1 (LMF1) (Roberts et al., 2018). This protein contains several thiols in its cytosolic loops, transmembrane regions and lumenal domain that are required for activity and could be involved in disulfide exchange. Unfortunately, we did not identify LMF1 in our proteomics data, so we could not identify any changes to its redox status. Hence, LMF1 remains a potential candidate for shuttling disulfides across

Journal of Cell Science (2020) 133, jcs241976. doi:10.1242/jcs.241976

Table 1. Proteins showing a significant change to their oxidised thiols along with information on their subcellular location, position and identity of the modified cysteine(s)

Location of cysteine modified	Gene name	Protein location	Type	Cysteine modified	More Red/Ox
Cytosol	GAPDH	Cytoplasm	Soluble	152, 156	Red
	CCS	Cytoplasm	Soluble	227	Red
	WDFY3	Cytoplasm	Soluble	952	Ox
	RPL37A	Cytoplasm	Soluble	39, 42	Ox
	PBXIP1	Nucleus	Soluble	559, 565	Ox
Endomembrane system	COL6A1	ECM	Soluble	745	Red
	COL6A3	ECM	Soluble	1823, 1824	Red
	EFEMP1	ECM	Soluble	40, 47	Red
	LAMB3	ECM	Soluble	451, 453, 511, 534, 536	Red
	LAMC1	ECM	Soluble	416, 418, 474, 751, 804, 807, 954, 956	Ox
	LAMC2	ECM	Soluble	28, 30, 53, 56	Red
	MMP9	ECM	Soluble	256	Red
	CALR	ER	Soluble	105	Red
	ERO1L	ER	Soluble	131	Red
	PLOD1	ER	Soluble	267, 270	Red
	POFUT1	ER	Soluble	283	Red
	TMX2	ER	Single pass	59	Red
	GPAA1	ER	Multipass	266	Red
	VKORC1L1	ER	Multipass	50	Red
	LMAN1	ER/Golgi	Single pass	230	Red
	LOXL2	ER/secreted	Soluble	395	Red
	PRDX6	Lysosomal	Soluble	47	Ox
	LAMP1	Lysosomal	Single pass	338	Ox
	CTSA	Lysosomal	Soluble	239	Red
	IGF2R	Lysosomal	Soluble	1227	Red
	CTSB	Lysosomal	Soluble	211	Red
	KIDINS220	Endosome	Multipass	705	Red
	CD59	PM	GPI anchored	70	Red
	CPD	PM	Single pass	309	Red
	MFI2	PM	GPI anchored	199	Red
	MGAT5	PM	Single pass	338	Ox
	NOTCH2	PM	Single pass	1342, 1346	Red
	PLXNA1	PM	Single pass	358	Red
	AGRN	PM/secreted	Soluble	650	Red
	CYR61	Secreted	Soluble	337, 314, 317	Red
	ENDOD1	Secreted	Soluble	34	Red
	FN1	Secreted	Soluble	87, 97, 135, 141, 179, 231, 508	Red
	IGFBP7	Secreted	Soluble	156	Ox
	PLAT	Secreted	Soluble	419	Red
	PLAU	Secreted	Soluble	45	Red
	PSAP	Secreted	Soluble	42	Red
	SPARC	Secreted	Soluble	130	Red
	STC1	Secreted	Soluble	170	Red
	VEGFC	Secreted	Soluble	328	Red
Mitochondrion	NDUFA8	Mitochondrion	Soluble	66	Red
	COA6	Mitochondrion	Soluble	44	Red
Unknown	NUMB	Membrane	Unknown	130, 132	Ox
	DPY19L1	Unknown	Multipass	647	Ox

ECM, extracellular matrix; PM, plasma membrane; Ox, oxidised; Red, reduced.

the ER membrane. Of the 41 microsomal proteins whose redox status changed during incubation with the TrxR1 system, four are multipass membrane proteins with VKORC1L1 and GPAA1 being known resident ER proteins. GPAA1 is a subunit of the GPI-anchor transamidase (Ohishi et al., 2000) whereas VKORC1L1 is a paralogue of vitamin K epoxide hydrolase with a potential function in vitamin K-dependent carboxylation (Tie et al., 2013). Whether these proteins are directly involved in disulfide exchange across the ER membrane is a focus of future studies.

MATERIALS AND METHODS

Generation of stable cell line expressing ER-SFGFP-iE

HT1080 cells were transfected with ER-SFGFP-iE using MegaTran 1.0 (OriGene, Cambridge, UK) following the manufacturer's protocol. Various dilutions (1:10 to 1:10,000) of transfected HT1080 cells were plated on 15 cm^2 dishes. Cells were grown in selective medium containing G418 (1 mg/ml) until colonies appeared. Single colonies were picked and transferred to 12-well plates (one colony per well) using trypsin-soaked Scienceware cloning discs (Sigma, Dorset, UK). Cells were grown until confluent and then transferred to 25 cm^2 flasks. The presence of ER-SFGFP-iE was confirmed by western blot using rabbit anti-GFP antibody (Santa Cruz, California, USA; cat# sc-8334, 1:200 dilution). All cell lines were regularly tested for mycoplasma infection.

Live cell microscopy and image analysis

HT1080 cells stably expressing ER-SFGFP-iE were seeded on coverslips. The cells were washed with buffer [HEPES (20 mM) pH 7.4, NaCl (130 mM), KCl (5 mM), $CaCl_2$ (1 mM), $MgCl_2$ (1 mM), D-glucose

Journal of Cell Science (2020) 133, jcs241976. doi:10.1242/jcs.241976

(10 mM)] before imaging on a Zeiss Axio Observer A1 inverted microscope equipped with a 40× FLUAR lens (Zeiss, Oberkochen, Germany). The cells were sequentially excited by 385 and 470 nm LEDs with fluorescence detection through a T495 lpxr beamsplitter (Chroma, Vermont). Images were captured at 30 s intervals and analysed with AxioVision 4.8 software. The 385/470 nm ratio images of untreated, diamide-treated (1 mM) and DTT-treated (10 mM) cells were false-coloured using a rainbow look-up table. The 385/470 nm ratio changes over time were quantified by defining regions of interest for individual cells and plotted as the average ratio with standard deviation.

Preparation of microsomal membranes

Cells were cultured using cell culture roller bottles (1700 cm^2) (Greiner Bio-One). Confluent cells were detached from the roller bottle by incubation with 100 ml PBS containing EDTA (1 mM) for 15 min. Cells were pelleted, washed three times in HEPES–KOH (35 mM) buffer at pH 7.5 containing NaCl (140 mM) and glucose (11 mM) followed by washing once in extraction [HEPES–KOH (20 mM) pH 7.5, KOAc (135 mM), KCl (30 mM), MgOAc (1.65 mM)]. An equal volume of extraction buffer to the cell volume was used for resuspension. The cells were disrupted in a Mini-Bomb Cell disruption chamber (Kontes) using a nitrogen pressure of 1.0 MPa for 30 min. Cell homogenates were centrifuged at 6000×***g*** for 5 min at 4°C and the post-nuclear supernatant retained. The supernatant was centrifuged at 50,000×***g*** (Optima Max-XP Ultracentrifuge, Beckman Coulter) for 15 min at 4°C to pellet the membrane fraction. The membrane pellet was resuspended in buffer A [Tris-HCl (50 mM) pH 7.4, sucrose (0.25 M), KCl (50 mM), MgOAc (6 mM), EDTA (1 mM)] to give an A_{280} value of 50 units/µl (the absorbance was determined in water in the presence of 1% SDS). Aliquots of the microsomal membranes were frozen in liquid nitrogen and stored at −80°C.

Measurement of changes to the redox state of microsomal ER-SFGFP-iE

Microsomes were pipetted into Dulbecco's phosphate-buffered saline (PBS) (1.5 µl microsomes in 48.5 µl PBS) in the absence or presence of 0.1% Triton X-100 (Thermo Fisher). The solution was added into a CELLSTA 96-Well Polystyrene Flat Bottom Cell Culture Microplate (Greiner Bio-One) (final volume 50 µl per well; three wells per condition). Fluorescence intensities at 520 nm were measured following excitation at 390 nm and 460 nm excitations wavelengths using PHERAstar FS microplate reader (BMG Labtech). After 10 min of measurement to obtain a baseline, DTT, diamide or different concentrations of tris-(2-carboxyethyl)phosphine (TCEP) (Thermo) were injected into the wells. Fluorescence intensities were recorded for up to 50 min. In some experiments, the same amount of microsomes were untreated or treated either with immobilized TCEP Disulfide Reducing Gel beads (Thermo) that had been washed twice with PBS to remove soluble TCEP or with PBS that had been preincubated with TCEP beads for 60 min. The samples were incubated for 60 min and then transferred into microplate wells to measure fluorescence intensity at 520 nm following excitation at 390 and 460 nm.

To calculate the rate of change of the redox status of ER-SFGFP-iE at different TCEP concentrations, microsomes were treated with various concentrations of TCEP in the absence or presence of Triton X-100 (0.1% v/v). The fluorescence ratio (390/460 nm) change was followed over time after addition of TCEP and the resulting time course fitted to an exponential decay function [$y=-A(e^{-k(t-t0)}-1)+c$] to calculate the rate (k), where t_0 is time of addition of TCEP, c the initial fluorescence ratio and A the difference in fluorescence ratio between t_0 and t. The rate was then plotted against TCEP concentration. Measurement of the rate of reduction of ER-SFGFP-iE at different concentrations of TCEP was performed in triplicate.

Recombinant protein purification

Recombinant human thioredoxins (Trx1), wild type and mutants, were expressed and purified from *Escherichia coli* BL21-DE3 cells as described previously (Schwertassek et al., 2007). Purification was by successive HisTrap affinity and size exclusion (Superdex 200 10/300) chromatography (GE Healthcare). The protein concentration was determined following OD_{280nm} measurement and calculated using an extinction coefficient of 12.49 mM^{-1} cm^{-1}. The purified protein aliquots were flash frozen in liquid nitrogen and stored −80°C.

Determining the redox state of Trx1

Purified thioredoxin (25 µM) was incubated in KHM buffer [HEPES (20 mM) pH 7.2 containing KOAc (110 mM) and MgOAc (2 mM)] at 30°C for 60 min in the absence or presence of NADPH (1 mM), human TrxR1 (16.25 nM; IMCO), G6P (1.25 mM) and G6PDH (10 U/ml). The reaction was stopped by the addition of NEM (20 mM). Samples were incubated with streptavidin agarose resin (Thermo) in isolation buffer (IB) [Tris-HCl (50 mM) pH 7.5, Triton (1% v/v), NaCl (150 mM), EDTA (2 mM), PMSF (0.5 mM), sodium azide (0.02% w/v)] at 4°C for 60 min. The streptavidin beads were pelleted by centrifugation and washed three times in isolation buffer to remove unbounded proteins. Trx1 was eluted from the streptavidin beads by incubating at room temperature (RT) for 15 min with PBS containing SDS (2% w/v) and biotin (3 mM). The samples were boiled at 105°C for 15 min and incubated with TCEP (10 mM) at RT for 10 min to break existing disulfides, followed by a 1.5 h incubation with AMS (20 mM; Invitrogen) in the dark to alkylate free thiols. The samples were separated by SDS-PAGE and a western blot performed using Streptavidin Protein DyLight 800 (ThermoFisher, cat#21851; 1:5000 dilution).

Preparation of SP cells

SP cells were prepared as described previously (Wilson et al., 1995). Following digitonin treatment, cells were resuspended in KHM buffer containing $CaCl_2$ (1 mM) and treated with *Staphylococcus aureus* nuclease (150 U/ml; Calbiochem) at RT for 12 min to remove endogenous mRNA. The reaction was stopped with EGTA (4.5 mM; Sigma). SP cells were pelleted by centrifugation and resuspended in 100 µl KHM buffer to be used in translation reactions. For ERp57 redox state determination experiments, SP cells were prepared from cells expressing V5-tagged ERp57 (Jessop et al., 2007); nuclease treatment was not included during the preparation.

Determining the redox state of ER-localised ERp57

The redox state of ERp57 in SP cells was determined as described previously (Jessop and Bulleid, 2004). SP cells were either untreated or treated with diamide (10 mM) at RT for 10 min. Samples were washed twice with 500 µl KHM buffer to remove diamide. Oxidised SP cells were incubated at 30°C for 60 min in KHM buffer with or without DTT or with the purified reductive pathway components NADPH (1 mM), human Trx1 (25 µM), human TrxR1 (16.25 nM), G6P (1.25 mM) and G6PDH (10 U/ml). The SP cells were pelleted by centrifugation at 14,800×***g*** for 1 min and then incubated with 500 µl PBS containing NEM (25 mM) to block free thiols. The samples were washed twice with 1 ml PBS to remove excess NEM. The cells were lysed on ice with lysis buffer [Tris-HCl (50 mM), NaCl (150 mM), EDTA (2 mM), PMSF (0.5 mM), Triton X-100 (1% v/v)] for 10 min. The lysate was centrifuged at 14,800×***g*** at 4°C for 10 min. The supernatant was removed and boiled with SDS (2% w/v; VWR chemicals) to denature the protein. Denatured samples were incubated at RT with TCEP (10 mM) to break existing disulfide bonds, followed by a 1.5 h incubation with AMS (20 mM; Invitrogen) in the dark. The samples were separated by SDS-PAGE and a western blot performed with antibody to V5-tag to detect different redox states of ERp57.

Western blotting

Following SDS-PAGE, proteins were transferred to nitrocellulose blotting membrane (GE Healthcare). The membrane was blocked with 3% w/v dried skimmed milk (Marvel) in TBST buffer [Tris-HCl pH 8.0 (150 mM), NaCl (150 mM), Tween-20 (0.5% v/v)] for 1 h. The membrane was incubated in TBST including V5-antibody (Invitrogen, cat#R960-25; 1:10,000 dilution) for 1 h. After primary antibody incubation, the membrane was incubated in 5 ml TBST with secondary antibody (Fisher Scientific, cat #10751195; 1:10,000 dilution) in the dark for 45-60 min. The membrane was scanned using a Li-Cor Odyssey 9260 Imager. Quantification of gel intensity was by ImageJ (National Institutes of Health, Bethesda, MD); experiments were carried out three times. Values quoted are averages, with error bars depicting standard deviation.

Journal of Cell Science (2020) 133, jcs241976. doi:10.1242/jcs.241976

Proteinase K treatment

SP cells were incubated on ice with proteinase K (20 µg/ml; Roche) for 25 min in the presence of $CaCl_2$ (10 mM). Proteinase K was inactivated by incubation with PMSF (0.5 mM). Proteinase K and PMSF were removed by washing twice with KHM buffer.

Preparation of ADAM10 domain construct and *in vitro* translation

The human ADAM10 construct codes for residues 456-550 and contains the human-β2 M signal sequence residues (1-20). The generation of this construct and its transcription and translation were described previously (Robinson et al., 2020). Essentially, plasmid DNA was used as a template for the polymerase chain reaction (PCR) using an appropriate forward primer that adds a T7 promoter and a reverse primer that lacks a stop codon. The PCR product was transcribed into an RNA template using T7 RNA polymerase. Translations were performed using the Flexi Rabbit Reticulocyte Lysate System (Promega) supplemented with DTT (10 mM) or purified water but in the absence of added G6P. SP cells were added to a concentration of ∼10^5 cells per 25 µl translation reaction. Following assembly of components, translation reactions were incubated at 30°C for 15 min. For post-translational assays, G6P (5 mM) was added following translation or the SP cells were isolated by centrifugation and resuspended in KHM buffer in the presence or absence of a TrxR1 reduction system [NADPH (1 mM), human Trx1 (25 µM), human TrxR1 (16.25 nM), G6P (1.25 mM) and G6PDH (1 U) or TCEP (1 mM)]. An additional incubation was carried out in the presence of the TrxR1 reduction system without Trx1. The reactions were stopped after a 60 min incubation by the addition of NEM (final concentration 25 mM) prior to immunoisolation, SDS-PAGE and phosphorimage analysis.

Immunoisolation

SP cells from the translation reactions were resuspended in 1 ml IB containing 50 µl 10% Protein A Sepharose FF Resin (Generon). After 30 min incubation, the beads were isolated by centrifugation at 16,000 ***g*** for 30 s. The supernatant was transferred into a new tube containing 10% Protein A Sepharose (50 µl). Anti-V5 antibody (Invitrogen, cat #10751195; 1 µl) was added and the suspension incubated at 4°C overnight. The beads were pelleted by centrifugation and washed three times with 1 ml IB buffer. The beads were heated for 5 min at 105°C with SDS-PAGE loading buffer [Tris/HCl (200 mM) pH 6.8, glycerol (10% v/v), SDS (2% w/v), Bromophenol Blue (0.1% w/v)]. The samples were separated by SDS-PAGE. Gels were fixed in 10% acetic acid and 10% methanol, dried and exposed to a phosphorimager plate. A FLA-7000 bioimager (Fujifilm) was used to scan the plate to obtain the image.

Sample preparation for mass spectrometry analysis

Samples were prepared for redox proteomics as previously described (van der Reest et al., 2018) with some modifications. Microsomes were incubated in the presence of the reductive system as described above, either in the presence or absence of Trx1. After 60 min incubation at 30°C, microsomes were lysed in a buffer containing SDS (4%), triethylammonium bicarbonate (50 mM) pH 8.5 and unlabelled iodoacetamide (55 mM; light IAA, $^{12}C_2H_4INO$; Sigma) to alkylate free cysteine thiols. For each experimental replicate, 30 µg of protein was subsequently tagged with iodoacetamide labelled with stable isotope (heavy IAA, $^{13}C_2D_2H_2INO$; Sigma) to alkylate reversibly oxidised cysteines. Differentially alkylated proteins were precipitated using trichloroacetic acid (TCA) and digested first with endoproteinase Lys-C (enzyme:lysate ratio 1:33) for 1 h, followed by overnight digestion with trypsin (enzyme:lysate ratio 1:33). The digested peptides from each experiment, and a pool sample, were differentially labelled using the Tandem Mass Tag (TMT) 10-plex reagent set (Thermo Scientific). Fully labelled samples were mixed in equal amounts and desalted using 100 mg Sep Pak C18 reverse phase solid-phase extraction cartridges (Waters).

LC/MS/MS protocol

We analysed three different experimental conditions. For each condition, we analysed three biological replicates, which were labelled with nine tags of the TMT 10-plex. The remaining TMT tag was used to label a pool generated by mixing equal amounts of each sample, which was used to normalise the data using the internal reference scaling method (Plubell et al., 2017).

TMT-labelled peptides were analysed as previously described (van der Reest et al., 2018) with minor modifications. First, peptides were fractionated using high pH reverse phase chromatography on a C18 column [150×2.1 mm internal diameter; Kinetex EVO (5 µm, 100 Å)] on a HPLC system (LC 1260 Infinity II, Agilent). A two-step gradient was applied: from 1-28% buffer B in 42 min, then from 28-46% buffer B in 13 min to obtain a total of 21 fractions for LC/MS/MS analysis.

Fractionated peptides were separated by nanoscale C18 reverse-phase liquid chromatography using an EASY-nLC II 1200 (Thermo Scientific) coupled to an Orbitrap Fusion Lumos mass spectrometer (Thermo Scientific). Elution was carried out using a binary gradient with buffer A (2% acetonitrile) and B (80% acetonitrile), both containing 0.1% formic acid. Samples were loaded with 6 µl of buffer A into a 50 cm fused silica emitter (New Objective) packed in-house with ReproSil-Pur C18-AQ, 1.9 µm resin (Dr Maisch, Ammerbuch, Germany). Packed emitter was kept at 50°C by means of a column oven (Sonation) integrated into the nanoelectrospray ion source (Thermo Scientific). Peptides were eluted at a flow rate of 300 nl/min using different gradients optimised for three sets of fractions: 1-7, 8-15 and 16-21. The initial percentage of buffer B (%B) was kept constant for 3 min, then a two-step gradient was used, all with 113 min for step one and 37 min for step two. The %B was changed as follows: for F1-7, %B was 2 at the start, 17 at step one and 26 at step two. For F8-14, %B was 4 at the start, 23 at step one and 35 at step two. For F15-21, %B was 6 at the start, 27 at step one and 43 at step two. All gradients were followed by a washing step (95% B) of 10 min followed by a 5 min re-equilibration step at the initial %B of each gradient, for a total gradient time of 168 min. Eluting peptides were electrosprayed into the mass spectrometer using a nanoelectrospray ion source (Thermo Scientific). An Active Background Ion Reduction Device (ESI Source Solutions) was used to decrease air contaminant signal level. The Xcalibur software (Thermo Scientific) was used for data acquisition. A full scan over mass range of 350-1400 m/z was acquired at 60,000 resolution at 200 m/z, with a target value of 500,000 ions for a maximum injection time of 20 ms. Higher energy collisional dissociation fragmentation was performed on the 15 most intense ions, selected through an isolation window of 0.8 m/z, for a maximum injection time of 100 ms, or a target value of 100,000 ions. Peptide fragments were analysed in the Orbitrap at 50,000 resolution.

MS data analysis

The MS Raw data were processed with MaxQuant software (Cox and Mann, 2008) version 1.6.3.3 and searched with Andromeda search engine (Cox et al., 2011), querying SwissProt (UniProt, 2010). First and main searches were performed with precursor mass tolerances of 20 ppm and 4.5 ppm, respectively, and MS/MS tolerance of 20 ppm. The minimum peptide length was set to six amino acids and specificity for trypsin cleavage was required, allowing up to two missed cleavage sites. MaxQuant was set to quantify on 'Reporter ion MS2', and TMT 10-plex was chosen as isobaric label. Interference between TMT channels were corrected by MaxQuant using the correction factors provided by the manufacturer. The 'Filter by PIF' option was activated and a 'Reporter ion tolerance' of 0.003 Da was used. Modification by light [H(3)NOC(2)] and heavy [HNOCx(2)Hx(2)] iodoacetamide on cysteine residues (carbamidomethylation) were specified as variable, as well as methionine oxidation and N-terminal acetylation modifications; no fixed modifications were specified. The peptide, protein and site false discovery rate (FDR) was set to 1%. MaxQuant outputs were analysed with Perseus software version 1.6.2.3 (Cox and Mann, 2008). The MaxQuant output ModSpecPeptide.txt file was used for quantification of cysteine-containing peptide oxidation, whereas the ProteinGroup.txt file was used for protein quantification analysis. Peptides with a cysteine count lower than one were excluded from the analysis, together with Reverse and Potential Contaminant flagged peptides. From the ProteinGroups.txt file, Reverse and Potential Contaminant flagged proteins were removed, as well as protein groups identified with no unique peptides. The TMT corrected intensities of proteins and peptides were normalised to the median of all intensities measured in each replicate. Only cysteine-containing peptides uniquely assigned to one protein group within

each replicate experiment, and robustly quantified in three out of three replicate experiments, were normalised to the total protein levels and included in the analysis. To determine significantly regulated cysteine-containing peptides, a Student's *t*-test with a 5% FDR (permutation-based) was applied using normalised reporter ion intensities.

Acknowledgements
We wish to acknowledge the generosity of all our colleagues for contributing reagents, and other members of the Bulleid group for critical reading of the manuscript. We would like to acknowledge Dr Martin Rennie for advice on curve fitting.

Competing interests
The authors declare no competing or financial interests.

Author contributions
Methodology: X.C., S.L., Z.C., O.B.V.O., P.J.R., M.v.L., S.Z.; Software: S.L.; Formal analysis: S.L.; Investigation: X.C., Z.C., M.A.P., O.B.V.O., P.J.R., T.S., M.v.L.; Writing - original draft: N.J.B.; Writing - review & editing: X.C., Z.C., M.A.P., O.B.V.O., P.J.R., M.v.L., S.Z.; Supervision: S.Z., N.J.B.; Project administration: M.A.P.; Funding acquisition: S.Z., N.J.B.

Funding
This work was funded by the Biotechnology and Biological Sciences Research Council (grant BB/P017665), the Wellcome Trust (grant 103720), the China Scholarship Council and Cancer Research UK (A29800 and A17196). Deposited in PMC for immediate release.

Data availability
The raw files and the MaxQuant search results files have been deposited as a partial submission to the ProteomeXchange Consortium via the PRIDE partner repository with the dataset identifier PXD017923.

Peer review history
The peer review history is available online at
https://jcs.biologists.org/lookup/doi/10.1242/jcs.241976.reviewer-comments.pdf

References
Abramovich, C., Chavez, E. A., Lansdorp, P. M. and Humphries, R. K. (2002). Functional characterization of multiple domains involved in the subcellular localization of the hematopoietic Pbx interacting protein (HPIP). *Oncogene* **21**, 6766-6771. doi:10.1038/sj.onc.1205784

Appenzeller-Herzog, C., Riemer, J., Christensen, B., Sorensen, E. S. and Ellgaard, L. (2008). A novel disulphide switch mechanism in Ero1α balances ER oxidation in human cells. *EMBO J.* **27**, 2977-2987. doi:10.1038/emboj.2008.202

Appenzeller-Herzog, C., Riemer, J., Zito, E., Chin, K. T., Ron, D., Spiess, M. and Ellgaard, L. (2010). Disulphide production by Ero1α-PDI relay is rapid and effectively regulated. *EMBO J.* **29**, 3318-3329. doi:10.1038/emboj.2010.203

Baker, K. M., Chakravarthi, S., Langton, K. P., Sheppard, A. M., Lu, H. and Bulleid, N. J. (2008). Low reduction potential of Ero1α regulatory disulphides ensures tight control of substrate oxidation. *EMBO J.* **27**, 2988-2997. doi:10.1038/emboj.2008.230

Braakman, I. and Bulleid, N. J. (2011). Protein folding and modification in the mammalian endoplasmic reticulum. *Annu. Rev. Biochem.* **80**, 71-99. doi:10.1146/annurev-biochem-062209-093836

Bulleid, N. J. and Ellgaard, L. (2011). Multiple ways to make disulfides. *Trends Biochem. Sci.* **36**, 485-492. doi:10.1016/j.tibs.2011.05.004

Cao, Z., Mitchell, L., Hsia, O., Scarpa, M., Caldwell, S. T., Alfred, A. D., Gennaris, A., Collet, J.-F., Hartley, R. C. and Bulleid, N. J. (2018). Methionine sulfoxide reductase B3 requires resolving cysteine residues for full activity and can act as a stereospecific methionine oxidase. *Biochem. J.* **475**, 827-838. doi:10.1042/BCJ20170929

Chakravarthi, S. and Bulleid, N. J. (2004). Glutathione is required to regulate the formation of native disulfide bonds within proteins entering the secretory pathway. *J. Biol. Chem.* **279**, 39872-39879. doi:10.1074/jbc.M406912200

Chakravarthi, S., Jessop, C. E. and Bulleid, N. J. (2006). The role of glutathione in disulphide bond formation and endoplasmic-reticulum-generated oxidative stress. *EMBO Rep.* **7**, 271-275. doi:10.1038/sj.embor.7400645

Chen, W., Helenius, J., Braakman, I. and Helenius, A. (1995). Cotranslational folding and calnexin binding during glycoprotein synthesis. *Proc. Natl. Acad. Sci. USA* **92**, 6229-6233. doi:10.1073/pnas.92.14.6229

Cho, S.-H., Porat, A., Ye, J. and Beckwith, J. (2007). Redox-active cysteines of a membrane electron transporter DsbD show dual compartment accessibility. *EMBO J.* **26**, 3509-3520. doi:10.1038/sj.emboj.7601799

Cox, J. and Mann, M. (2008). MaxQuant enables high peptide identification rates, individualized p.p.b.-range mass accuracies and proteome-wide protein quantification. *Nat. Biotechnol.* **26**, 1367-1372. doi:10.1038/nbt.1511

Cox, J., Neuhauser, N., Michalski, A., Scheltema, R. A., Olsen, J. V. and Mann, M. (2011). Andromeda: a peptide search engine integrated into the MaxQuant environment. *J. Proteome Res.* **10**, 1794-1805. doi:10.1021/pr101065j

Cunnea, P. M., Miranda-Vizuete, A., Bertoli, G., Simmen, T., Damdimopoulos, A. E., Hermann, S., Leinonen, S., Huikko, M. P., Gustafsson, J. A., Sitia, R. et al. (2003). ERdj5, an endoplasmic reticulum (ER)-resident protein containing DnaJ and thioredoxin domains, is expressed in secretory cells or following ER stress. *J. Biol. Chem.* **278**, 1059-1066. doi:10.1074/jbc.M206995200

Dierks, T., Dickmanns, A., Preusser-Kunze, A., Schmidt, B., Mariappan, M., von Figura, K., Ficner, R. and Rudolph, M. G. (2005). Molecular basis for multiple sulfatase deficiency and mechanism for formylglycine generation of the human formylglycine-generating enzyme. *Cell* **121**, 541-552. doi:10.1016/j.cell.2005.03.001

Ellgaard, L., Sevier, C. S. and Bulleid, N. J. (2018). How are proteins reduced in the endoplasmic reticulum? *Trends Biochem. Sci.* **43**, 32-43. doi:10.1016/j.tibs.2017.10.006

Hagiwara, M., Maegawa, K., Suzuki, M., Ushioda, R., Araki, K., Matsumoto, Y., Hoseki, J., Nagata, K. and Inaba, K. (2011). Structural basis of an ERAD pathway mediated by the ER-resident protein disulfide reductase ERdj5. *Mol. Cell* **41**, 432-444. doi:10.1016/j.molcel.2011.01.021

Hoseki, J., Oishi, A., Fujimura, T. and Sakai, Y. (2016). Development of a stable ERroGFP variant suitable for monitoring redox dynamics in the ER. *Biosci. Rep.* **36**, e00316. doi:10.1042/BSR20160027

Jansens, A., van Duijn, E. and Braakman, I. (2002). Coordinated nonvectorial folding in a newly synthesized multidomain protein. *Science* **298**, 2401-2403. doi:10.1126/science.1078376

Jessop, C. E. and Bulleid, N. J. (2004). Glutathione directly reduces an oxidoreductase in the endoplasmic reticulum of mammalian cells. *J. Biol. Chem.* **279**, 55341-55347. doi:10.1074/jbc.M411409200

Jessop, C. E., Chakravarthi, S., Garbi, N., Hämmerling, G. J., Lovell, S. and Bulleid, N. J. (2007). ERp57 is essential for efficient folding of glycoproteins sharing common structural domains. *EMBO J.* **26**, 28-40. doi:10.1038/sj.emboj.7601505

Kadokura, H., Katzen, F. and Beckwith, J. (2003). Protein disulfide bond formation in prokaryotes. *Annu. Rev. Biochem.* **72**, 111-135. doi:10.1146/annurev.biochem.72.121801.161459

Lavery, G. G., Walker, E. A., Draper, N., Jeyasuria, P., Marcos, J., Shackleton, C. H., Parker, K. L., White, P. C. and Stewart, P. M. (2006). Hexose-6-phosphate dehydrogenase knock-out mice lack 11β-hydroxysteroid dehydrogenase type 1-mediated glucocorticoid generation. *J. Biol. Chem.* **281**, 6546-6551. doi:10.1074/jbc.M512635200

Lillig, C. H. and Holmgren, A. (2007). Thioredoxin and related molecules–from biology to health and disease. *Antioxid Redox Signal.* **9**, 25-47. doi:10.1089/ars.2007.9.25

Molteni, S. N., Fassio, A., Ciriolo, M. R., Filomeni, G., Pasqualetto, E., Fagioli, C. and Sitia, R. (2004). Glutathione limits Ero1-dependent oxidation in the endoplasmic reticulum. *J. Biol. Chem.* **279**, 32667-32673. doi:10.1074/jbc.M404992200

Ohishi, K., Inoue, N., Maeda, Y., Takeda, J., Riezman, H. and Kinoshita, T. (2000). Gaa1p and gpi8p are components of a glycosylphosphatidylinositol (GPI) transamidase that mediates attachment of GPI to proteins. *Mol. Biol. Cell* **11**, 1523-1533. doi:10.1091/mbc.11.5.1523

Oka, O. B., Pringle, M. A., Schopp, I. M., Braakman, I. and Bulleid, N. J. (2013). ERdj5 is the ER reductase that catalyzes the removal of non-native disulfides and correct folding of the LDL receptor. *Mol. Cell* **50**, 793-804. doi:10.1016/j.molcel.2013.05.014

Oliver, J. D., van der Wal, F. J., Bulleid, N. J. and High, S. (1997). Interaction of the thiol-dependent reductase ERp57 with nascent glycoproteins. *Science* **275**, 86-88. doi:10.1126/science.275.5296.86

Palde, P. B. and Carroll, K. S. (2015). A universal entropy-driven mechanism for thioredoxin-target recognition. *Proc. Natl. Acad. Sci. USA* **112**, 7960-7965. doi:10.1073/pnas.1504376112

Plubell, D. L., Wilmarth, P. A., Zhao, Y., Fenton, A. M., Minnier, J., Reddy, A. P., Klimek, J., Yang, X., David, L. L. and Pamir, N. (2017). Extended multiplexing of tandem mass tags (TMT) labeling reveals age and high fat diet specific proteome changes in mouse epididymal adipose tissue. *Mol. Cell. Proteomics* **16**, 873-890. doi:10.1074/mcp.M116.065524

Poet, G. J., Oka, O. B., van Lith, M., Cao, Z., Robinson, P. J., Pringle, M. A., Arner, E. S. and Bulleid, N. J. (2017). Cytosolic thioredoxin reductase 1 is required for correct disulfide formation in the ER. *EMBO J.* **36**, 693-702. doi:10.15252/embj.201695336

Ponsero, A. J., Igbaria, A., Darch, M. A., Miled, S., Outten, C. E., Winther, J. R., Palais, G., D'Autreaux, B., Delaunay-Moisan, A. and Toledano, M. B. (2017). Endoplasmic reticulum transport of glutathione by Sec61 is regulated by Ero1 and Bip. *Mol. Cell* **67**, 962-973.e5. doi:10.1016/j.molcel.2017.08.012

Rishavy, M. A., Usubalieva, A., Hallgren, K. W. and Berkner, K. L. (2011). Novel insight into the mechanism of the vitamin K oxidoreductase (VKOR): electron relay through Cys43 and Cys51 reduces VKOR to allow vitamin K reduction and

facilitation of vitamin K-dependent protein carboxylation. *J. Biol. Chem.* **286**, 7267-7278. doi:10.1074/jbc.M110.172213

Roberts, B. S., Babilonia-Rosa, M. A., Broadwell, L. J., Wu, M. J. and Neher, S. B. (2018). Lipase maturation factor 1 affects redox homeostasis in the endoplasmic reticulum. *EMBO J.* **37**. doi:10.15252/embj.201797379

Robinson, P. J., Kanemura, S., Cao, X. and Bulleid, N. J. (2020). Protein secondary structure determines the temporal relationship between folding and disulfide formation. *J. Biol. Chem.* **295**, 2438-2448. doi:10.1074/jbc.RA119.011983

Schwertassek, U., Balmer, Y., Gutscher, M., Weingarten, L., Preuss, M., Engelhard, J., Winkler, M. and Dick, T. P. (2007). Selective redox regulation of cytokine receptor signaling by extracellular thioredoxin-1. *EMBO J.* **26**, 3086-3097. doi:10.1038/sj.emboj.7601746

Sevier, C. S., Qu, H., Heldman, N., Gross, E., Fass, D. and Kaiser, C. A. (2007). Modulation of cellular disulfide-bond formation and the ER redox environment by feedback regulation of Ero1. *Cell* **129**, 333-344. doi:10.1016/j.cell.2007.02.039

Shepherd, C., Oka, O. B. V. and Bulleid, N. J. (2014). Inactivation of mammalian Ero1alpha is catalysed by specific protein disulfide-isomerases. *Biochem. J.* **461**, 107-113. doi:10.1042/BJ20140234

Tavender, T. J., Springate, J. J. and Bulleid, N. J. (2010). Recycling of peroxiredoxin IV provides a novel pathway for disulphide formation in the endoplasmic reticulum. *EMBO J.* **29**, 4185-4197. doi:10.1038/emboj.2010.273

Tie, J.-K., Jin, D.-Y., Tie, K. and Stafford, D. W. (2013). Evaluation of warfarin resistance using transcription activator-like effector nucleases-mediated vitamin K epoxide reductase knockout HEK293 cells. *J. Thromb. Haemost.* **11**, 1556-1564. doi:10.1111/jth.12306

Tie, J.-K., Jin, D.-Y. and Stafford, D. W. (2014). Conserved loop cysteines of vitamin K epoxide reductase complex subunit 1-like 1 (VKORC1L1) are involved in its active site regeneration. *J. Biol. Chem.* **289**, 9396-9407. doi:10.1074/jbc.M113.534446

Tsunoda, S., Avezov, E., Zyryanova, A., Konno, T., Mendes-Silva, L., Pinho Melo, E., Harding, H. P. and Ron, D. (2014). Intact protein folding in the glutathione-depleted endoplasmic reticulum implicates alternative protein thiol reductants. *Elife* **3**, e03421. doi:10.7554/eLife.03421

UniProt, C. (2010). The universal protein resource (UniProt) in 2010. *Nucleic Acids Res.* **38**, D142-D148.

Ushioda, R., Hoseki, J., Araki, K., Jansen, G., Thomas, D. Y. and Nagata, K. (2008). ERdj5 is required as a disulfide reductase for degradation of misfolded proteins in the ER. *Science* **321**, 569-572. doi:10.1126/science.1159293

van Lith, M., Tiwari, S., Pediani, J., Milligan, G. and Bulleid, N. J. (2011). Real-time monitoring of redox changes in the mammalian endoplasmic reticulum. *J. Cell Sci.* **124**, 2349-2356. doi:10.1242/jcs.085530

van der Reest, J., Lilla, S., Zheng, L., Zanivan, S. and Gottlieb, E. (2018). Proteome-wide analysis of cysteine oxidation reveals metabolic sensitivity to redox stress. *Nat. Commun.* **9**, 1581. doi:10.1038/s41467-018-04003-3

Wang, M. and Kaufman, R. J. (2016). Protein misfolding in the endoplasmic reticulum as a conduit to human disease. *Nature* **529**, 326-335. doi:10.1038/nature17041

Wilson, R., Allen, A. J., Oliver, J., Brookman, J. L., High, S. and Bulleid, N. J. (1995). The translocation, folding, assembly and redox-dependent degradation of secretory and membrane proteins in semi-permeabilized mammalian cells. *Biochem. J.* **307**, 679-687. doi:10.1042/bj3070679